9-Substituted Paullones: Synthesis and Analysis of Structure-Activity Relationships

Dissertation

zur Erlangung des Doktorgrades
der Universität Hamburg
Fachbereich Chemie

vorgelegt von
Tanja Pies
aus Darmstadt

Hamburg 2003

Referees: PD Dr. C. Kunick
Prof. Dr. D. Geffken

Date of thesis defense: 11 July 2003

In Liebe und Dankbarkeit
meinem Vater gewidmet

Die vorliegende Arbeit entstand in der Zeit von Oktober 1999 bis Mai 2003 am Institut für Pharmazie der Universität Hamburg unter der Leitung von **Herrn PD Dr. C. Kunick**, dem ich für die Überlassung des Themas und seine vorbildlich engagierte Betreuung ganz besonders herzlich danke.

Herrn Prof. Dr. D. Geffken gilt mein Dank für die freundliche Aufnahme in seinen Arbeitskreis und seine großzügige Förderung sowie für die Übernahme des Korreferats.

Für die Unterstützung bei der Durchführung der QSAR-Studie bin ich **Herrn Dr. K.-J. Schaper** (Forschungszentrum Borstel) außerordentlich dankbar.

Meinen herzlichen Dank möchte ich auch **Herrn Dr. Th. Lemcke** für die Erstellung der Molecular Modeling-Abbildungen aussprechen.

Weiterhin sei der Arbeitsgruppe von **Dr. L. Meijer** (CNRS, Station Biologique, Roscoff, Frankreich), **Herrn Dr. D. Zaharevitz** und dem National Cancer Institute (Bethesda, Maryland, USA) sowie **Herrn M. Kaiser** und dem Schweizer Tropeninstitut (Basel, Schweiz) für die Durchführung der biologischen Testungen gedankt.

Zudem danke ich **Frau Dr. K. Wieking**, **Frau J. Möllenbeck**, **Herrn C. Prühs**, **Frau S. Kohfeld**, **Frau Dr. X. Xie**, **Frau Dr. K. Lauenroth** und **Herrn Dr. Z. Zeng** für die erfolgreiche und angenehme Zusammenarbeit sowie allen übrigen Mitarbeitern des Institutes für Pharmazie und des Institutes für Chemie, die zum Gelingen dieser Arbeit beigetragen haben.

Sehr dankbar bin ich **Frau Dr. K. Wieking**, **Frau J. Möllenbeck** und **Herrn Scott Veals** für die Hilfe beim Lesen der Korrekturen.

Abschließend gilt mein besonderer Dank meiner Familie und meinen Freunden für die fortwährende Unterstützung, die sie mir während der Erstellung dieser Arbeit zuteil werden ließen.

List of Abbreviations

abs.	absolute
Ala	alanine
Ar	aromatic (spectra)
Asp	aspartic acid
ATP	adenosine 5’-triphosphate
avg	average
br	broadened (spectra)
BSA	bovine serum albumin
CAK	cyclin activating kinase
calcd.	calculated
CDI	*N*,*N*’-carbonyldiimidazole
CDK	cyclin-dependent kinase
cf.	compare (Latin confer)
CIP	CDK2-interacting proteins
^{13}C-NMR	carbon nuclear magnetic resonance
CNS	central nervous system
COSY	correlation spectroscopy
m-CPBA	*meta*-chloroperbenzoic acid
CPK	Corey-Pauling-Koltun
CRK	CDK-related kinase
Δ	reflux
Δm	difference in mass
δ	chemical shift
d	day
d	doublet (spectra)
d. h.	das heißt
2D	two-dimensional
3D	three-dimensional
DCC	*N*,*N*’-dicyclohexylcarbodiimide

DEPT	Distortionless Enhancement by Polarization Transfer
DIC	*N*,*N*'-diisopropylcarbodiimide
DMAP	4-dimethylaminopyridine
DMF	*N*,*N*-dimethylformamide
DMSO	dimethyl sulfoxide
DNA	deoxyribonucleic acid
e.g.	for example (Latin exempli gratia)
EDC	1-ethyl-3-(3-dimethylamino)propylcarbodiimide
EGTA	ethylene glycol bis(β-aminoethylether)-*N*,*N*,*N*',*N*'-tetraacetic acid
equiv.	equivalent(s)
expt.	experiment
FAB-MS	fast atom bombardment mass spectrometry
GI_{50}	50% growth inhibition
Glu	glutamic acid
GS	glycogen synthase
GSK	glygogen synthase kinase
GST	glutathione-S-transferase
h	hour
HETCOR	Heteronuclear Correlation Spectroscopy
HMQC	Heteronuclear Multiple Quantum Correlation
^{1}H-NMR	proton nuclear magnetic resonance
HOBt	1-hydroxy-1*H*-benzotriazole
HPLC	high-performance liquid chromatography
HRMS	high-resolution mass spectrometry
Hz	hertz
i.e.	that is (Latin id est)
IC_{50}	50% inhibitory concentration
Ile	isoleucine
IR	infrared
J	coupling constant

λ	wavelength
LC_{50}	lethal concentration for 50%
Leu	leucine
log	logarithm to the base 10
log_{10}	logarithm to the base 10
LOO	Leave-One-Out
M	molar
m	multiplet (spectra)
m	*meta*
MAP-kinase	mitogen-activated protein kinase
Met	methionine
MG_MID	Meangraph Midpoint
MOPS	3-(*N*-morpholino)propanesulfonic acid
mp	melting point
MPLC	medium pressure liquid chromatography
MS	mass spectrometry
m/z	mass-to-charge ratio
n/a	not applicable
NCI	National Cancer Institute
NMP	*N*-methyl-2-pyrrolidinone
#	number
p	*para*
PENDANT	Polarization Enhancement During Attached Nucleus Testing
Phe	phenylalanine
PHF	paired helical filaments
PKC	protein kinase C
ppm	parts per million
pRb	retinoblastoma protein
q	quartet (spectra)
QSAR	quantitative structure-activity relationship

quat.	quaternary (spectra)
quint	quintet (spectra)
quot.	quotient
rct.	reaction
recr.	recrystallization
rel.	relative
RT	room temperature
s	singlet (spectra)
sept	septet (spectra)
sext	sextet (spectra)
S_N2	second-order nucleophilic substitution
t	triplet (spectra)
tert.	tertiary (spectra)
tert	tertiary
TGI	total growth inhibition
THF	tetrahydrofuran
Thr	threonine
t_R	retention time
UV/VIS	ultraviolet/visible
w/o	without
wat	water

Contents

1 Introduction and Aim of Thesis

1.1 7,12-Dihydroindolo[3,2-*d*][1]benzazepin-6(5*H*)-ones (Paullones)

Paullones are defined to be 7,12-dihydroindolo[3,2-*d*][1]benzazepin-6(5*H*)-ones and constitute a class of cyclin-dependent kinase (CDK) inhibitors.[1] Their discovery has its roots in the National Cancer Institute (NCI)-COMPARE algorithm which enables the detection of substances with similar mechanisms of cell growth inhibition by comparing the patterns of compound action resulting from the NCI Human Tumor Cell Line Anti-Cancer Drug Screening.[2] Flavopiridol, the first CDK inhibitor involved in clinical trials[3,4], was taken as a reference substance, and thus 9-bromo-7,12-dihydroindolo[3,2-*d*][1]benzazepin-6(5*H*)-one (**1**) (kenpaullone) was identified as a potential CDK inhibitor. Consequentially, various kinases were assayed with kenpaullone (**1**) and a strong preference for CDK1, CDK2, and CDK5 was observed.[2] Further experiments exposed the paullones to additionally act as potent inhibitors of GSK-3β.[5] Kinetic studies with enzymes proved the kinase inhibition to be caused by the competitive replacement of ATP at the CDK ATP binding site.[2] However, the NCI in vitro anti-cancer drug screening revealed kenpaullone (**1**) to show only moderate anti-proliferative activity. Therefore, kenpaullone (**1**) was comprehensively modified in order to pave the way for the performance of structure-activity relationship analyses and thus optimize the compound structure to yield a derivative with potent enzyme inhibition and high anti-proliferative activity. The synthesis of alsterpaullone (**2**) represents the successful achievement of this aim.[6]

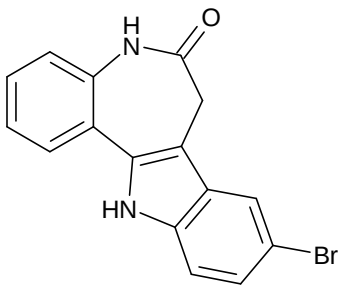

1

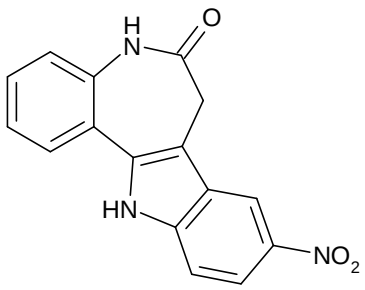

2

1.2 Cyclin-Dependent Kinases

Cyclin-dependent kinases represent a family of serine/threonine kinases that play a major part in the process of cell cycle division.[7-8]

Cyclin-dependent kinases are heterodimeric kinases composed of a catalytic CDK-subunit and a regulatory cyclin-subunit. The former consists of approximately 300 amino acids and can be subdivided into two lobes: a smaller N-terminal loop, rich in β-sheets and containing the PSTAIRE helix, a conserved subdomain serving as a binding site for the associated cyclins, and a larger C-terminal loop, mostly α-helical. The cleft between these lobes, called the hinge-region, features the ATP binding site. The entrance to this active site cleft is controlled by a flexible loop, the T-loop, which blocks protein substrate binding if the CDK catalytic subunit is still unmodified, that is, not yet connected to a cyclin. The latter, cyclins, show a distinctive diversity. Their size ranges from about 35 to 90 kDa. However, a homologous sequence exists: it consists of circa 100 amino acids and represents the “cyclin-box” which is responsible for CDK binding.

As an example, the CDK2/cyclin A-complex is illustrated in figure 1-1.

Figure 1-1: CDK2/cyclin A-complex with bound ATP

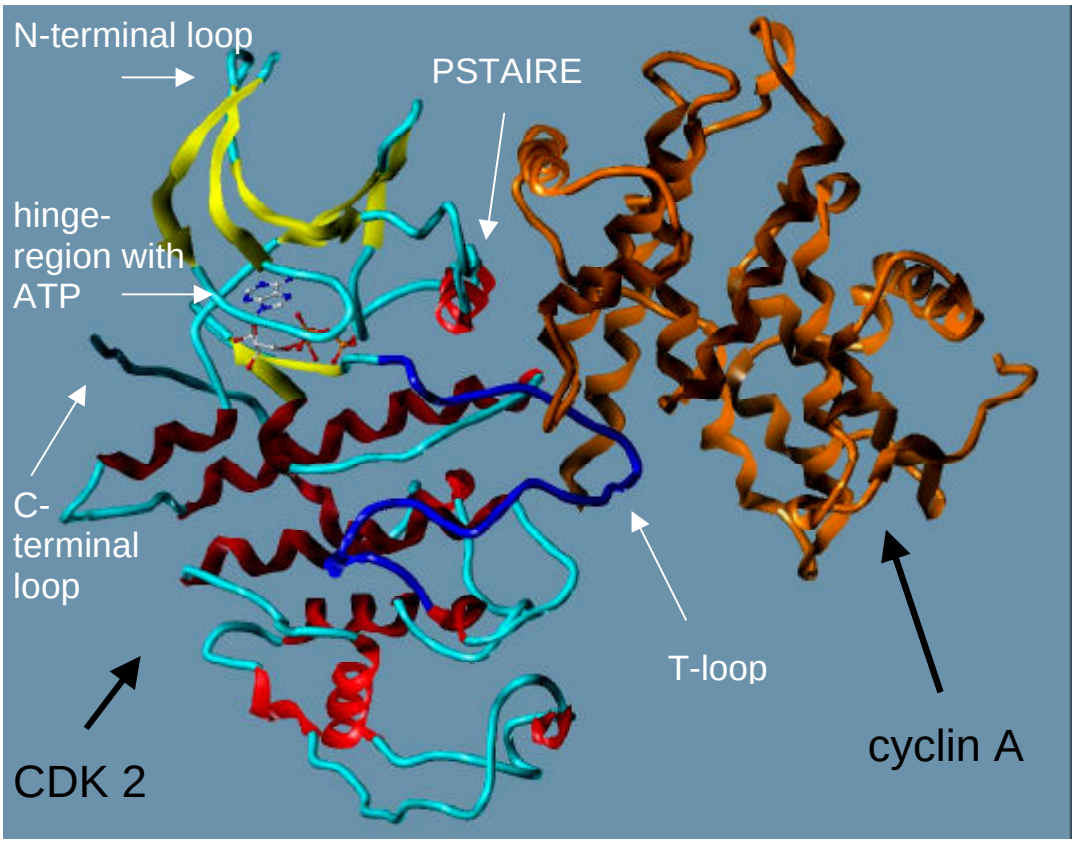

The characteristic elements were depicted in color as follows:

- α-Helices: red spirals
- β-Sheets: yellow ribbons
- Connecting structures: cyan
- T-loop: blue
- ATP: depicted in “balls & sticks”-illustration
- Cyclin A: brown

The coordinates were adopted from the Brookhaven Protein Data Bank[9] (PDB ID: 1JST[10]) and illustrated using SYBYL[11].

As deducible from their name, the catalytic activity of CDKs is linked to the formation of a complex between the cognated units. Up to today, at least 9 CDKs (CDK1-9) and 15 cyclins (cyclin A-T) have been discovered.[4] Various CDK-cyclin combinations are known, each catalyzing phosphotransfer reactions and playing a unique role in cell cycle progression or other events like gene transcription or neural differentiation (table 1-1).[4,7,12]

Table 1-1: Functions of CDK/cyclin-complexes

CDK	associated cyclin(s) or protein(s)	function
CDK1	cyclin A	transition S/G2 phase
CDK1	cyclin B1-3	transition G2/M phase
CDK2	cyclin A	S phase
CDK2	cyclin E	transition G1/S phase
CDK3	?	G1 phase
CDK4	cyclin D1-3	G1 and G2 phase
CDK5	cyclin D1-3	neural functions
CDK5	p35/p25	neural differentiation
CDK6	cyclin D1-3	G1 phase
CDK7	cyclin H	CAK, transcription
CDK8	cyclin C	transcription
CDK9	cyclin K	transcription
CDK9	cyclin T	transcription
?	cyclin F	?
?	cyclin G	?
?	cyclin I	?

Most paullones display their main activity towards the CDK1/cyclin B-holoenzyme. As depicted above (table 1-1), this complex orchestrates the transition of G2 into M phase, a crucial event in the cell cycle division process. Being aware of the fact that orderly cell cycle progression is of fundamental importance to all eukaryotic organisms concerning healthy reproduction and thus life in general, the specific sites of action of cyclin dependent kinases as the driving force within the cell cycle machinery is of special interest with regard to potential new drug targets.[8] The following figure gives an overview (figure1-2).[4]

Figure 1-2: Cell cycle driven by CDK/cyclin-complexes

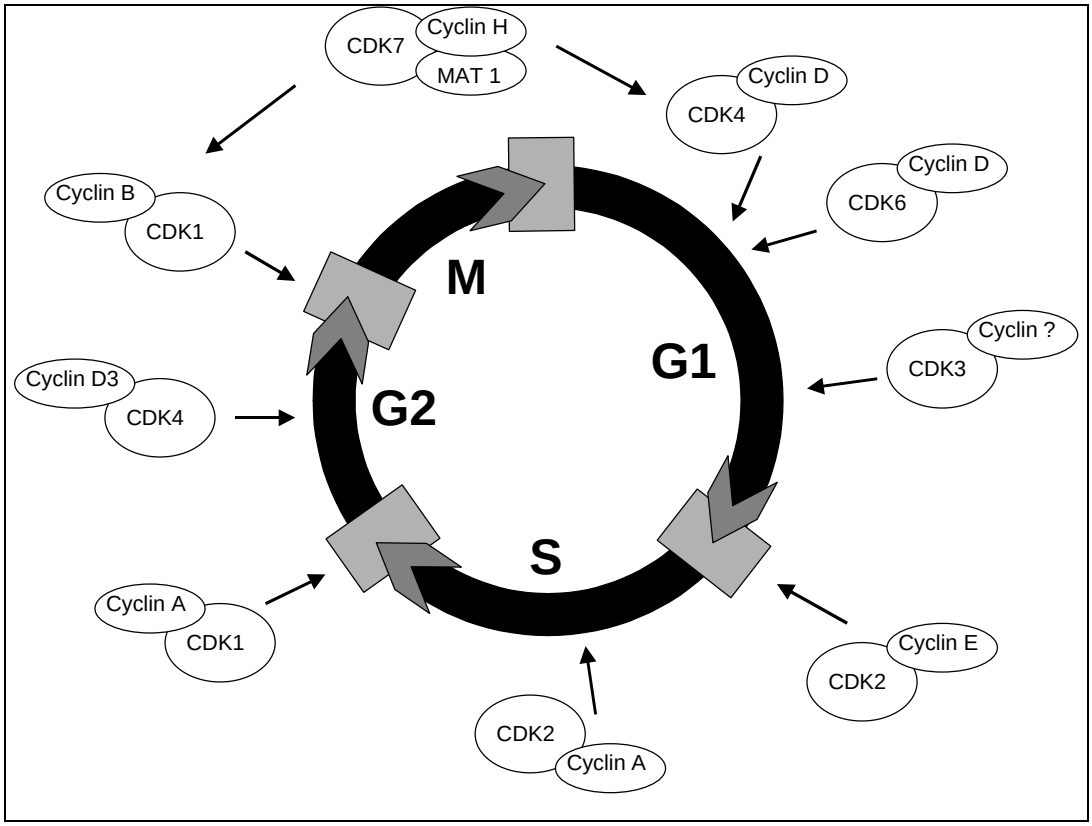

This figure was adapted from an illustration by Zhai.[4]

The abbreviation "G" stands for "gap", "S" for "synthesis", and "M" for "mitosis". "MAT1" represents "ménage à trois 1", an assembly factor and targeting unit of the cyclin activating kinase (CAK).

There are a number of different possibilities of regulating the CDK activity which results in a distinct flexibility concerning the control of cell cycle progression.[7,8,13] As mentioned before, CDKs are only able to catalyze phosphotransfer reactions when associated with a proper cyclin. In contrast to the catalytic subunits, the cyclin concentration oscillates in cells traversing the cycle, and thus cyclins serve as regulators. The variations in concentration are navigated by gene transcription, that is, synthesis and degradation processes of the cyclins. Another route of controlling CDK activity lies within post-translational modifications performed by kinases and phosphatases. Depending on the site of action, phosphorylation can give rise to both activation and deactivation of the holoenzyme; dephosphorylation has the opposite effects, respectively.[14] For example, phosphorylation of Thr160 (executed by CDK7/cyclin H) activates the CDK2/cyclin A-complex while phosphorylation of Thr14 (carried out by Myt1-kinase) deactivates it. Deactivation can also be caused by interaction with natural inhibitors: the fairly small proteins (e.g., p15 or p21) unfold their inhibitory potency by causing conformational alterations within the holoenzyme and/or by blocking the active sites, and thus thwart substrate interaction.

A great number of cellular proteins are designated substrates of cyclin-dependent kinases. Tumor suppressor proteins (e.g., retinoblastoma protein and p53), transcription factors (E2F, for example), replication factors (like replication protein A) and organizational factors (e.g., histones or lamins) constitute representative categories within this large variety.[13] The identification of further CDK substrates is a perpetual process.

1.3 Cyclin-Dependent Kinase Inhibitors

As mentioned in the previous subchapter, the catalytic activity of cyclin-dependent kinases is partially regulated by small inhibitory proteins. These natural inhibitors are categorized into two families: the INK4- and the CIP-family.[8,15]

Proteins of the INK4-family inhibit CDK4 and CDK6 and thus affect the G1 phase of the cell division cycle. They act by binding to the unmodified CDK-subunits, being competitive to the proper cyclins. Another possibility comprises the interaction with CDK in a different location than the cyclin binding site, resulting in the provocation of conformational changes within the binding site, and thus averting the formation of the CDK/cyclin-complex. In both cases, catalytic activation is impeded. Members of this family are, for example, p15, p16, p18, and p19.

CDK2-interacting proteins (CIP) display a wider range of inhibitory activity. They have impact on the G1 phase as well as the G1/S phase transition by interacting with CDK2/cyclin-complexes. The interaction occurs by clasping the holoenzyme which entails the change of conformation of the catalytic cleft as well as the partial occupation of the ATP binding site, hence impeding enzymatic activity. Exemplary members of the CIP-family are p21, p27, and p57.

Concerning proliferative diseases, lack or malfunction of these natural inhibitory proteins is very frequently at hand. Therefore, the creation of small synthetic inhibitory molecules became a salient aim in medicinal chemistry research. The specific targeting of cyclin-dependent kinases represents a challenging venture due to the fact that an immensely large number of protein kinases exists in the human body that all utilize ATP as a phosphate donor and thus show great similarities with respect to the structure of the ATP binding site.[13,16] Nonetheless, the ATP binding pocket represents the dedicated site of action because small molecules, their size being obligatorily limited in order to enable cell transport, can usually not unfold their activity and foil substrate interaction by other means like, for instance, the establishment of large protein-protein contact surfaces. As a matter of fact, most synthetic CDK inhibitors indeed evolve their potency through binding in the deep grove normally occupied by ATP.[17] With ATP serving as the chemical lead structure,

thought has to be given to the circumstance that there is a considerable risk of provoking undesired effects because of the enclosed adenine ring representing a popular structure in the whole human metabolism. Consequentially, research is focused on the synthesis of inhibitors that interact with the target enzyme in the surroundings of the catalytic cleft as well as the ATP binding pocket itself in order to attain selectivity for a specific enzyme. Actually, residues typical of CDK can be found in the direct neighborhood of the ATP binding site, thus enabling specific CDK interactions without simultaneously addressing a broad spectrum of other kinases.[18]

Hitherto, various structures representing ATP-competitive inhibitors have been discovered:

Indolinones

The indolinone group comprises indirubins like indirubin 5-sulfonic acid **3**, inhibiting CDK1, CDK2, and CDK4, as well as the oxindole-based inhibitors of CDK2 like compound **4**. The latter causes cell cycle arrest and reduces the sensitivity of the epithelium against cytotoxic agents, hence demonstrating potential utility in the prevention of chemotherapy-induced alopecia. Topical application provides regional delivery, and therefore no antagonism of the antitumor efficacy of the applied therapeutic drugs is observed.[19,20]

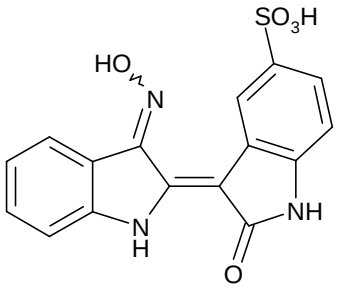

3

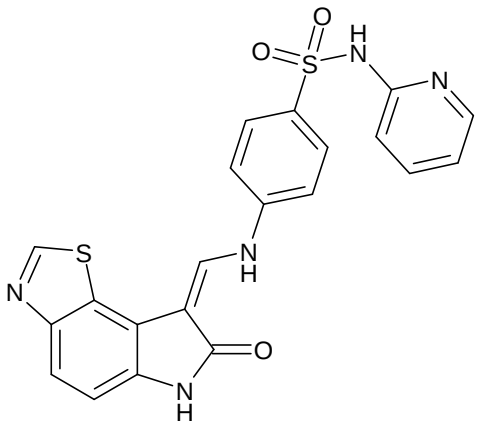

4

Flavopiridol

Flavopiridol (**5**) is a synthetic flavonoid developed from rohitukine (**6**), an alkaloid extracted from the Indian plant *Dysoxylum binectariferum*, and is a potent inhibitor of CDK1, CDK2, and CDK4. Its anti-proliferative activity is unfolded through a variety of mechanisms besides CDK inhibition, for instance, through apoptosis, DNA interaction, and cyclin D1 decrease.[4] Currently, flavopiridol is undergoing clinical trials phase I and phase II.[17]

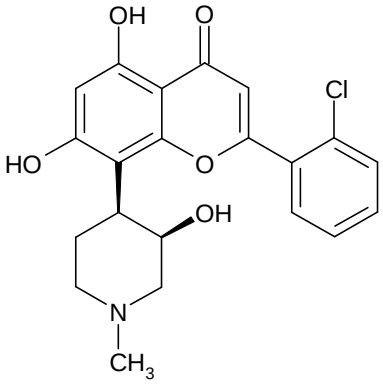

5

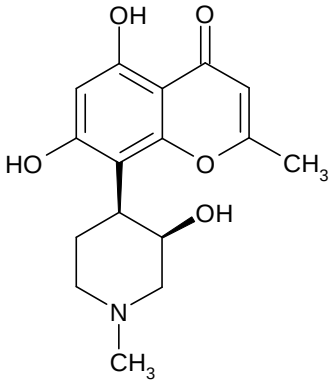

6

Benzylidene-benzofuranones

Designed as flavopiridol mimics, 2-benzylidene-benzofuran-3-ones show significant inhibition of CDK1, CDK2, and CDK4.[21] The derivative 2-benzylidene-4,6-dihydroxy-7-(1-methyl-piperidin-4-yl)-benzofuran-3-one (**7**) displays an improved inhibitory activity towards CDK1 and CDK2, and thus shows selectivity against CDK4.

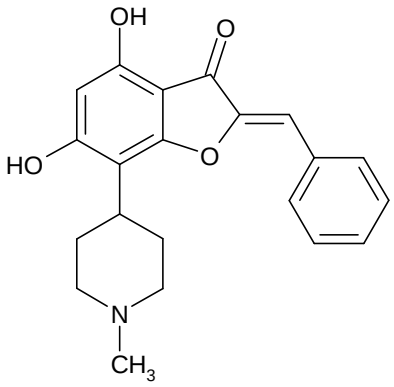

7

Pyridopyrimidones

Pyrido[2,3-*d*]pyrimidin-7-ones are CDK4 inhibitors, displaying only a modest selectivity for CDK4 versus other kinases (CDK1, CDK2). Selectivity turned out to be a function of the choice of N8- and C2-substituents.[22] Depicted exemplary structures **8** and **9** are compounds with optimized potency against CDK4.

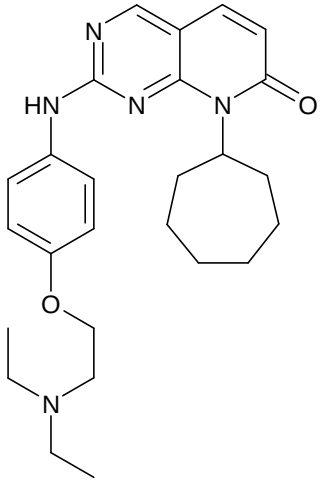

8

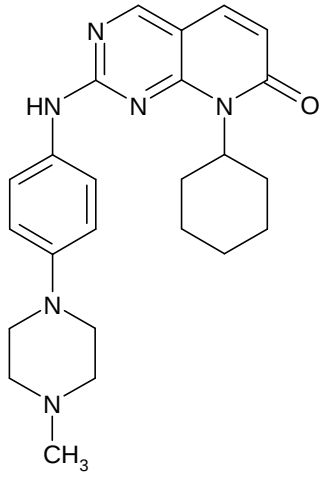

9

Indenopyrazolones

A novelty in the field of cyclin-dependent kinase inhibitors are indeno[1,2-*c*]pyrazol-4-ones, inhibitors of CDK2 and CDK4. Semicarbazide-based derivatives like **10** show high potency while maintaining selectivity against other serine/threonine kinases.[23,24]

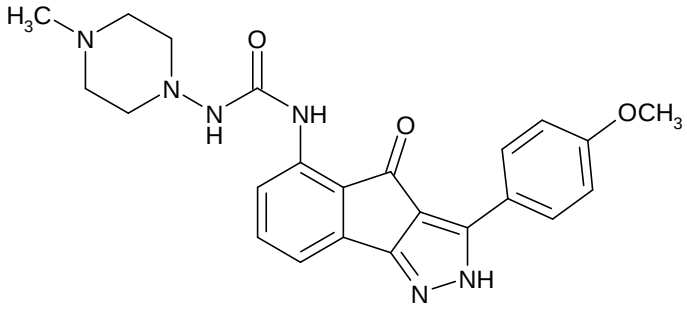

10

Aminothiazoles

Very recently, aminothiazoles were discovered as a novel class of CDK2 inhibitors.[25] Developed from the acetic ester derivative **11**, which became unstable in plasma and inactive in cells because of metabolic hydrolysis, the oxazole-containing derivative **12** is metabolically stable against esterases and exhibits potent CDK2-inhibitory activity while displaying a 10 to 100-fold selectivity over CDK1 and CDK4 as well as other kinases. Cell population in S phase is reduced, and a significant level of apoptosis is induced.

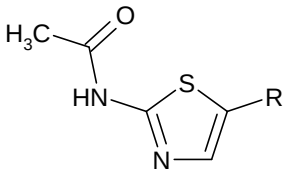

11 R = 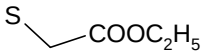

12 R = 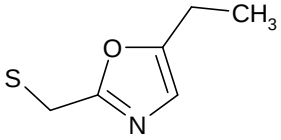

Paullones

The CDK-inhibitory activity of paullones, which are fused benzazepin-2-ones, was discovered in the late nineties.[6] The best known representative of this novel inhibitor class, alsterpaullone (**2**), shows high potency concerning CDK1, CDK2, CDK5, and GSK-3β inhibition and demonstrates distinct anti-proliferative qualities.[5,6] Alsterpaullone (**2**) was chosen for preclinical development at the NCI.[17]

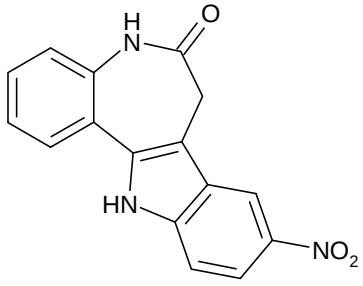

2

Butyrolacton I

Butyrolacton I (**13**), a natural product isolated from an Aspergillus species, displays inhibitory activity against CDK1, CDK2, and CDK5.[12] In consequence, cell proliferation is blocked, and cell cycle progression is perturbed at the G1/S and G2/M phase transitions.[13]

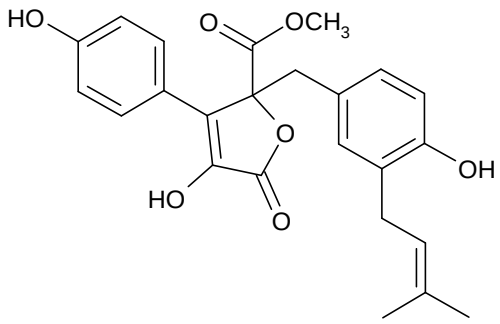

13

Suramin

Suramin (**14**) represents a non-selective CDK inhibitor. For many years, it has been prescribed for parasitic diseases like sleeping sickness, for instance. As other enzymes, for example, topoisomerase II and reverse transcriptases, are also reported to be inhibited by suramin (**14**), its efficacy cannot be solely attributed to the inhibition of CDK function.

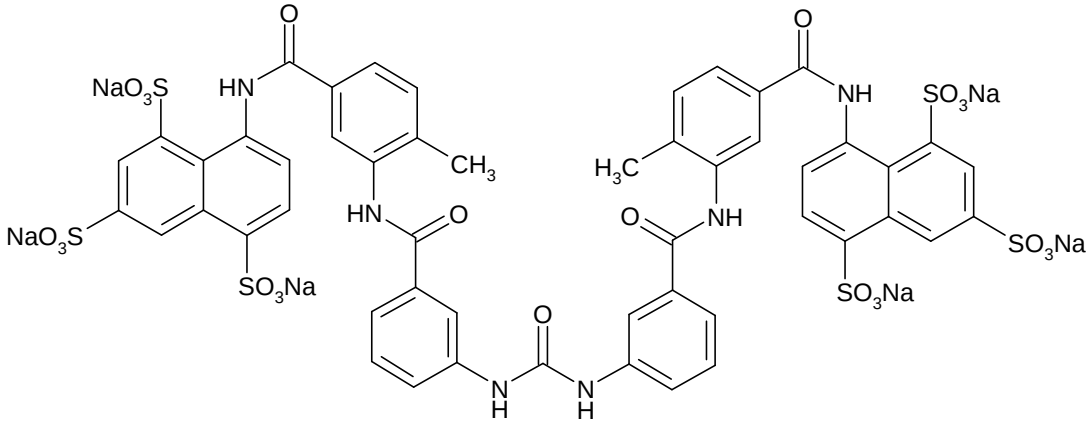

14

Staurosporine

Staurosporine (**15**) and its 7-hydroxy-derivative UCN-01 (**16**) are both natural products originating from *Streptomyces staurosporeus*. The indolocarbazoles are potent but non-selective CDK inhibitors. They also show activity against other kinases, especially against members of the protein kinase C (PKC) family. Hence, the observed restraint of tumor cell proliferation cannot necessarily be ascribed to CDK inhibition.[12,13,17]

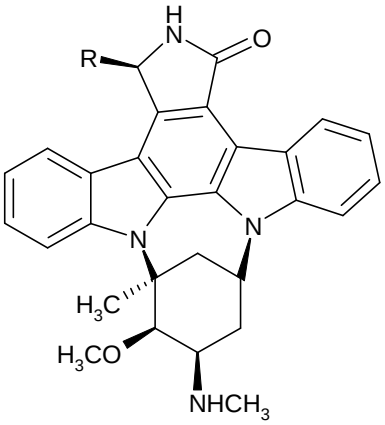

15 R = H

16 R = OH

9-Hydroxyellipticin

Derived from the alkaloid ellipticin, 9-hydroxyellipticine (**17**) is a fairly non-selective CDK inhibitor. Inhibitory activity has also been described against topoisomerase II and reverse transcriptases.[13]

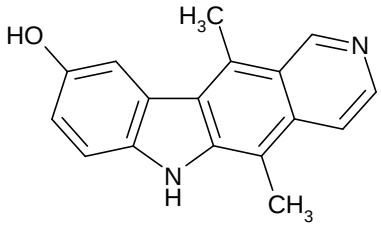

17

Purine derivatives

The C2, N6, N9-trisubstituted purines represent bicyclic ATP-competitive inhibitors. Olomoucine (**18**) and roscovitine (**19**) were the first purine inhibitors to be diligently analyzed, followed by purvalanol A (**20**) and purvalanol B (**21**).[17] Very recently, a promising new derivative has been synthesized, olomoucine II (**22**), displaying the tenfold CDK1-inhibitory activity of roscovitine (**19**) and exceeding the in vitro cytotoxic activity of purvanalol A (**20**), the most potent CDK inhibitor.[26]

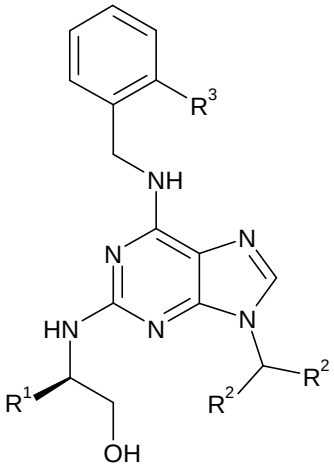

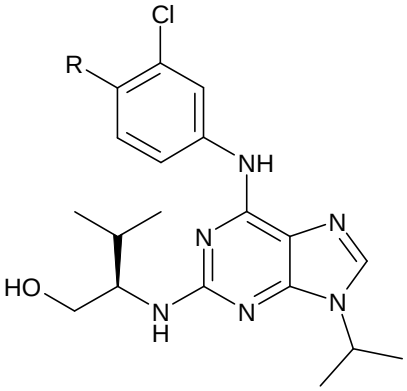

18 R^1, R^2, R^3 = H

19 $R^1 = C_2H_5$, $R^2 = CH_3$, R^3 = H

22 $R^1 = C_2H_5$, $R^2 = CH_3$, R^3 = OH

20 R = H

21 R = COOH

Overview

Concluding the introduction to cyclin-dependent kinase inhibitors, the following table (table 1-2) provides an overview of the inhibitory activity of the presented structures.

Table 1-2: Inhibitory activity [μM] of the introduced CDK inhibitors

CDK inhibitor		CDK1/ cyc B	CDK2/ cyc A	CDK2/ cyc E	CDK4/ cyc D	CDK5/ p35
olomoucine[12]	**18**	7.0	7.0	7.0		3.0
olomoucine II[26]	**22**	0.020				
roscovitin[12]	**19**	0.650	0.700	0.700		0.160
purvalanol A[12]	**20**	0.004	0.070	0.035	0.850	0.075
purvalanol B[12]	**21**	0.006	0.006	0.009	>10.0	0.006
flavopiridol[21]	**5**	0.100	0.220		0.400	
benzylidene-benzofuranone[21]	**7**	0.110	1.3		4.4	
indolinone/indirubin[17]	**3**	0.055		0.150	0.300	
indolinone/oxindole[19]	**4**	0.110		0.010	0.130	
pyridopyrimidone[22]	**8**				0.004	
pyridopyrimidone[22]	**9**				0.004	
aminothiazole[25]	**12**	0.300		0.020	2.3	
indenopyrazole[23]	**10**			0.012	0.009	
butyrolactone I[12]	**13**	0.680	1.5		1000	1.5
staurosporine[17]	**15**	0.006				
UCN-01[17]	**16**	0.100				
9-hydroxyellipticin[12]	**17**	1.0				
suramin[12]	**14**	4.0				
alsterpaullone[12]	**2**	0.035	0.015	0.200		0.040

The values listed represent the IC_{50}-values [μM] determined for the isolated enzymes, respectively.

The references are indicated separately for each presented CDK inhibitor.

It is important to be aware of the fact that measurements of IC_{50}-values may vary depending on the ATP concentration applied in the particular assays.

Void spaces symbolize the nonavailability of data.

1.4 Potential Applications of Cyclin-Dependent Kinase Inhibitors

Initially, research focused on CDK inhibitors because of their antitumor potential.[27-29] In cancer cells, the cell cycle machinery no longer works in a coordinated manner, resulting in aberrant cell proliferation. As cyclin-dependent kinases trigger and coordinate the phase transitions in the cell division cycle, the inhibition of abnormally active CDKs was expected to stop malignant growth, and thus enable the recovery of homeostasis concerning cell proliferation.[12] Indeed, cyclin-dependent kinase inhibitors show inspiring properties with regard to the treatment of cancer: they display a profound antimitotic activity, for some compounds with a preferential effect on transformed versus normal cells[30], induce apoptosis in dividing cells, or facilitate antitumor drug-enhanced apoptosis. CDK inhibitors unfold effects independent of tumor suppressor proteins like p53 and pRb, and they have proven antitumoral qualities in animal models.[27]

By now, other putative applications of CDK inhibitors are also being evaluated since there are several diseases deriving from unbalanced but non-tumoral proliferation of certain cells:[27-29]

Pathologies in the cardiovascular area like atherosclerosis, restenosis, and tumor angiogenesis are linked to a deficient proliferation process of vascular cells. Cyclin-dependent kinase inhibitors may contribute to regaining proper control of the process.

Antiviral properties are based on the fact that many viruses require active CDKs for replication which is then restrained by CDK inhibitors. Promising experiments have been performed with human cytomegalovirus[31], herpes virus[32], and varicella zoster virus[33].

Of very high interest are potential applications in the field of neurodegenerative disorders. Protection of neuronal cells from apoptosis, the underlying mechanisms still being unclear though, has been observed in recent past.[34] With respect to Alzheimer's disease, the CDK5/p35-complex plays a key role in the abnormal hyperphosphorylation of the microtubule-associated proteins tau[35,36] and MAP-1B[37]. This hyperphosphorylation causes the appearance of the paired helical filaments (PHF) that are typical of Alzheimer's disease. Moreover, the holoenzyme CDK1/cyclin B is abnormally expressed in Alzheimer brain

tissue.[38] Therefore, CDK inhibitors represent imaginable pharmacological agents for the modulation of neurodegeneration.

Captivating ongoing investigations deal with the use of cyclin-dependent kinase inhibitors and their analogs against parasitic protozoa. Multiplication and development of these eukaryotic organisms are believed to depend on the activity of CDK-related kinases (CRKs).[29,39] Members of the CRK enzyme family have been cloned from several species of parasitic protozoa, for example *Plasmodium falciparum*[40], *Trypanosoma cruzi*[41], *Leishmania mexicana*[42], *Toxoplasma gondii*[43], and microsporidia. These proteins show distinct homology with the CDKs found in vertebrates (40-60 % identical) and thus allow their classification as CDK-related kinases. Yet the divergence from human cyclin-dependent kinases is significant, and therefore a potentially important therapeutic window is opened. Possibly, structural differences between parasite and host CDKs result in divergent affinities towards inhibitory compounds, and some inhibitors may turn out to be effective against the parasite CDKs but less so against the human counterparts.[28,29] Furthermore, the ATP binding pocket serves as a target that does not allow many variations, thus resistance is more unlikely to emerge compared to more variable targets.

Other current investigations center potential applications in dermatology (psoriasis) and nephrology (glomerulonephritis).[28]

1.5 Aim of Thesis

The aim of this thesis was the synthesis of further paullones with electron-withdrawing substituents at the 9-position (figure 1-3). The electronic properties of the residues at that position are known to be a critical factor concerning the biological activity of the compounds.[6] Hence, it was striven for the discovery of more potent CDK inhibitors than hitherto synthesized as well as the improvement of physical properties like solubility of the compounds in order to facilitate biological testing.

Figure 1-3: Basic paullone structure

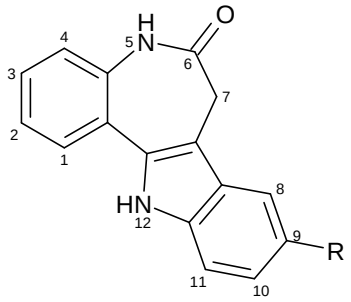

Furthermore, it was planned to perform quantitative structure-activity relationship (QSAR) studies, utilizing the biological data of all suitable paullone compounds produced, including the new derivatives. Emphasis was to be put on the execution of a multiple regression analysis in order to have the ability to survey the influence of steric and lipophilic as well as electronic properties of the substituents at the 9-position on the biological activities of the substances.

2 Syntheses

2.1 Educts and Standard Paullone Synthesis

This thesis focuses on paullone derivatives that are substituted at the 9-position which is known to have a major impact on the biological activity of the molecules.[6] There is a standard procedure for the synthesis of the basic paullone ring structure consisting of a four-step reaction sequence developed by Kunick[44], Link[45], and Schultz[46]:

First, the anthranilic acid ethyl esters **23a** and **23b** were reacted with ethyl succinyl chloride (**24**) to yield the amides **25a** and **25b** (scheme 2-1) which then performed a Dieckmann condensation catalyzed by potassium hydride and thus furnished the benzazepine derivatives **26a** and **26b** (scheme 2-2).

Scheme 2-1:

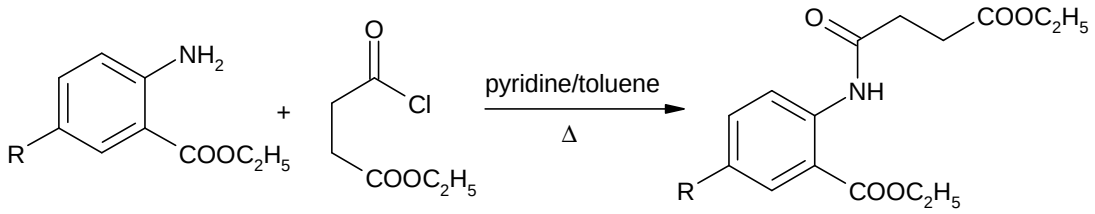

23a R = H **24** **25a** R = H

23b R = OCH_3 **25b** R = OCH_3

Scheme 2-2:

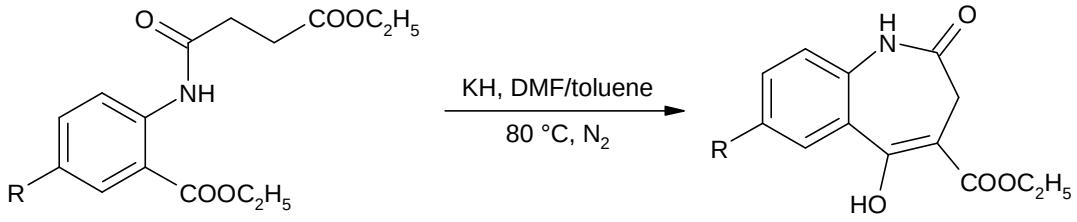

25a R = H **26a** R = H

25b R = OCH_3 **26b** R = OCH_3

Heating **26a** and **26b** in wet DMSO provoked a dealkoxycarbonylation resulting in the synthesis of 3,4-dihydro-1*H*-[1]-benzazepine-2,5-diones **27a** and **27b**, respectively (scheme 2-3).

Scheme 2-3:

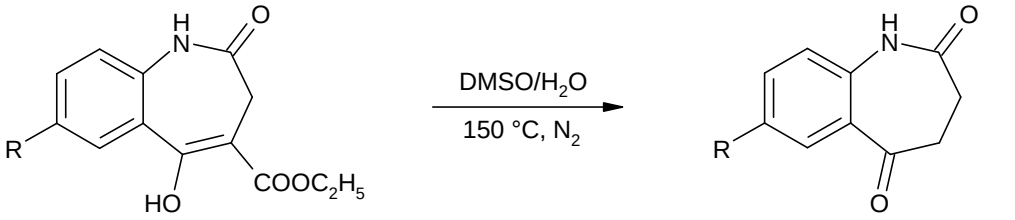

26a R = H **27a** R = H

26b R = OCH_3 **27b** R = OCH_3

Finally, the paullone products **28a** and **28b** were obtained by performing a Fischer indole synthesis with a phenylhydrazine derivative **29** (scheme 2-4).

Scheme 2-4:

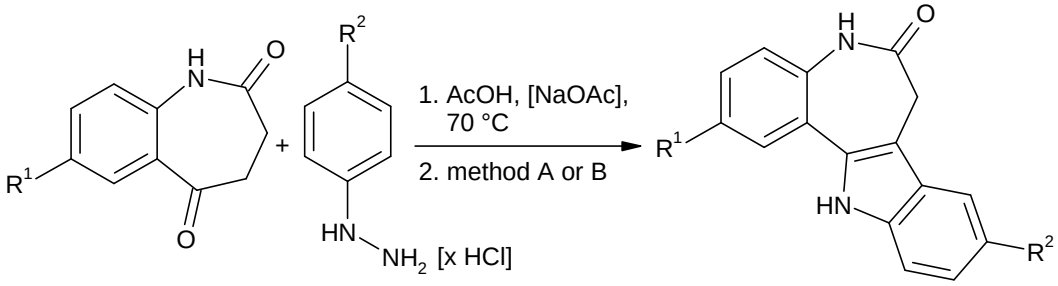

27a R^1 = H **29** **28a** R^1 = H

27b R^1 = OCH_3 **28b** R^1 =OCH_3

The last step involved the formation of the phenylhydrazones **30a** and **30b** as intermediate products which usually cyclized instantaneously upon addition of concentrated sulfuric acid to the reaction mixture (method A). However, low electron density within the aromatic ring system, for example, caused by electron-withdrawing substituents, may aggravate an acid-catalyzed Fischer synthesis or even completely impede it.[47] In these cases, a thermally induced Fischer indole synthesis (method B) represented an alternative route to paullones **28a** and **28b** (scheme 2-5).

Scheme 2-5:

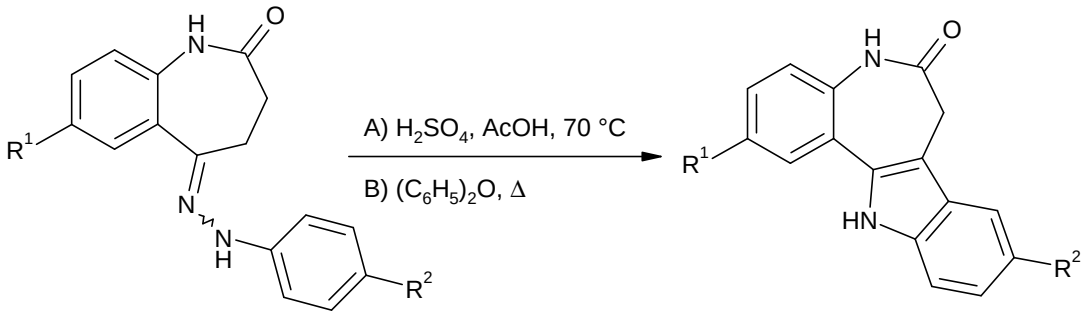

30a $R^1 = H$ **28a** $R^1 = H$

30b $R^1 = OCH_3$ **28b** $R^1 = OCH_3$

As further variations of the paullone structure at other positions than the 9-position were of secondary interest, the standard cyclic ketone utilized for the paullone syntheses was the unsubstituted 3,4-dihydro-1*H*-[1]-benzazepine-2,5-dione (**27a**). Its preparation is depicted in the beginning of this chapter (schemes 2-1 to 2-3).

The synthesis of the cyclic ketone **27b** was performed using 5-methoxy-anthranilic acid ethyl ester (**23b**) instead of ethyl 2-aminobenzoate (**23a**), also following the synthetic sequence outlined in schemes 2-1 to 2-3.

The component **23b** was obtained by a two-step synthesis (scheme 2-6): first, 5-methoxy-2-nitrobenzoic acid (**31**) was reduced with tin(II) chloride, following a procedure stated by Smith.[48] The proximate esterification was achieved adding gaseous hydrogen chloride to the previously obtained 5-methoxy-anthranilic acid (**32**) dissolved in ethanol**,** as described by Schultz[46], yielding the desired 5-methoxy-anthranilic acid ethyl ester (**23b**).

Scheme 2-6:

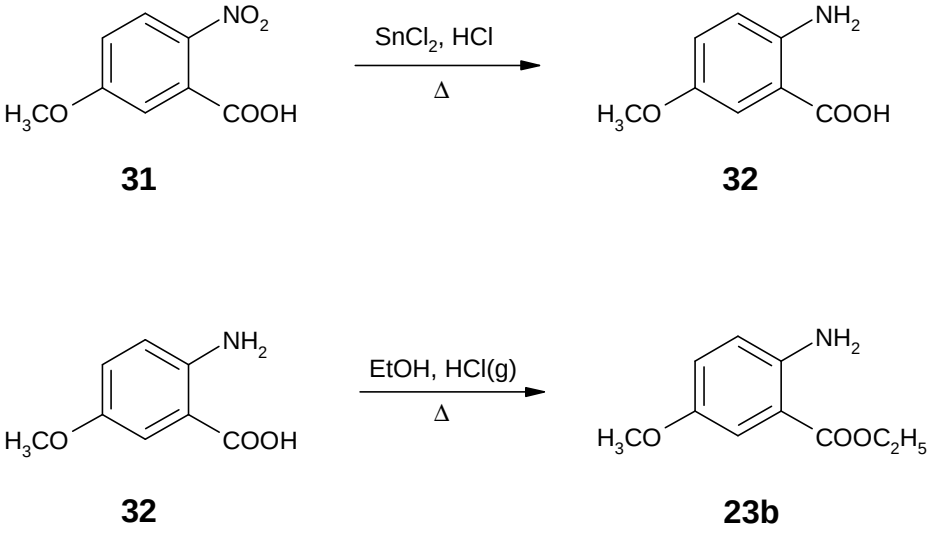

The other reagents needed for the synthesis of 9-substituted paullones, *para*-substituted phenylhydrazines **29**, were either commercially purchased or produced by performing diazotization and reduction reactions.

The aromatic amines **33a** and **33b** formed diazonium ions **34a** and **34b** by reacting with the electrophilic nitrosonium ions generated from nitrous acid in acidic solution. The subsequent reduction was carried out with tin(II) chloride dissolved in hydrochloric acid and yielded the hydrazine derivatives **29a** and **29b** (scheme 2-7). Methods issued by Hodgson[49] and Enders[50] served as references for the synthesis of [4-(methylthio)phenyl]hydrazine (**29a**), and a method by Soliman[51] was referred to for the synthesis of 4-hydrazinobenzenesulfonamide (**29b**).

Scheme 2-7:

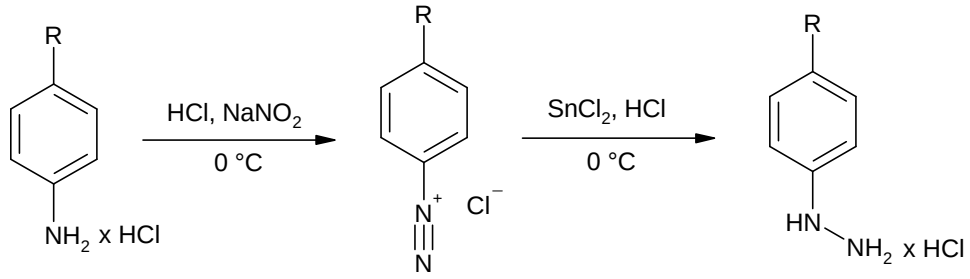

33a R = SCH_3 **34a** R = SCH_3 **29a** R = SCH_3

33b R = SO_2NH_2 **34b** R = SO_2NH_2 **29b** R = SO_2NH_2

In two cases, the acid-catalyzed Fischer indole synthesis was not applied for the production of the proper paullones. Instead, the corresponding phenylhydrazone derivatives **30c** and **30d** were synthesized and isolated, thereupon serving as reagents for the alternative route, the thermally induced Fischer indole synthesis (cf. scheme 2-5, method B).

The synthesis of the phenylhydrazones **30c** and **30d** was performed by heating 3,4-dihydro-1*H*-[1]benzazepine-2,5-dione (**27a**) with 4-hydrazinobenzenesulfonamide (**29b**) or 4-hydrazinobenzoic acid (**29c**) in glacial acetic acid as reported by Schultz[46] (scheme 2-8).

Scheme 2-8:

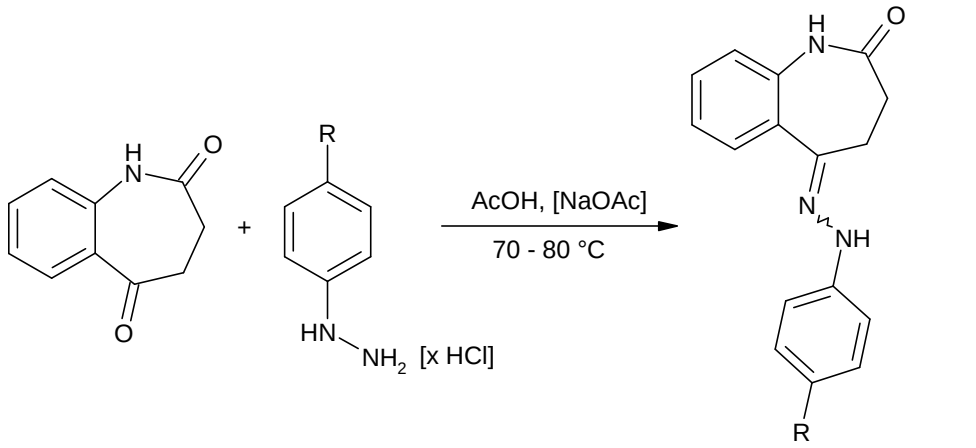

27a **29b** R = SO_2NH_2 **30c** R = SO_2NH_2

29c R = COOH **30d** R = COOH

2.2 Synthesis of 9-Substituted Paullones

Synthetic efforts targeted the preparation of paullones with different substituents at the 9-position, putting special emphasis on sulfur and carbonyl residues. Furthermore, various experiments have been performed in order to achieve the introduction of a tetrazolyl substituent.

2.2.1 Synthesis of Paullones with Sulfur Substituents at the 9-Position

Paullones substituted with sulfur derivatives at the 9-position were considered to be very interesting compounds as residues like sulfonyl or sulfamoyl are fairly similar to a nitro group concerning electronegativity and steric dimensions. Keeping in mind that 9-nitro-paullone, alsterpaullone (**2**), showed outstanding CDK-inhibitory activity and antiproliferative potency, the attempt to create novel paullones with comparable or even better biological qualities seemed very promising. Moreover, it was hoped to improve the solubility of the substances.

The 9-(methylthio)-paullones **35a** and **35b** and 2-methoxy-6-oxo-5,6,7,12-tetrahydroindolo[3,2-*d*][1]benzazepine-9-sulfonamide (**35c**) were synthesized, following the standard procedure by Kunick[52], by heating the cyclic ketones **27a** and **27b** with [4-(methylthio)phenyl]hydrazine (**29a**) or 4-hydrazinobenzenesulfonamide (**29b**), respectively, and sodium acetate in glacial acetic acid. As a final step, concentrated sulfuric acid was added which catalyzed the Fischer indole synthesis (scheme 2-9).

Scheme 2-9:

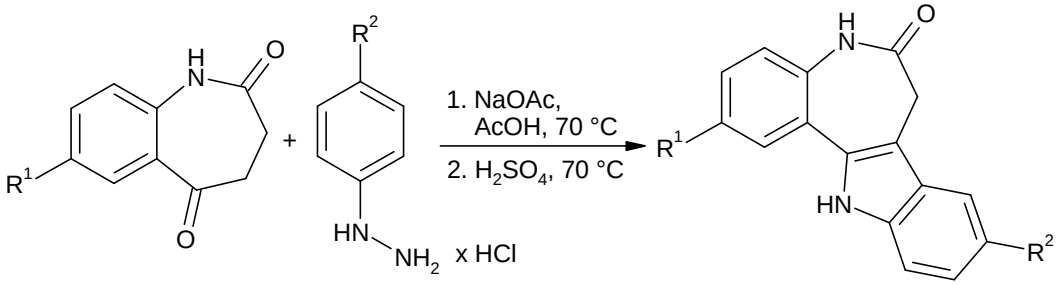

27a $R^1 = H$ **29a** $R^2 = SCH_3$ **35a** $R^1 = H$, $R^2 = SCH_3$

27b $R^1 = OCH_3$ **29b** $R^2 = SO_2NH_2$ **35b** $R^1 = OCH_3$, $R^2 = SCH_3$

35c $R^1 = OCH_3$, $R^2 = SO_2NH_2$

The careful choice of proper reagents paved the way for the well directed synthesis of the differently oxidized derivatives of the previously obtained thio ethers **35a** and **35b**. Usage of *meta*-chloroperbenzoic acid (*m*-CPBA) at temperatures below 0 °C, as stated by Potts[53], led to the 9-(methylsulfinyl)-paullones **36a** and **36b**. The employment of hydrogen peroxide and heating to 60-80 °C resulted in the 9-(methylsulfonyl)-paullones **37a** and **37b**, taking methods by Page[54], Bordwell[55], and Ternay[56] as references (scheme 2-10).

Scheme 2-10:

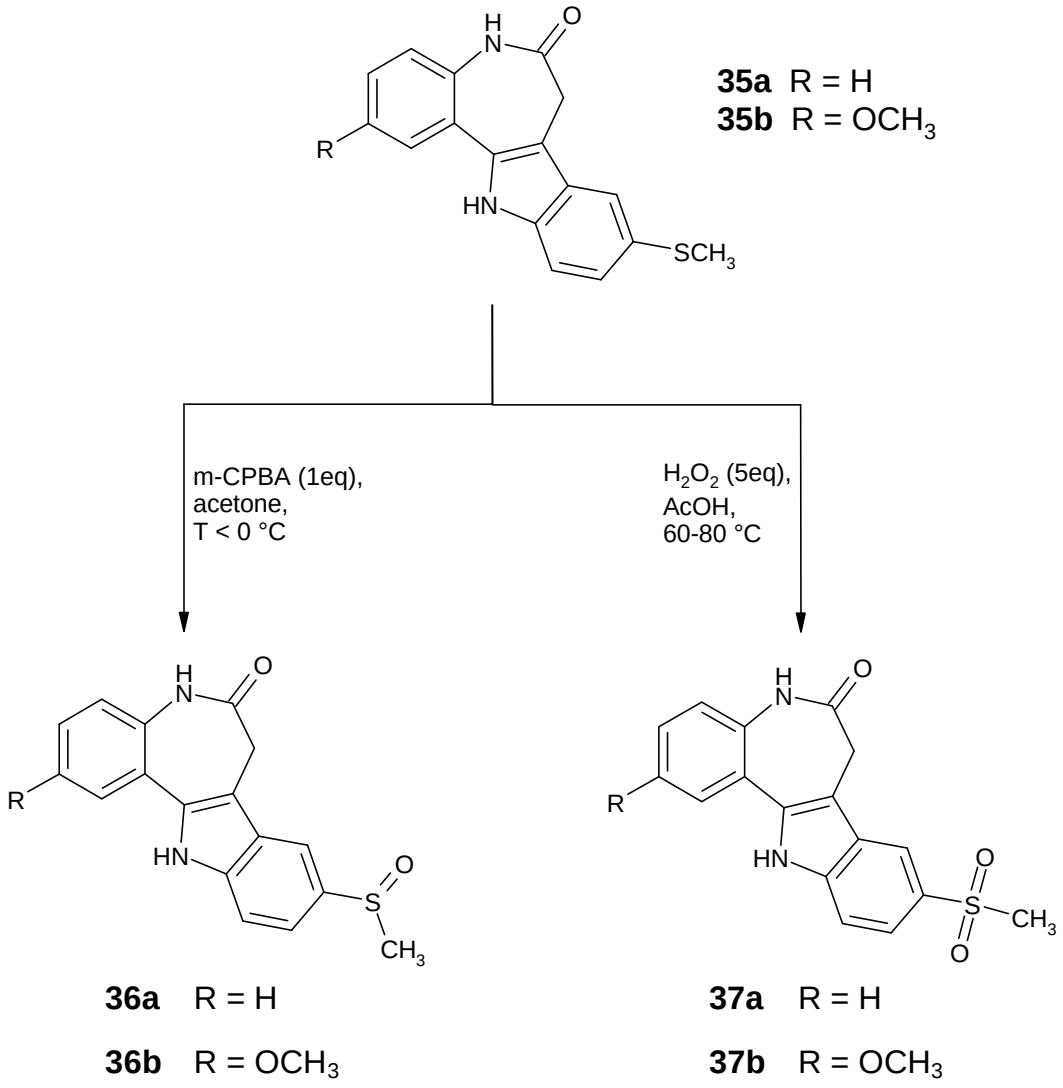

The sulfoxide derivatives **36a** and **36b** feature a very interesting analytical phenomenon with respect to their ^{1}H-NMR spectra: due to the fact that sulfoxides represent stereocenters, the protons of the CH_2-group of the azepinone ring become diastereotopic.

By definition[57,58], two atoms or groups of a molecule are called diastereotopic if they are constitutionally equivalent but surrounded by non-identical substituents of which one embodies a chiral center. Diastereotopic atoms or groups cannot be exchanged by any symmetry operations. Replacement of one or two diastereotopic atoms or groups results in the formation of one pair of diastereomers. Diastereotopicity can frequently be detected by ^{1}H-NMR as the diastereotopic atoms or groups are chemically nonequivalent and have different electronic environments. Hence, diastereotopic protons will generate ^{1}H-NMR signals at different chemical shifts.

Consequentially, the ^{1}H-NMR spectra of the methylsulfinyl-paullones **36a** and **36b** depicted separate signals for each proton of the azepinone CH_2-group (figure 2-1).

Figure 2-1: ^{1}H-NMR spectrum of sulfoxide derivative **36a**

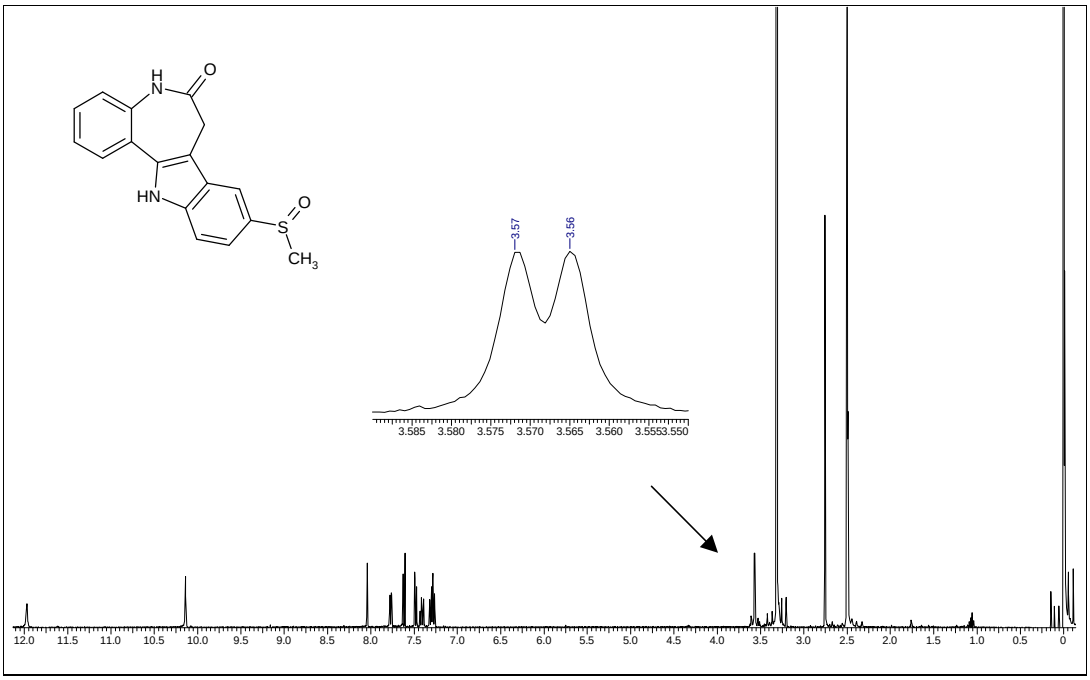

In comparison, the CH_2-group protons of other paullone molecules, like the sulfone derivative **37a**, for example, generated only one signal (with doubled intensity). There is no present stereocenter and the paullone azepinone ring is flexible in its conformation, thus performing ring inversion at a high pace. This fast innermolecular motion causes the considered protons to become chemically and magnetically equivalent, resulting in the generation of one single signal (figure 2-2).

Figure 2-2: ^{1}H-NMR spectrum of sulfone derivative **37a**

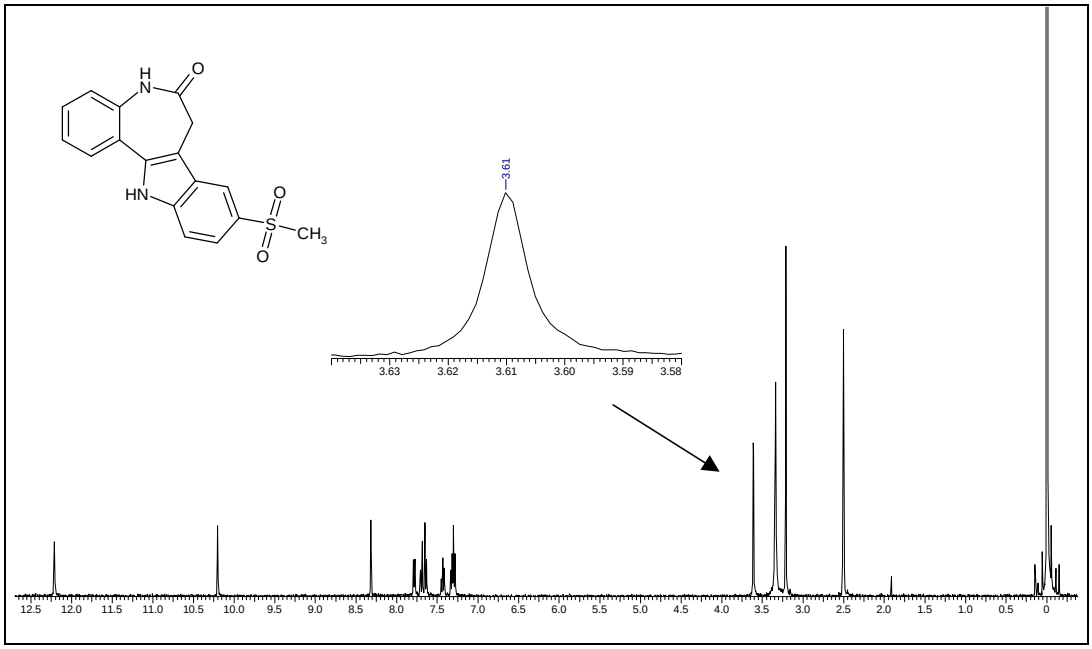

One derivative of the sulfur-substituted paullones, the sulfonamide **38**, had to be obtained by utilizing the thermally induced Fischer indole synthesis developed by Schultz[46], the alternative path described in the introductory part of this chapter (cf. schemes 2-8 and 2-5). Acid-catalyzed Fischer synthesis did not lead to the desired product **38**, hence, the hydrazone derivative **30c** was first produced and isolated. Heating **30c** in diphenyl ether under reflux supplied paullone-9-sulfonamide (**38**) (scheme 2-11).

Scheme 2-11:

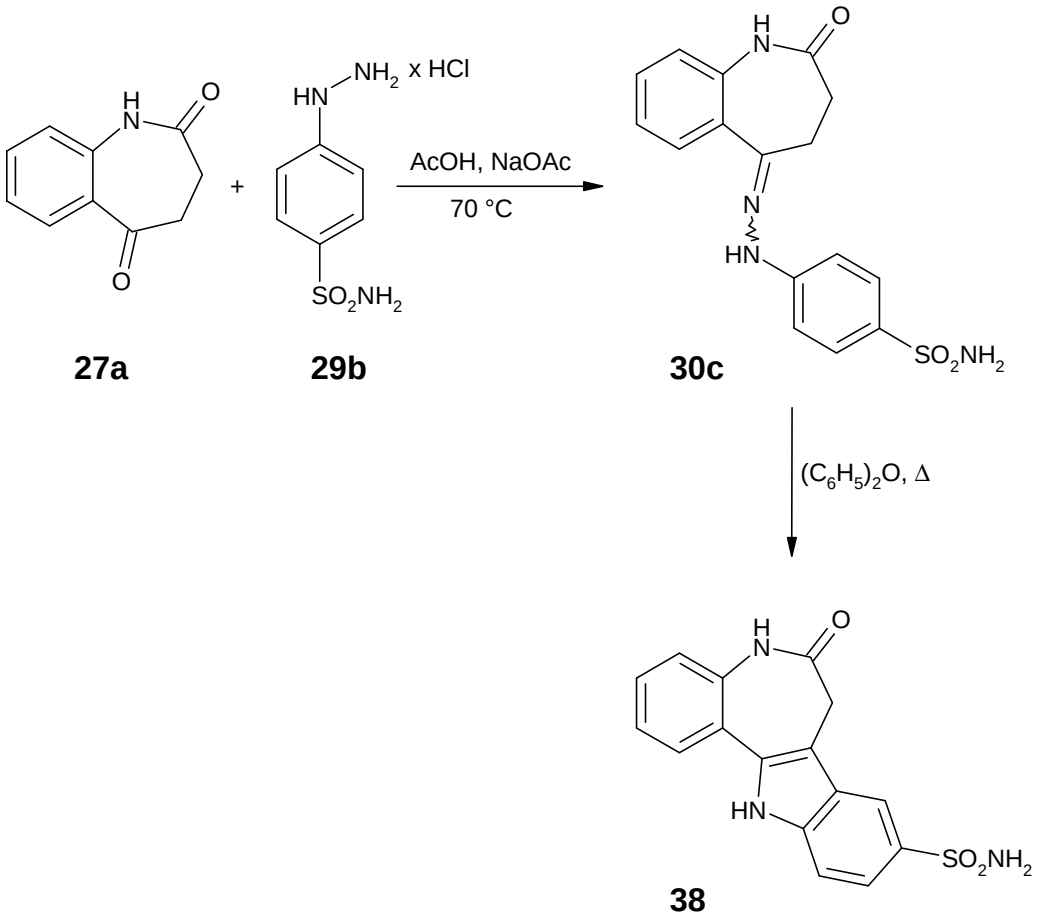

27a **29b** **30c** **38**

2.2.2 Synthesis of Paullones with Carbonyl Substituents at the 9-Position

All carbonyl substituents possess electron-withdrawing properties, and thus represent suitable residues for the synthesis of novel paullone derivatives with interesting substituent characteristics at the 9-position. The creation of a group of homologous substances holds the possibility of investigating the advisable substituent properties at that position concerning steric dimensions and lipophilicity, for instance, by systematically varying bulkiness or chain length of the introduced residues. Esters and amides embody eligible substance classes for the performance of these investigations.

2.2.2.1 Synthesis of Paullone-9-carboxylic Acid

Paullone-9-carboxylic acid (**39**) represented a suitable educt for the synthesis of ester and amide derivatives. Due to the fact that rather large amounts of carboxylic acid **39** would be needed, the careful evaluation of synthesis routes was recommendable.

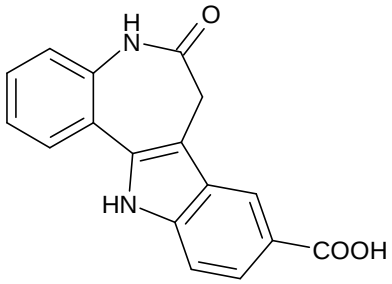

39

Acid-catalyzed[52] and thermally induced[46] Fischer indole synthesis both yielded paullone-9-carboxylic acid (**39**). The acid-catalyzed synthesis at regular reaction temperatures (70-80 °C) only supplied low yields which triggered experiments employing the thermally induced indole synthesis. Yields could be raised but were still not completely satisfactory. Finally, returning to the acid-catalyzed synthesis, the increase of reaction temperature to 90 °C supplied the desired high yields (scheme 2-12).

Scheme 2-12:

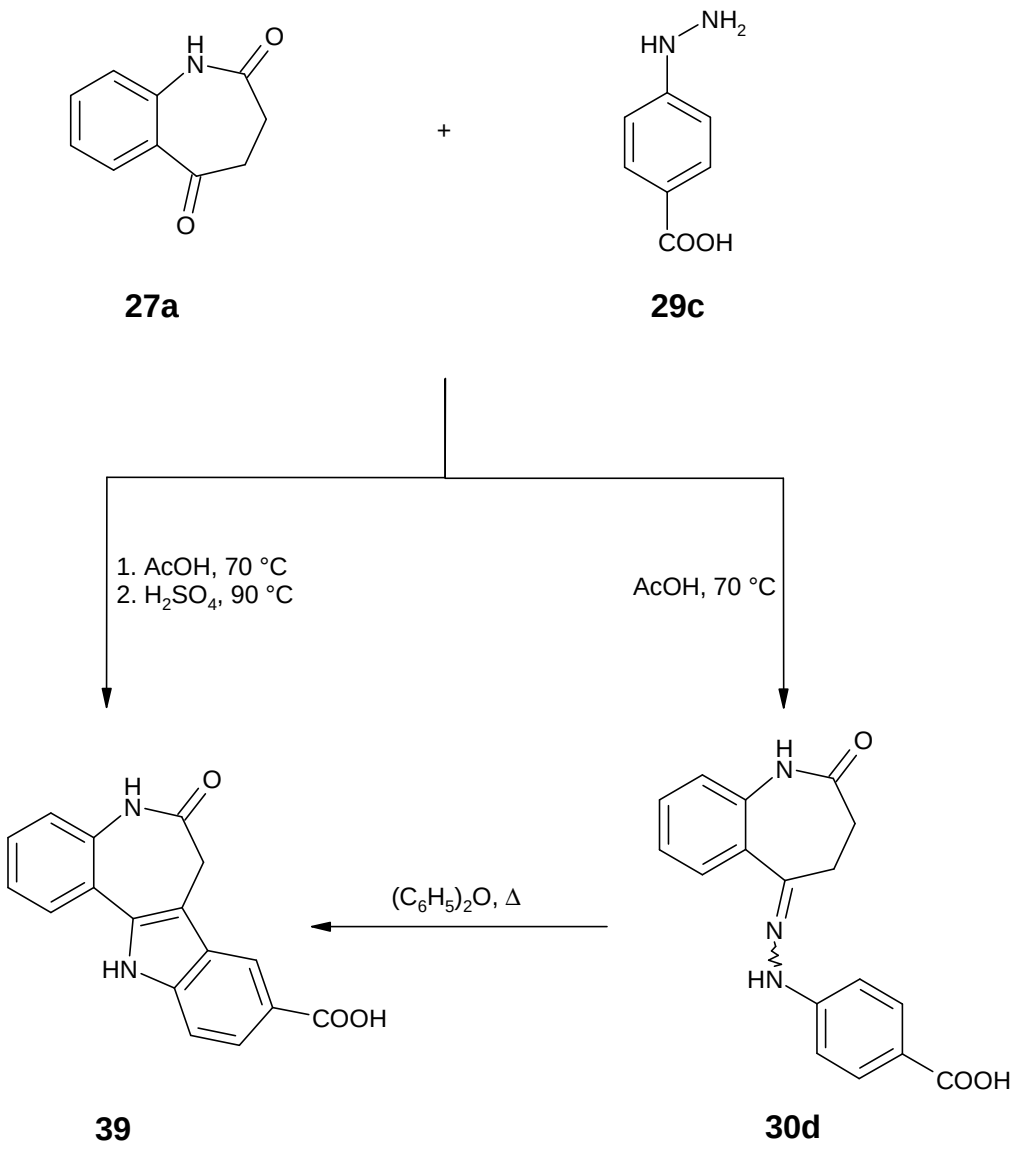
H
N
O
O
+
HN
NH2
COOH
27a
29c
1. AcOH, 70 °C
2. H2SO4, 90 °C
AcOH, 70 °C
(C6H5)2O, Δ
39
30d

The reactions experimented with so far were adapted from conventional chemical synthesis methods. A completely different approach concerning the physical conditions but not the employed reagents was based on microwave technology, that is, microwave-assisted synthesis.

The basic principle of microwave assisted synthesis is the “dielectric heating” of reactants and solvents by applying microwave radiation. According to Lidström[59], there are two components to microwave radiation: an electric field component and a magnetic field component. Two major mechanisms are responsible for the dielectric heating caused by the mentioned electric field component - the so called dipolar polarization mechanism and the conduction mechanism.

The former is based on the fact that a dipole, when exposed to external electric fields, will try to align itself with the field by rotation. The frequency of the applied irradiation is crucial. It has to be low enough to give the dipoles time to respond to the changing electric field and rotate. But it must not allow for the rotation to precisely follow the field. The microwave radiation region fits those requirements, thus creating a phase difference between the orientation of the field and that of the dipole. The phase difference is caused by the field changing faster than the dipole is capable of re-orientating itself. Molar friction and collisions are enhanced, resulting in a loss of energy, and therefore giving rise to dielectric heating.

The conduction mechanism represents the stronger interaction with respect to heat-generating capacity. If influenced by an electric field, ions present in a sample will be moving around, causing an increasing number of collisions and converting the kinetic energy into heat.

Another important requirement for microwave-assisted synthesis is the usage of an oven with a single mode cavity which prevents the formation of “hot and cold spots”, and therefore provides a uniform heating pattern. Modes are described as three dimensional stationary patterns of standing waves within a cavity, caused by microwaves being reflected of the walls after entering the cavity. That uniform increase in temperature throughout the whole sample may be a reason for producing less by-products and/or decomposition products.

In general, microwave technology enables rapid heating, producing unique heat profiles not reproducible by other heating techniques. That

paves the way for an increased range of accessible reactions and shorter reaction times compared to conventional chemical synthesis.[60]

With respect to the synthesis of paullone-9-carboxylic acid (**39**), emphasis was put on the shortening of reaction times, the reaction already being well accessible by conventional synthesis.

Due to the limited size of the certified microwave vessels, a small reaction scale was chosen. Under these conditions, the hydrazone derivative **30d** was formed instantly at room temperature. Therefore, the evaluation of the acquired data will focus on the course of the Fischer indole synthesis (scheme 2-13).

Scheme 2-13:

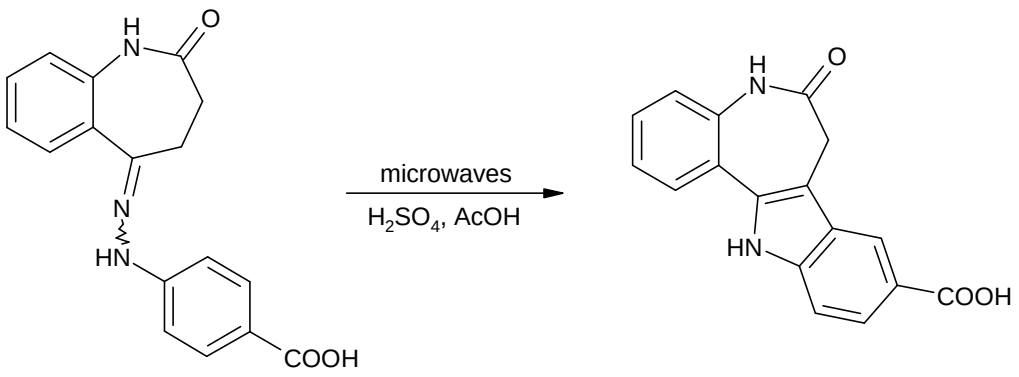

30d **39**

Diverse irradiation times and reaction temperatures were experimented with in order to optimize the reaction process (tables 2-1 and 2-2).

Table 2-1: Variation of irradiation times at 90 °C

time	yield
3 min	97.5%
5 min	96.3%
10 min	96.6%

Yield values determined by HPLC, evaluation: 100%-method, integration wavelength range: 240-261 nm

Table 2-2: Variation of reaction temperatures (3 min irradiation time)

temperature	yield
90 °C	97.5%
120 °C	97.4%
150 °C	96.7%
180 °C	95.8%

Yield values determined by HPLC, evaluation: 100%-method, integration wavelength range: 240-261 nm

The interpretation of the listed results led to the conclusion that neither irradiation times longer than 3 minutes nor temperatures higher than 90 °C resulted in higher yields. Compared to the conventional chemical synthesis of paullone-9-carboxylic acid (**39**), which required one hour at the same scale, a considerable improvement concerning reaction time was accomplished.

2.2.2.2 Synthesis of Paullone-9-carboxylic Acid Esters

Besides the intention of creating a group of homologous substances for the investigation of favorable substituent properties, the synthesis of the paullone esters **40a-h** seemed promising with respect to their biological activity. Transport through cell membranes should be facilitated because of the ester chain increasing the lipophilicity of the molecule. Another motive for the preparation of carboxylic acid esters was the eventuality of these compounds constituting prodrugs of the corresponding carboxylic acid. The possibility of esterases cleaving the esters within the cell and hence liberating paullone-9-carboxylic acid (**39**) at the scene of action, providing direct access to the target enzymes, was considered and striven for.

The first ester derivative synthesized was paullone-9-carboxylic acid ethyl ester (**40a**), accessible by refluxing the educt **39** in dried ethanol and concentrated sulfuric acid (method A) as described by Fischer[61], or alternatively, in dried ethanol saturated with anhydrous hydrogen chloride gas (method B) as performed by Schultz[46] (scheme 2-14).

Scheme 2-14:

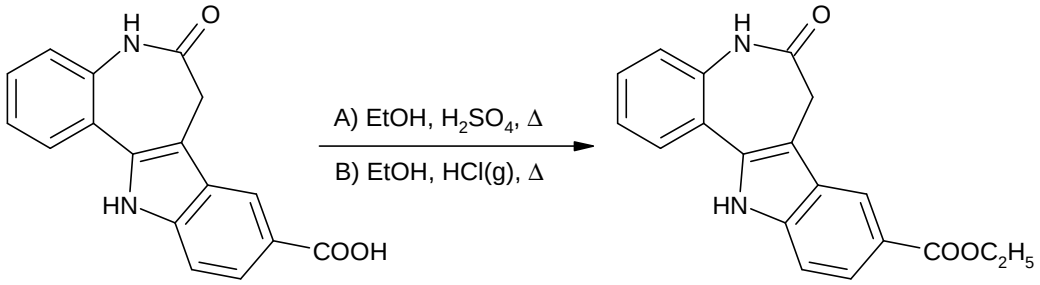

39 **40a**

Carboxylic acids can also be converted into ester derivatives by applying the Mitsunobu esterification reaction.[62-64] The reagents needed for the performance of this reaction are triphenylphosphine (**41**) and di-*tert*-butyl azodicarboxylate (**42**).

The mechanism is postulated as follows (scheme 2-15): First, triphenylphosphine (**41**) is added to the azodicarboxylic acid ester **42**, forming the quaternary phosphonium salt **43**, a zwitterion. Protonation by the employed carboxylic acid leads to **44** which reacts with the alcohol component under cleavage of di-*tert*-butyl hydrazinedicarboxylate (**45**), yielding the alkoxy-phosphonium salt **46**. The latter compound **46** is believed to proceed through an S_N2 type displacement, resulting in the formation of the desired carboxylic acid ester **47** and triphenylphosphine oxide (**48**).

The reagents triphenylphosphine (**41**) and di-*tert*-butyl azodicarboxylate (**42**) represent a redox system. In the course of the Mitsunobu reaction, the former is oxidized to triphenylphosphine oxide (**48**) and the latter is reduced to di-*tert*-butyl hydrazinedicarboxylate (**45**). These side products can cause severe problems in the work-up procedures.

The solvent has to be aprotic and completely anhydrous. For the esterification of paullone-9-carboxylic acid (**39**), tetrahydrofuran (THF) was chosen because of the lacking solubility of the paullone derivatives **40a-h** in THF. This fact enabled the isolation of the desired products by suction-filtration, traces of the side products **45** and **48** remaining though. The strenuous work-up procedures necessary for the comprehensive purification led to rather low yields.

Scheme 2-15:

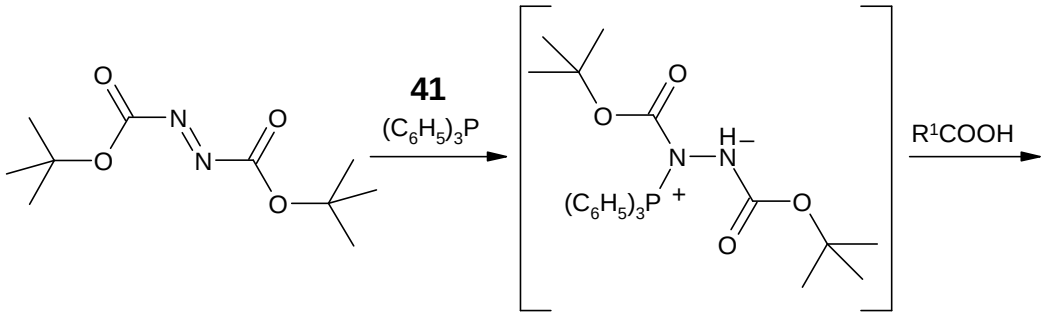

42 **43**

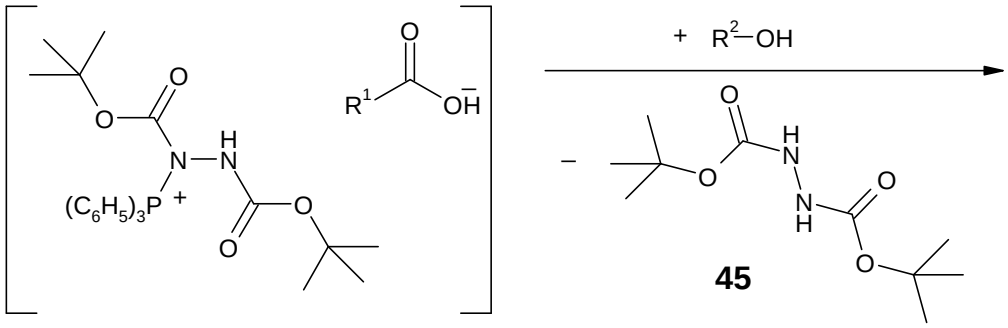

44 **45**

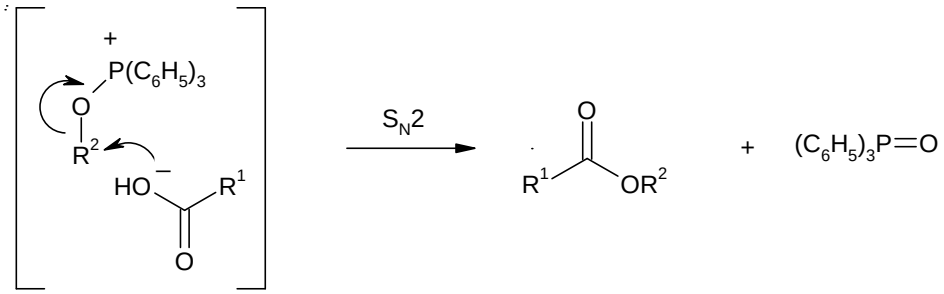

46 **47** **48**

A number of paullone ester derivatives **40a-h** were obtained by employing the described reaction conditions (scheme 2-16).

Scheme 2-16:

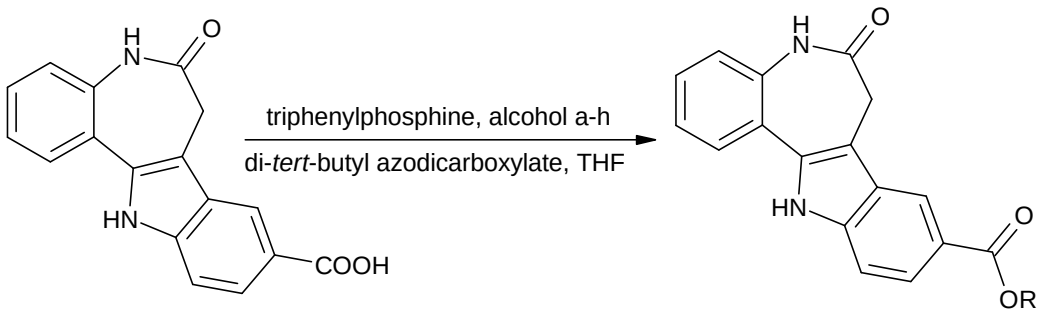

39	**a**	ethanol	**40a**	R = C_2H_5
	b	methanol	**40b**	R = CH_3
	c	1-propanol	**40c**	R = C_3H_7
	d	1-butanol	**40d**	R = C_4H_9
	e	1-pentanol	**40e**	R = C_5H_{11}
	f	2-pentanol	**40f**	R = $CH(CH_3)(C_3H_7)$
	g	1-hexanol	**40g**	R = C_6H_{13}
	h	1-octanol	**40h**	R = C_8H_{17}

2.2.2.3 Rearrangement Reaction via DIC

In the course of performing experiments dealing with the synthesis of paullone-9-carboxylic acid esters **40**, the condensation reagent *N*,*N*'-diisopropylcarbodiimide (DIC) was employed, and its applicability to the production of paullone ester derivatives by an alternative route was evaluated.[65]

Carbodiimides, which can be regarded as anhydrides of urea, represent highly reactive compounds and thus versatile reagents in organic synthesis. Their wide application includes the employment as condensing agents which are, for instance, utilized for the formation of acid anhydrides, esters, and amides. Dicyclohexylcarbodiimide (DCC) and DIC constitute familiar examples of the group of symmetrical carbodiimides.[66]

Carboxylic acids react with aliphatic carbodiimides **49** to yield the corresponding acid anhydrides **50** and the appropriate disubstituted ureas **51**. The protonation of the carbodiimide **49** is postulated to initialize the reaction. The coupling procedure is believed to be mediated by the formation of O-acylisourea **52** as an intermediate product, leaving room for side reactions like the oxygen-to-nitrogen migration which results in the production of the stable N-acylurea **53** (scheme 2-17).[65-67]

Scheme 2-17:

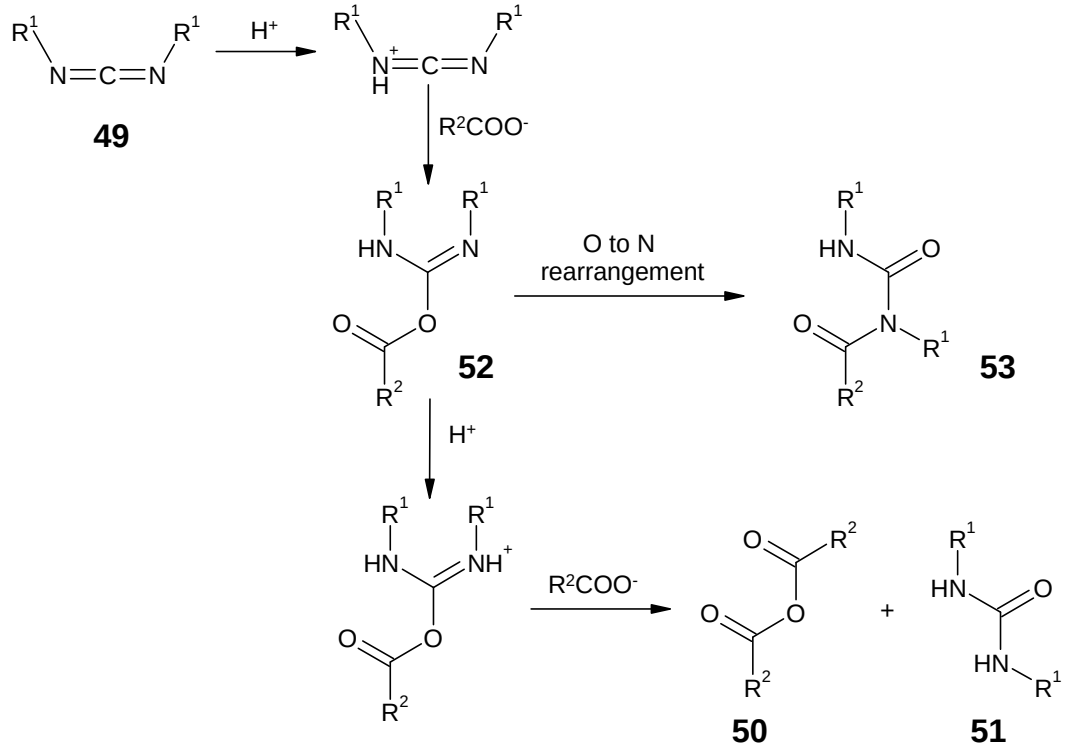

Depending on the nature of reagents and reaction conditions, the outcome of the coupling procedure varies, resulting either in the formation of the acid anhydride **50** and the proper urea **51** or in the formation of the rearranged N-acylurea **53**.

Experiments have shown that lower reaction temperatures, shorter reaction times, or the use of unsymmetrical carbodiimides may suppress the cyclic electronic displacement and therefore impede the production of the chemically inactive N-acylurea **53**.[65,68]

In contrast, aprotic dipolar solvents show a tendency to slow down the reactions and thus enhance the rearrangement procedure.[65] As reported by Hudson[67], for example, DMF concentrations exceeding 25% may accelerate the formation of N-acylurea **53**. It is also claimed that the presence of organic bases like pyridine or triethylamine provokes the oxygen-to-nitrogen migration and may even result in the exclusive preparation of the stable N-acylurea **53**.[66]

For the conversion of paullone-9-carboxylic acid (**39**), DIC was chosen as the carbodiimide component due to the fact that it is rather soluble in organic solvents (more soluble than DCC, for example), leading to facilitated work-up procedures.[69] With 4-dimethylaminopyridine (DMAP), N-ethyldiisopropylamine and DMF as employed reagents and solvent, the coupling reaction led to the N-acylurea derivative **54** (scheme 2-18).

Scheme 2-18:

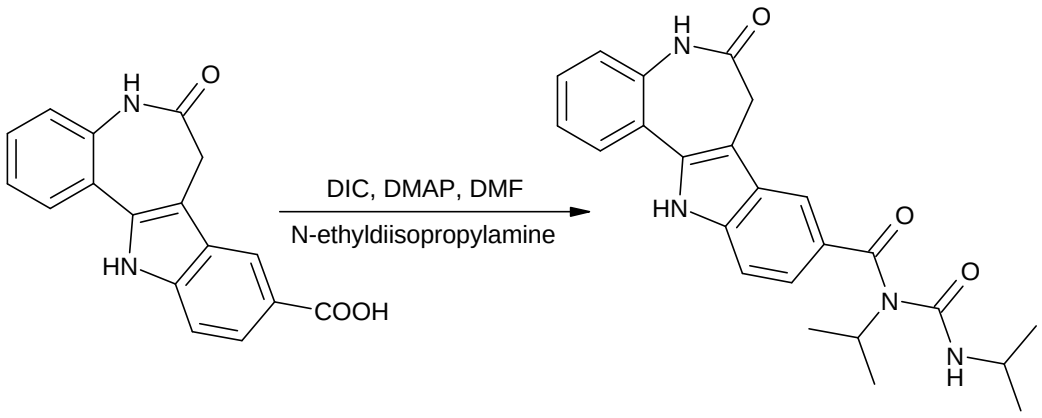

39 **54**

Recapitulatory, the use of DIC did not yield a desired paullone ester derivative **40** but resulted in the rearrangement reaction stated above. Applying the gained insights concerning carbodiimides as condensing agents, DIC was not utilized in the course of conducting experiments which aimed at the synthesis of paullone-9-carboxamides (**55**) as described in the following subchapter (chapter 2.2.2.4).

2.2.2.4 Synthesis of Paullone-9-carboxamides

Literature provides a large number of reaction procedures dealing with the synthesis of amide derivatives from their corresponding carboxylic acids. However, with regard to paullone-9-carboxylic acid (**39**) as the designated educt, the majority of these methods becomes inexpedient. The feasibility of the reactions is negatively affected by the rather high electron density present in the reaction center, caused by the indole residue, and by the poor solubility of the educt **39**, thus aggravating the preparation of paullone-9-carboxamides (**55**) (scheme 2-19).

Scheme 2-19:

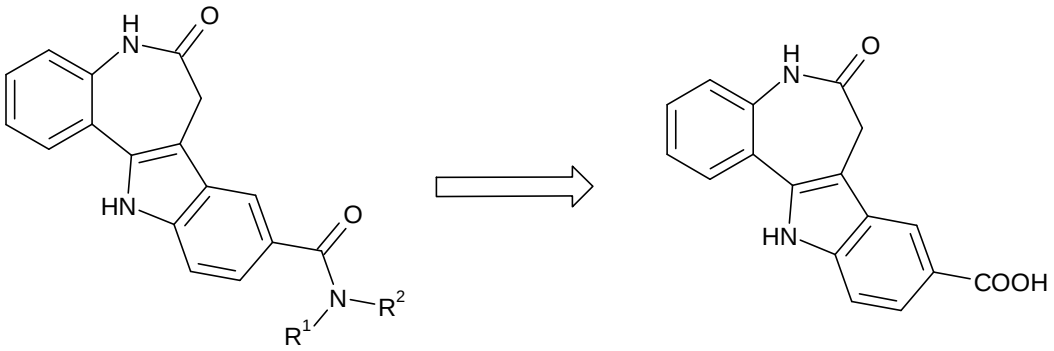

55 **39**

Experiments were performed applying several different methods, hence varying reagents and reaction conditions. Except for the pyrolysis procedure, the postulated reaction mechanisms comprise the activation of the carboxylic acid function by a proper reagent prior to the nucleophilic attack of the amine component. This will be further elucidated by discussing the different routes and their underlying mechanisms.

Pyrolysis

A carboxylic acid **56** reacts with an amine **57** to form a salt **58**. By means of pyrolysis, the salts of ammonia, primary, or secondary amines can be converted into amides **59** (scheme 2-20).[70]

Scheme 2-20:

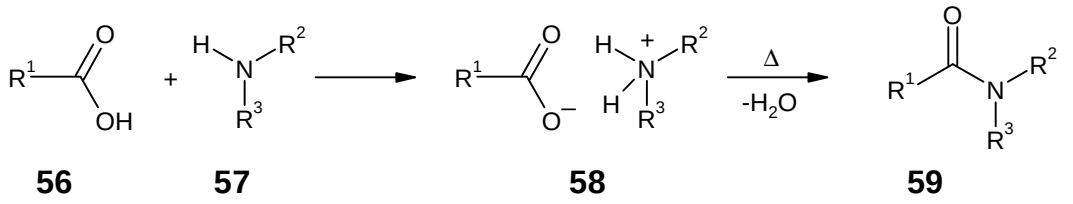

56 **57** **58** **59**

Refluxing the paullone educt **39** in a large excess of benzylamine as the amine component did not yield the paullone-9-carboxamide **55a**.

Use of isocyanide

With reference to Wackerle[71] and Aigner[72], an isocyanide **60** undergoes an α-addition with carboxylic acid **56**, resulting in the intermediate product acyl formimidate **61** which acylates the employed amine **57**. Under cleavage of the formamide derivative **62**, the amide product **59** is obtained (scheme 2-21).

Scheme 2-21:

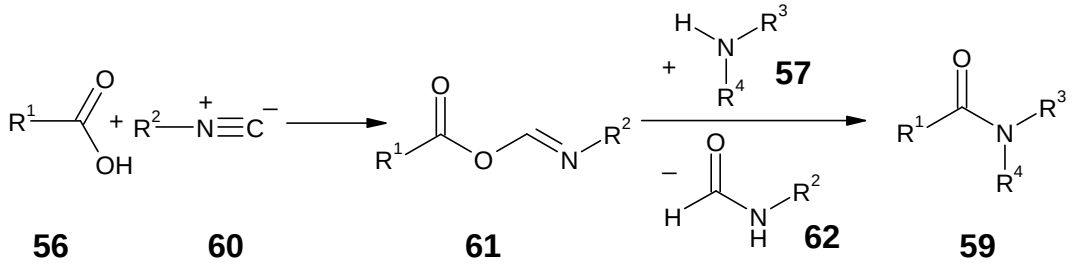

56 **60** **61** **62** **59**

The experiments performed with *tert*-butyl isocyanide and varying amine components (e.g., benzylamine, isopropylamine) did not provide the desired paullone amide product **55**.

Use of triphenyl phosphite

It is postulated by Prabhakaran[73] that an aromatic carboxylic acid, in the presence of pyridine existing as the carboxylate anion **63**, reacts with triphenyl phosphite **64** to yield the ester intermediate **65** which is then attacked by pyridine, leading to the strongly activated acylpyridinium salt **66**. Upon the reaction with urea **67**, the final product **68** is obtained. The stated reaction is supposed to occur in a similar fashion when employing other nucleophiles like alcohols or amines instead of urea (scheme 2-22).

Scheme 2-22:

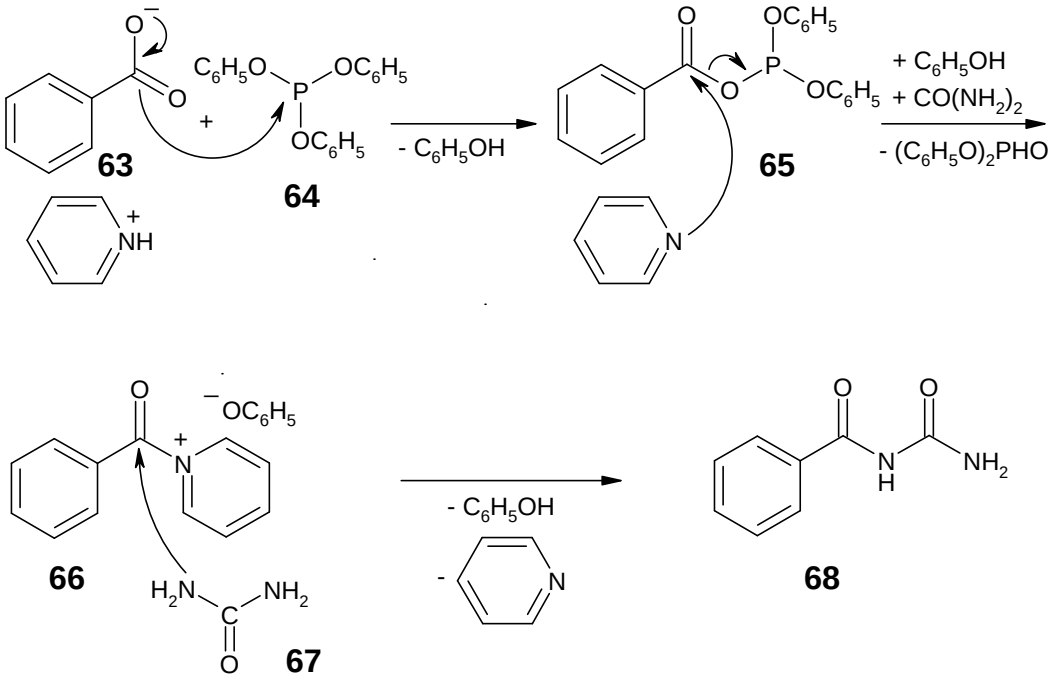

It was first investigated whether the designated paullone educt **39**, the indole carboxylic acid substructure representing the reaction center, would perform an amidation reaction with urea similar to the process depicted above. Because of the failure of that attempt, it was refrained from substituting an amine for the urea as the nucleophile component, and instead methods employing other reagents than triphenyl phosphite were experimented with.

Use of CDI

According to Harada[74] and Walter[75], *N*,*N*'-carbonyldiimidazole (CDI) (**69**) activates the carboxylic acid **56** by forming the imidazolide derivative **70** which subsequently reacts with the amine component to yield the desired amide **59** (scheme 2-23).

Scheme 2-23:

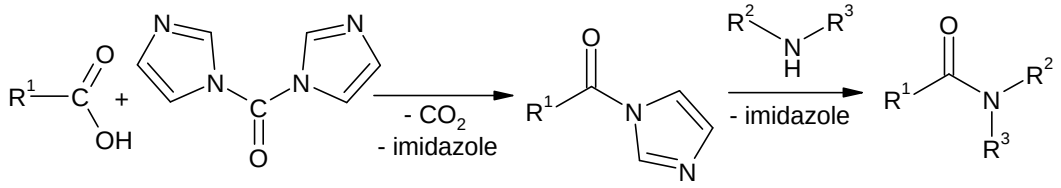

56 **69** **70** **59**

The paullone educt **39** did not react with CDI and benzylamine to provide the amide product **55a**.

Use of EDC

1-Ethyl-3-(3-dimethylamino)propylcarbodiimide (EDC) (**71**) constitutes an example of an unsymmetrical carbodiimide.[65] A brief insight into the chemistry of carbodiimides has been mediated in the previous subchapter (chapter 2.2.2.3), discussing the rearrangement reaction performed via *N*,*N*'-diisopropylcarbodiimide (DIC).

In this case, the synthesis of a paullone-9-carboxamide **55** was striven for, and hence the choice concerning reagents and reaction conditions had to be made very carefully in order to avoid the rearrangement reaction. With reference to Ito[68] and Tartar[69], the formation of the N-acylurea derivative **53** is noticeably suppressed when using an unsymmetrical carbodiimide like EDC (**71**). According to Bailey[76], the addition of co-reagents like 1-hydroxysuccinimide or 1-hydroxy-1*H*-benzotriazole (HOBt) (**72**) may also aid in the avoidance of this side reaction. The *N*-hydroxy compounds are believed to moderate the reactivity of the intermediate product O-acylisourea **52** by trapping out the acylating agent as the active ester **73**. The latter then reacts with the amine component to yield the amide derivative **59** (scheme 2-24).

Scheme 2-24:

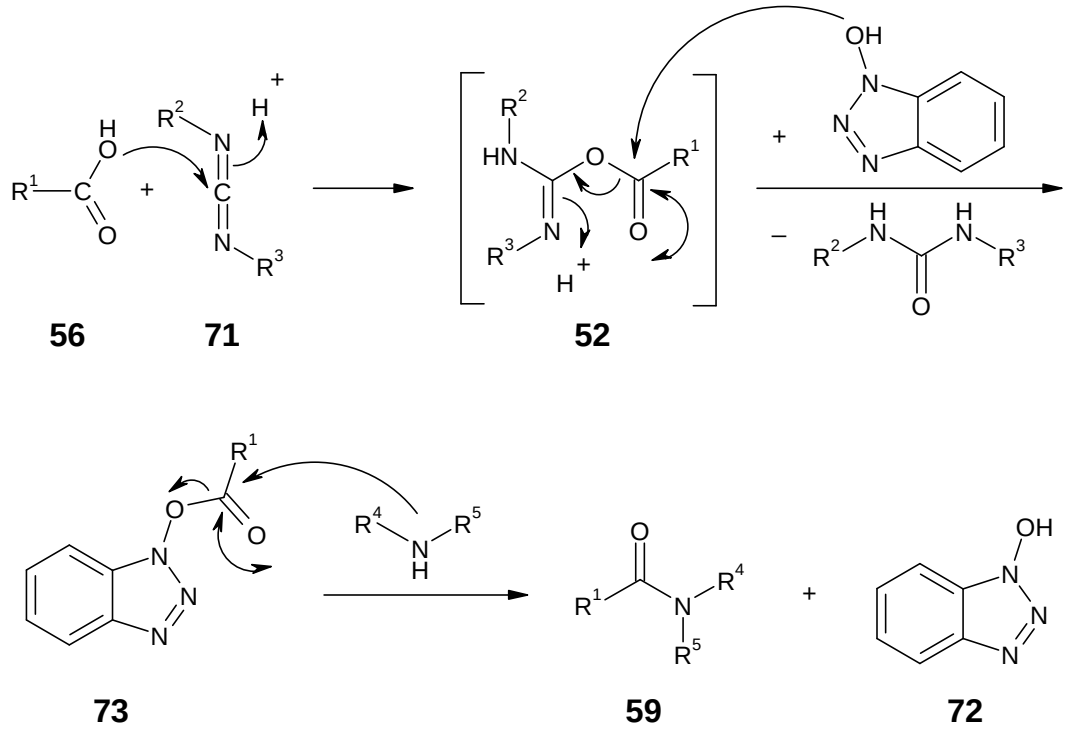

Methods published by Madson[77] and Albrecht[78] also recommended the employment of the co-reagent HOBt which indeed proved to be favorable for the outcome of the reaction. When adapting the procedure for the synthesis of paullone-9-carboxamides **55**, careful adjustments had to be made concerning the utilized equivalents of the reagents EDC and HOBt, the activation time with EDC, and the total reaction time. The preparation of several amide derivatives **55a-h** could then be achieved (scheme 2-25).

Scheme 2-25:

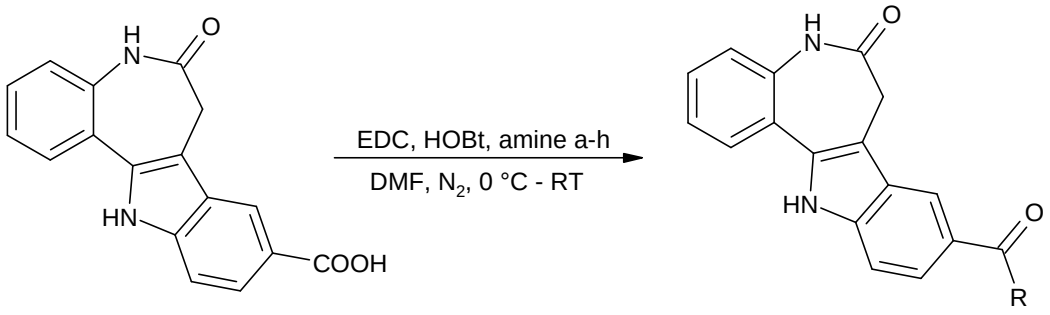

39	**a** benzylamine	**55a**	R = $NHCH_2C_6H_5$
	b morpholine	**55b**	R = NC_4H_8O
	c octadecylamine	**55c**	R = $NHC_{18}H_{37}$
	d 1-benzylpiperazine	**55d**	R = $NC_4H_8NCH_2C_6H_5$
	e pyrrolidine	**55e**	R = NC_4H_8
	f butylamine	**55f**	R = NHC_4H_9
	g (4-methoxybenzyl)amine	**55g**	R = $NHCH_2C_6H_4OCH_3$
	h 2,4-dichlorobenzylamine	**55h**	R = $NHCH_2C_6H_3Cl_2$

In the course of performing the amidation reaction by means of the reagents EDC/HOBt, some experiments provided unexpected products, yielding compounds with a seemingly different basic ring structure. This matter will be elaborately discussed thereinafter (chapter 2.3).

2.2.3 Synthesis of 9-Tetrazolyl-Paullone

Tetrazole represents a structural element that may serve as a bioisostere for the carboxylic acid moiety similar to other functional groups like carboxamides, sulfonamides, and phosphates, for example. Referring to Herr[79], it is common practice to interchange the term bioisosterism with the term non-classical isosterism, relating to the concept that functional groups with similar physical properties may be interchangeable, possibly resulting in similar biological properties. Tetrazoles feature physical properties analogous to those of carboxylic acids, yet they are considerably influenced by the effect of the substituents at the C5-position. In medicinal chemistry, tetrazoles constitute favored isosteres because of their characteristic of being metabolically resistant to many biological transformations. Furthermore, the ring structure causes a raise in lipophilicity, and thus tetrazoles are believed to pass through cell membranes more easily.[79]

Being aware of the possibility that insufficient cell membrane transport might be responsible for some of the paullone derivatives exhibiting only poor in vitro antitumor activity in contrast to excellent biological activity against the isolated kinases (e.g., carbonitrile derivative **74**)[6], the synthesis of the tetrazole derivative **75** was considered to be a promising venture.

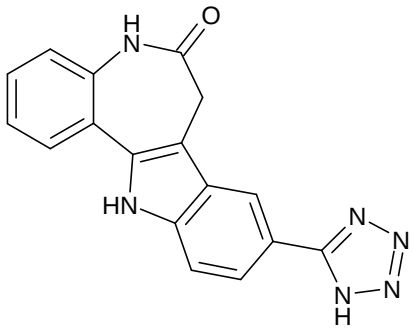

75

It should be pointed out that tetrazoles in possession of a free N-H bond, also denominated as tetrazolic acids, are believed to exist as an approximate 1:1 ratio of 1*H*- and 2*H*-tautomeric forms.[79] The tetrazole

structures depicted in this subchapter should therefore be regarded as mixtures of the N-1 and N-2 regioisomers.

As the cyano functionality is transformable into a tetrazole, paullone-9-carbonitrile (**74**) constituted a suitable educt for the synthesis of the desired paullone product **75** (scheme 2-26).[80]

Scheme 2-26:

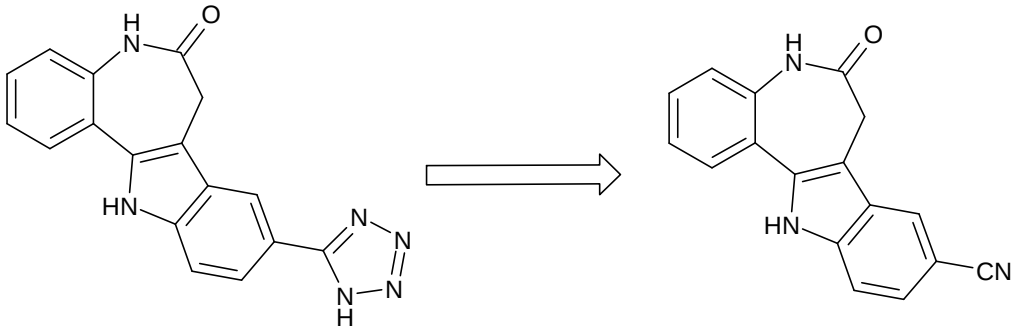

75 **74**

The carbonitrile derivative **74** was accessible by the performance of a Rosenmund-von-Braun reaction, referring to a method stated by Agarwal[81] and modified by Schultz[46]. This comprised the conversion of the starting material kenpaullone (**1**), synthesized applying the standard reaction sequence for paullones described earlier (cf. chapter 2.1), into the desired compound **74** by employment of cuprous cyanide as the reagent and 1-methyl-2-pyrrolidinone (NMP) as the solvent (scheme 2-27).

Scheme 2-27:

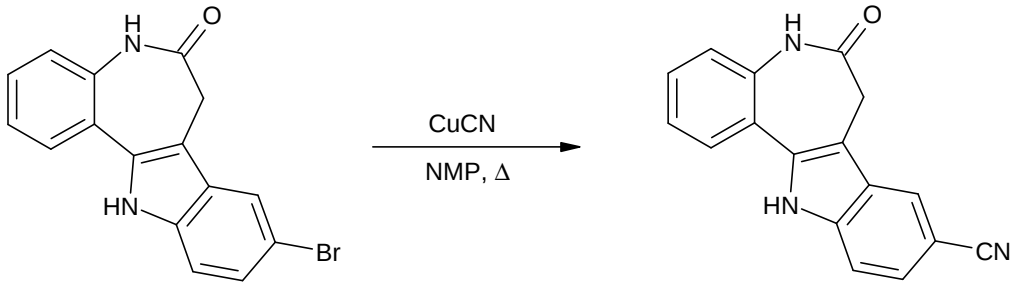

1 **74**

In literature, numerous articles deal with the synthesis of tetrazoles from carbonitriles and can therefore serve as references. However, most of these methods document the employment of rather electron-poor carbonitriles as educts, for example, compounds with cyano functionalities activated by electron-withdrawing groups. In contrast to these findings, the paullone derivative **74** provides an electron-rich vicinity to the designated reaction center. This might impair the feasibility of the considered reactions.

The physicochemical properties of the paullone educt **74** indeed proved to have a negative impact on the aspired reaction process. Various reagents and reaction conditions were experimented with, yet no procedure led to the desired product **75** (table 2-3).

Table 2-3: Futile attempts at tetrazole **75** synthesis

reagents	solvent	reference(s)
NaN_3, NH_4Cl	DMF	Finnegan[82], Peet[83]
NaN_3, NH_4Cl, LiCl	DMF	Ried[84,85]
NaN_3, AcOH	n-butyl alcohol	Herbst[86]
NaN_3, $AlCl_3$	THF	Arnold[87]

More sophisticated procedures than the metal salt strategy, which uses sodium azide as the cycloaddition reagent, have been published in recent past, leading to the preparation of 5-substituted tetrazoles by tin- and silicon-mediated methods. The new azide reagents like trialkyltin azide or trimethylsilyl azide are soluble in organic solvents, and furthermore they are considered to be the better alternative with respect to safety issues.[79]

A method published by Duncia[88], preferably designed for electron-rich carbonitriles, was chosen to serve as the reference procedure for the next experiment aiming at the synthesis of 9-tetrazolyl-paullone **75**.

The employed reagent trimethyltin azide (**76**) was generated from trimethyltin chloride (**77**) and aqueous sodium azide solution as described by Kricheldorf[89] and Luijten[90] (scheme 2-28).

Scheme 2-28:

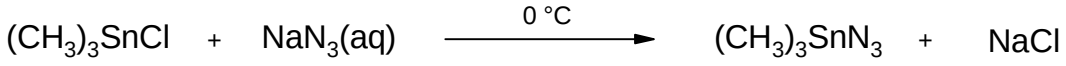

77 **76**

The starting material **74** was refluxed with trimethyltin azide **76** in toluene, forming a tin-tetrazole adduct **78** as an intermediate product. Subsequently, the performance of acid hydrolysis yielded the tetrazole product **75** (scheme 2-29).

Scheme 2-29:

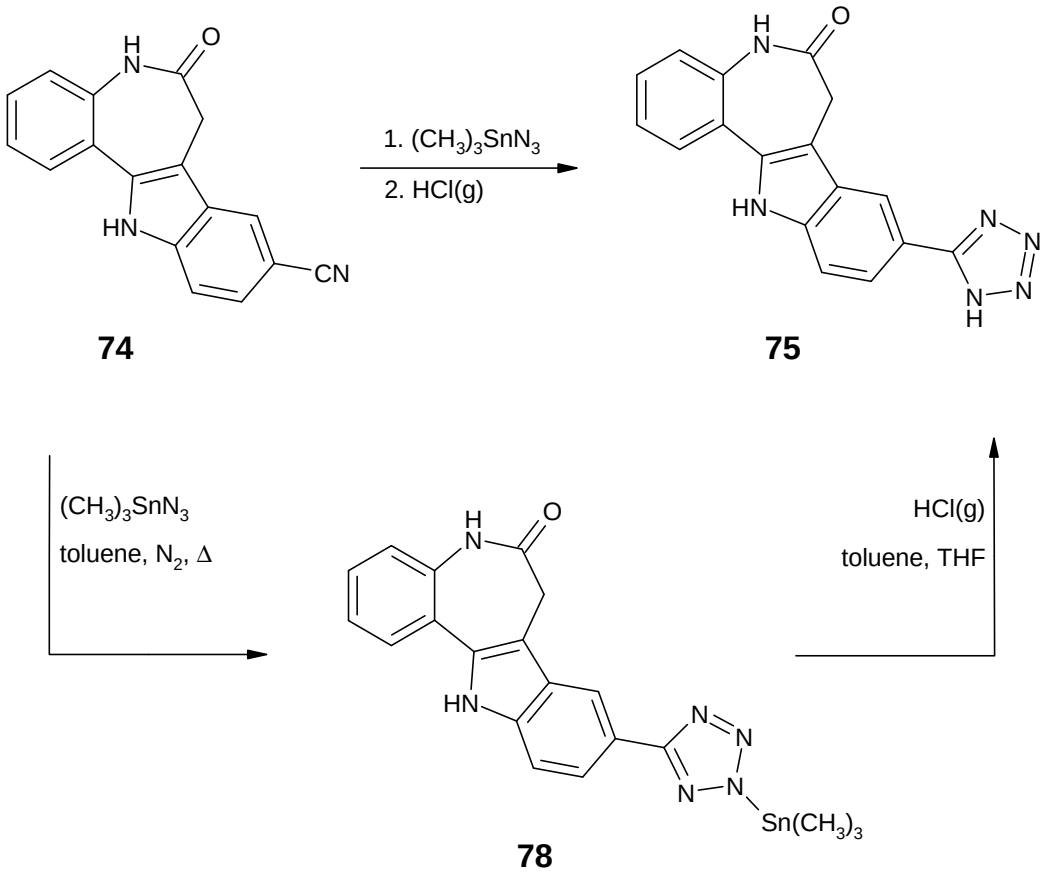

74 **75**

78

In spite of reaction times exceeding one hundred hours, only a partial conversion of the carbonitrile **74** into the tetrazole **75** could be achieved. Thus, the compounds had to be carefully separated. For that purpose, an HPLC method which had been established for monitoring the reaction progress was converted into an MPLC procedure. The poor solubility of 9-tetrazolyl-paullone **75** severely aggravated the purification process, yet small amounts of the pure product could be obtained. Proofs of identity and purity were provided by HPLC (figure 2-3) and mass spectrometry (figure 2-4).

Figure 2-3: HPLC chromatogram of isolated MPLC fraction containing **75**

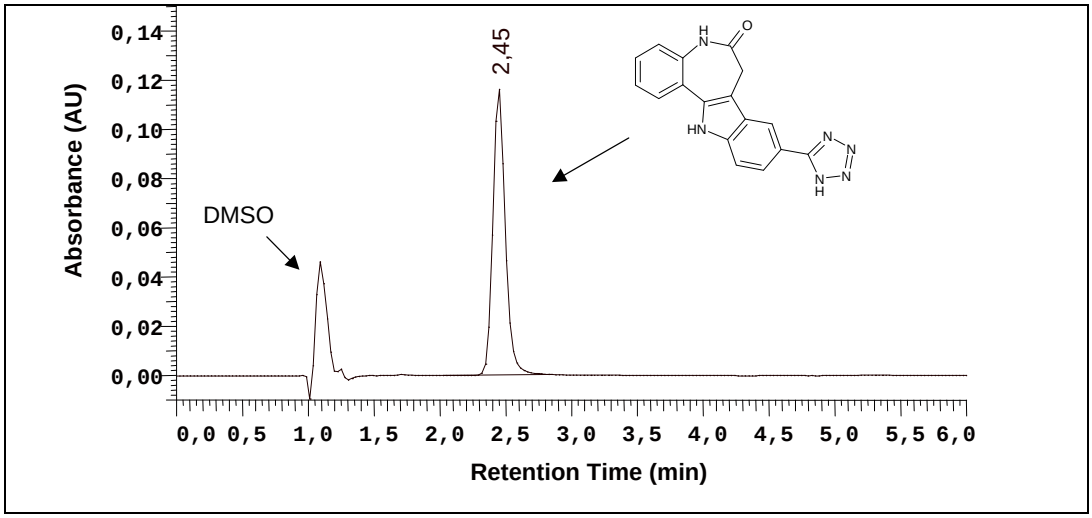

Elution solvent: acetonitrile/water pH 1.5 (35/65), detection wavelength: 254 nm

Figure 2-4: High resolution FAB spectrum of **75**

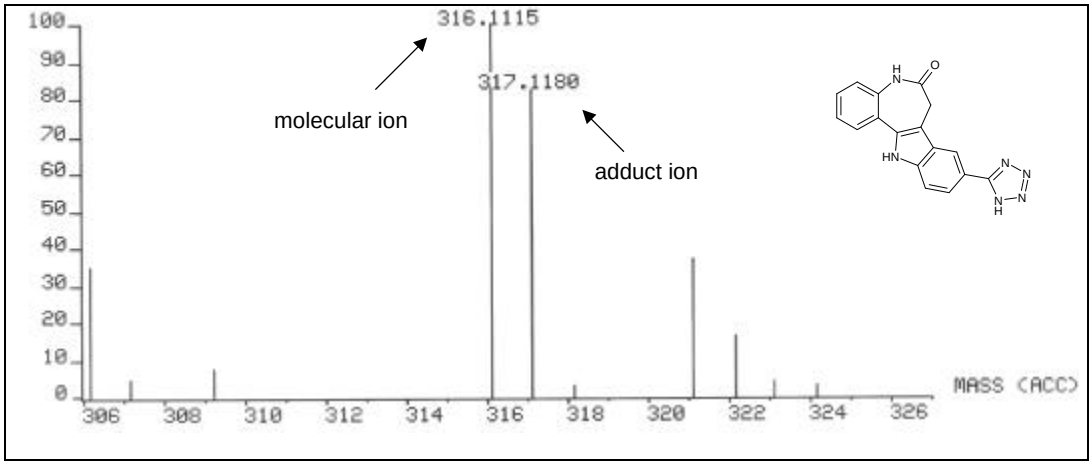

Calculated molecular ion $[M]^+$ at 316.1073, calculated adduct ion $[M + H]^+$ at 317.1151

Because of the complications associated with the conventional chemical synthesis of the tetrazole derivative **75**, a strong interest existed in applying the microwave technology to this reaction. As previously elucidated (cf. chapter 2.2.2.1), flash heating by microwave irradiation often exhibits a positive effect on the feasibility of reactions that are considered problematic for conventional chemistry and/or shortens reaction times. This enterprise was further encouraged by an article published by Alterman[80], reporting on the smooth conversion of aryl nitriles into the corresponding tetrazoles by treatment with sodium azide and ammonium chloride in DMF.

Microwave-assisted synthesis of 9-tetrazolyl-paullone **75** was pursued employing the azide/ammonium salt combination documented in the publication by Alterman[80] (method A) as well as the trialkyltin azide reagent that had mediated the conventional tetrazole synthesis (method B) (scheme 2-30).

Scheme 2-30:

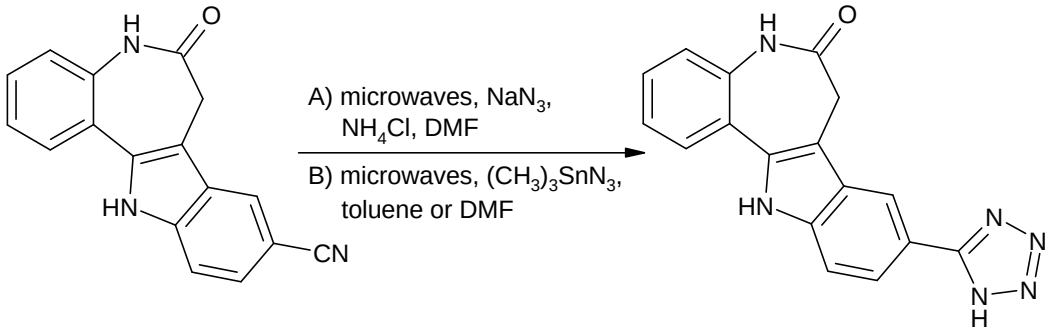

74 **75**

Different irradiation times and reaction temperatures were experimented with. Results concerning method A are presented in tables 2-4 and 2-5, those linked to method B are presented in table 2-6.

Table 2-4: NaN_3/NH_4Cl: variation of reaction temperatures (20 min irradiation time)

temperature	yield
130 °C	14.3% (13 min)
150 °C	52.8%
180 °C	49.7%
210 °C	4.5%

Yield values determined by HPLC, evaluation: 100%-method, integration wavelength range: 240-261 nm

Table 2-5: NaN_3/NH_4Cl: variation of irradiation times at 150 °C

time	yield
20 min	52.8%
40 min	68.2%
60 min	73.5%

Yield values determined by HPLC, evaluation: 100%-method, integration wavelength range: 240-261 nm

Table 2-6: $(CH_3)_3SnN_3$: variation of irradiation times at 200 °C

time	yield
15 min	23.9%
30 min	25.3%

Yield values determined by HPLC, evaluation: 100%-method, integration wavelength range: 240-261 nm

These values were obtained employing DMF as the solvent. Using toluene, a conversion into the tetrazole did not take place.

The progress of the reaction was continuously monitored by HPLC. The chromatograms shown below (figures 2-5 to 2-7) nicely depict the ongoing conversion of the educt **74** into the desired product **75** during the performance of method A.

Figure 2-5: Starting material **74**

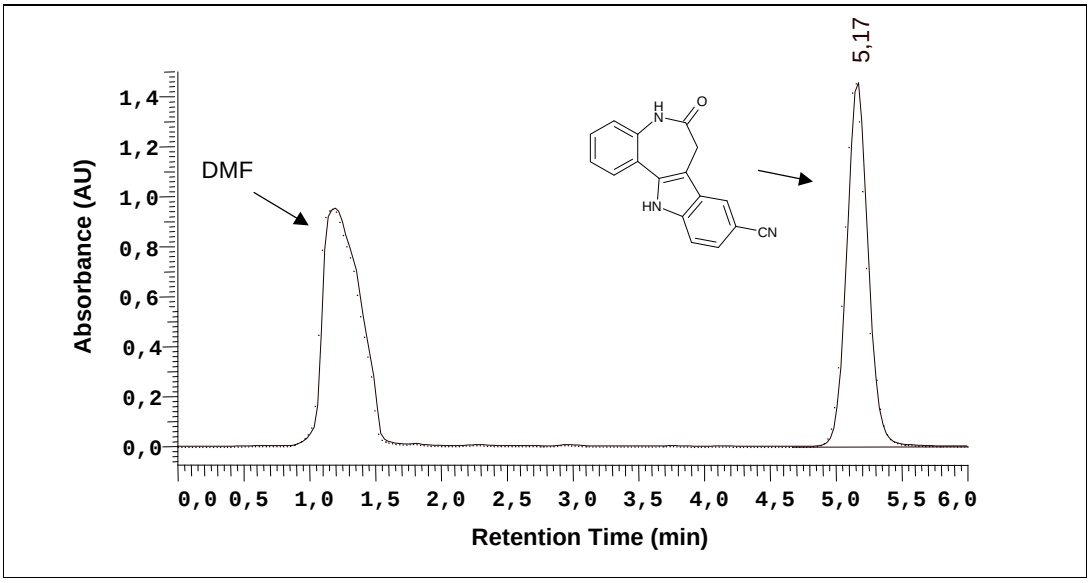

Elution solvent: acetonitrile/water pH 1.5 (35/65), sample solvent: DMF, detection wavelength: 254 nm

Figure 2-6: Reaction mixture after 20 min irradiation at 150 °C

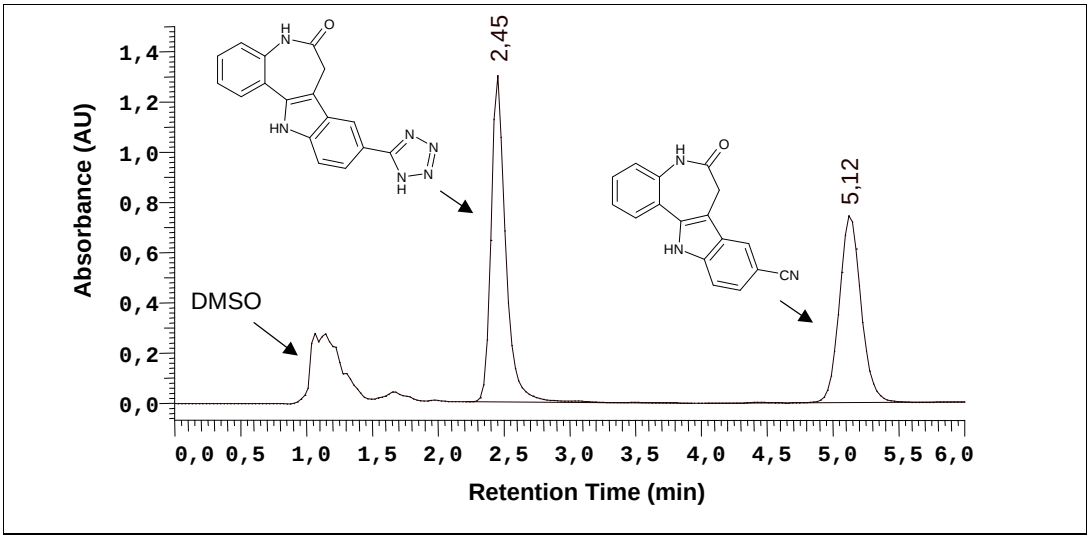

Elution solvent: acetonitrile/water pH 1.5 (35/65), sample solvent: DMSO, detection wavelength: 254 nm

Figure 2-7: Reaction mixture after 60 min irradiation at 150 °C

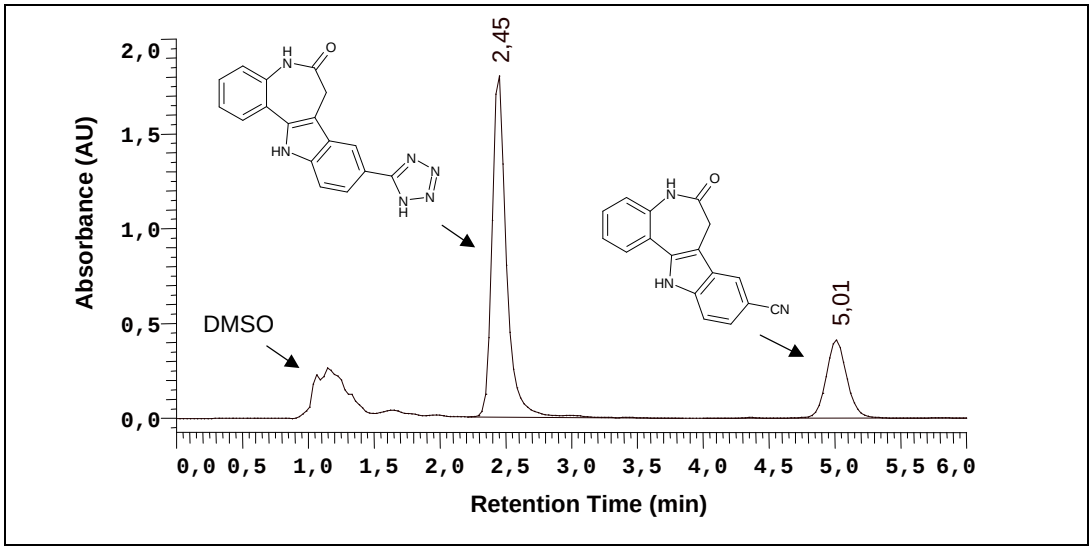

Elution solvent: acetonitrile/water pH 1.5 (35/65), sample solvent: DMSO, detection wavelength: 254 nm

The evaluation of the results allowed the conclusion that both methods were capable of achieving the transformation of paullone-9-carbonitrile **74** into the tetrazole product **75**.

Remarkably, the reagents sodium azide and ammonium chloride only mediated the cycloaddition reaction by treatment with microwave irradiation. The most eligible reaction temperature was 150 °C, yields rising as the reaction time was prolonged. This procedure constituted a fine example of improving the accessibility of a reaction by means of flash heating.

Concerning the use of trimethyltin azide as the cycloaddition reagent, it was proven that a partial synthesis of 9-tetrazolyl-paullone **75** was achieved in a very short reaction time.

2.2.4 Determination of Purity of the Synthesized Paullones

In several cases, the purification of paullone derivatives by means of recrystallization or column chromatography turned out to be difficult, mainly because of the low solubility of the compounds in the common organic solvents. Consequently, the purity and the identity of the compounds that lacked a satisfactory elemental analysis were determined by performing HPLC and mass spectrometry (i.e., FAB-MS) analyses.

Different HPLC methods were developed, varying the composition of the elution solvent. In order to move the equilibrium of dissociation to one side and assure the presence of the acidic form of a compound only, hence prompting the appearance of a single and narrow peak in the chromatogram, the aqueous phase was acidified via trifluoroacetic acid to pH 1.5. Substances susceptible to acid hydrolysis, like the paullone ester **40e**, for instance, contained no acid additive in the aqueous phase of the elution solvent.

For the affected paullones, an overview of purity values and retention times (t_R) corresponding to the proper elution solvent composition is given in table 2-7.

Table 2-7: Purity analyses of paullones performed by HPLC

Sample	grade of purity	t_R	elution solvent composition
40b	95.6%	9.3 min	acetonitrile/water pH 1.5 (30/70)
40e	97.0%	3.6 min	acetonitrile/water (60/40)
40f	94.6%	3.3 min	acetonitrile/water (60/40)
40h	99.2%	5.0 min	acetonitrile/water (70/30)
55a	93.4%	4.2 min	acetonitrile/water (40/60)
55b	98.4%	3.1 min	acetonitrile/water pH 1.5 (30/70)
55d	96.3%	4.0 min	acetonitrile/water pH 1.5 (30/70)
55e	98.2%	2.9 min	acetonitrile/water (35/65)
55f	97.9%	3.0 min	acetonitrile/water (40/60)

Evaluation: 100%-method, integration wavelength range: 240-261 nm

As a representative example, the HPLC chromatogram (figure 2-8) and high resolution mass spectrum (figure 2-9) of pentyl paullone-9-carboxylate (**40e**) are depicted below.

Figure 2-8: Proof of purity for compound **40e** by HPLC

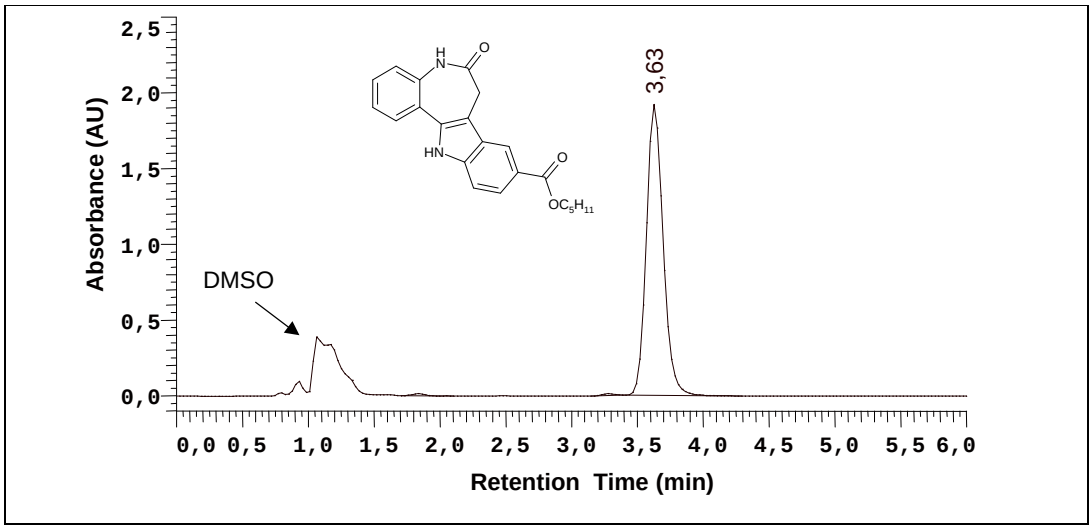

Elution solvent: acetonitrile/water (60/40), sample solvent: DMSO,
detection wavelength: 254 nm,
purity: 97%, evaluation: 100%-method, integration wavelength range: 240-261 nm
run time in total: 10 min (no further peaks detected)

Figure 2-9: Proof of identity for compound **40e** by FAB-MS

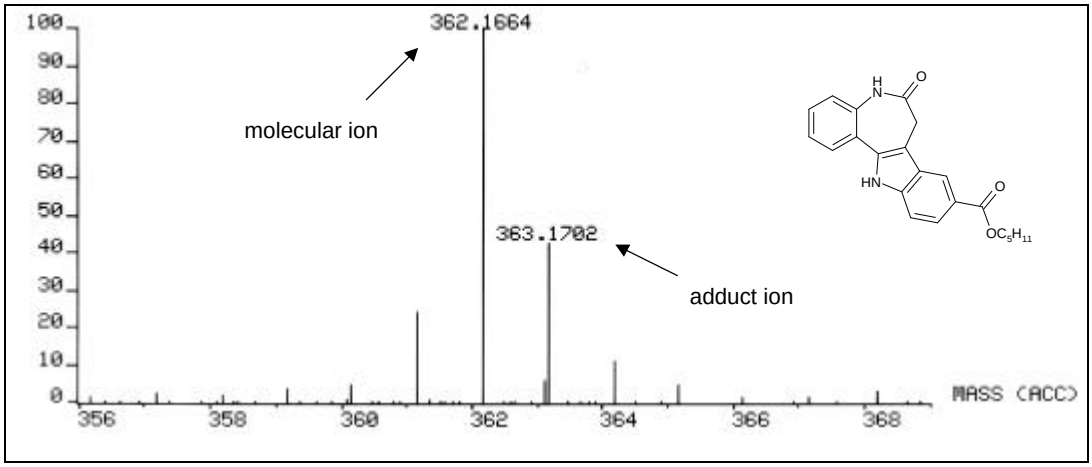

Calculated molecular ion $[M]^+$ at 362.1630, calculated adduct ion $[M + H]^+$ at 363.1709

The adsorption or incorporation of water into new, crystallized compounds constitutes another aspect that has to be taken into account when scrutinizing the purity of a substance. However, methods based on UV detection will certainly not reveal the presence of water within the examined crystals. Furthermore, elemental analyses only inform about the measured elemental composition of a target compound matching or differing from the calculated one – whether possible deviations are caused by impurities or water, possibly crystal water, remains unenlightened.

Thermogravimetry measures the change in weight of a sample as it is heated, cooled, or held at constant temperature. Due to the fact that water evaporates when heated to sufficiently high temperatures, thus entailing a decrease in sample mass, information concerning the amount of water present in a sample can be gathered by means of this methodology. According to Riesen[91], a thermobalance is a very sensitive device for measuring an alteration in mass of a sample affected by heating or cooling under an appropriate atmosphere. The process of the mass changing during the modification of the temperature acting on the sample is recorded and may be illustrated in curves depicting the sample mass as a function of temperature. The interpretation of the obtained curves can lead to conclusions concerning the water contained in a sample, and eventually even characterize the type of water (e.g., crystal water).

The paullone derivatives selected for the investigation had supplied elemental analyses that had matched the calculated composition values only after including certain amounts of crystal water into the calculation. It was to be determined whether the percentage of sample mass (i.e., water) lost during the thermogravimetric procedure coincided with the amounts of water theoretically present in the substance according to the recalculated elemental composition.

Sodium tartrate dihydrate, containing 15.66% of crystal water, served as a standard and was measured throughout the procedure in order to supervise the operation of the thermobalance. The measured water content of the standard samples and the absolute (abs.) and relative (rel.) deviations from the calculated value (i.e., 15.66%) are presented in table 2-8, a corresponding sample curve is illustrated in figure 2-10.

Table 2-8: Experimental results for sodium tartrate dihydrate (standard)

sample	water content	abs. deviation	rel. deviation
1	15.20%	-0.46%	-2.94%
2	14.80%	-0.86%	-5.49%
3	15.95%	+0.29%	+1.85%
4	17.26%	+1.60%	+10.22%
5	15.93%	+0.27%	+1.72%
6	15.84%	+0.18%	+1.15%
7	15.62%	-0.04%	-0.26%
8	14.39%	-1.27%	-8.11%

Statistics: x_{ar} = 15.62%, s = 0.87%, s_{rel} = 5.57%

Figure 2-10: Exemplary curve of a standard sample

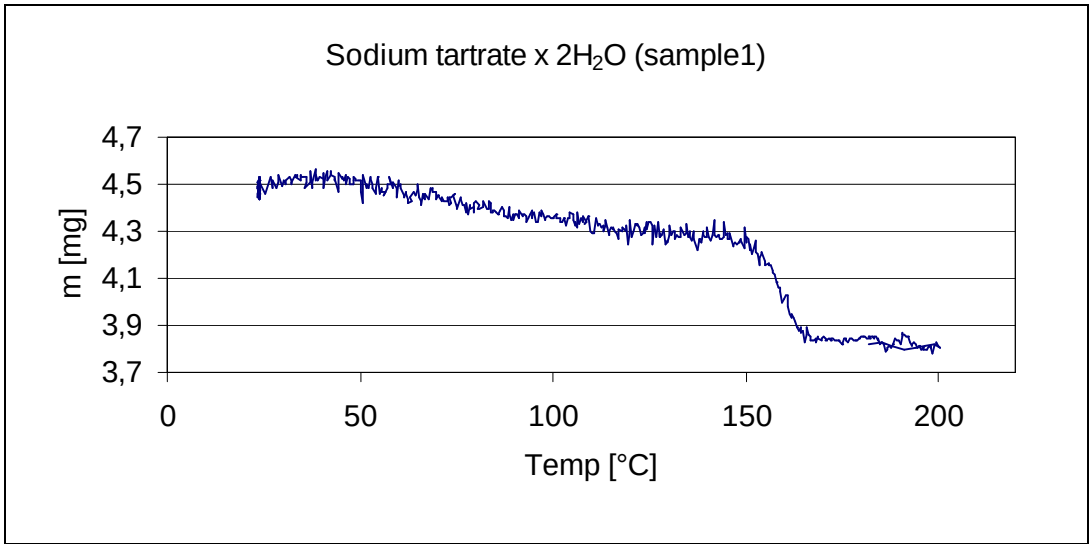

The loss of crystal water was observed between 150 °C and 165 °C.

Although the statistical evaluation of the measurements performed with the standard sodium tartrate dihydrate did not provide satisfactory results, the corresponding graphic illustrations clearly documented the loss of crystal water, indicated by the typical shape of the curve.

Hence, the thermogravimetric analysis of the designated paullone derivatives was carried into execution. The obtained results are listed in table 2-9, exemplary curves are depicted in figures 2-11 and 2-12.

Table 2-9: Analysis of paullone derivatives

sample	thermobalance (Δm [%])				theoretical	HPLC
	#1	#2	#3	avg	(Δm [%])	purity [%]
40h	[-0.58]	[0.38]	[1.08]	n/a	-1.10 (x ¼ H_2O)	99.2
55a	-1.81	-1.96	-1.67	-1.81	-2.31 (x ½ H_2O)	93.4
55b	[-1.26]	[0.23]	[-0.44]	n/a	-2.43 (x ½ H_2O)	98.4
55d	-0.57	-0.94	-0.56	-0.69	-2.91 (x ½ H_2O)	96.3
55e	-1.77	-1.62	-2.29	-1.89	-2.54 (x ½ H_2O)	98.2

Each paullone sample was analyzed three times in consecutive order (#1-#3), "avg" gives the average value, "n/a" is the abbreviation for "not applicable".

Thermogravimetric values in brackets are of no significance as they are derived from either illogical (mass increase under N_2-atmosphere) or unreliable curves.

The theoretical values listed are based on calculations that incorporated the amount of crystal water stated in parentheses.

HPLC-derived purity values are included in the table in order to ease the interpretation of the thermogravimetry data: they hint the presence of other impurities.

Figure 2-11: Illustration of the course of sample #2 of compound **55a**

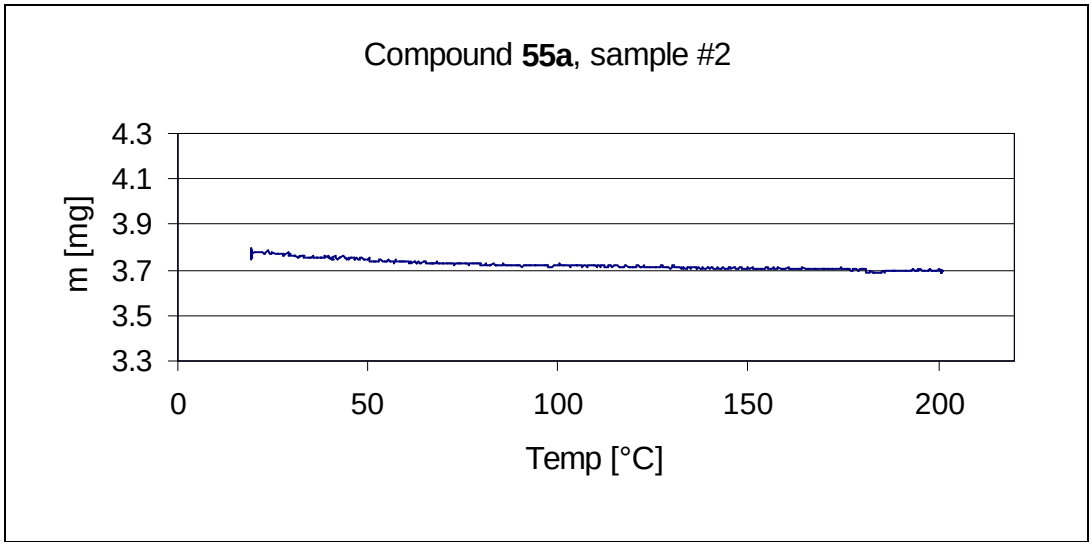

The scale is equivalent to the one applied to the standard depicted in figure 2-10.

No loss of crystal water can be observed.

Figure 2-12: Illustration of the course of sample #3 of compound **40h**

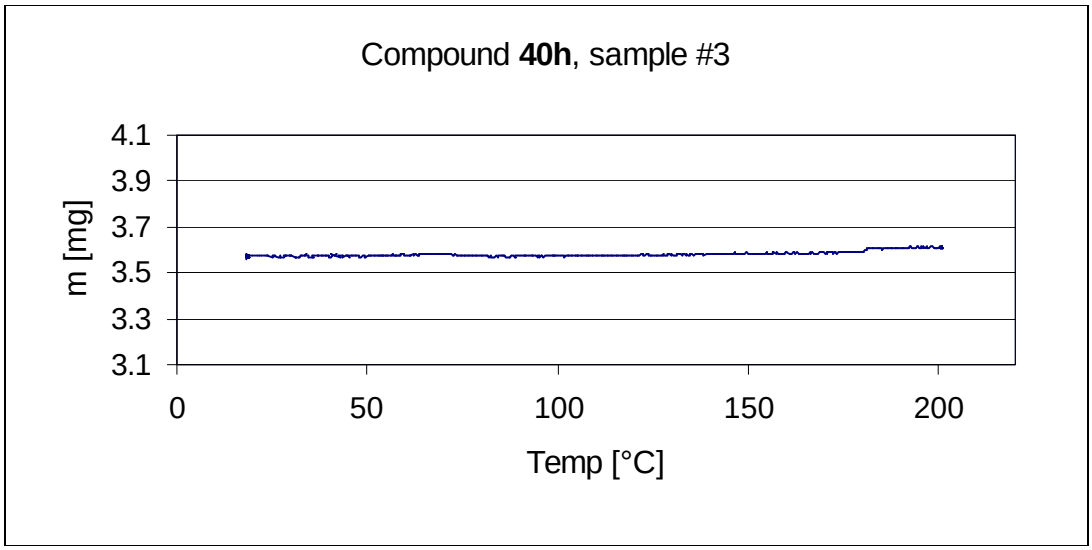

The scale is equivalent to the one applied to the standard depicted in figure 2-10.

No loss of crystal water can be observed. The curve even exhibits a slight increase in sample mass which is inexplicable under the given experimental conditions.

In conclusion, it could not be proven that the analyzed paullones contained crystal water. The experimental results did not correspond to the calculated theoretical values, and the corresponding curves did not illustrate the typical mass decrease seen during the loss of crystal water.

2.3 Skeletal Rearrangement of Paullones to 11*H*-Indolo[3,2-*c*] quinoline-6-carboxylic Acids

In the course of performing experiments dealing with the synthesis of paullone-9-carboxamide derivatives **55a-h**, using a combination of the reagents EDC (**71**) and HOBt (**72**) as described earlier (cf. chapter 2.2.2.4), the outcome of some reactions was unexpected and thus required further investigation. The cause of special interest being aroused was the absence of a certain peak typical of the basic paullone ring structure in the ^{1}H-NMR spectra of the affected compounds: the signal corresponding to the CH_2-group of the azepinone ring, previously mentioned in connection with the diastereotopicity phenomenon (cf. chapter 2.2.1), could not be detected after the targeted amidation reaction. This was first taken notice of when reacting paullone-9-carboxylic acid (**39**) (figure 2-13) with benzylamine, yielding an unknown new compound **79a** (figure 2-14).

Figure 2-13: ^{1}H-NMR spectrum of the educt **39**

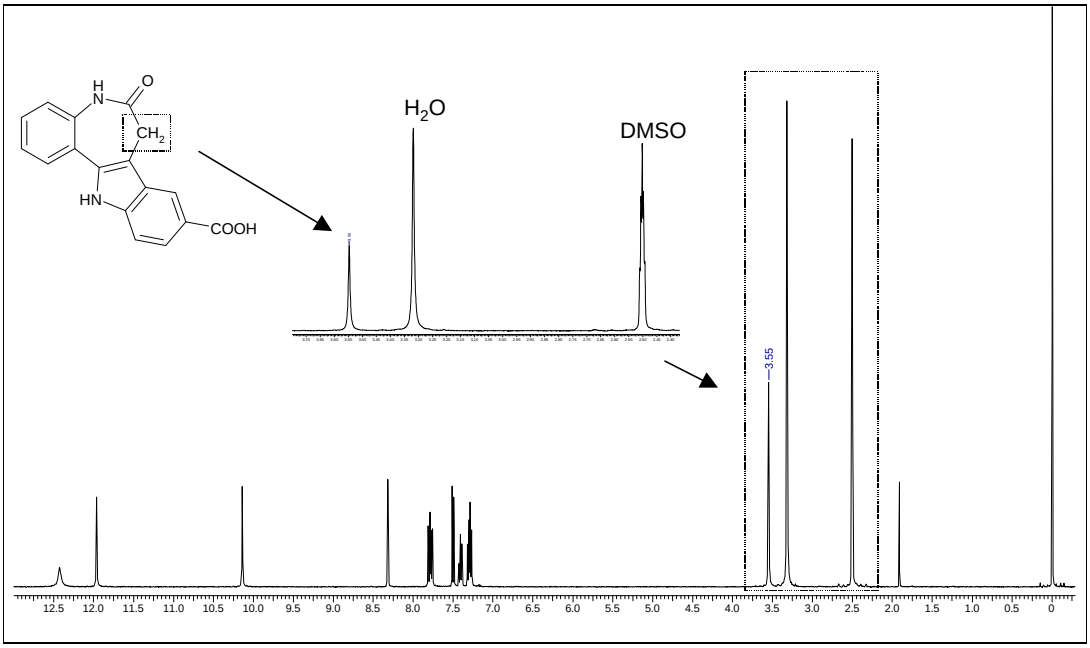

The peak corresponding to the azepinone CH_2-group appeared at δ = 3.55 ppm.

Figure 2-14: ^{1}H-NMR spectrum of the unknown product **79a**

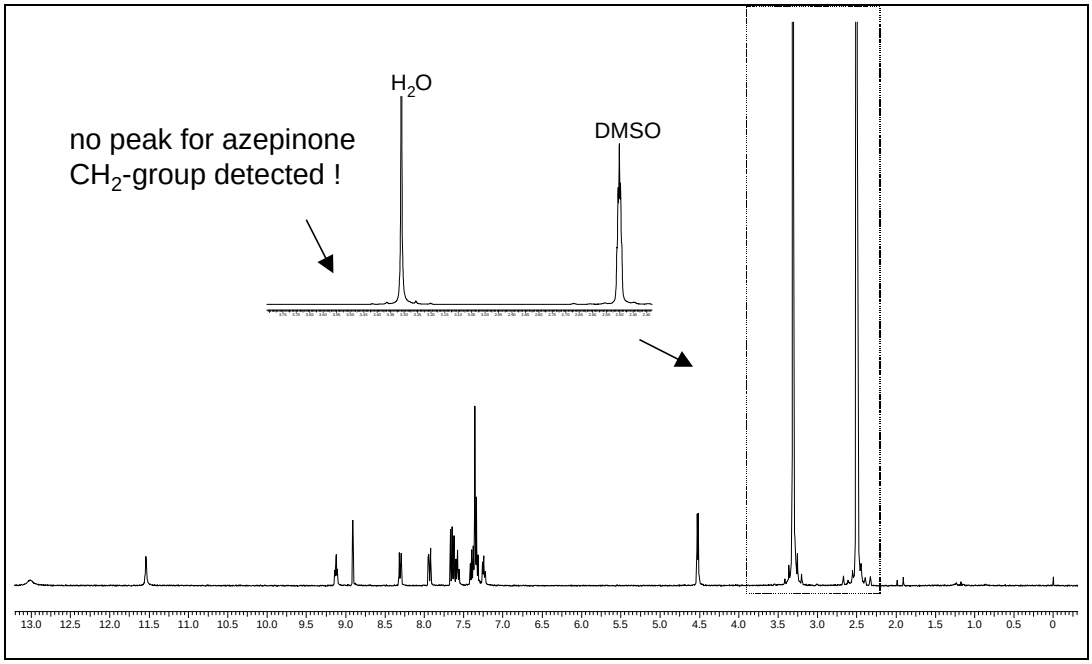

No peak corresponding to an azepinone CH_2-group could be detected.

The lack of the characteristic CH_2-group signal in the ^{1}H-NMR spectrum of the new compound **79a** constituted a fundamental divergence and hinted the occurrence of a skeletal rearrangement within the basic paullone ring structure.

Reflecting on rearrangement processes observed in the past that involve compounds playing a role in paullone chemistry, two examples can be referred to. However, each of the rearrangement procedures pertains to compounds representing intermediate products in the process of paullone synthesis - hence, in both cases, the characteristic paullone ring formation had not yet been established. Once created, the paullone structure had hitherto never been observed to have undergone any skeletal rearrangement processes.

The first rearrangement reaction referred to is related to the conversion of ethyl 5-hydroxy-2-oxo-2,3-dihydro-1*H*-1-benzazepine-4-carboxylate (**26a**) into 3,4-dihydro-1*H*-1-benzazepine-2,5-dione (**27a**). The conversion can be achieved by performing a dealkoxycarbonylation in wet DMSO as previously described by Kunick[44]. However, with reference to MacPhillamy[92] and Hörlein[93], the attempt at synthesizing the cyclic ketone **27a** by acidic or basic saponification of the ester with subsequent decarboxylation provokes a rearrangement reaction and leads to the ring-contracted product **80** (scheme 2-31).

Scheme 2-31:

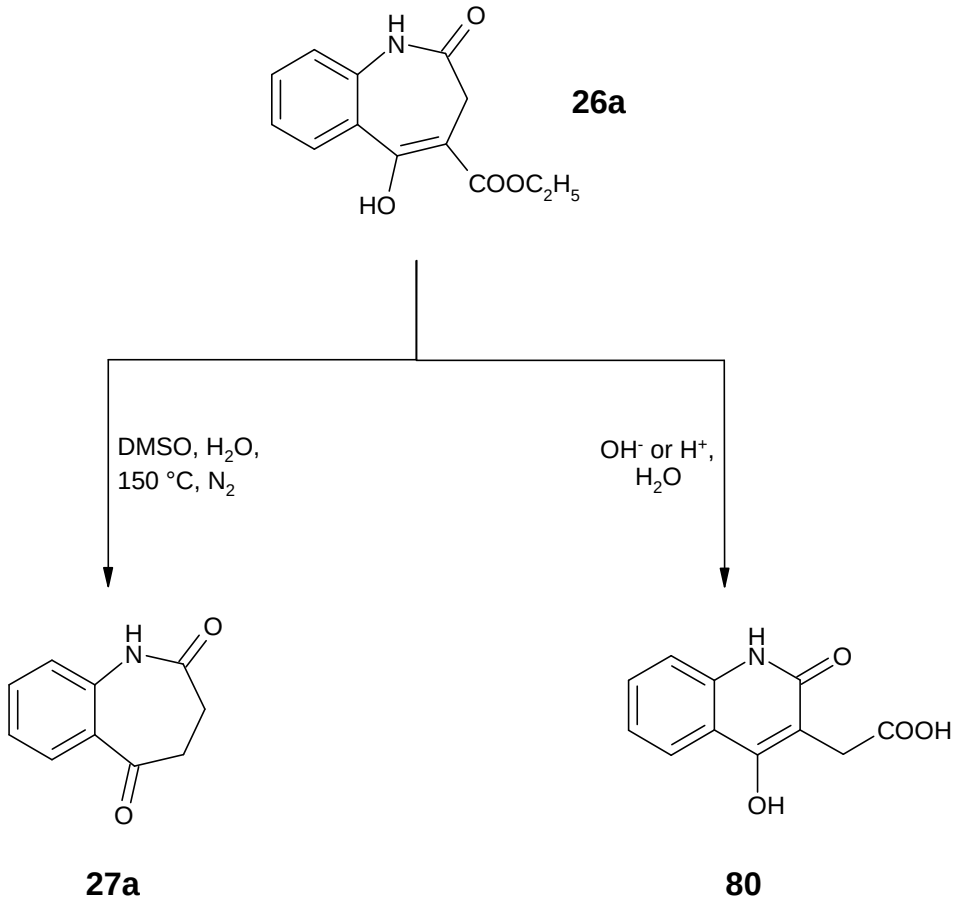

The other rearrangement reaction hitherto observed pertains to the last step of the paullone synthesis, that is, the acid-catalyzed Fischer indole synthesis (cf. chapter 2.1, scheme 2-4). Under certain reaction conditions, a cleavage of the azepinone ring occurs, located at the lactam bond, followed by a cyclization yielding a 4,5-dihydropyridazin-3(2*H*)-one **81**. According to Lauenroth[12], the progression of the reaction depends on the nature of the *para*-substituent of the employed phenylhydrazine as well as the anelland of the azepinone ring. In the reaction stated by Schultz[46] and exemplarily depicted below, the utilized phenylhydrazone **82** provided the rearranged product **81** when stirred in concentrated hydrochloric acid (scheme 2-32).

Scheme 2-32:

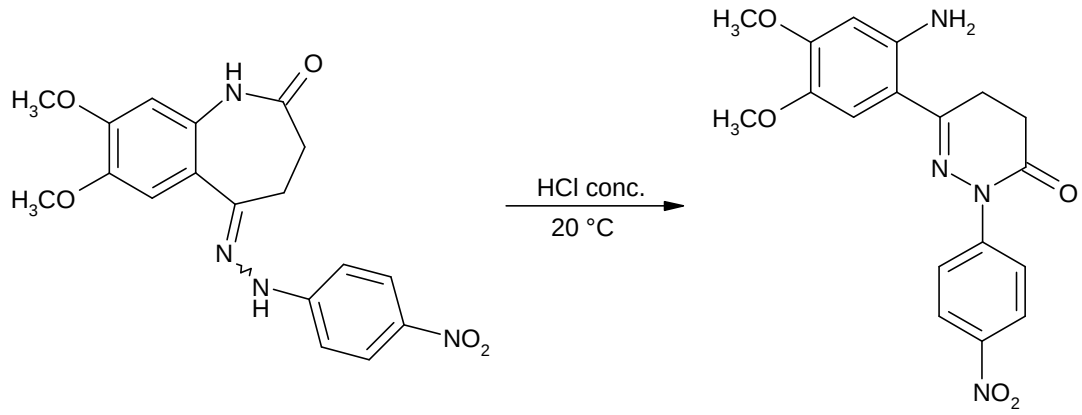

82 **81**

The rearrangement reactions stated above both comprised the decomposition of the azepinone substructure. In accordance with that, the ^{1}H-NMR spectra of the affected substances missed precisely the signal corresponding to the azepinone CH_2-group. These facts triggered further research to focus on the putative occurrence of ring contraction.

Consulting literature for references concerning the ring contraction of azepinone derivatives, several interesting publications were viewed that described rearrangement processes yielding quinoline carboxylic acids. Moore[94] reported on the treatment of an azepinedione “with hot strong aqueous sodium hydroxide”, resulting in the synthesis of an oxo-dihydro-quinoline carboxylic acid. The ring contraction of a 2-chloro-benzazepine-5-one yielding a 2-chloro-quinoline carboxylic acid, presumably via cation

intermediate, was described by Rees.[95] Furthermore, quinoline-2-carboxylic acid (**83**) was obtained by treating 1*H*-1-benzazepine-2,3-dione (**84**) with warm alkali as patented by Hughes[96] and illustrated by Jones[97] (scheme 2-33).

Scheme 2-33:

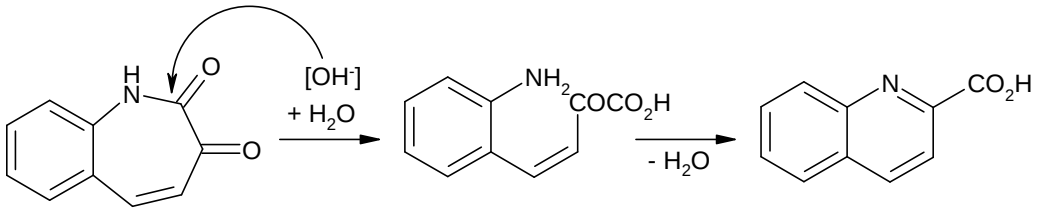

84 **83**

Taking the conversion of a paullone into an 11*H*-indolo[3,2-*c*]quinoline-6-carboxylic acid derivative into consideration, the ^{1}H-NMR spectrum of the unknown product **79a** was restudied (figure 2-15).

Figure 2-15: Integrated ^{1}H-NMR spectrum of compound **79a**

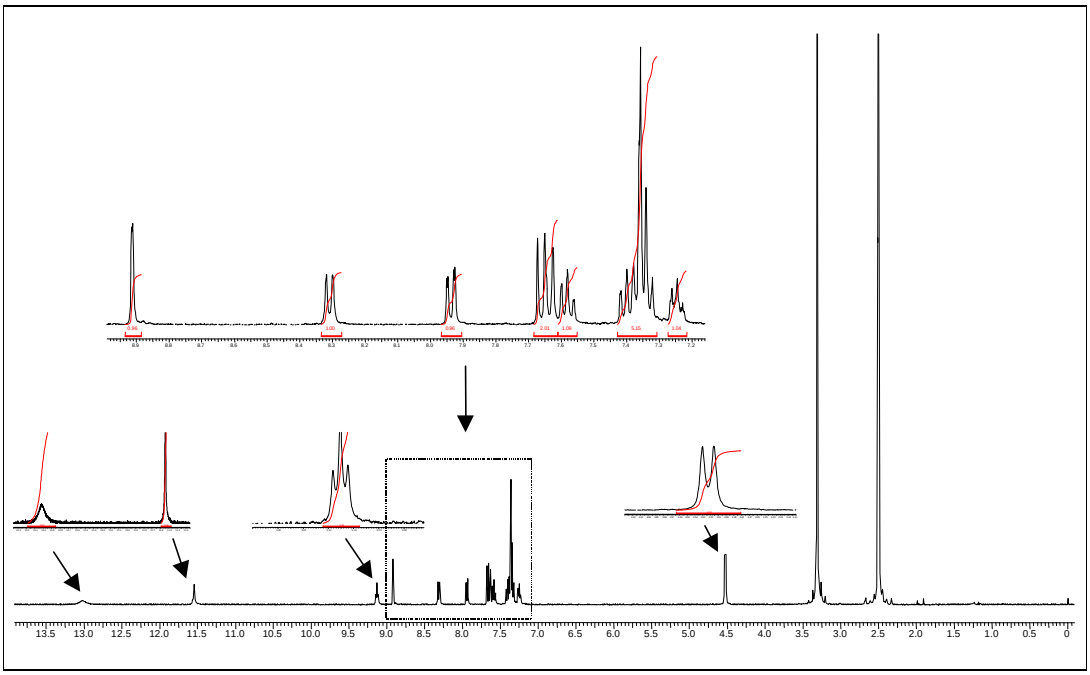

The integrated spectrum exhibits signals corresponding to twelve aromatic protons (δ = 7-9 ppm), to two downfield protons attached to heteroatoms (δ = 11.5 and 13 ppm) and to the NH-group (δ = 9.2 ppm) and CH_2-group (δ = 4.5 ppm) protons of the benzylamide component, displaying their mutual coupling.

The interpretation of the integrated ^{1}H-NMR spectrum supported the hypothesis that the treatment of the paullone educt **39** with EDC/HOBt and benzylamine in DMF led to a skeletal rearrangement process, yielding the 11*H*-indolo[3,2-*c*]quinoline-6-carboxylic acid derivative **79a** (scheme 2-34).

Scheme 2-34:

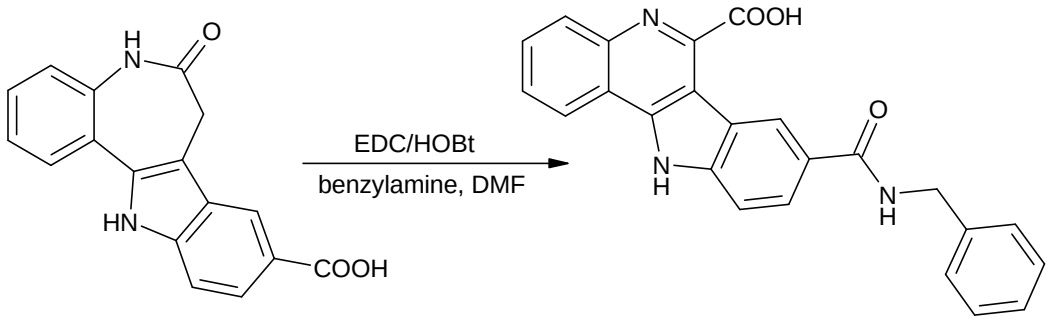

39 **79a**

The proposition of the novel ring structure was substantiated by a matching high-resolution FAB-MS analysis. Further experiments had to be performed in order to gather information about the reagents and reaction conditions provoking the rearrangement procedure.

One point of interest comprised the question whether a paullone-9-carboxamide like **55a** (cf. chapter 2.2.2.4), once synthesized and purified, could be converted into the corresponding quinoline derivative **79a** by means of recrystallization, employing different solvents and additives (scheme 2-35 and table 2-10).

Scheme 2-35:

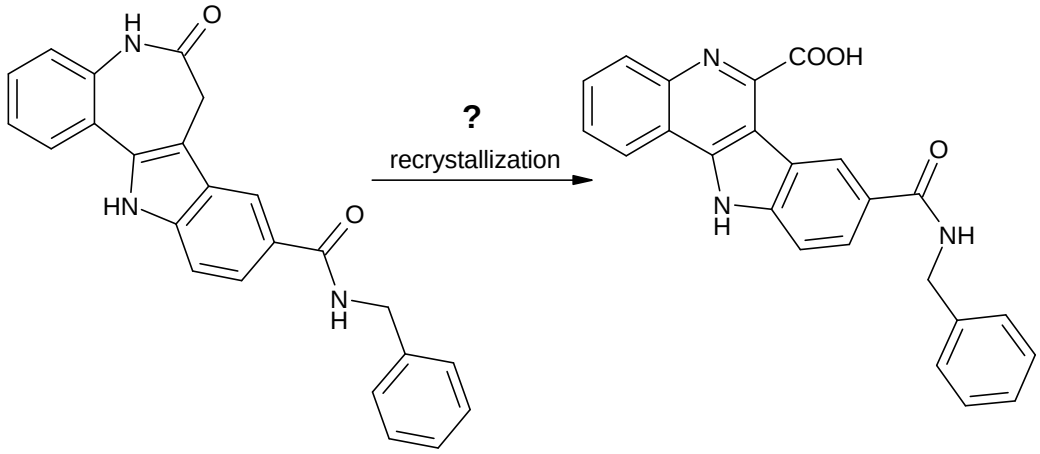

55a **79a**

Table 2-10: Applied conditions for recrystallization of **55a** under reflux

solvent(s)	additive(s)
toluene	-
toluene/ethanol (1/1)	-
toluene	benzylamine
ethyl acetate	-
hexanol	-
hexanol	hydrochloric acid
hexanol/ethyl acetate (1/1)	-
hexanol/ethyl acetate (1/1)	sodium hydroxide
hexanol/ethyl acetate (1/1)	water
hexanol/ethyl acetate (1/1)	water, benzylamine

The solvents hexanol and ethyl acetate were selected to play a major role in this experiment because the compound **79a** was detected for the first time after the recrystallization from hexanol/ethyl acetate (1/1) directly subsequent to the reaction of the educt **39** with EDC/HOBt and benzylamine.

Toluene was chosen due to its fairly high boiling point in order to take into account that high temperatures might serve as a trigger for the rearrangement reaction.

The additives were selected in order to examine whether acid, base, water, or the amine display catalytic effects with respect to the rearrangement process.

The recorded ^{1}H-NMR spectra of the recrystallized substances all show the initial signal pattern of the paullone derivative **55a** - no rearrangement process had taken place under any of the applied recrystallization conditions.

Hence, the possibility of the skeletal rearrangement procedure taking place during the amidation reaction was examined more closely. The next series of experiments therefore explored the effect of changing parameters like the reaction time or the added molar equivalents of the reagents EDC/HOBt. In addition to that, the ^{1}H-NMR spectra of the products before and after recrystallization were compared.

The experiments were performed with (4-methoxybenzyl)amine as the amine component which reacted with the carboxylic acid educt **39** (scheme 2-36 and table 2-11).

Scheme 2-36:

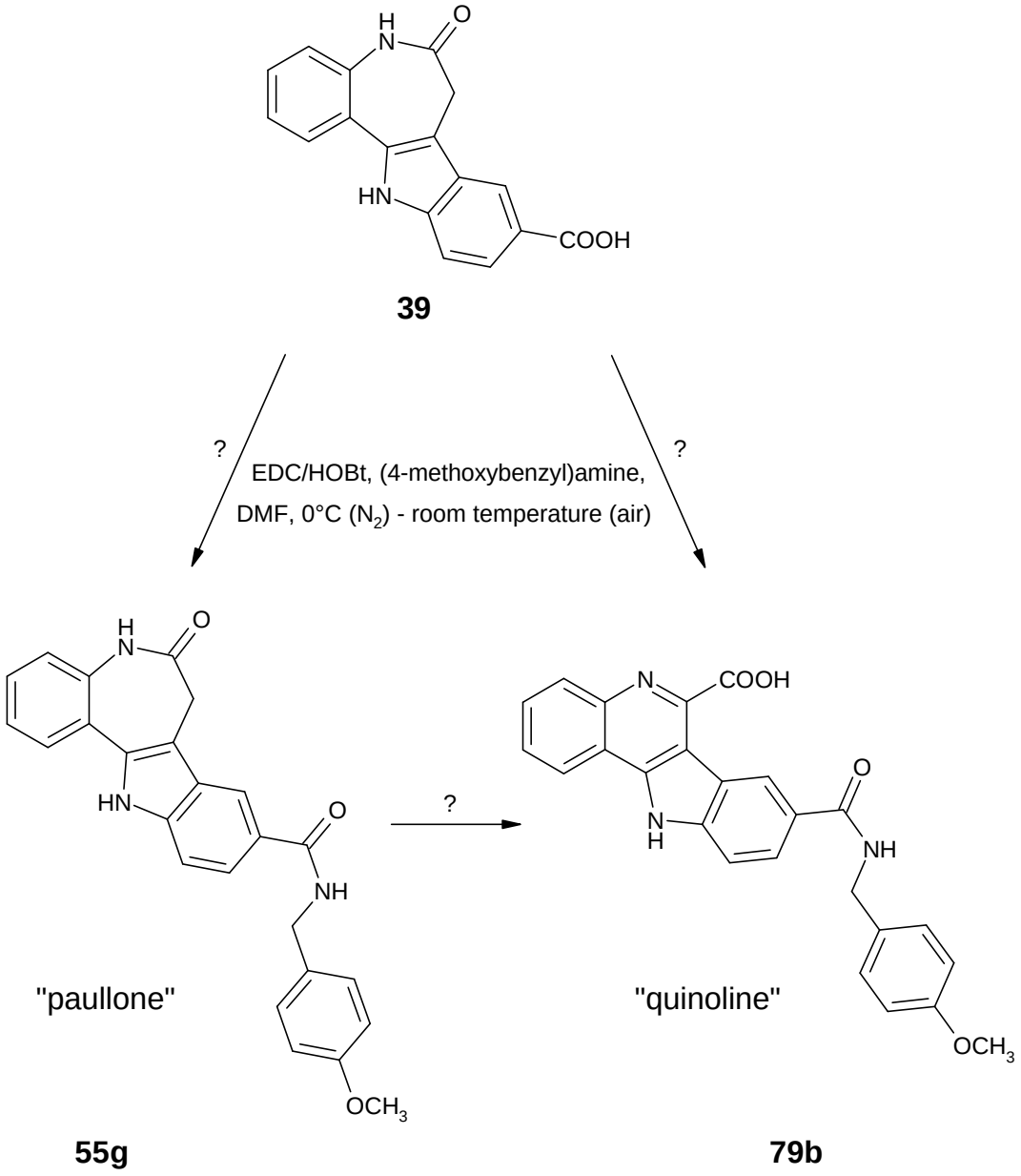

The simplified descriptions signalized with quotation marks serve as identifiers for table 2-11.

Table 2-11: Overview of the applied reaction conditions and the resulting products before and after recrystallization

Expt. #	equivalents EDC/HOBt	rct. time 0 °C/N_2	rct. time RT/air	product before recr.	product after recr.
1	1.2 eq	**3:00 h**	**5 d**	n/a	quinoline
2	1.5 eq	1:10 h	**3 d**	quinoline	quinoline
3	1.3 eq	1:00 h	24 h	paullone	paullone
4	1.3 eq	1:00 h	**4 d**	quinoline paullone	quinoline
5	1.3 eq	**3:00 h**	24 h	paullone	paullone
6	1.3 eq	1:20 h	**14 d**	quinoline	quinoline
7	**3.0 eq**	1:10 h	24 h	paullone quinoline	quinoline
8	**3.0 eq**	1:10 h	**14 d**	quinoline	quinoline

Standard conditions leading to a paullone product comprised 1.3 molar equivalents EDC/HOBt, one hour reaction time at 0 °C under nitrogen atmosphere and 24 hours reaction time at room temperature/air (as in experiment #3).

Parameters crucially differing from the experimentally determined standard reaction conditions are pointed out in bold letters.

The term “paullone” represents compound **55g** and the term “quinoline” represents compound **79b**.

If two products were identified, the one listed first constitutes the main product.

Recrystallization was performed from ethanol (expt. #2-#5, #8) or from ethanol/toluene (expt. #1, #6, #7) and under reflux (exception: expt. #7, no heat applied).

In experiment #1, an ^{1}H-NMR spectrum was not recorded before recrystallization; the primary product is thus unknown (“n/a”).

The evaluation of the collected data allowed certain conclusions to be drawn concerning the reaction conditions provoking the rearrangement process:

The reaction time at room temperature seems to be the crucial factor. If prolonged distinctly, the performed reaction yielded the quinoline derivative **79b** (expt. #6 and #8). In case of minor prolongation, both quinoline **79b** and paullone derivative **55g** (expt. #4) were obtained.

The amount of the added reagents EDC/HOBt only unfolds a minor effect. Increasing the excess of the reagents applied to the reaction mixture provided the paullone derivative **55g** as the main product and quinoline **79b** as a side product (expt. #7).

The prolongation of the reaction time at 0 °C under nitrogen atmosphere does not initiate the skeletal rearrangement procedure (expt. #5).

The process of recrystallization does not convert the paullone derivative **55g** into the corresponding quinoline **79b** (expt. #3, #5). In the case of both compounds being present before the recrystallization process, only the quinoline derivative **79b** was detected afterwards (expt. #4, #7). However, this occurrence might simply be based on a higher solubility of the paullone product **55g** in the recrystallization solvent. In order to further investigate this eventuality, an HPLC analysis was performed. The chromatogram of the precipitated product after recrystallization was compared to the one of the appropriate filtrate. The solid precipitate produced a large peak corresponding to the quinoline **79b** as expected from the recorded ^{1}H-NMR spectrum. The chromatogram of the filtrate though displayed two peaks, one representing the paullone **55g** and the other representing the quinoline **79b**, thus documenting the presence of both reaction products after the recrystallization process. The HPLC analysis therefore explicitly proved that the rearrangement procedure was not caused or promoted by recrystallization.

The performed experiments gave valuable insights concerning the initiation of the observed skeletal rearrangement, yet the drawn conclusions necessitated verification. It also remained to be elucidated whether the amide residue present in the affected compounds like **79a** and **79b** was of any significance for the rearrangement procedure. Hence, an experiment considering both issues was designed: the investigation of the impact unfolded by the long term treatment with the reagents EDC and HOBt at room temperature under air atmosphere on a well characterized paullone derivative not containing an amide residue, that is, kenpaullone (**1**).

The recorded ^{1}H-NMR spectra of the utilized educt **1** and the obtained product **79c** clearly illustrate that the applied reaction conditions indeed provoked a skeletal rearrangement process (scheme 2-37 and figure 2-16).

Scheme 2-37:

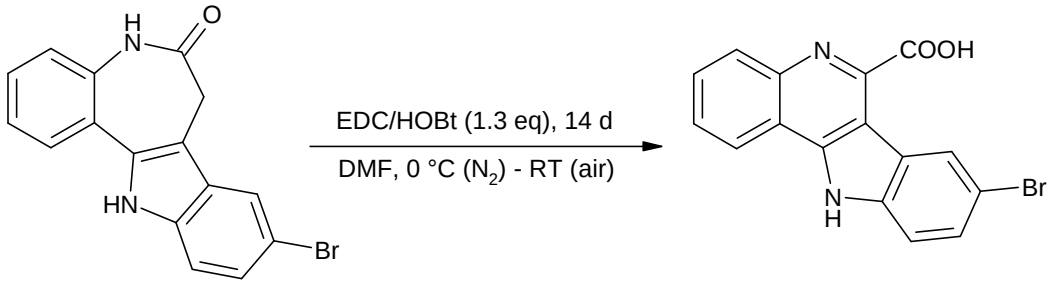

1 **79c**

Hence, it was proven that the amide residue did not play a role in the rearrangement procedure. Furthermore, a confirmation of the postulated reaction conditions triggering the process was achieved.

Figure 2-16: Comparison of the ^{1}H-NMR spectra of kenpaullone (**1**) and the corresponding quinoline derivative **79c**

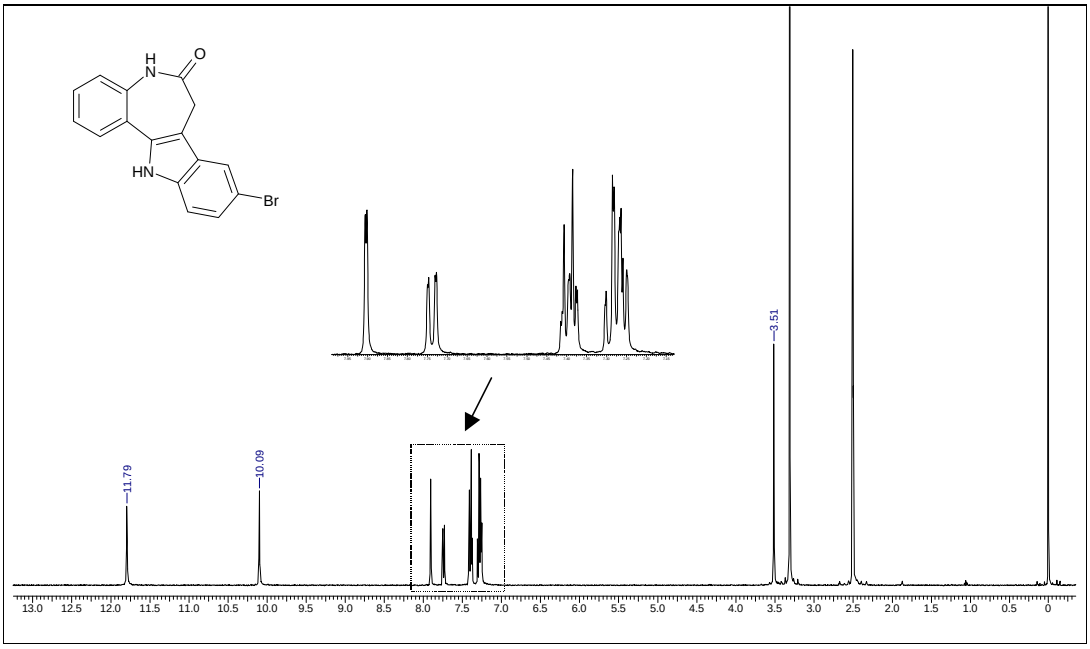

The azepinone CH_2-group displays a signal at δ = 3.5 ppm, and the protons attached to the nitrogen atoms are detected at δ = 10.1 and 11.8 ppm.

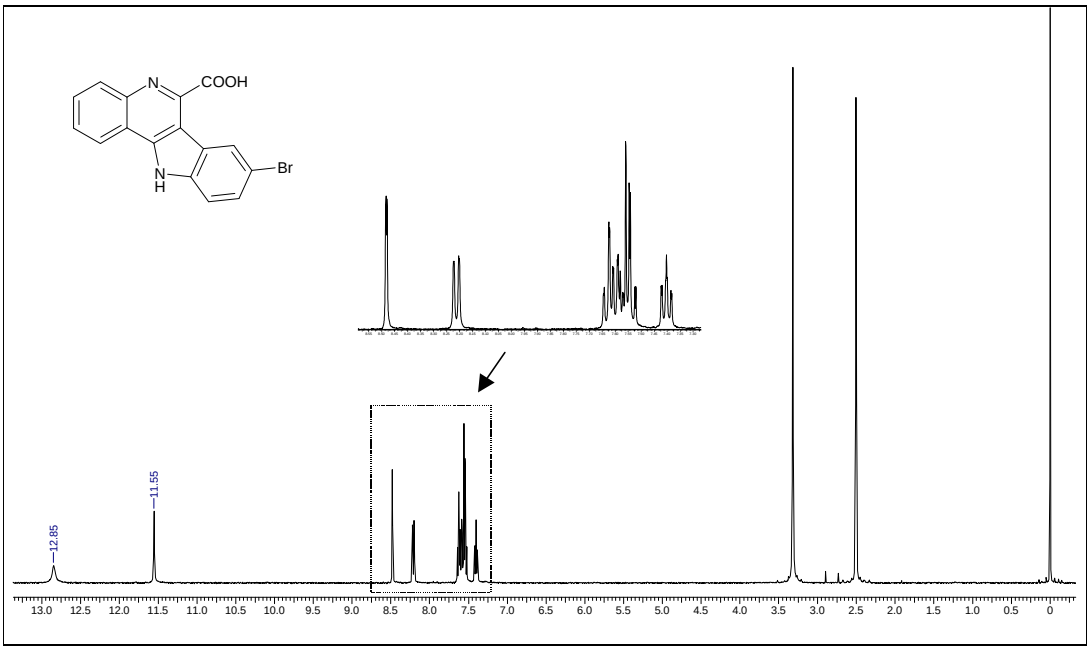

There is no signal representing a CH_2-group, the protons attached to the heteroatoms display singlets further downfield at δ = 11.6 and 12.9 ppm, and the aromatic region shows a different pattern.

The synthesized compound **79c** constituted a suitable representative of the new substance class for performing further analytical investigations, thus affording the opportunity to substantiate the assumption of obtaining 11*H*-indolo[3,2-*c*]quinoline-6-carboxylic acids as the actual products of the rearrangement procedure.

IR

The recorded IR spectra of the paullone educt **1** and the rearranged product **79c** document the change in the basic ring structure (figure 2-17).

Figure 2-17: Overlaid IR spectra of kenpaullone (**1**), upper curve, and the corresponding quinoline derivative **79c**, lower curve

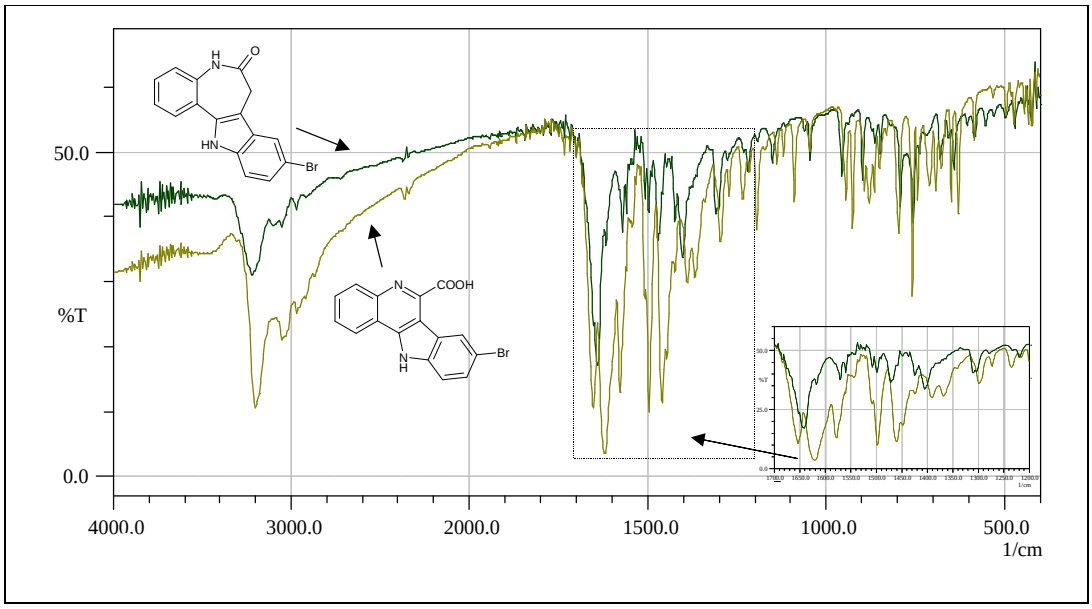

The enlarged section of the IR fingerprint region, depicted in the bottom right corner, clearly illustrates the differing molecular vibrations caused by the diverse structures of educt **1** and product **79c**.

The broad band visible in the high frequency region of the IR spectrum of the rearranged substance **79c** can be assigned to the OH-group of the carboxylic acid functionality comprised in the new ring structure.

The C=O stretching vibration corresponding to the carboxylic acid functionality is not observed in the vicinity of 1700 cm^{-1} as generally expected for carboxylic acids; it is instead detected in a lower wave number region. This phenomenon results from H-bonding formation between the carboxylic hydrogen and the nitrogen atom and is characteristic of the quinaldic acid substructure as stated by Thomas[98] and Goher[99].

NMR

The ^{1}H-NMR spectra of kenpaullone (**1**) and the corresponding quinoline derivative **79c** have already been depicted and elucidated (figure 2-16).

The evaluation of the obtained ^{13}C-NMR spectra provided further evidence for the creation of a new substance class (figures 2-18 and 2-19).

Figure 2-18: ^{13}C-NMR spectrum of kenpaullone (**1**)

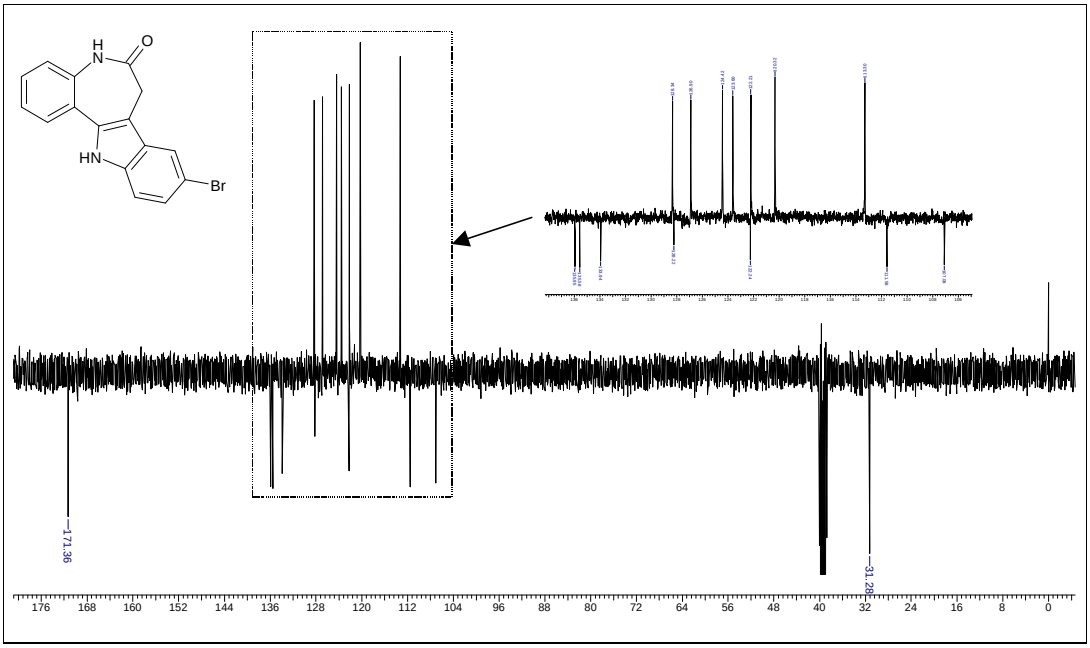

Signals for one secondary, seven tertiary and eight quaternary carbons are detected, thus matching the structure of kenpaullone (**1**).

The peak at δ = 31 ppm corresponds to the azepinone CH_2-group, the peak at δ = 171 ppm represents the carbonyl carbon of the lactam functionality.

Figure 2-19: ^{13}C-NMR spectrum of compound **79c**

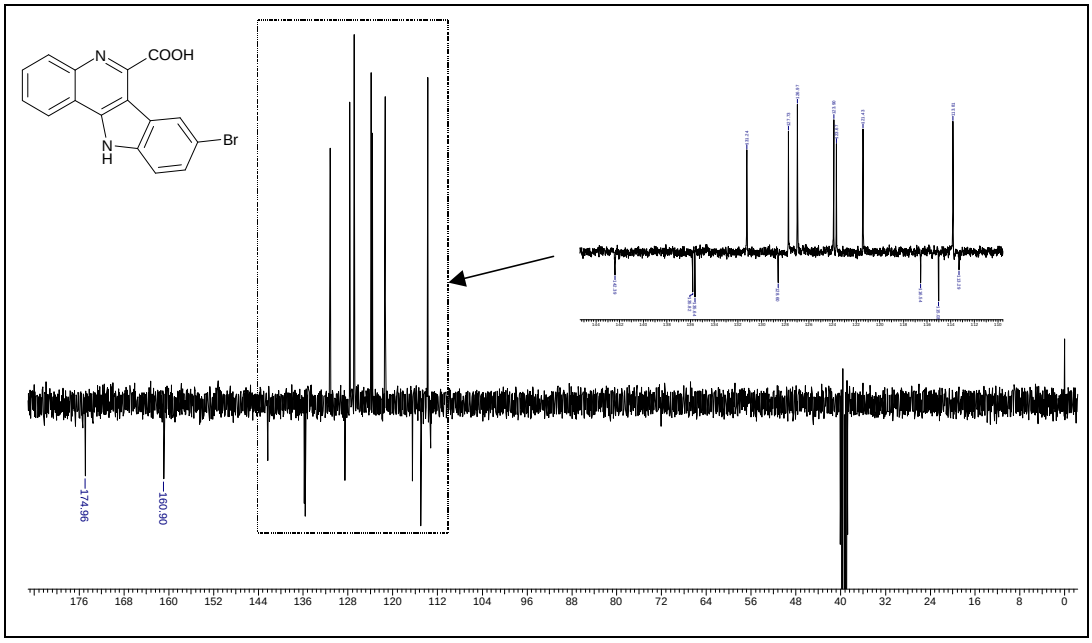

The spectrum displays peaks corresponding to seven tertiary and nine quaternary carbons, hence confirming the postulated ring structure of the rearranged product **79c**.

In consequence of the occurred ring contraction, a signal representing the secondary carbon incorporated in the azepinone substructure cannot be observed.

The quaternary carbons of the quinaldic acid derivative **79c** are located further downfield compared to the ones of the educt **1**. The peak representing the carbonyl carbon of the carboxylic acid functionality is detected at δ = 175 ppm.

In order to thoroughly substantiate the postulation concerning the ring structure of the product **79c**, 2D-NMR experiments were conducted.

The determination of the coupling existent between protons can be performed by ^{1}H-^{1}H correlation spectroscopy (^{1}H,^{1}H-COSY) which features the plotting of the proton spectrum on both axes.[100] The analysis of the resulting coupling pattern provides information about the exact location of the protons within the molecule. The enlarged aromatic region of the recorded ^{1}H,^{1}H-COSY spectrum of the rearranged product **79c** displays a proton coupling pattern that is in accordance with the assumed compound structure (figure 2-20).

Figure 2-20: $^{1}H,^{1}H$-COSY spectrum of compound **79c**

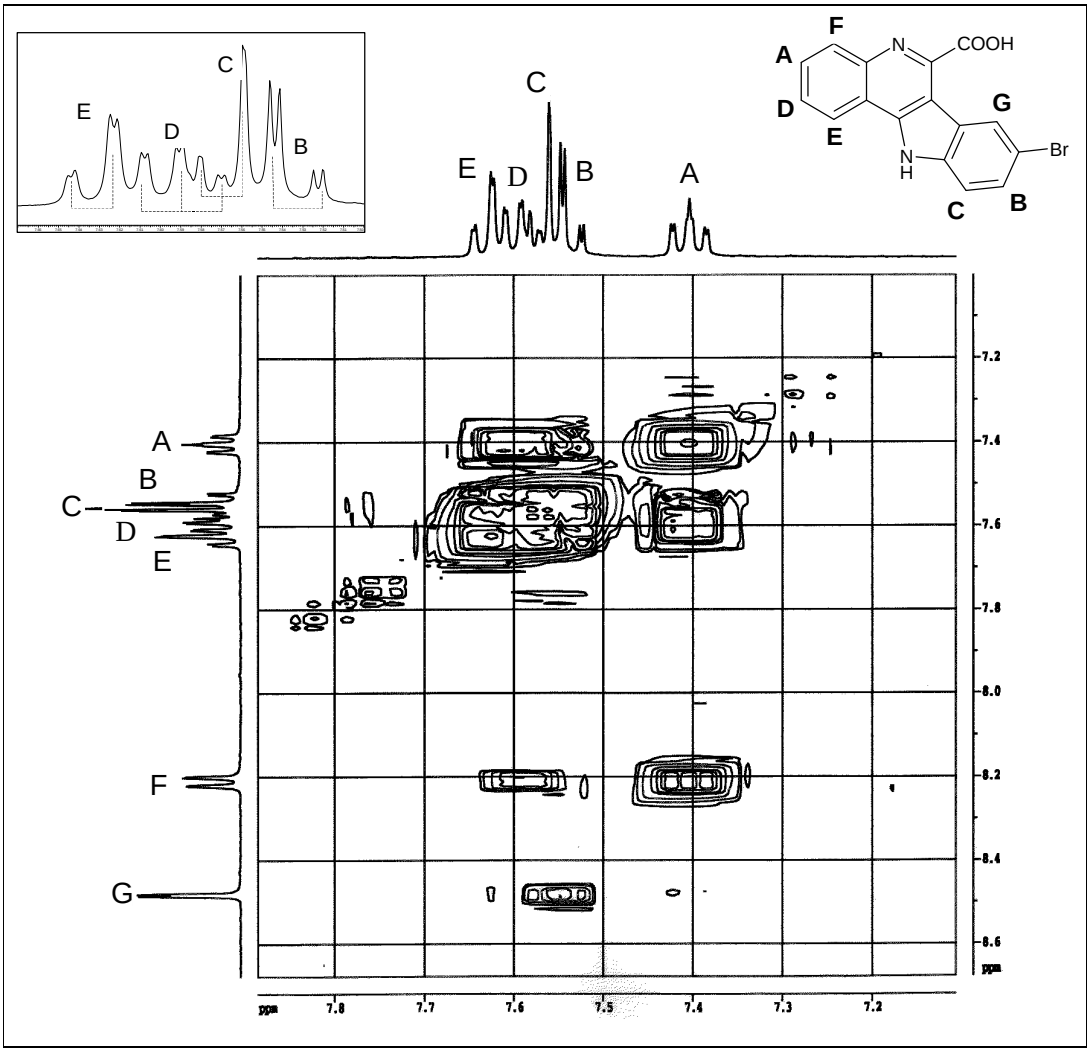

The signals depicted on the axes of the $^{1}H,^{1}H$-COSY spectrum, corresponding to the protons A-G, could be assigned to the proper positions of the hydrogen atoms within the molecule as shown in the upper right corner of the illustration.

Perspicuously visible are the *ortho* coupling between the protons A and F and the *meta* couplings between the protons B and G and the protons D and F.

The illustration showing an enlarged part of the aromatic region, displayed in the upper left corner, elucidates the composition of the signals corresponding to the protons B through E.

The coupling between the nuclei of different elements can be detected applying Heteronuclear Correlation Spectroscopy (HETCOR). The performance of an HMQC (Heteronuclear Multiple Quantum Correlation) experiment constitutes a suitable method for determining which protons of a molecule are bonded to which ^{13}C-nuclei. The HMQC spectrum recorded of the synthesized compound **79c** shows only signals originating from tertiary carbons which complies with the hypothetical product structure, hence serving as further evidence (figure 2-21).

Figure 2-21: HMQC spectrum of compound **79c**

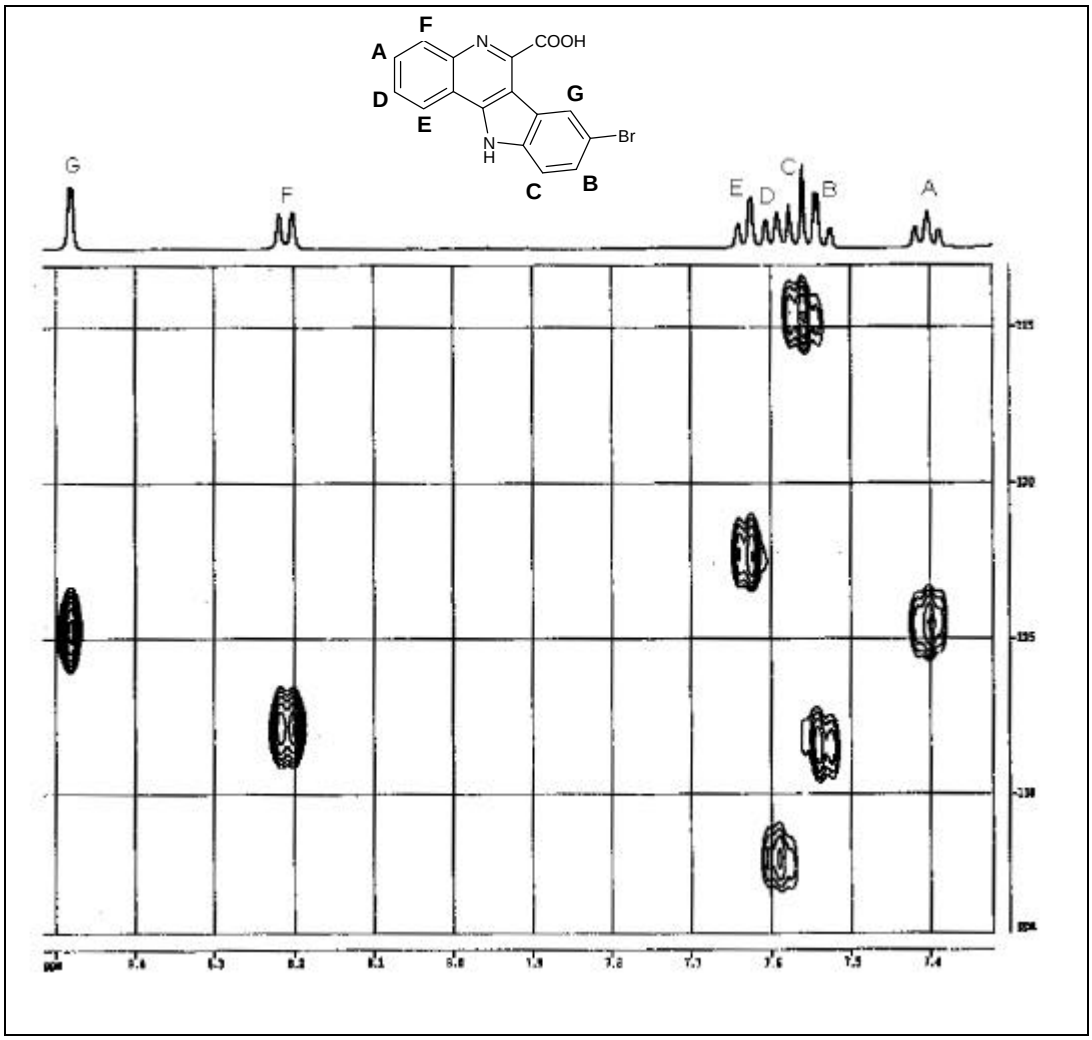

The illustration presents an enlarged view of the relevant field region and facilitates the assignment of the seven detected signals to the corresponding nuclei.

UV/VIS

An organic compound containing one or more chromophoric groups is susceptible to qualitative and quantitative analysis by means of ultraviolet/visible (UV/VIS) absorption spectroscopy.[101] Both the educt kenpaullone (**1**) and the quinoline product **79c** constitute aromatic substances, and thus comprise chromophoric groups. However, the ring structures of the two substance classes differ, and therefore altering UV/VIS spectra should be obtained. The performed experiments did provide different absorption curves, thus verifying the established assumption (figure 2-22).

A publication by Goher[99], dealing with the analytical characterization of free and coordinated quinaldic acid, states that the UV/VIS spectrum of the free quinaldic acid (**85**) shows two absorption bands in the UV region at 230 nm and 280 nm together with a shoulder at 315 nm. In the spectrum of the rearranged product **79c** (figure 2-22), an absorption band appearing with a shoulder can be detected at the described wavelengths. A second absorption band is located in a higher wavelength region which constitutes a bathochromic shift compared to the described spectrum of the free quinaldic acid. This can be explained by the additional aromatic rings comprised in the structure of compound **79c**, resulting in the expansion of the chromophoric system, and thus in a decrease in required excitation energy.

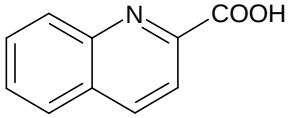

85

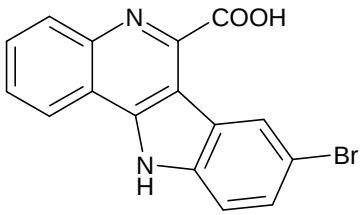

79c

Figure 2-22: UV/VIS spectra of kenpaullone **1** and compound **79c**

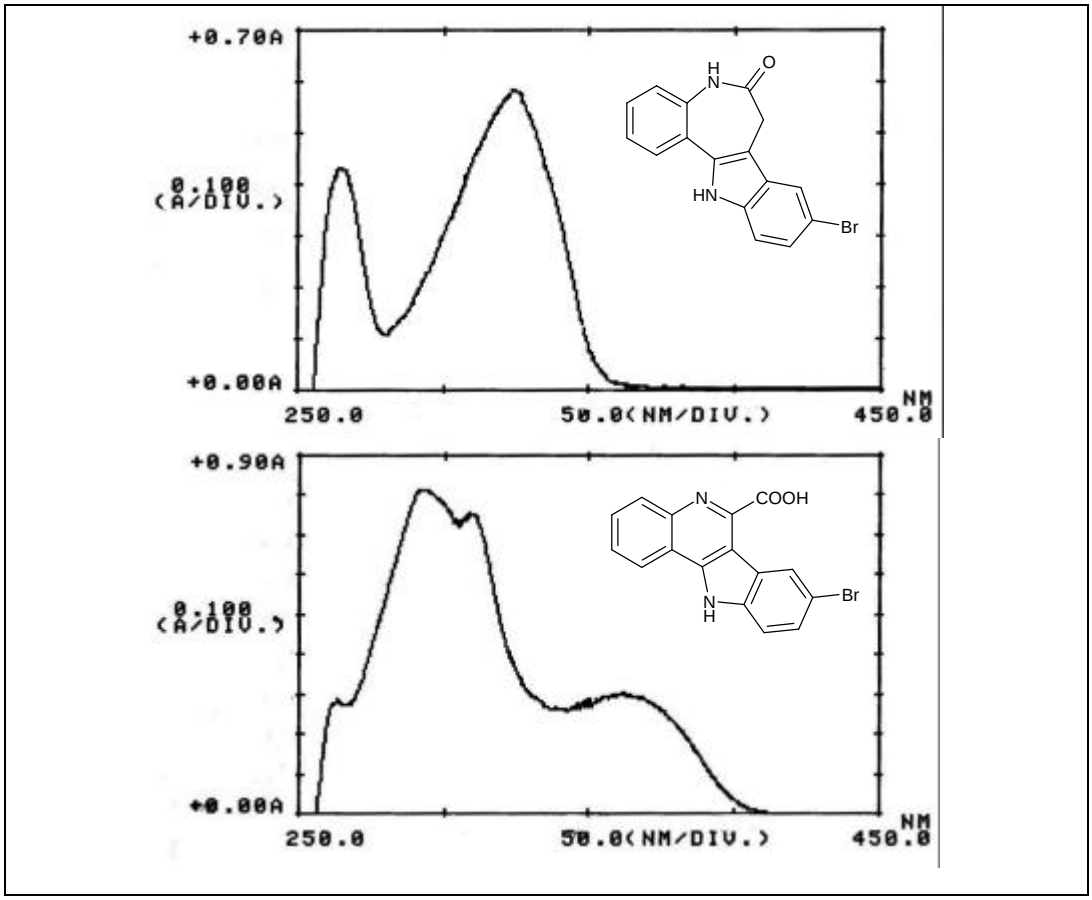

The compounds **1** and **79c** are clearly distinguishable by their UV/VIS spectra. Maxima and minima of the absorption curves are located at different wavelengths.

Having elucidated the constitution of the novel compound **79c** by various analytical procedures and confirmed it by obtaining a correct elemental analysis, the next target constituted the clarification of the reaction mechanism which the rearrangement procedure was based on.

It had to be examined whether both reagents played an essential role in the skeletal rearrangement process. In literature, references concerning rearrangement reactions in connection with either EDC or HOBt could not be found. Thus, a series of experiments was performed in order to gain crucial insights:

Kenpaullone (**1**) was treated under reaction conditions similar to the ones applied before but with the exception of employing EDC as the only reagent. Interestingly, a rearrangement process yielding the compound **79c** could not be observed.

The experiment was repeated substituting HOBt for EDC as the single utilized reagent. The ^{1}H-NMR spectrum recorded of the obtained product revealed that the rearranged compound **79c** had been produced. It was therefore concluded that the presence of HOBt alone sufficed for triggering the skeletal rearrangement under the applied reaction conditions (scheme 2-38).

Scheme 2-38:

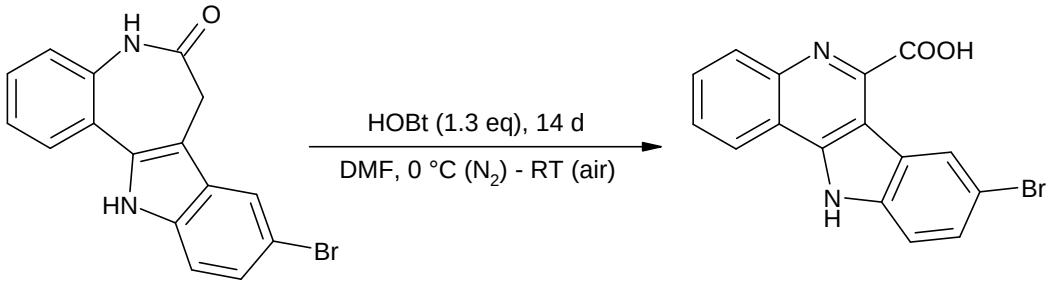

1 **79c**

As a follow-up, it was investigated whether a change in the utilized reaction conditions could impede the rearrangement process. Hence, the experiment was performed again with HOBt as the single utilized reagent, this time supplying nitrogen atmosphere throughout the whole reaction procedure, that is, additionally during the reaction time at room temperature. This alteration led to the preservation of kenpaullone (**1**) –

the quinoline derivative **79c** was not synthesized. Consequently, it was deduced that an oxidation reaction must constitute the first step of the skeletal rearrangement procedure.

Searching literature for references dealing with oxidation reactions that involve the usage of HOBt, several publications were discovered that reported on oxidation procedures executed by a redox system consisting of laccase in combination with HOBt.[102-105]

Laccases are enzymes defined as multi-copper oxidases. HOBt serves as a “laccase mediator” within this redox system. Redox-active mediators shuttle electrons between acceptor and donor molecules. With reference to Niku-Paavola[104], current theories state that laccase oxidizes HOBt as well as other *N*-hydroxy [-N(OH)-] mediators to radical intermediates. In accordance with that, Xu[103,105] and Li[102] propose that a single-electron oxidation of *N*-hydroxy compounds yields N-O· radicals which subsequently cause the oxidation of the substrates. These N-O· radicals constitute highly unstable intermediates and quickly decay into catalytically inactive products. A scheme adapted from Li[102] illustrates the proposed mechanism for the “laccase-mediator oxidation” with HOBt (scheme 2-39).

Scheme 2-39:

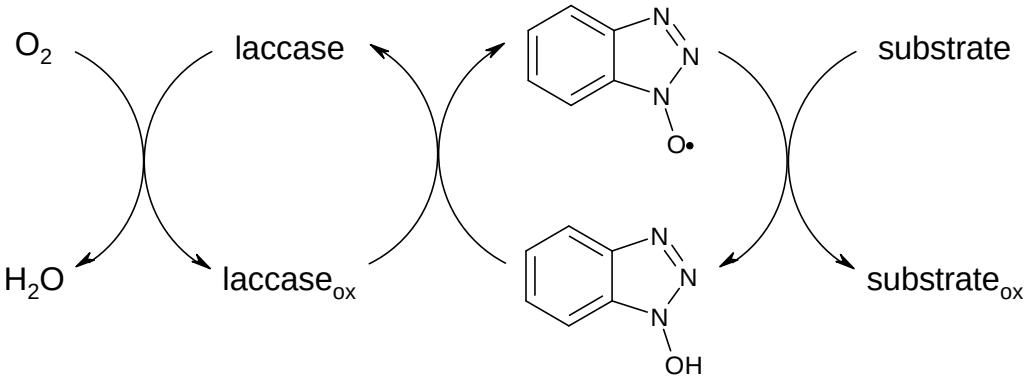

Recently, interesting reports have been published concerning the catalytic activity of *N*-hydroxyphthalimide in the aerobic oxidation of hydrocarbons and other organic substrates. The oxidation reactions were performed under non-electrochemical and non-enzymatic reaction conditions, catalyzed by the N-OH compound utilizing molecular oxygen (dioxygen) as the primary oxidant.[106-108]

The underlying reaction mechanism was investigated by Ishii[106] who suggested, based on the fact that the reaction could be completely inhibited by adding a radical inhibitor, that the oxidation proceeded via a radical process. It was also proposed that the reaction pathway resembled a free radical autoxidation, claiming the formation of the phthalimide N-oxyl radical **86** from dioxygen and *N*-hydroxyphthalimide (**87**) to be the initiating step of the oxidation reaction. In order to verify this postulation, experiments were performed in which *N*-isopropoxy-phthalimide (**88**) was substituted for *N*-hydroxyphthalimide (**87**). As a consequence thereof, no oxidation reactions were observed, and thus the generation of a phthalimide radical **89** by nitrogen-oxygen bond cleavage was deemed improbable (scheme 2-40).

Scheme 2-40:

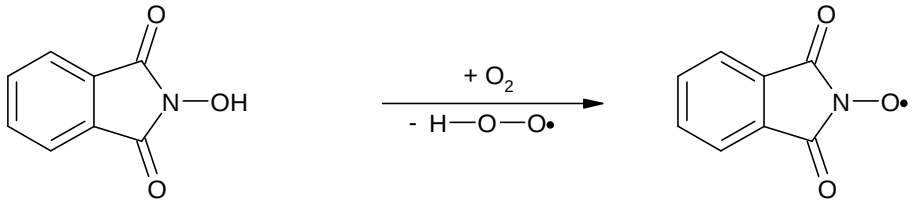

87 **86**

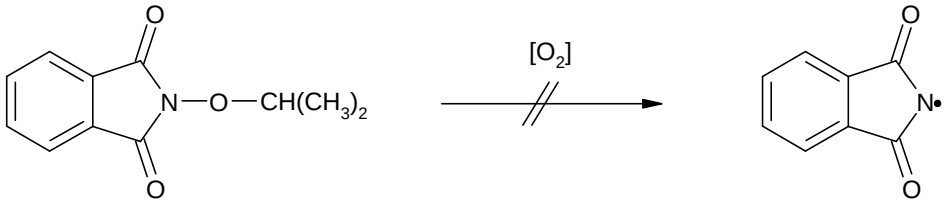

88 **89**

The postulated reaction mechanism further comprised the abstraction of a hydrogen atom from the substrates by the generated N-oxyl radical **86**, resulting in alkyl radicals. Subsequent oxygenations by molecular oxygen produced peroxy radicals which were, according to Ishii[106], converted into ketones or dicarboxylic acids.

In further experiments, analogs of *N*-hydroxyphthalimide (**87**), that is, *N*-hydroxysuccinimide and *N*-hydroxymaleinimide, were proven to be also applicable as catalysts in aerobic oxidation reactions.[106]

With respect to the skeletal rearrangement of kenpaullone (**1**), it is thus imaginable that the *N*-hydroxy compound HOBt might serve as a radical catalyst, provoking the oxidation of the paullone **1** and therewith the production of the corresponding benzazepinedione **90** (scheme 2-41).

Scheme 2-41:

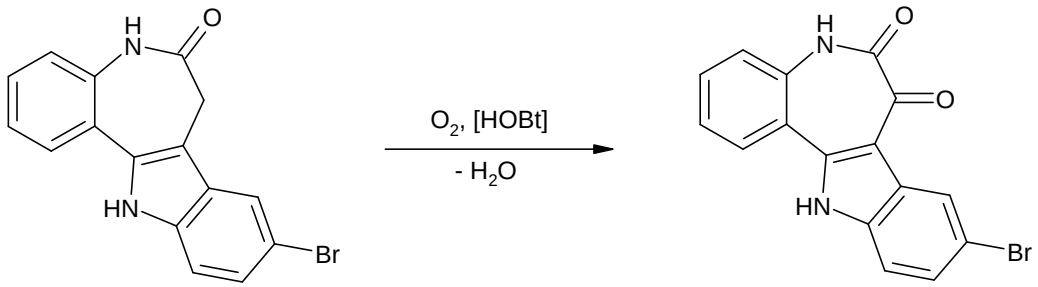

1 **90**

The oxidation reaction of kenpaullone (**1**) by molecular oxygen can be postulated to proceed in a similar fashion as the described catalysis involving *N*-hydroxyphthalimide (**87**). Therefore, the underlying reaction mechanism is proposed analogously (scheme 2-42).

Scheme 2-42:

I)

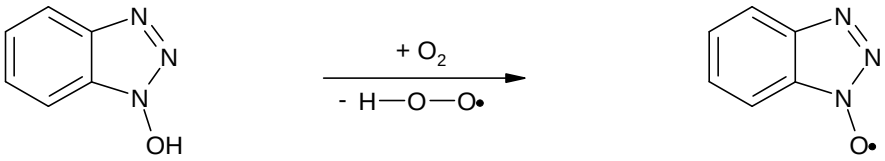

72 **91**

II)

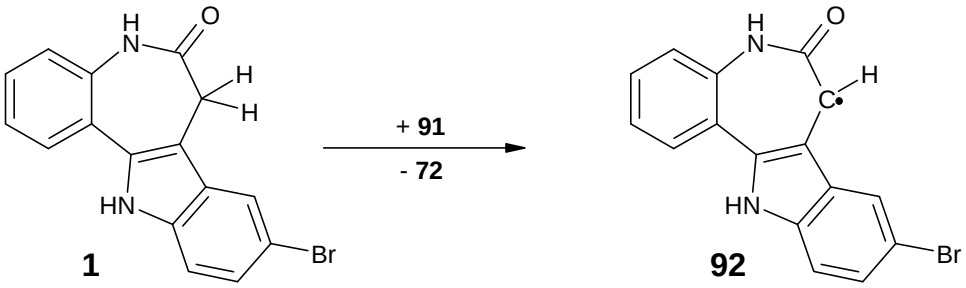

1 **92**

III)

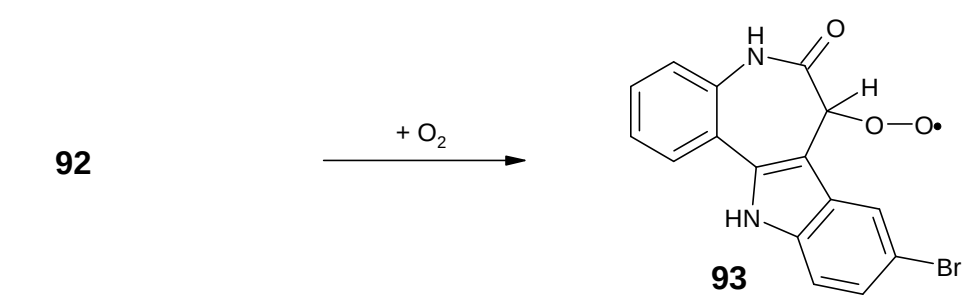

93

IV)

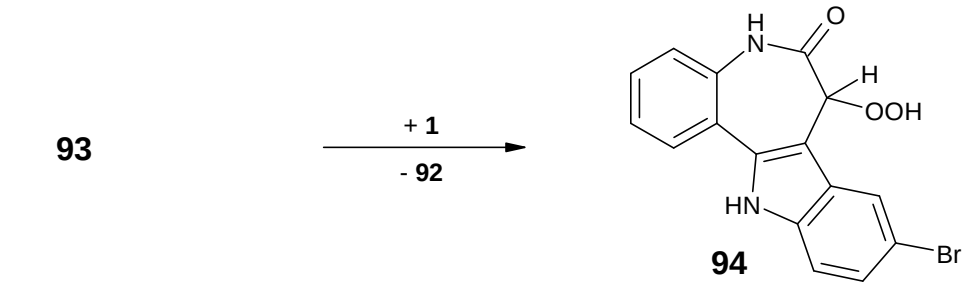

94

V)

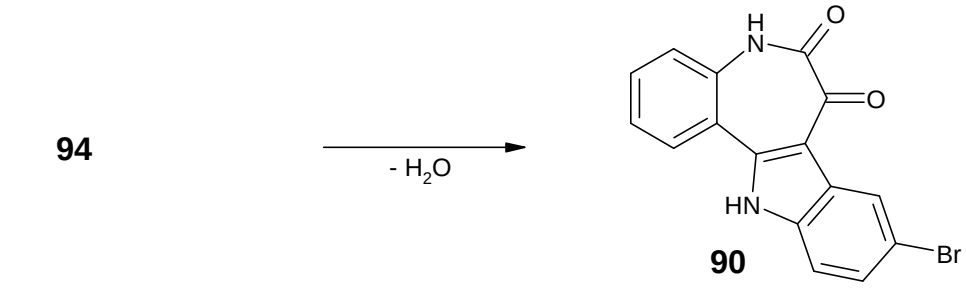

90

As the initiating step, the benzotriazole N-oxyl radical **91** is generated from HOBt (**72**) and molecular oxygen (equation I).

The created radical **91** then abstracts a hydrogen atom from kenpaullone (**1**) and forms the corresponding alkyl radical **92** (equation II).

The following oxygenation of the alkyl radical **92** by dioxygen results in the formation of the appropriate peroxy radical **93** (equation III).

Representing the characteristic propagation reaction, the peroxy radical **93** abstracts a hydrogen atom from kenpaullone (**1**), supplying the alkyl radical **92** for further oxygenations. The peroxy radical **93** is converted into the hydroperoxide **94** (equation IV).

In the final step, the hydroperoxide **94** decomposes, yielding the benzazepinedione derivative **90** (equation V).

Hydroperoxides are known to be the principal reaction products of the autoxidation of organic compounds with cleavable hydrogen atoms.[109] With reference to Criegee[110], secondary hydroperoxides that carry an aromatic residue are particularly accessible to conversion reactions yielding ketones. Furthermore, Cullis[111] reports on the production of 1,2-dicarbonyl compounds through aerobic oxidation, however in small yields only. It is suggested that the mechanism of such reactions involves the formation of an α-hydroperoxy ketone which is concordant with the reaction pathway postulated above.

The autoxidation of tetralin constitutes a relevant example of this type of reaction as the subsequent decomposition of tetralin hydroperoxide provides the corresponding ketone **95** as a major product. Tetralone (**95**) itself is autoxidized, yielding an α-hydroperoxy ketone **96** as an intermediate product, resulting in the formation of tetrahydro-1,2-naphthalenedione (**97**) and the enol tautomeride **98** among other products (scheme 2-43).[111,112]

Scheme 2-43:

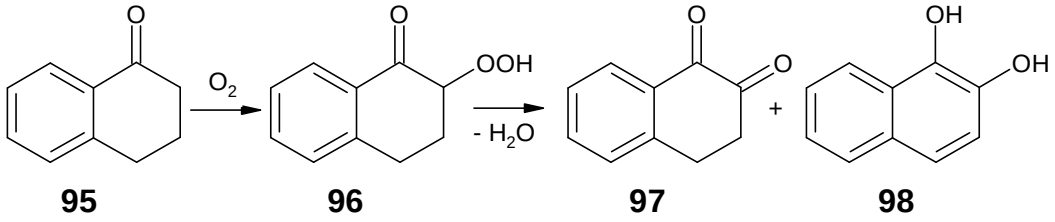

95 **96** **97** **98**

Having proposed an imaginable reaction pathway for the generation of the dioxobenzazepine derivative **90** from kenpaullone (**1**) by aerobic oxidation with HOBt as a catalyst, the subsequent conversion of **90** into the corresponding quinoline derivative **79c** needed to be analyzed next.

In the beginning of this subchapter, it was referred to Hughes[96] and Jones[97] who had reported on a reaction dealing with the conversion of 1*H*-1-benzazepine-2,3-dione into quinoline-2-carboxylic acid under treatment with warm alkali (illustrated in scheme 2-33). In this reaction, the oxygen atom of the hydroxide anion had supposedly attacked the carbonyl carbon atom of the lactam functionality, provoking ring cleavage. Subsequently, the amino group reacted with the α,β-unsaturated ketone carbonyl functionality, resulting in the ring-contracted quinaldic acid.

It is conceivable that the oxygen atom of the catalyst HOBt **72** attacks the carbonyl carbon atom of the lactam functionality present in the oxidized kenpaullone derivative **90** in a similar fashion. Compared to kenpaullone (**1**), the benzazepinedione **90** is more susceptible to this ring cleavage reaction because of the stronger activation of the attacked lactam carbonyl carbon which is neighbored by the additional electron-withdrawing carbonyl functionality. The intermediate product **99** is believed to undergo a condensation reaction which provides the quinaldic acid ester derivative **100**. The last step of this postulated reaction mechanism consists in the hydrolysis of the ester **100**, providing 8-bromo-11*H*-indolo[3,2-*c*]quinoline-6-carboxylic acid (**79c**) as the final product of the skeletal rearrangement procedure (scheme 2-44).

Scheme 2-44:

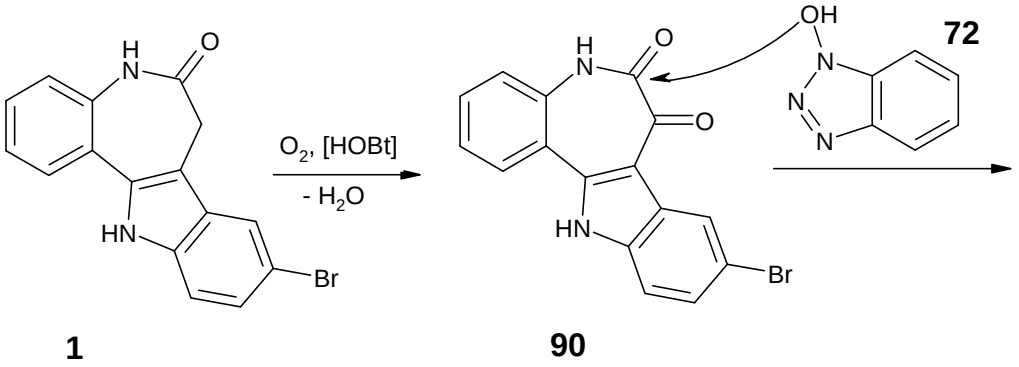

1 **90**

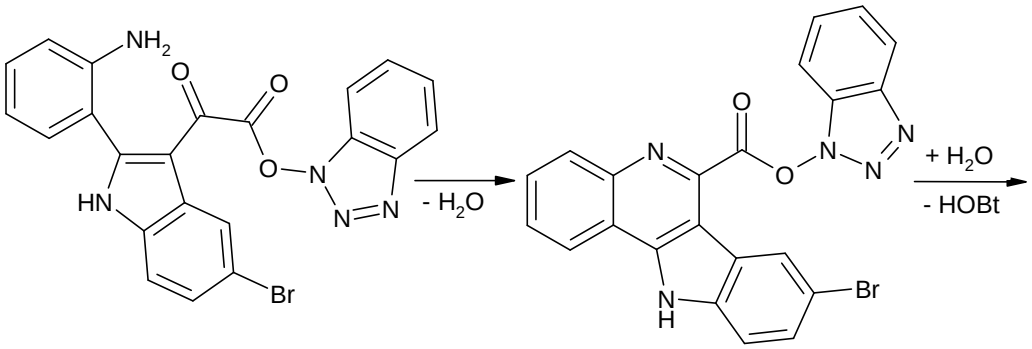

99 **100**

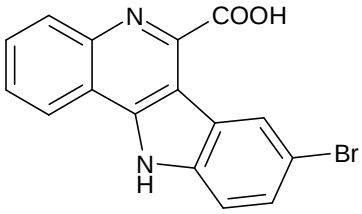

79c

By applying reaction conditions to paullone-9-carboxylic acid (**39**) that provoke the amidation reaction as well as the skeletal rearrangement reaction, the synthesis of several different 8-(aminocarbonyl)-11*H*-indolo [3,2-*c*]quinoline-6-carboxylic acid derivatives **79a**, **b**, **d** was achieved (scheme 2-45).

Scheme 2-45:

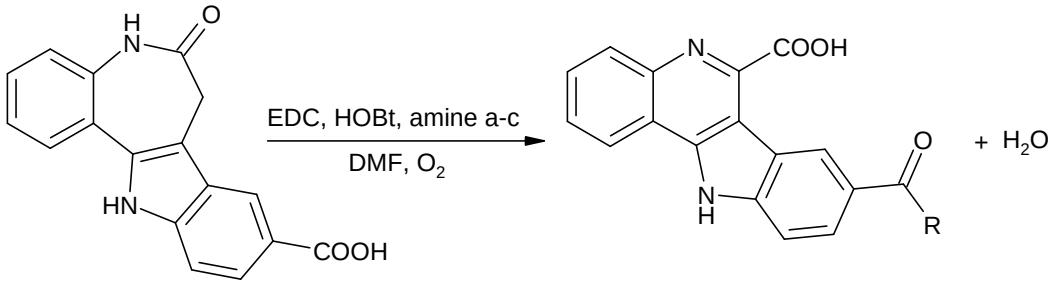

39 **a** benzylamine — **79a** R = $NHCH_2C_6H_5$

b (4-methoxybenzyl)amine — **79b** R = $NHCH_2C_6H_4OCH_3$

c 4-methylpiperidine — **79d** R = $NC_5H_9CH_3$

3 Biological Activity of Paullones

3.1 CDK1/Cyclin B-, CDK5/p25- and GSK-3b-Inhibitory Activity

The inhibitory effect on the isolated enzymes CDK1/cyclin B, CDK5/p25 and GSK-3β exhibited by the compounds synthesized within the scope of this thesis as well as other paullone derivatives was assayed by the group of Laurent Meijer (CNRS, Station Biologique, Roscoff, France).

It is commonly assumed that the inhibition of these enzymes, respectively, might play an important role in the treatment of a variety of diseases (cf. chapter 1.4):

In a number of human primary tumors and tumor cell lines, the deregulation of the CDK1/cyclin B-complex has been documented. Inhibitors of the holoenzyme therefore constitute putative drugs for the treatment of cancer.[2,46]

The activation of CDK5 is considered to be most likely involved in the cytoskeletal abnormalities and neuronal death observed in connection with Alzheimer's disease. The inhibition of CDK5 is thus regarded to be of major interest concerning the development of drugs for the treatment of Alzheimer's disease.[5]

Glykogen synthase kinase-3 (GSK-3) represents a serine/threonine protein kinase which is known to be involved in the regulation of the glycogen metabolism, and to play important roles in various biological processes like developmental patterning and cell survival. GSK-3 inhibitors may thus exhibit therapeutic potential for the treatment of several human diseases such as diabetes, stroke and neurological diseases.[113,114]

The activity of the kinases CDK1/cyclin B and CDK5/p25 was determined by measuring the phosphorylation of the histone H1 which is catalyzed by these enzymes. Histones constitute basic proteins found in the nuclei of all eukaryotic cells where they are complexed to DNA.

Concerning GSK-3β, the kinase activity was analyzed in a similar fashion as stated above but with the exception of substituting glycogen-synthase-1 (GS-1) peptide for the histone H1 as the employed substrate.

Dose-response curves were constructed for every compound tested and used for the calculation of the corresponding IC_{50}-values. All assays were carried out in triplicate.

The table below gives an overview of the inhibitory activity of the newly synthesized paullone derivatives, substituted at the 9-position, against the enzymes CDK1/cyclin B, CDK5/p25 and GSK-3β, additionally listing the previously obtained IC_{50}-values of kenpaullone (**1**), paullone-9-carbonitrile (**74**), and alsterpaullone (**2**) in order to facilitate the comparison and evaluation of the presented data (table 3-1).

Table 3-1: Inhibition of CDK1/cyclin B, CDK5/p25, and GSK-3β activity by 9-substituted paullone derivatives, IC_{50}-values [µM]

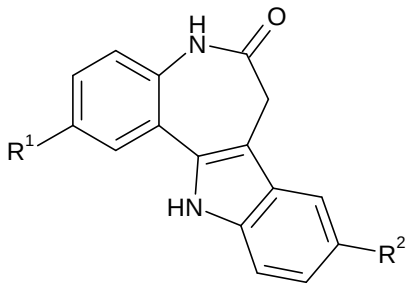

	R^1	R^2	CDK1/ cyc B	CDK5/ p25	GSK-3β
1	H	Br	0.400	0.850	0.023
74	H	CN	0.024	0.044	0.010
2	H	NO_2	0.035	0.040	0.004
35a	H	SCH_3	0.400	1.5	1.2
35b	OCH_3	SCH_3	0.340	1.5	1.6
36a	H	$SOCH_3$	0.28	0.40	13.0
36b	OCH_3	$SOCH_3$	0.080	0.150	7.0

Table 3-1: Inhibition of CDK1/cyclin B, CDK5/p25, and GSK-3β activity by 9-substituted paullone derivatives, IC_{50}-values [µM] (continuation)

	R^1	R^2	CDK1/ cyc B	CDK5/ p25	GSK-3β
37b	OCH_3	SO_2CH_3	0.009	0.042	2.0
38	H	SO_2NH_2	0.320	0.400	0.350
35c	OCH_3	SO_2NH_2	0.18	0.29	0.30
39	H	COOH	47.0	100.0	30.0
40b	H	$COOCH_3$	4.2	>10	7.2
40a	H	$COOC_2H_5$	25.0	240.0	>100
40c	H	$COOC_3H_7$	13.0	200.0	700.0
40d	H	$COOC_4H_9$	>10	>10	>10
40e	H	$COOC_5H_{11}$	25.0	210.0	600.0
40g	H	$COOC_6H_{13}$	7.0	>10	>10
40h	H	$COOC_8H_{17}$	40.0	700.0	>1000
54	H	$CON(C_3H_7)CONH(C_3H_7)$	750.0	>1000	>1000
55a	H	$CONHCH_2C_6H_5$	9.0	100.0	500.0
55c	H	$CONHC_{18}H_{37}$	6.2	240.0	1000.0

The compounds presented in the table are depicted as separate groups in order to demonstrate the particular classification. The reference substances are listed first; the order of appearance of the newly introduced paullone derivatives is similar to the arrangement within the synthesis chapter (chapter 2).

The determined inhibitory activity of the newly synthesized compounds towards the enzymes differs in extent depending on the particular chemical functionality at the 9-position.

CDK1/Cyclin B

The paullones with sulfur substituents are approximately as effective as kenpaullone (**1**), exhibiting IC_{50}-values in the same order of magnitude, with the exception of the 2-methoxy-substituted sulfoxide **36b** and the 2-methoxy-substituted sulfone **37b**. These derivatives show a remarkably high inhibitory activity, especially compound **37b** which is fourfold more active than alsterpaullone (**2**) and threefold more active than the cyano-substituted derivative **74**. Thus, the sulfone **37b** constitutes one of the most potent CDK1/cyclin B inhibitors existing so far, purvalanol A (IC_{50} = 0.004µM) being the most active representative. Subdividing the sulfur-substituted paullone derivatives with respect to their functional groups and the corresponding inhibitory activity, the sulfone **37b** embodies the most potent derivative, followed by the sulfoxides **36b** and **36a**, the sulfonamides **35c** and **38**, and finally the thioethers **35b** and **35a**. In all these cases, the 2-methoxy-substituted paullones show a higher inhibitory activity towards CDK1/cyclin B than the unsubstituted derivatives. However, this cannot be regarded as a basic phenomenon as examined and pointed out by Wieking.[115]

Paullone-9-carboxylic acid (**39**) and the ester derivatives **40a-h** all display less inhibitory activity than the paullones with sulfur substituents at the 9-position, the acid **39** being the weakest inhibitor. These carbonyl-substituted compounds are less active than kenpaullone (**1**) and alsterpaullone (**2**) by 1-2 orders of magnitude and 2-3 orders of magnitude, respectively. Furthermore, it is remarkable that the extent of inhibitory activity of the ester derivatives **40a-h** does not increase or decrease in a manner congruous with the ester chain length – no pattern can be assigned.

The N-acylurea derivative **54** shows only very poor inhibitory activity towards CDK1/cyclin B and constitutes the least active substance of the newly tested compounds.

The inhibition of CDK1/cyclin B by the paullone-9-carboxamides **55a** and **55c** occurs in an extent comparable to the one exhibited by the more potent ester derivatives, that is, the methyl and hexyl ester derivatives **40b** and **40g**, respectively. These substances are approximately 20-fold less active than kenpaullone (**1**). Interestingly, the amides **55a** and **55c** unfold a certain selectivity for CDK1/cyclin B over CDK5/p25 and GSK-3β inhibition.

CDK5/p25

All introduced substances display less inhibitory activity towards CDK5/p25 than towards CDK1/cyclin B.

The compounds with sulfur substituents at the 9-position show a decreasing effect on CDK5/p25 in an order resembling the one concerning the inhibition of CDK1/cyclin B. Within this group of compounds, the sulfone **37b** represents the strongest inhibitor, exhibiting a potency comparable to the one of alsterpaullone (**2**), and the thioethers **35a** and **35b** display the least activity.

None of the paullone derivatives with carbonyl substituents at the 9-position inhibit the enzyme CDK5/p25 to a noteworthy extent. Significant differences between the IC_{50}-values corresponding to the carboxylic acid **39**, to the ester derivatives **40a-h**, and to the amides **55a** and **55c** cannot be observed. However, some results are just stated as limits (e.g., IC_{50} >10), thus aggravating the comparison with the exactly determined IC_{50}-values.

GSK-3β

The reference substances kenpaullone (**1**), paullone-9-carbonitrile (**74**), and alsterpaullone (**2**) show a 2- to 40-fold higher inhibitory activity towards GSK-3β than towards CDK1/cyclin B and CDK5/p25. This phenomenon cannot be observed for the newly synthesized compounds. With the exception of the sulfonamide **38** and the carboxylic acid **39**, all tested substances displayed less activity towards GSK-3β than towards the cyclin-dependent kinases.

Compared to the reference substances, the sulfur derivatives are less active towards GSK-3β by 1-3 orders of magnitude. Solely the sulfonamide derivatives **38** and **35c** inhibit all three kinases to a fairly similar extent.

The 9-carbonyl-substituted paullones do not show a remarkable inhibition of GSK-3β; the IC_{50}-values lie within the same range as those corresponding to CDK5/p25. An exception is merely constituted by the amides **55a** and **55c** which are considerably less active towards the glycogen synthase kinase-3β than towards the CDK5/p25 enzyme.

Hitherto, the biological activity of only two of the newly synthesized compounds containing the quinoline substructure has been determined. The obtained IC_{50}-values [µM] are presented in the following table which also includes kenpaullone (**1**) and the paullone-9-carboxamide derivative **55a** as reference substances (table 3-2).

Table 3-2: Inhibition of CDK1/cyclin B, CDK5/p25, and GSK-3β activity by 8-substituted 11*H*-indolo[3,2-*c*]quinoline-6-carboxylic acids **79b** and **79d**, IC_{50}-values [µM]

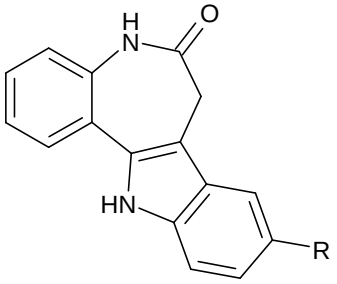

1, 55a

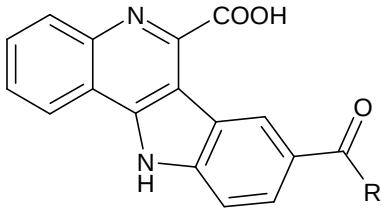

79b, 79d

	R	CDK1/cyc B	CDK5/p25	GSK-3β
1	Br	0.400	0.850	0.023
55a	$CONHCH_2C_6H_5$	9.0	100.0	500.0
79b	$NHCH_2C_6H_4OCH_3$	40.0	120.0	500.0
79d	$NC_5H_9CH_3$	25.0	85.0	130.0

The compounds presented in the table are depicted as separate groups in order to demonstrate the particular classification. The reference substances are listed first, the newly synthesized compounds afterwards.

The quinoline derivatives **79b** and **79d** do not display an inhibitory activity comparable to that of the reference substance kenpaullone (**1**), being less active by 2-4 orders of magnitude. The degree of discrepancy is particularly high concerning the inhibition of GSK-3β.

The reference substance paullone-9-carboxamide **55a** unfolds an inhibitory activity towards CDK1/cyclin B that is 3- to 5-fold higher than the one of the new compounds **79d** and **79b**. The enzymes CDK5/p25 and GSK-3β are inhibited to a similar extent; all three amides **55a**, **79b**, and **79d** show only moderate activity towards the former and moderate to poor activity towards the latter enzyme.

A direct comparison of kenpaullone (**1**) to the corresponding bromo-substituted quinoline derivative **79c** is aspired in order to evaluate the qualities of the rearranged ring structure. The necessary biological test results are awaited.

3.2 In Vitro Antitumor Activity

Investigations concerning the in vitro antitumor activity of the compounds synthesized within the scope of this thesis were performed by the National Cancer Institute, Bethesda, Maryland, USA by means of the NCI anti-cancer drug screen.[116-121] Experimental data was collected against sixty different tumor cell lines and the results were converted into response parameters like, for example, "GI_{50}" (concentration at which 50% of the cells are inhibited in growth). For the comparative interpretation of the obtained data corresponding to the synthesized compounds, the $\log_{10} GI_{50}$-values of two particular cell lines and the mean $\log_{10} GI_{50}$-value calculated from all cell lines tested, referred to as $\log_{10} GI_{50}$ MG_MID, were chosen to be presented in the tables depicted within this subchapter. The cell lines SR (leukemia) and RXF 393 (renal cancer) were selected for this purpose because they have proven to be eminently sensible to the anti-proliferative effects caused by the introduced substances.

Five different inhibitor concentrations (10^{-4} to 10^{-8} M) were applied for determining the particular antitumor activity of the compounds. Even if the highest concentration applied (i.e., 10^{-4} M) did not provoke a 50% tumor cell growth inhibition, this maximum concentration was employed in the calculation of the mean antitumor activity ($\log_{10} GI_{50}$ MG_MID) of that substance. Hence, the GI_{50} MG_MID-value may not be the actual mean of the GI_{50}-values. Furthermore, a $\log_{10} GI_{50}$ MG_MID-value of –4 implies that none of the utilized tumor cell lines provoked a 50% inhibition.

The first table shows the data collected for the new paullone derivatives, additionally depicting the $\log_{10} GI_{50}$-values of kenpaullone (**1**), paullone-9-carbonitrile (**74**), and alsterpaullone (**2**) which serve as reference substances (table 3-3).

Table 3-3: Antitumor activity of 9-substituted paullone derivatives, log_{10} GI_{50}-values [M]

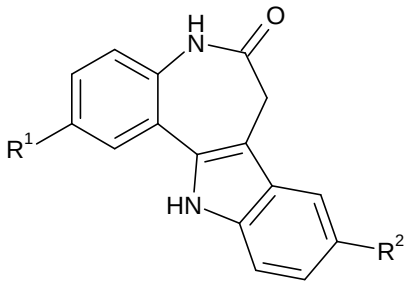

	R^1	R^2	SR	RXF 393	MG_MID
1	H	Br	-5.38	-5.29[a]	-4.35[a]
74	H	CN	-5.54	-4.0	-4.05
2	H	NO_2	-6.82	-6.52	-6.24[a]
35a	H	SCH_3	n/a	n/a	-4.19
35b	OCH_3	SCH_3	-4.76	-4.59	-4.11
36a	H	$SOCH_3$	-5.42	n/a	-4.56
36b	OCH_3	$SOCH_3$	-5.26	-4.71	-4.59
37b	OCH_3	SO_2CH_3	n/a	-4.02	-4.14
38	H	SO_2NH_2	n/a	-4.72	-4.19
35c	OCH_3	SO_2NH_2	-5.35[b]	-4.46[a]	-4.78[b]
39	H	COOH	-4.0	n/a	-4.05
40b	H	$COOCH_3$	-5.14	n/a	-4.42
40a	H	$COOC_2H_5$	-4.77	-4.0	-4.11
40c	H	$COOC_3H_7$	-4.49	-4.0	-4.03

Table 3-3: Antitumor activity of 9-substituted paullone derivatives, log_{10} GI_{50}-values [M] (continuation)

	R^1	R^2	SR	RXF 393	MG_MID
40d	H	$COOC_4H_9$	-4.59	-4.59	-4.05
40e	H	$COOC_5H_{11}$	-5.85[a]	-4.32[a]	-4.38[a]
40f	H	$CH(CH_3)(C_3H_7)$	-6.98[a]	-4.72[a]	-5.23[a]
40g	H	$COOC_6H_{13}$	-4.0	-7.58	-4.07
40h	H	$COOC_8H_{17}$	-4.0	-4.52[a]	-4.14[a]
54	H	$CON(C_3H_7)CONH(C_3H_7)$	-4.09	-4.0	-4.15
55a	H	$CONHCH_2C_6H_5$	n/a	-5.44	-4.91
55b	H	$CONC_4H_8O$	n/a	-5.04	-4.22
55c	H	$CONHC_{18}H_{37}$	-4.0	-4.4	-4.04
55d	H	$CONC_4H_8NCH_2C_6H_5$	-5.48	-5.09[a]	-4.63[a]
55e	H	$CONC_4H_8$	n/a	-5.45	-4.08
55g	H	$CONHCH_2C_6H_4OCH_3$	-5.34	-5.18[a]	-4.59[a]

The compounds presented in the table are depicted as separate groups in order to demonstrate the particular classification. The reference substances are listed first; the order of appearance of the newly introduced paullone derivatives is similar to the arrangement within the synthesis chapter (chapter 2).

Values marked with a superscript represent the mean log_{10} GI_{50}-values originating from two (a) or four (b) individual data sets.

If certain cell lines were not available and thus not utilized in the NCI drug screen, the proper data was not applicable (“n/a”).

As a general evaluation of the presented data of the 9-substituted paullone derivatives, the statement has to be made that none of the compounds unfold an outstanding anti-proliferative activity like alsterpaullone (**2**). The antitumor activity displayed only ranges from poor to moderate.

The derivatives carrying sulfur substituents at the 9-position show an antitumor activity comparable to that of kenpaullone (**1**) which is not very remarkable. Implying a modest anti-proliferative activity, the $\log_{10} GI_{50}$ MG_MID-value of -4.78 corresponding to the 2-methoxy-substituted sulfonamide **35c** represents the best result within the group. However, that value constitutes the average of four performed experiments, having resulted in $\log_{10} GI_{50}$ MG_MID-values of -6.26, -4.43, -4.18, and -4.20. Therefore, it has to be presumed that the first experiment led to incorrectly high activity values and that the other three experiments disclosed the actual status.

Paullone-9-carboxylic acid (**39**), the ester derivatives **40a-h**, and the N-acylurea compound **54** do not display a noteworthy antitumor activity, the $\log_{10} GI_{50}$ MG_MID-values being as poor as the one of the reference substance **74**. The pentyl ester derivatives **40e** and **40f** constitute exceptions, unfolding a slightly stronger anti-proliferative effect on the tumor cell lines. Furthermore, it has to be noted that the hexyl ester **40g** strongly inhibits the cell growth of RXF 393, a renal tumor cell line, exhibiting a $\log_{10} GI_{50}$-value of -7.58, but nevertheless features an extremely poor $\log_{10} GI_{50}$ MG_MID-value of -4.07. This is very unusual, and thus the testing result concerning RXF 393 has to be critically questioned.

The amide derivatives **55a**, **55d**, and **55g**, all comprising a benzyl substructure in the substituent at the 9-position, unfold a moderate antitumor activity which is slightly superior to that of kenpaullone (**1**). The other tested amides did not show a noteworthy inhibition of the tumor cell lines, the long-chained octadecylamide **55c** providing the overall poorest results.

In general, the extent of inhibition of the tumor cell lines caused by the synthesized substances does not correlate with the corresponding inhibitory activity towards the isolated kinases. Hence, a strong inhibition

of the isolated enzymes does not necessarily entail a strong inhibitory effect on the tumor cell lines. For example, the sulfone derivative **37b** displays an extremely high activity towards the isolated cyclin-dependent kinases (cf. table 3-1) but shows basically no inhibition of the tumor cell lines. This insight has already been gained by Schultz[46] when evaluating the data describing the inhibitory activity of paullone-9-carbonitrile (**74**). In the case of alsterpaullone (**2**), the strong inhibition of the isolated kinases does coincide with the pronounced inhibitory effect on the tumor cell lines. However, the observed inhibition of tumor cell growth could also be caused by cellular mechanisms triggered by the 9-nitro-compound **2** that do not involve CDK-inhibition. Up to today, it is not known to what extent the inhibition of cyclin-dependent kinases contributes to the extraordinary anti-proliferative activity unfolded by alsterpaullone (**2**). Investigations concerning this matter are ongoing.

So far, the antitumor activity of only two quinoline derivatives (i.e., **79b** and **79d**) has been examined by means of the NCI anti-cancer drug screen. The obtained $\log_{10}$ GI_{50}-values [M] are presented in the following table which also includes kenpaullone (**1**) and the paullone-9-carboxamide derivative **55g** as reference substances (table 3-4).

Table 3-4: Antitumor activity of 8-substituted 11*H*-indolo[3,2-*c*]quinoline-6-carboxylic acids **79b** and **79d**, $\log_{10}$ GI_{50}-values [M]

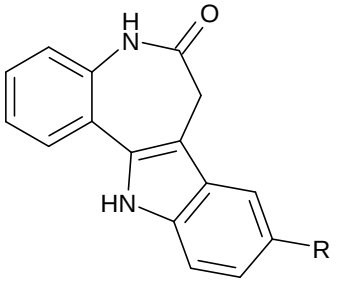

1, 55g

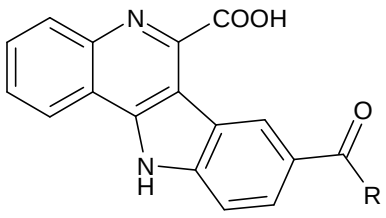

79b, 79d

	R	SR	RXF 393	MG_MID
1	Br	-5.38	-5.29[a]	-4.35[a]
55g	$CONHCH_2C_6H_4OCH_3$	-5.34	-5.18[a]	-4.59[a]
79b	$NHCH_2C_6H_4OCH_3$	n/a	n/a	-4.10
79d	$NC_5H_9CH_3$	-4.0	-4.88[a]	-4.27[a]

The compounds presented in the table are depicted as separate groups in order to demonstrate the particular classification. The reference substances are listed first, the newly synthesized compounds afterwards.

Values marked with the superscript “a” represent the mean $\log_{10}$ GI_{50}-values originating from two individual data sets.

If certain cell lines were not available and thus not utilized in the NCI drug screen, the proper data was not applicable (“n/a”).

The rearranged substances **79b** and **79d** do not display a noteworthy anti-proliferative activity. These quinoline derivatives are even less active than the reference substances **1** and **55g** which cause only a moderate inhibitory effect on the tumor cell lines.

An evaluation of the new indolo[3,2-*c*]quinoline-ring structure is accomplishable by comparing the quinoline derivative **79b** with the paullone **55g** as both are substituted with the same residue. The contracted basic ring structure seems to be less favorable with respect to the antitumor activity.

3.3 In Vitro Antiprotozoic Activity

In vitro assays exploring the antiprotozoic qualities of paullone derivatives were performed by the Swiss Tropical Institute, Basel, Switzerland. Several representatives of the compounds synthesized within the scope of this thesis were included in these investigations. As previously discussed (cf. chapter 1.4), cyclin-dependent kinase inhibitors may constitute putative drugs for the treatment of diseases caused by parasitic protozoa.

In the conducted assays, the antiprotozoic activity exhibited by the synthesized substances against *Leishmania donovani* (*L. donovani*), *Plasmodium falciparum* (*P. falc.*), *Trypanosoma brucei rhodesiense* (*T. b. rhod.*), and *Trypanosoma cruzi* (*T. cruzi*) was determined. In addition to that, the corresponding cytotoxicicity of the paullone derivatives towards rat skeletal myoblasts (L-6 cells) was investigated. This enables the evaluation of the eligibility of the tested compounds for potentially subsequent in vivo assays.

Leishmania donovani is the protozoan parasite responsible for visceral leishmaniasis (kala-azar, dumdum fever) among other diseases. Sandflies acting as vectors, a systemic infection is produced that comprises reticuloendothelial cells and macrophages in all organs. The course of the infection may be subclinical; the clinical disease is fatal if untreated.

The protozoan parasite *Plasmodium falciparum* is the most pathogenic representative of the four species of *Plasmodium* causing malaria. Transmitted by anopheline mosquitoes, an infection can result in the development of multi organ disease including coma, renal failure, and pulmonary disfunction, and thus may be rapidly fatal.

Trypanosoma brucei rhodesiense is the protozoan parasite causing the disease African sleeping sickness (East African trypanosomiasis). Tsetse flies serve as vectors. The invasion of the bloodstream is followed by waves of parasitaemia with accompanying fever and malaise. An infection of the central nervous system can occur within a time span of several weeks. The disease can be rapidly fatal.

The protozoan parasite *Trypanosoma cruzi* is the causative agent of the Chagas disease (American trypanosomiasis). The transmission to humans occurs by the contamination of abraded skin with the feces of infected kissing bugs (*Triatoma infestans*). The initial acute phase of Chagas disease, lasting several weeks and being often asymptomatic, subsides into a chronic phase which may continue for decades, possibly leading to irreversible heart and gastrointestinal tract lesions. Chagas disease represents the main cause of heart attack among infected people.[122,123]

The results of the assays investigating the inhibitory activity towards the parasites *Trypanosoma brucei rhodesiense* and *Trypanosoma cruzi* are depicted in the tables shown below (tables 3-5 and 3-6). No antiprotozoic activity of the tested paullone derivatives could be observed against *Leishmania donovani* and *Plasmodium falciparum*: the particular IC_{50}-values all exceeded the highest test concentration applied, corresponding to 30 µg/ml and 5 µg/ml, respectively.

Table 3-5: Antiprotozoic activity of 9-substituted paullone derivatives against *Trypanosoma brucei rhodesiense*, IC_{50}-values [µg/ml] and [µM]

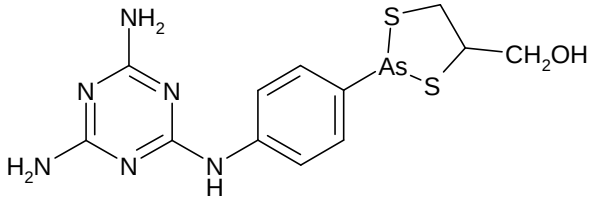

101

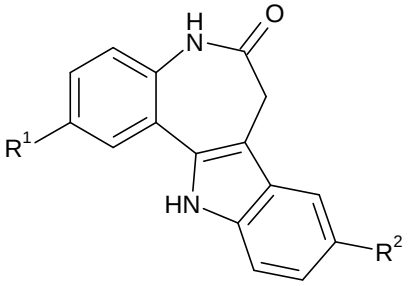

1, **2**, **35a**, **35b**, **36a**, **36b**, **37b**, **38**, **35c**, **39**, **40a**, **40d**, **40g**

	R^1	R^2	*T. b. rhod.*		Cytotoxicity L6		quot.[b]
			[µg/ml]	[µM]	[µg/ml]	[µM]	
101[a]	-	-	0.00206	0.005	3.9	9.8	1893
1	H	Br	2.46	7.5	>90	>275	>37
2	H	NO_2	0.26	0.9	0.26	0.9	1
35a	H	SCH_3	0.97	3.3	>90	>306	>93
35b	OCH_3	SCH_3	11.9	36.7	n/a	n/a	n/a
36a	H	$SOCH_3$	0.82	2.6	19.9	64	24
36b	OCH_3	$SOCH_3$	1.49	4.4	>90	>264	>60
37b	OCH_3	SO_2CH_3	0.97	2.7	>90	>253	>93
38	H	SO_2NH_2	>90	>275	n/a	n/a	n/a
35c	OCH_3	SO_2NH_2	14.7	41	n/a	n/a	n/a
39	H	COOH	81.4	278	n/a	n/a	n/a
40a	H	$COOC_2H_5$	>90	>281	45.2	141	<0.5
40d	H	$COOC_4H_9$	>90	>258	n/a	n/a	n/a
40g	H	$COOC_6H_{13}$	>90	>239	n/a	n/a	n/a

The compounds presented in the table are depicted as separate groups in order to demonstrate the particular classification. The standard and the reference substances are listed first; the order of appearance of the newly introduced paullone derivatives is similar to the arrangement within the synthesis chapter (chapter 2).

For some compounds, the obtained data did not substantiate a cytotoxicity test. In these cases, the appropriate values were not applicable (“n/a”).

[a] Melarsoprol represents the standard for the *Trypanosoma brucei rhod.*-assay. It is a drug employed in the treatment of the African sleeping sickness.

[b] The quotient (“quot.”) is defined as the IC_{50}-value expressing the cytotoxicity of the tested compound towards host cells divided by the appropriate IC_{50}-value describing the inhibitory effect on the parasite. Therefore, it serves as an approximation for the assessment of the potential therapeutic window of the substance.

Table 3-6: Antiprotozoic activity of 9-substituted paullone derivatives against *Trypanosoma cruzi*, IC_{50}-values [µg/ml] and [µM]

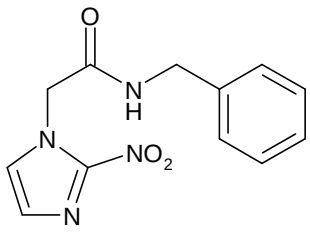

102

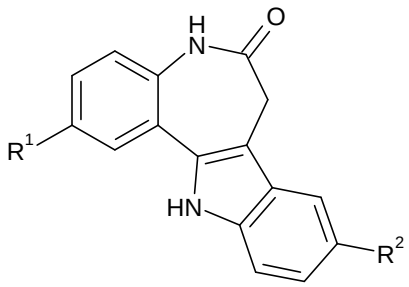

1, **2**, **35a**, **35b**, **36a**, **36b**, **37b**, **38**, **35c**, **39**, **40a**, **40d**, **40g**

	R^1	R^2	*T. cruzi*		Cytotoxicity L6		quot.[b]
			[µg/ml]	[µM]	[µg/ml]	[µM]	
102[a]	-	-	0.4056	1.6	>1000	>3842	>2465
1	H	Br	35.1	107.3	>90.0	>275.1	>2.6
2	H	NO_2	0.013	0.04	0.26	0.9	22.5
35a	H	SCH_3	17.4	59.1	>90.0	>305.7	>5.2
35b	OCH_3	SCH_3	>90.0	>277.4	n/a	n/a	n/a
36a	H	$SOCH_3$	2.7	8.7	19.9	64.1	7.4
36b	OCH_3	$SOCH_3$	32.2	94.6	>90.0	>264.4	>2.8
37b	OCH_3	SO_2CH_3	49.7	139.5	>90.0	>252.5	>1.8
38	H	SO_2NH_2	17.4	53.2	n/a	n/a	n/a
35c	OCH_3	SO_2NH_2	>90.0	>251.8	n/a	n/a	n/a

Table 3-6: Antiprotozoic activity of 9-substituted paullone derivatives against *Trypanosoma cruzi*, IC_{50}-values [µg/ml] and [µM] (continuation)

	R^1	R^2	*T. cruzi*		Cytotoxicity L6		quot.[b]
			[µg/ml]	[µM]	[µg/ml]	[µM]	
39	H	COOH	40.7	139.2	n/a	n/a	n/a
40a	H	$COOC_2H_5$	0.8	2.5	45.2	141.1	56.6
40d	H	$COOC_4H_9$	>90.0	>258.3	n/a	n/a	n/a
40g	H	$COOC_6H_{13}$	>90.0	>239.1	n/a	n/a	n/a

The compounds presented in the table are depicted as separate groups in order to demonstrate the particular classification. The standard and the reference substances are listed first; the order of appearance of the newly introduced paullone derivatives is similar to the arrangement within the synthesis chapter (chapter 2).

For some compounds, the obtained data did not substantiate a cytotoxicity test. In these cases, the appropriate values were not applicable ("n/a").

[a] Benznidazol represents the standard for the *Trypanosoma cruzi*-assay. It is a drug employed in the treatment of the Chagas disease.

[b] The quotient ("quot.") is defined as the IC_{50}-value expressing the cytotoxicity of the tested compound towards host cells divided by the appropriate IC_{50}-value describing the inhibitory effect on the parasite. Therefore, it serves as an approximation for the assessment of the potential therapeutic window of the substance.

In general, two conditions need to be fulfilled by a new substance in order to arouse interest and to qualify for further investigations: the compound should unfold a high inhibitory activity towards the targeted parasite but, at the same time, exhibit no or little toxic effects on the host organism.

Concerning the inhibitory activity towards *Trypanosoma brucei rhod.*, none of the tested paullones gave results comparable to the extraordinary values determined for the standard melarsoprol (**101**). Taking the corresponding quotients into account, the sulfur-substituted derivatives **35a**, **36b**, and **37b** supplied the best results. None of the substances was selected for further test programs though.

With respect to the inhibitory effect on *Trypanosoma cruzi*, the examined compounds did not display activities similar or close to the activity

exhibited by the standard benznidazol (**102**). Including the determined quotient in the overall evaluation, only one new substance shows an interesting profile: the paullone-9-carboxylic acid ethyl ester (**40a**). This compound displays a remarkable inhibitory activity towards the parasite accompanied by only moderate cytotoxicity towards host cells, leading to a favorable quotient.

Because of these qualities, the ester derivative **40a** was chosen to be further investigated by means of in vivo experiments, conducted at the London School of Hygiene and Tropical Medicine. Up to today, the results mirroring the in vivo antitrypanosomal activity of **40a** have not been obtained.

3.4 Qualitative Structure-Activity Relationships

The performance of structure-activity relationship analyses constitutes a valuable tool with respect to the realization of lead optimization. Since the discovery of the anti-proliferative potential of paullones, over a hundred derivatives have been synthesized up to today. The biological activities displayed by the individual compounds were interpreted with regard to the differences in the compound structure, leading to valuable conclusions concerning the qualitative relation between structure and activity.[46,124]

A substitution at the 9-position of the paullone molecule is obligatory for unfolding CDK-inhibitory activity; electron-withdrawing substituents have proven to be of advantage. Furthermore, substituents at the 2- and the 3-position are tolerated. In all other positions, the molecule should remain unsubstituted. Especially the lactam functionality and the indole-NH need to be preserved in order to avoid a severe loss of biological activity. The qualitative structure-activity relationships established in the literature are illustrated in figure 3-1.

Figure 3-1: Qualitative structure-activity relationships of paullones

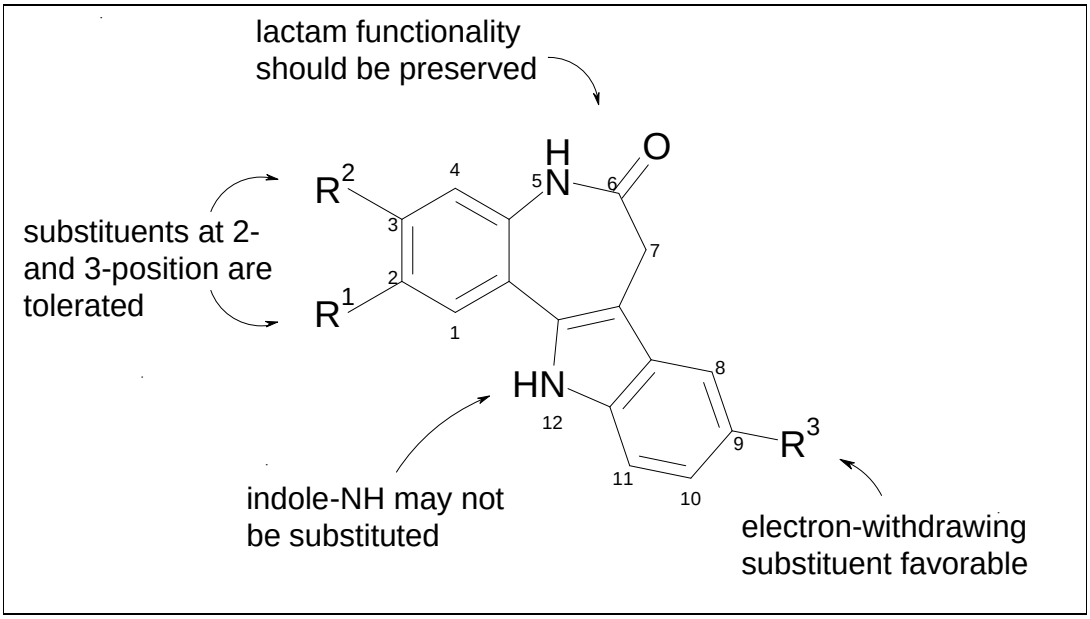

Adapted from an illustration by Kunick[124]

An excellent opportunity for exploring and vividly understanding the structure-activity relationships of a compound interacting with an enzyme is offered by molecular modeling. With a view to investigate the possible interactions that may occur between certain structural elements of the paullone molecule and the surrounding binding pocket of the target enzyme, a computer model of the CDK1/cyclin B-ATP binding pocket was created by homology building. It was developed from the crystal structure of CDK2/cyclin A which was used as a template to generate the initial coordinates. The paullones were docked into the ATP binding pocket of the CDK1/cyclin B model and optimized with molecular mechanics as reported by Gussio.[125]

Major contacts between the paullone molecule and the amino acids building up the ATP binding site of CDK1 are created by the formation of hydrogen bonds: paired hydrogen bonding occurs between the paullone lactam functionality and both the backbone carbonyl and amide of Leu83, and another hydrogen bond is formed by the paullone indole-NH and the carboxyl functionality of Asp86. These findings explain why the involved structural elements of the paullone molecule need to remain unsubstituted. Furthermore, the paullone ring system is positioned between the lipophilic residues of the amino acids Ile10 and Leu134 like a sandwich. Substituents located at the 2- or the 3-position of the molecule though are given the possibility of expanding into the surroundings of the binding pocket without the occurrence of significant steric hindrance. This is the reason for these substituents to be tolerated without causing a decrease in biological activity. Moreover, a hydrophobic pocket is formed by the side chains of the amino acids Ala144 and Phe80 among others. A structural water (wat539) is postulated to hydrogen bond to the π-cloud of Phe80. As hypothesized by Schultz[46], a polar substituent at the 9-position should enable the formation of a hydrogen bond to wat539, and thus improve the inhibitory activity of the compound. The described interactions are illustrated in figures 3-2 and 3-3.[2,124,125]

Figure 3-2: Hydrogen bonds formed between the paullone **38** and the ATP binding pocket of CDK1/cyclin B

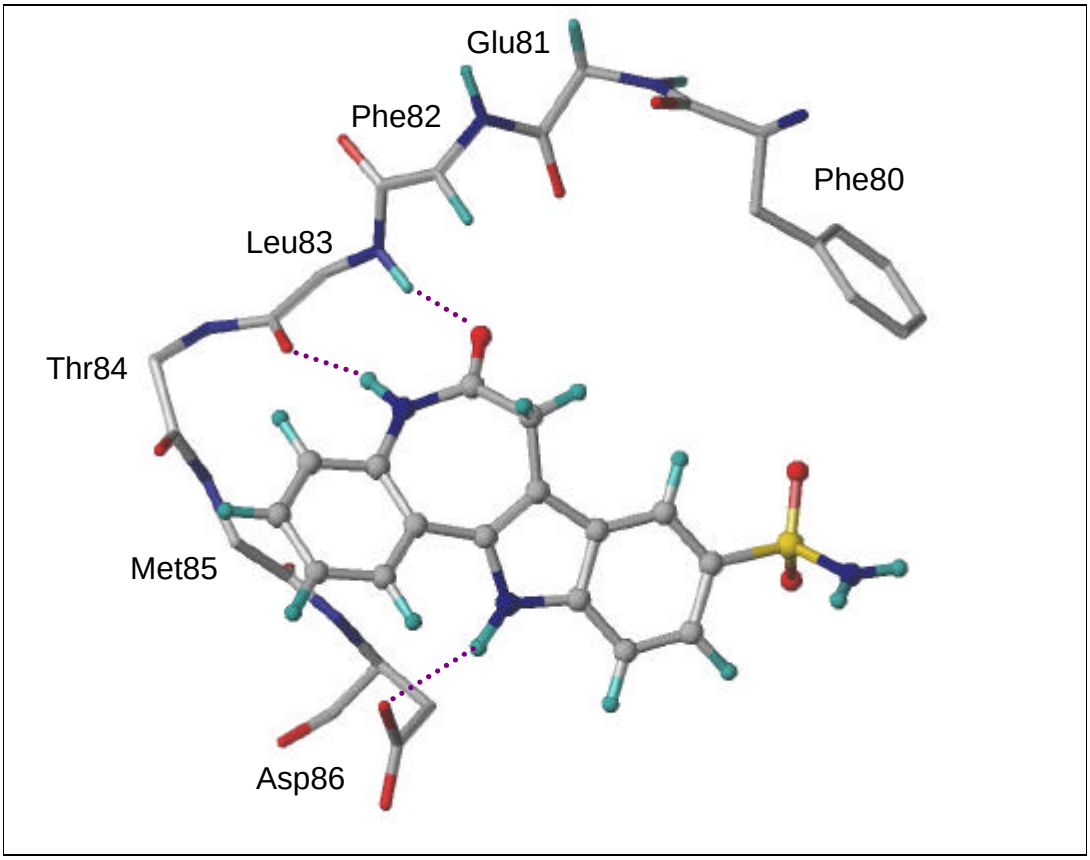

This illustration was created using SYBYL[11], employing the CDK1/cyclin B homology model developed by R. Gussio[125]. The manual docking and the subsequent minimization process, which was performed using the MAB force field implemented in the program MOLOC[126,127], were carried out by Th. Lemcke.

In order to provide a good lucidity of the illustration, the side chains of the amino acids Glu81 through Met85 were not depicted.

The magenta-colored dotted lines represent the hydrogen bonds formed between the paullone molecule and the amino acids Leu83 and Asp86.

Figure 3-3: Paullone **38** docked into the ATP binding site of CDK1/cyclin B, enzyme surface illustrating lipophilic properties

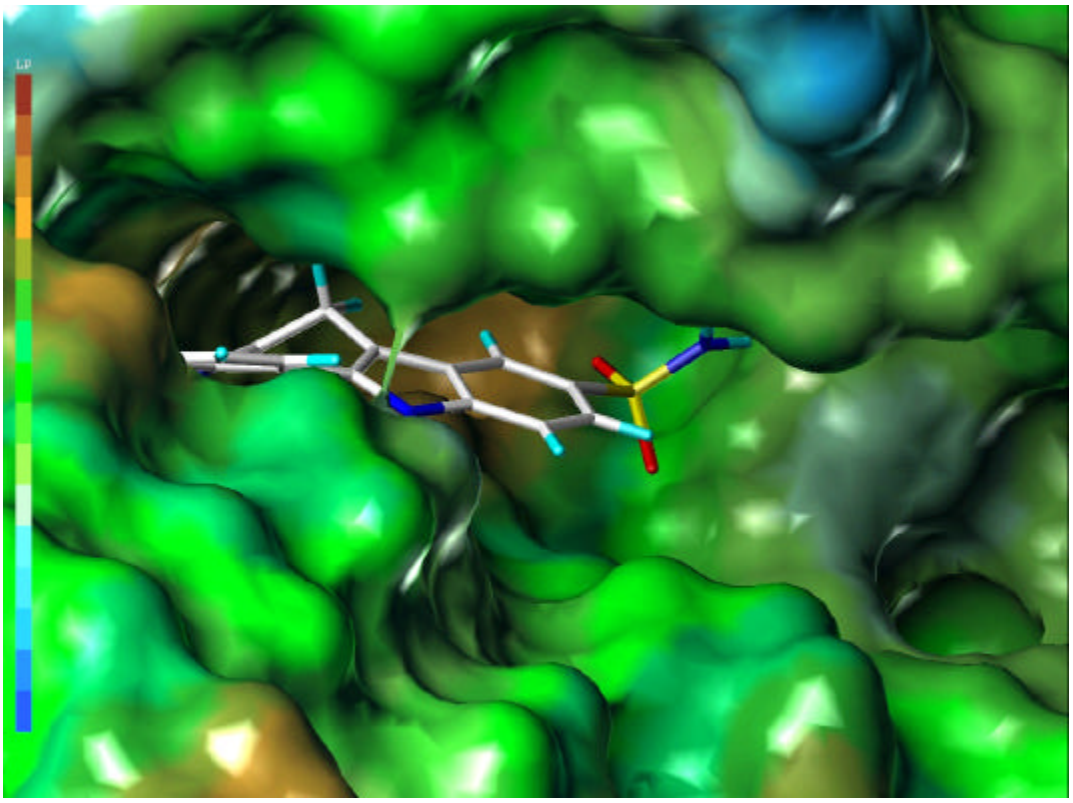

This illustration was created using SYBYL[11], employing the CDK1/cyclin B homology model developed by R. Gussio[125]. The manual docking and the subsequent minimization process, which was performed using the MAB force field implemented in the program MOLOC[126,127], were carried out by Th. Lemcke.

Lipophilicity decreases as shown on the left hand side, the color brown representing the most lipophilic areas.

The paullone molecule is placed like a sandwich between the lipophilic residues of the amino acids. The side chains present a unique, hydrophobic surface that is accessible for interactions with the lipophilic portions of the paullone.[125]

The space provided within the ATP binding pocket is not fully exploited by the paullone molecule. The available free space is visible at the right hand side of the illustration.

As the paullone derivatives synthesized within the scope of this thesis all carry different substituents at the 9-position, the discussion of structure-activity relationships will focus on the properties of the newly introduced substituents and their impact on the biological activity towards CDK1/cyclin B.

As previously stated, the introduction of electron-withdrawing substituents is expected to have a positive effect on the biological activity. The sulfone derivative **37b**, carrying the substituent with the most electronegative potential, indeed constitutes the compound with the highest inhibitory activity towards CDK1/cyclin B. The sulfonamides **38** (depicted in figures 3-2 and 3-3) and **35c** and the sulfoxides **36a** and **36b**, all equipped with electron-withdrawing substituents, also unfold a strong inhibitory effect, and thus are in agreement with the established hypothesis. The thioethers **35a** and **35b** represent substances with electron-donating residues, hence giving rise to the assumption of exhibiting a lower biological activity than the other derivatives, for example, the esters **40a-h**. However, the derivatives **35a** and **35b** are almost as active as the other sulfur-substituted paullones and unfold a much stronger inhibitory effect than the synthesized carboxylic acid **39**, the ester derivatives **40a-h**, and the amides **55a** and **55c**. With the exception of the methyl and hexyl esters **40b** and **40g** and the amides **55a** and **55c**, these carbonyl-substituted paullones show no remarkable biological activity towards CDK1/cyclin B in spite of their electron-withdrawing substituents.

Concerning the formation of hydrogen bonds between the carbonyl oxygen of the carbonyl-substituted derivatives and the mentioned wat539 present in the binding pocket, the interaction either does not occur or does not lead to the desired improvement of the inhibitory activity. On the other hand, hydrogen bonding between the polar sulfur-substituted compounds and wat539 might contribute to the observed noteworthy biological activity.

As shown in figure 3-3, the paullone molecule does not exploit all the space available within the ATP binding pocket. It is hence imaginable that a substituent located at the 9-position might expand into that free space, create further contacts with the surrounding amino acids and improve the inhibitory activity of the compound. With a view to explore this possibility,

esters with altering chain lengths were synthesized. However, the obtained biological data does not coincide with the variations in ester chain length: the methyl and hexyl esters **40b** and **40g** show the highest inhibitory activity towards CDK1/cyclin B, followed by the propyl ester **40c**, then the butyl, ethyl and pentyl esters **40d**, **40a**, and **40e**. The octyl ester **40h** represents the least active derivative. A logical pattern cannot be assigned and further structure-activity relationships cannot be deduced.

4 Quantitative Structure-Activity Relationships (QSAR)

4.1 Objective of the Paullone QSAR Study

The performance of a qualitative structure-activity relationship analysis within the paullone series (cf. chapter 3.4) yielded the conclusion that the introduction of electron-withdrawing substituents at the 9-position of the paullone molecules affected the exhibited inhibitory activity in a favorable manner.

It was desirable to also quantitatively characterize the determined correlation between the electronic properties of the introduced substituents and the resulting biological activity of the created paullone derivatives, and additionally, to acquire the capability to survey the influence of other physicochemical substituent parameters like hydrophobicity and steric dimensions. This aim could be achieved by performing a quantitative structure-activity relationship analysis using multiple regression correlation methodology, a Hansch analysis. An extracted mathematical relationship between the physicochemical substituent parameters and the biological activity would offer the opportunity to effectively continue the paullone lead optimization process.

Multiple regression correlation studies were conducted with the aim of investigating two different issues: the major interest consisted in the quantitative determination of the influence exerted by the substituents located at the 9-position of the paullone molecules on the inhibition of the isolated enzyme CDK1/cyclin B. In the second study, the degree of contribution made by each inhibited enzyme (i.e., CDK1/cyclin B, CDK5/p25, and GSK-3β) to the observed cell growth inhibition caused by paullones was to be analyzed.

4.2 Introduction to QSAR Studies

The objective of QSAR analyses is to investigate the quantitative relationship between the chemical structure of a compound and its biological activity. The classical QSAR methodology was principally molded by Hansch in the 1960s; today, it is strongly rivaled by modern 3D-QSAR methods like CoMSIA (Comparative Molecular Similarity Indices Analysis) and CoMFA (Comparative Molecular Field Analysis).[128,129] Nevertheless, the Hansch analysis is still regarded as a valuable tool, and thus is continuously employed. For instance, the QSAR study recently published by Lee[130] was performed by means of a Hansch analysis, reporting on purine analogs and their CDK-inhibitory activity.

The substances selected to be incorporated in a QSAR data set need to fit certain requirements: the chemical structures have to be closely related, and the biological target must be identical, including the mechanism underlying the biological activity.[128] Thus, the evaluation of the contribution of particular substituents can be performed by correlating the physicochemical properties of the substituents with the biological activity of the compounds.

There is a variety of substituent constants commonly used for the description of the physicochemical properties of the different residues. These descriptors can be experimentally or computationally derived. According to Hansch[131], the use of substituent constants provides the possibility to describe “the role of substituents on organic and biochemical processes in terms of polar, resonance, steric, hydrophobic and polarizability vectors”.

Having conducted a QSAR analysis by means of multiple regression correlation methodology, it is of uttermost importance to critically evaluate the obtained results. Certain statistical quantities aid in assessing the quality of the proposed correlation. However, the sole examination of the statistic quantities with respect to their significance and the additional performance of other evaluation methods like cross-validation cannot serve as a definite proof of having established a true mathematical relationship. A statistically significant correlation does not necessarily allow a physicochemical interpretation of the obtained biological data. A proposed relationship should be thoroughly scrutinized by taking further

inspection measures like surveying the orthogonality of the employed substituent constants, assuring a sufficiently high number of tested compounds incorporated in the regression analysis when using several explanatory variables, and varying the composition of the data set.[129,132]

The relevant substituent constants and the applied statistical quantities will be elucidated in the following subchapters (chapters 4.2.1 and 4.2.2).

4.2.1 Substituent Constants for Structure-Activity Correlations

The substituent constants used for correlating structure with reactivity can be grouped into electronic, hydrophobic, and steric parameters.

Electronic parameters

The Hammett constant σ is an electronic substituent constant reflecting the electron-donating or electron-withdrawing properties of a substituent. It thus serves as a quantitative measure of the change in electronic density in the reaction center caused by the introduced substituent. The σ–values were experimentally determined by Hammett through the examination of the dissociation constants of differently substituted benzoic acids in water, and also through the analysis of the rate constants corresponding to the hydrolysis reactions of differently substituted benzoic acid esters. Positive σ-values are defined to represent residues that unfold a stronger electron-withdrawing effect than the hydrogen present in the unsubstituted derivative, negative σ-values vice versa. Many sets of σ–values for special systems or applications have been created since the original proposal of the Hammett equation; the two most frequently applied pairs will be elucidated herein.[133,134]

$$\sigma_X = \log K_X - \log K_H$$

where σ_X is the Hammett constant characteristic of the *meta*- or *para*-substituent X,

K_X is the ionization constant for the *meta*- or *para*- substituted derivative of benzoic acid, and

K_H is the ionization constant for benzoic acid in water at 25 °C.

It is possible to express the electronic effect of a substituent in terms of non-resonance and resonance capability. The parameter σ_m describes the inductive effect on the electron density present in the reaction center, hence emphasizing on the non-resonance capability. The mesomeric effect on the electron density is characterized by σ_p, putting emphasis on the resonance capability.[133-136]

$$\sigma_m = \sigma_I + \alpha\sigma_R$$

$$\sigma_p = \sigma_I + \sigma_R$$

where σ_m is the Hammett *meta* constant,

σ_p is the Hammett *para* constant,

σ_I is the inductive effect,

σ_R is the resonance effect, and

α is the transmission coefficient.

As resonance conjugation cannot be performed from the *meta*-position, σ_R contributes indirectly to σ_m.

A distinction between non-resonance and resonance capability can also be made by employing the parameters F and R, which are the field (F) and resonance (R) constants calculated by Swain and Lupton from Hammett σ_m- and σ_p-values. Swain and Lupton[136] claim the descriptors F and R “to be more accurately defined and more physically significant independent variables for correlating or predicting substituent effects” than any other pair of Hammett values. F and R are supposed to be independent of the performed reaction, of the solvent, and of the

temperature. Hansch[135] attests the field and resonance constants a remarkable orthogonality and thus the avoidance of the common problem of multi-collinearity.

$$\sigma = fF + rR$$

where σ is the Hammett constant,

f is the field weighting factor,

F is the field constant,

r is the resonance weighting factor, and

R is the resonance constant.

The empirical weighting factors f and r are independent of the substituent but different for each substituent constant (i.e., σ_m, σ_p).

Hydrophobic parameters

The gap between mere organic and biochemical-biomedicinal systems can be bridged with the aid of the hydrophobic parameters log P and π.

The partition coefficient, referred to as log P, represents a parameter expressing the hydrophobicity of the molecule as a whole. The log P-value of a compound is commonly determined by measuring the distribution behavior in a biphasic system consisting of 1-octanol, representing the lipid phase, and water.[133]

$$P = \frac{c\,(\text{lipid phase})}{c\,(\text{water phase})}$$

where P is the partition coefficient of the compound,

c (lipid phase) is the concentration of the compound present in the lipid phase, and

c (water phase) is the concentration of the compound present in the water phase.

The Hansch constant π describes the contribution of a substituent to the lipophilicity of a compound. The π-values are usually derived from the benzene solute system, that is, by partitioning substituted benzene derivatives between 1-octanol and water. Subtraction of the log P-value of the unsubstituted benzene from the log P-value of the substituted compound yields the π-value of the appropriate substituent. Positive π-values represent an amplification of the lipophilic character caused by the substituent; negative π-values symbolize an increase in hydrophilicity.[131,133,135]

$$\pi_X = \log P_{R-X} - \log P_{R-H}$$

where π_X is the Hansch constant characteristic of the substituent X,

$P_{R\text{-}X}$ is the partition coefficient of the X-substituted benzene, and

$P_{R\text{-}H}$ is the partition coefficient of the unsubstituted benzene.

Steric parameters

The Taft steric substituent constant E_S is defined as a parameter describing the retardation of a reaction rate caused by the size of the substituent. It was experimentally determined by observing the change in reaction rate when performing the acidic hydrolysis of differently substituted benzoic acid ethyl esters.[137]

$$E_S = \log\left(\frac{k_X}{k_0}\right) \quad [H^+]$$

where E_S is Taft's steric constant characteristic of the substituent X,

k_X is the rate constant for the acidic hydrolysis of the ester substituted with the residue X, and

k_0 is the rate constant for the acidic hydrolysis of the methyl-substituted ester.

By definition, $E_S = 0$ when $X = CH_3$. To obtain the value for hydrogen, one must consider the acid hydrolysis of formate. As it was found to be equal to 1.24, the value 1.24 needs to be subtracted from the values established by Taft in order to refer the E_S-scale to hydrogen.

The E_s-values mirror the extent to which the substituents shield the reaction center. Large substituents provide strong shield effects and are represented by small E_s-values. The Taft substituent constant constitutes the most widely used parameter for steric substituent effects in organic reaction mechanism studies. However, for a large number of substituents, the E_s-constants have not been determined so far, and therefore other parameters describing steric interactions are of interest.[133,135]

The molecular volume MV, introduced by Exner, represents another parameter directly related to the steric influence of the substituent. MV is defined as the molecular weight of the substituent divided by its density. By measuring the density of a series of homologous compounds, Exner experimentally determined the molecular volume of a number of substituents.[133]

$$MV = \frac{M}{d}$$

where MV is the molecular volume of the substituent,

M is the molecular weight of the substituent, and

d is the density of the substituent.

A parameter readily available for each substituent is MR, the molar refractivity. The molar refractivity is described as the molar volume of the substituent corrected by the refractive index. The refractive index being a part of the definition hints a contribution of the polarizability of the substituent to the MR-value which must be regarded as an electronic contribution. The equivalence of MR with only steric requirements can therefore be misleading. Nevertheless, the molar refractivity constitutes a useful measure for describing general “steric bulk”.[133,135,137,138]

$$MR = \frac{M \cdot (n^2 - 1)}{d \cdot (n^2 + 2)}$$

where MR is the molar refractivity of the substituent,

M is the molecular weight of the substituent,

d is the density of the substituent, and

n is the refractive index, measured at 20 °C, Na D line.

This equation is referred to as the Lorenz-Lorentz equation.

A purely geometrical definition of the size of a substituent is provided by Verloop who thereby wanted to overcome the problem of asymmetry of substituents. In order to be able to describe substituents deviating from a spherical shape, a set of five parameters was developed. The length parameter L and the four width parameters $B_{1\text{-}4}$, representing the four rectangular directions perpendicular to the axis describing the length, were calculated by means of the STERIMOL computer program. The program simulates the three-dimensional model building of molecules or molecular groups on the basis of the Corey-Pauling-Koltun (CPK) atomic models.[133,137,139]

Due to the fact that the common steric parameters were not available for several of the substituents introduced at the 9-position of the paullone molecules within the scope of this thesis, an amenable steric substituent constant was created. The Verloop parameter L served as a basic orientation. The parameter was termed “distance”, abbreviated “dist”, and was defined as the distance between the C9-carbon of the paullone basic ring structure and the most remote atom of the substituent, measured in Angström (Å). The value was derived from the 3D-optimized structure of the substituted paullone molecule by means of the ACDLabs computer program. In literature, the parameter “distance” also appears in tables listing substituent parameters. There, “distance” stands for the substituents’ distance from hydrogen.[140]

4.2.2 Statistical Quantities in QSAR Studies

Performing the multiple linear regression of a dependent variable (y) on a computer offers the possibility of choosing a large number of explanatory variables (x) and thus raises the question of significance in an acute form. Statistical quantities need to be calculated in order to assess the success of the correlation.[132,141]

The correlation coefficient r measures the degree to which the dependent variable is linearly related to the explanatory variables. With respect to the QSAR study presented hereafter, the multiple correlation coefficient of the established regression equation expresses the extent to which the observed biological activity coincides with the calculated hyperplane defined by the applied descriptors and their regression coefficients, that is, the extent to which the experimentally measured biological activity coincides with the calculated biological activity. As r will continuously approach its optimum value of 1 with the number of explanatory variables increasing, further statistical quantities need to be consulted.

$$r = \sqrt{\frac{\sum_{j=1}^{k} b_j \left(\sum_i y_i x_{ji} - \frac{\sum_i y_i \sum_i x_{ji}}{n}\right)}{\sum_i y_i^2 - \frac{\left(\sum_i y_i\right)^2}{n}}}$$

where r is the multiple correlation coefficient,

x_{ji} is the value of the *j*th explanatory variable of compound *i*,

y_i is the value of the *j*th dependent variable of compound *i*,

k is the number of employed explanatory parameters,

b_j is the regression coefficient of descriptor *j*, and

n is the number of considered compounds.

The F-distribution mirrors the ratio of the variance, which is a measure of the spread of data, that is explained by the established regression equation to the variance not explained, taking the degrees of freedom into account. The F-distribution can be regarded as a measure of significance of the established regression equation as a whole.

$$F = \frac{\frac{\sum_i (\hat{y}_i - \bar{y}_i)^2}{k}}{\frac{\sum_i (y_i - \hat{y}_i)^2}{(n-k-1)}}$$

where F is the F-value corresponding to the multiple regression equation,

y_i is the observed value of compound *i*,

y_i is the calculated value of compound *i*,

n is the number of considered compounds, and

k is the number of employed explanatory parameters.

The standard deviation of the estimate s is defined as the square root of the variance and represents the most commonly used measure of spread. With respect to the performed QSAR study, the standard deviation s expresses the degree of deviation of the calculated biological activity from the experimentally determined biological activity.

$$s = \sqrt{\frac{\sum_i (y_i - \hat{y}_i)^2}{(n-k-1)}}$$

where s is the standard deviation corresponding to the multiple regression equation,

y_i is the observed value of compound *i*,

y_i is the calculated value of compound *i*,

n is the number of considered compounds, and

k is the number of employed explanatory parameters.

The t-value describes the ratio of the regression coefficient b of a single parameter to the standard deviation s_b of that parameter. It can be regarded as a measure of significance of that single variable in the established regression equation.

$$t = \frac{b_i}{s_{b_i}}$$

where t is the t-value corresponding to the variable x_i,

b_i is the regression coefficient of the variable x_i, and

s_{b_i} is the standard deviation of the variable x_i.

The coefficient of determination r^2 represents the percent of the variance that can be explained by the regression equation, mathematically defined as the explained variance divided by the total variance.

$$r^2 = \frac{\sum_{j=1}^{k} b_j \left(\sum_i y_i x_{ji} - \frac{\sum_i y_i \sum_i x_{ji}}{n}\right)}{\sum_i y_i^2 - \frac{\left(\sum_i y_i\right)^2}{n}}$$

where r^2 is the coefficient of determination corresponding to the multiple regression equation,

x_{ji} is the value of the *j*th explanatory variable of compound *i*,

y_i is the value of the *j*th dependent variable of compound *i*,

k is the number of employed explanatory parameters,

b_j is the regression coefficient of descriptor *j*, and

n is the number of considered compounds.

In QSAR studies, the cross-validated coefficient of determination, referred to as q^2, is widely adopted to quantitatively express the predictive power of a correlation. Cross-validation can be performed by the Leave-One-Out (LOO) method. The q^2-values were calculated by the computer program employed for the paullone multiple regression correlation studies (cf. chapter 7.4.1) as shown below.

$$q^2 = 1 - \left(\frac{PRESS}{MS}\right)$$

where q^2 is the cross-validated coefficient of determination corresponding to the multiple regression equation,

PRESS stands for "prediction error sum of squares",

$$PRESS = \sum_{i=1}^{n} (y_i - \hat{y}_i)^2$$

MS stands for "mean squares",

$$MS = \sum_{i=1}^{n} (y_i - \bar{y}_i)^2$$

y_i is the observed value of compound *i*,

y_i is the calculated value of compound *i*, and

n is the number of considered compounds.

If the sum of the squared deviations of the calculated values from the observed values (PRESS) is larger than the sum of the squared deviations of the observed values from the mean observed value (MS), q^2 adopts a negative value. This implies that the proposed regression equation does not provide reasonable predictions.

The confidence interval represents the range of values that is believed to encompass the "true" value with a high probability (usually 95%). It can be regarded as a measure of precision of an estimated value. Wider intervals indicate lower precision and vice versa.

The number of compounds n indicates the number of derivatives incorporated in the calculation of a regression equation.

4.2.3 Evaluation of the Statistical Quantities

The evaluation process obligatorily comprises the consideration of all the statistical quantities determined for the established regression equation. Several guidelines aid in comprehensively judging the obtained results:

- The correlation coefficient r and the cross-validated coefficient of determination q^2, the latter representing the more critical value, should be as high as possible, the standard deviation s as low as possible. In case of a negative q^2-value being obtained, no predictive power can be assigned to the established regression equation.
- Every explanatory variable employed in the regression equation has to make a valuable contribution. The fulfillment of this requirement is surveyed by analyzing the particular t-values. An explanatory variable is regarded to be significant if the t-value exceeds 2.2. In addition to that, the corresponding F-distribution-value should increase and thus mirror the significance of the additionally employed descriptor. In case a distinctive rise in the F-value cannot be observed, the particular variable should not be incorporated into the regression equation, regardless of the corresponding t-value.
- The ratio of the number of compounds n incorporated into the calculation to the number of the employed explanatory variables should be greater than five. As few descriptors as possible should be utilized for establishing a regression equation.

The insights gained by the careful evaluation of the statistical quantities corresponding to the multiple regression equations provide the basis for the decisions made on the selection of the parameters employed in future analyses.

4.3 Performed Multiple Regression Analyses

An overview of the selection of compounds, the employed literature parameters, the calculated substituent parameters, and the obtained regression equations with the corresponding statistical quantities are presented in the experimental section of this thesis (chapter 7.4).

4.3.1 Substituent Properties and Enzyme Inhibition

An iterative procedure was chosen for the performance of the QSAR analysis. First, random combinations of electronic, hydrophobic, and steric parameters were tested. The subsequent evaluation of the statistical quantities corresponding to the resulting regression equations then revealed the most suitable substituent parameters, the mathematical functionalities to be applied, respectively, and the most significant parameter combinations.

In the next phase, it was aimed at applying the best parameter combinations established for the initial small data set to the large data set which also included the new paullone derivatives synthesized within the scope of this thesis. Encountered difficulties during this adaptation procedure were tried to overcome by designing individual analyses for the investigation of the different critical issues.

4.3.1.1 Initial Experiments with 9-Substituted Paullones

The initial data set considered all the tested paullone derivatives that were substituted at the 9-position only, resulting in a compound number n of 14 (compounds 1-14, listed in table 7-1, chapter 7.4.2). Different choices of two to four descriptors were employed for correlating the physicochemical properties of the residues with the inhibitory activity towards the isolated enzyme CDK1/cyclin B (cf. chapter 7.4.5, regression equations 1-52). Consequently, the ratio of compounds to variables was in many cases not above the desired threshold level of five. This reality was tolerated because the purpose of these first correlation calculations consisted in the comparison of the substituent constants within their groups (electronic, hydrophobic, or steric descriptors), and in the gain of

first insights. The best results were provided by regression equations containing one representative of each group of substituent constants, the hydrophobic descriptor π being raised to the power of 2. The most advantageous electronic descriptors were σ_p and σ_m, the most favorable steric substituent constants MR and L. The steric parameter can be applied in its linear and square function (e.g., MR + MR^2) in order to imitate a hyperbolic relationship, mirroring a consistent steric contribution of the residue to the inhibitory activity of the compound after having attained a certain size. The regression equations supplying the best results, employing three and four explanatory variables, are depicted below (regression equations 10 and 48).

Regression Equation 10: π^2, σ_m, MR

$$pIC_{50}(\text{CDK1/cyclin B}) = 5.25(\pm0.44) - 0.26(\pm0.25)\,\pi^2 + 2.65(\pm0.83)\,\sigma_m + 0.05(\pm0.06)\,MR$$

n = 14	$t(\pi^2) = 2.35$	$t(\sigma_m) = 7.15$	t(MR) = 2.05
r = 0.927	s = 0.331	F = 20.24	$q^2 = 0.731$

Regression Equation 48: π^2, σ_p, L, L^2

$$pIC_{50}(\text{CDK1/cyclin B}) = 1.60(\pm2.11) - 0.25(\pm0.13)\,\pi^2 + 1.45(\pm0.33)\,\sigma_p + 2.24(\pm1.20)\,L - 0.26(\pm0.16)\,L^2$$

n = 14	$t(\pi^2) = 4.28$	$t(\sigma_p) = 9.82$	t(L) = 4.21	$t(L^2) = 3.57$
r = 0.977	s = 0.199	F = 47.01	$q^2 = 0.851$	

In both regression equations, the highest t-value is provided by the electronic parameter. As a matter of fact, the electronic descriptor provides the highest t-value in all the performed correlation calculations, respectively. This hints an outstanding significance of the electronic properties of a substituent and a subordinate impact of the hydrophobic and steric substituent properties on the biological activity.

Further regression analyses with this data set were performed substituting CDK5/p25 or GSK-3β for CDK1/cyclin B as the dependent variable (cf. chapter 7.4.5, regression equations 53-69). However, the previously approved combinations of explanatory variables did not provide similarly good results. It was thus decided to concentrate on establishing a quantitative relationship between the substituent properties and the inhibitory activity towards CDK1/cyclin B.

4.3.1.2 Integration of 2- and 3-Methoxy-Substituted Paullones

In order to increase the number of compounds n, and thus to meet the conditions concerning the ratio of considered compounds to employed variables, it was investigated whether 9-substituted paullone derivatives that additionally carry a methoxy residue at the 2- and/or 3-position could be incorporated into the existing data set. The qualitative structure-activity relationship analysis had provided the insight that substituents introduced at the 2- or 3-position were tolerated without affecting the inhibitory activity (cf. chapter 3.4). Therefore, it was assumed that the additional compounds (compounds 15-25, listed in table 7-1, chapter 7.4.2) could be properly integrated, and a larger data set could hence be created. In order to prove this assumption, analyses were performed in which similar combinations of variables were used for both the initial and the enlarged data set (cf. chapter 7.4.5, regression equations 7, 10, 70-79). The resulting statistical data was then compared, carefully analyzing whether the matching q^2-values, derived from the initial and the enlarged data set, respectively, diverged in a significant manner. Table 4-1 gives an overview of the obtained results.

Table 4-1: Comparison of initial and enlarged data set

parameters	equation	n	F	q^2
π^2, σ_p, MR	7	14	20.64	0.716
	70	25	26.29	0.700
π^2, σ_m, MR	10	14	20.24	0.731
	71	25	26.73	0.718

Table 4-1: Comparison of initial and enlarged data set (continuation)

parameters	equation	n	F	q^2
π^2, σ_p, dist	72	14	16.70	0.648
	73	25	20.38	0.639
π^2, σ_m, dist	74	14	13.34	0.644
	75	25	18.90	0.628
π, σ_p	76	14	15.56	0.612
	77	25	18.13	0.527
π, σ_m	78	14	19.66	0.679
	79	25	26.04	0.625

As expected, the matching q^2-values are nearly identical, thus legitimizing the integration of the methoxy-substituted paullone derivatives into the data set. The only pair of q^2-values showing a certain divergence resulted from the employment of the parameter combination π, σ_p and was considered negligible. The increased number of compounds n exerts a positive effect on the F-values, increasing the significance of the regression equations as a whole.

4.3.1.3 Integration of Newly Synthesized Paullones and Use of Calculated Parameters

In the next phase of the paullone QSAR study, it was aimed at applying the approved parameter combinations to the large data set which included further tested paullone derivatives (compounds 25-29, listed in table 7-1, chapter 7.4.2) and newly synthesized paullones (compounds 30-41, listed in table 7-1, chapter 7.4.2), for example, ester derivatives. It had to be surveyed whether the mathematical relationships derived from the small and the enlarged data sets could still be regarded as true correlations after further increasing the number of considered compounds and the variability within the data set.

The analysis could not be performed employing the common literature parameters, which had been operated with up to now, due to the fact that literature parameters were not available for many of the newly introduced substituents (cf. chapter 7.4.3, table 7-2). Therefore, the substituent constants corresponding to the residues introduced at the 9-position of the paullone molecules were all (re)calculated by means of the ACDLabs computer program (cf. chapter 7.4.4). The calculated parameters were utilized for all the correlation calculations performed with the new, large data set.

The parameter combination π^2, σ_m, MR, which had previously supplied the best regression equations, provided poor results when applied to the large data set (regression equation 89).

Regression Equation 89: π^2, σ_m, MR

$$pIC_{50}(CDK1/cyclin\ B) = 5.78(\pm0.76) + 0.08(\pm0.08)\ \pi^2 + 2.45(\pm1.30)\ \sigma_m - 0.07(\pm0.05)\ MR$$

n = 36	$t(\pi^2) = 1.96$	$t(\sigma_m) = 3.83$	t(MR) = 2.56
r = 0.674	s = 0.742	F = 8.86	$q^2 = 0.123$

The values for r, F and q^2 are extremely low, the standard deviation s is very high, and the descriptor π^2 does not play a significant role. In this case, the employed parameters π^2, σ_m, and MR did not lead to the establishment of a quantitative relationship between substituent properties and enzyme inhibition.

Hence, many other combinations of electronic, hydrophobic, and steric parameters were tested. The number of considered compounds ranged between 36 and 40, the number of utilized descriptors between 1 and 4 (cf. chapter 7.4.5, regression equations 80-118). None of the correlation calculations supplied acceptable results; the best regression equation merely reached a q^2-value of 0.382 (regression equation 94).

Regression Equation 94: π^2, σ_p, dist

pIC_{50}(CDK1/cyclin B) = 6.57(±0.56) + 0.11(±0.07) π^2 + 1.33(±0.74) σ_p - 0.31(±0.16) dist

n = 37	t(π^2) = 2.96	t(σ_p) = 3.68	t(dist) = 3.94
r = 0.695	s = 0.718	F = 10.25	q^2 = 0.382

Again, the s-value is unacceptably high while the values for r, F, and q^2 remain poor. In consequence, it had to be investigated whether the dramatic change in quality of the obtained results had to be ascribed to the usage of the calculated parameters, the usage of the large data set, or the combination of both.

4.3.1.4 Comparison of Literature and Calculated Parameters

In order to be able to properly compare the results obtained using the calculated parameters to those derived from the literature parameters, the data sets worked with needed to be similar. The enlarged data set, consisting of the primary 9-substituted paullones and the additionally 2- and/or 3-methoxy-substituted paullones but not the newly synthesized derivatives, was chosen to be employed. Significant results had been obtained using the literature parameters (cf. chapter 4.3.1.2), so the results provided by the employment of the calculated parameters would be suitable for a direct comparison. The validity of the calculated parameters could be evaluated.

Correlation calculations were performed with a variety of descriptor combinations, separately applying calculated and literature parameters (cf. chapter 7.4.5, regression equations 119-136 and 137-147). A summary of the selected descriptors and the obtained results is presented in table 4-2.

Table 4-2: Comparison of literature and calculated parameters under application of the enlarged data set

parameters	source	equation	n	F	q^2
σ_p	lit	137	25	37.66	0.555
	calc	119	25	35.48	0.537
σ_m	lit	138	25	54.17	0.650
	calc	120	25	51.99	0.639
MR	lit	139	25	2.40	-0.039
	calc	121	23	0.25	-0.158
dist	lit	140	25	3.23	-0.095
	calc	123	25	2.16	-0.048
π	lit	141	25	0.22	-0.144
	calc	124	24	0.65	-0.160
π, σ_m, MR	lit	142	25	19.00	0.626
	calc	125	23	13.04	0.562
π, σ_p, MR	lit	143	25	15.45	0.577
	calc	126	23	12.01	0.550
π^2, σ_p, MR	lit	70	25	26.29	0.700
	calc	127	23	17.51	0.645
π^2, σ_m, MR	**lit**	**71**	**25**	**26.73**	**0.718**
	calc	128	23	19.17	0.665
π^2, σ_m, MR, MR^2	lit	144	25	19.97	0.708
	calc	129	23	13.66	0.487
π, π^2, σ_m, MR	lit	145	25	22.21	0.707
	calc	130	23	16.45	0.672
π^2, σ_m, dist	lit	75	25	18.90	0.628
	calc	**132**	**24**	**26.15**	**0.738**

Table 4-2: Comparison of literature and calculated parameters under application of the enlarged data set (continuation)

parameters	source	equation	n	F	q^2
π^2, σ_p, dist	lit	73	25	20.38	0.639
	calc	133	24	19.98	0.686
π^2, σ_m, dist, $dist^2$	lit	146	25	13.52	0.598
	calc	134	24	19.03	0.715
π^2, σ_m, $dist^2$	lit	147	25	18.92	0.625
	calc	135	24	24.92	0.723
π, σ_m	lit	79	25	26.04	0.625
	calc	136	24	22.02	0.605

The abbreviation “lit” signalizes the employment of the parameters stated in literature (cf. chapter 7.4.3), “calc” stands for the usage of the parameters calculated with the ACDLabs computer program (cf. chapter 7.4.4).

The regression equations providing the best results are depicted in bold letters, respectively.

Several observations were made when evaluating the data presented in the table above:

The usage of the calculated parameters resulted in q^2-values that differed slightly from the ones obtained with literature parameters. The parameter combination π^2, σ_m, MR, MR^2 (regression equations 144 and 129) was regarded as an exception; here, the corresponding q^2-values showed a significant divergence.

If the parameter “dist” was included in the applied parameter combination, the q^2-values originating from the calculated parameters were higher than those derived from the literature parameters. Again, it has to be pointed out that the definition for the calculated parameter “distance” differs from the definition stated in literature (cf. chapter 4.2.1). As the calculated parameter “dist” was especially designed for the paullone derivatives based on the optimized 3D-structures, the more favorable results are well explicable. For the same reason, the slightly higher divergence in the corresponding q^2-values seems deducible.

If the substituent constants MR, dist, or π were applied as sole explanatory variables, respectively, negative q^2-values were obtained, conferring no predictive power to the established regression equations. However, the descriptors σ_m and σ_p each provided respectable results if employed as the only explanatory variable. This serves as further evidence for the outstanding significance of the electronic substituent constant within the regression equations.

The employment of the calculated parameters under application of the enlarged data set resulted in regression equations of fairly similar quality as observed for the ones obtained with the literature parameters. The best result derived from calculated parameters (regression equation 132) is even slightly superior to the best result obtained with literature parameters. Therefore, the impairment of the data obtained under the application of the large data set and the usage of the calculated parameters (cf. chapter 4.3.1.3) does not seem to be caused by the change in employed parameters.

Regression Equation 132: π^2, σ_m, dist

$$pIC_{50}(\text{CDK1/cyclin B}) = 4.92(\pm0.52) - 0.24(\pm0.16)\,\pi^2 + 2.55(\pm0.65)\,\sigma_m + 0.29(\pm0.20)\,\text{dist}$$

n = 24	$t(\pi^2) = 3.28$	$t(\sigma_m) = 8.18$	t(dist) = 3.03
r = 0.893	s = 0.338	F = 26.15	$q^2 = 0.738$

4.3.1.5 Comparison of Small and Large Data Set

The investigation now focused on the size and on the composition of the data set. It was important to analyze whether the application of the large data set (compounds 1-41, listed in table 7-1, chapter 7.4.2) would impair the previously obtained results that were derived from literature parameters under application of the smaller data sets (cf. chapters 4.3.1.1 and 4.3.1.2). For that purpose, the same parameter combinations used in the beginning of the paullone QSAR study (cf. chapter 7.4.5, regression equations 1-69) were applied to the large data set (cf. chapter 7.4.5, regression equations 164-233), thus assuring the ability to directly compare the corresponding results. In addition to that, other parameter

combinations were employed (cf. chapter 7.4.5, regression equations 234-261), including the ones previously applied under usage of the calculated parameters (cf. chapter 4.3.1.3). The most representative data is depicted in tables 4-3 and 4-4.

Table 4-3: Comparison of small and large data set employing literature parameters

parameters	equation	n	F	q^2
π^2, σ_p, L	39	14	26.90	0.712
	203	28	5.00	0.097
π^2, σ_p, MR	7	14	20.64	0.716
	170	28	4.72	0.084
π^2, F, R, MR	16	14	17.36	0.711
	181	32	4.82	0.131
π^2, σ_p, L, L^2	48	14	47.01	0.851
	212	28	4.97	0.268
π^2, σ_m, MR, MR^2	33	14	20.68	0.788
	196	31	4.70	0.064

Table 4-4: Comparison of enlarged and large data set and of literature and calculated parameters

parameters	equation		n		F		q^2	
	lit	calc	lit	calc	lit	calc	lit	calc
π^2, σ_p, MR	70	127	25	23	26.29	17.51	0.700	0.645
	171	88	33	36	4.85	6.61	0.096	0.046
π^2, σ_m, dist	75	132	25	24	18.90	26.15	0.628	0.738
	247	93	33	36	7.74	8.86	0.312	0.123

The abbreviation “lit” signalizes the employment of the literature parameters (cf. chapter 7.4.3), “calc” the usage of the calculated parameters (cf. chapter 7.4.4).

Both tables clearly demonstrate the loss of significance that occurs when applying the large data set instead of the small or the enlarged one. The impairment of statistical quantities like F- and q^2-values takes place without being affected by the choice of parameters (i.e., literature or calculated parameters). As a matter of fact, a significant regression equation could not be established under application of the large data set.

Critically revising the composition of the large data set (compounds 1-41, listed in table 7-1, chapter 7.4.2), it was once more analyzed whether the incorporation of the additionally methoxy-substituted paullone derivatives into the data set constituted a legitimate action. This time, a “dummy-parameter” was employed. Dummy-parameters, also called indicator variables, are commonly used in QSAR analyses to indicate merely the presence or absence of a substituent or substructure. Thus, a dummy-parameter represents a descriptor that can only assume the two values 1 or 0, depending on the presence or absence of a given condition. In the resulting regression equation, the t-value corresponding to the dummy-parameter then indicates whether the examined condition makes a significant contribution to the established quantitative relationship.[133] In this case, a methoxy group at the 3-position of the paullone molecules represented the structural feature to be characterized by the employed dummy-parameter. Analyses were performed with three different descriptor combinations under application of the large data set, utilizing the literature parameters as well as, in separate correlation calculations, the calculated parameters (cf. chapter 7.4.5, regression equations 161-163 and 258, 259, and 261). The results are shown in table 4-5.

Table 4-5: Employment of a dummy-parameter

parameter	source	equation	n	t(Y/N)	F	q^2
π^2, σ_p, MR, Y/N	lit	258	33	0.10	3.52	0.048
	calc	161	36	0.37	4.86	0.005
π^2, σ_m, dist, Y/N	lit	259	33	0.14	5.62	0.275
	calc	162	37	0.91	9.88	0.428

Table 4-5: Employment of a dummy-parameter (continuation)

parameter	source	equation	n	t(Y/N)	F	q^2
π, σ_m, Y/N	lit	261	33	0.13	6.59	0.275
	calc	163	37	0.49	8.65	0.270

The column "t(Y/N)" lists the t-values corresponding to the utilized dummy-parameter.

"Y/N" stands for "yes/no", indicating the presence or the absence of a methoxy group at the 3-position of the paullone molecules.

All t-values corresponding to the employed dummy-parameter range between 0 and 1 and hence lie below the limit of significance of 2.2 (cf. chapter 4.2.3). Consequently, the presence or absence of a methoxy group at the 3-position of a paullone molecule does not make a significant contribution to the regression analysis. The integration of the additionally methoxy-substituted paullone derivatives into the data set can therefore be regarded as a qualified action.

4.3.1.6 Data Set Variations

The composition of the large data set was further examined. It was analyzed whether the loss of quality of the obtained QSAR results could be assigned to certain compounds or to a specific group of compounds (e.g., ester derivatives). For that purpose, a parameter combination was chosen which was constantly employed for the performed analyses in order to be able to observe the impact of the data set variations. Having supplied the best results under utilization of the calculated parameters, the descriptors π^2, σ_m, and dist were selected. The data set was diversified in numerous ways, trying to discover the trigger for the loss of significance of the established quantitative relationship (cf. chapter 7.4.5, regression equations 262-290). First, compounds with certain functional groups were excluded from the large data set, then substances whose substituent size exceeded a defined limit. Finally, the newly synthesized compounds were added individually to the enlarged data set which had supplied significant regression equations. In spite of carefully analyzing the obtained results, which remained fairly poor, the responsible factor could not be identified. Table 4-6 shows some examples of the performed data set variations.

Table 4-6: Examples of the diversification of the large data set under employment of the parameter combination π^2, σ_m, dist

performed variation	equation	n	F	q^2
w/o esters, amides	262	30	6.81	0.266
w/o esters, carboxylic acid	287	30	14.89	0.526
w/o esters, amides, carboxylic acid	264	29	12.16	0.471
w/o esters, amides, $SO_{(2)}$-derivatives	263	25	4.76	0.225
w/o derivatives with dist > 5	283	32	7.70	0.280
w/o derivatives with dist > 4	284	30	7.92	0.310
w/o derivatives with dist > 3	285	21	10.34	0.479

The column “performed variation” displays which paullone derivatives were excluded from the large data set. “W/o” stands for “without”.

The ester derivatives were more closely examined. It was analyzed whether a correlation between substituent properties and biological activity could be determined within this compound group (cf. chapter 7.4.5, regression equations 291-293). The resulting q^2-values were negative; the corresponding regression equations expressed no predictive power. The lack of a comprehensible correlation within the group of ester derivatives had already been presumed in the discussion of the qualitative structure-activity relationships (cf. chapter 3.4).

4.3.1.7 Conclusions

The descriptors π^2, σ_m, and dist proved to be the best parameter combination for describing the quantitative relationship between the physicochemical properties of the substituents located at the 9-position of the paullone molecules and the inhibitory activity of the derivatives towards the enzyme CDK1/cyclin B. Correlation calculations based on a data set comprising 25 compounds resulted in the establishment of a significant regression equation as depicted in figure 4-1.

Figure 4-1: Regression analysis without newly synthesized paullones

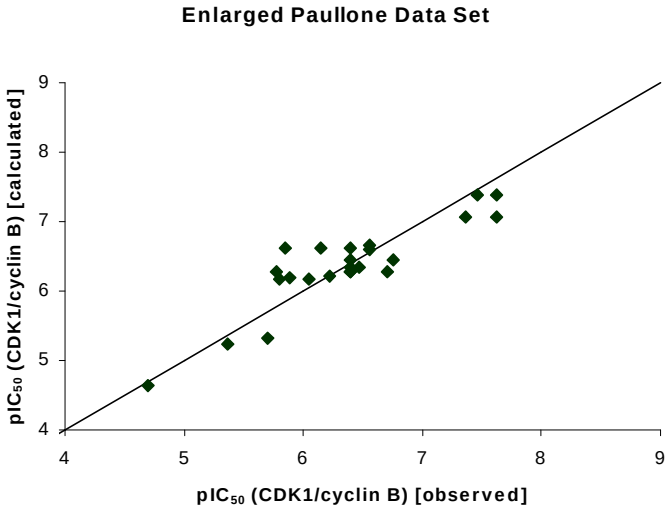

pIC_{50}(CDK1/cyclin B) = 4.92(±0.52) - 0.24(±0.16) p^2 + 2.55(±0.65) s_m + 0.29(±0.20) dist

This figure illustrates regression equation 132 (cf. chapter 7.4.5).
Statistical quantities: n = 24, r = 0.893, s = 0.338, F = 26.15, q^2 = 0.738.
The drawn straight line represents the imaginary perfect correlation where r = 1.

The depicted regression equation reveals that the electronic parameter σ_m clearly represents the most significant descriptor. The hydrophobic parameter π^2 and the steric parameter dist are of little significance. The previously assumed outstanding relevancy of the electronic properties of the substituents at the 9-position of the paullone molecules was thus confirmed.

The incorporation of the newly synthesized paullone derivatives, for example, compounds carrying carbonyl substituents at the 9-position, resulted in the loss of significance of the established quantitative relationship. The proposed correlation could not be verified when varying the composition of the data set. This is illustrated in figure 4-2.

Correlation calculations based on the large data set comprising 41 compounds did not lead to the establishment of a significant regression equation. A valuable mathematical relationship between the substituent properties and the biological activity could not be derived.

Figure 4-2: Regression analysis including the new paullone derivatives

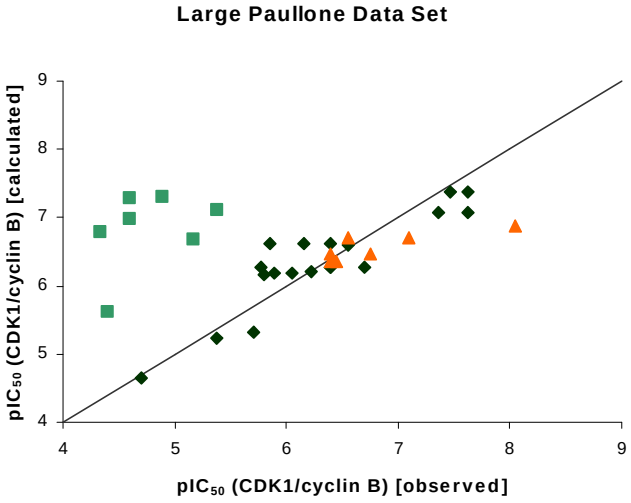

pIC_{50}(CDK1/cyclin B) = 4.92(±0.52) - 0.24(±0.16) p^2 + 2.55(±0.65) s_m + 0.29(±0.20) dist

The triangles represent the 9-sulfur-substituted paullone derivatives, the squares represent the compounds carrying carbonyl residues at the 9-position.
The rhomboid symbols embody the primarily synthesized paullones, also depicted in figure 4-1.

In this figure, primarily synthesized 9-sulfur-substituted paullones that were employed for establishing the shown regression equation, are shown as triangles and not as rhomboid symbols like in figure 4-1.

The pIC_{50}-values of the sulfur and the carbonyl derivatives were calculated employing the depicted regression equation.

The drawn straight line represents the imaginary perfect correlation where r = 1.

The prediction of the inhibitory activity of the derivatives carrying a sulfur residue at the 9-position of the paullone molecule, based on the regression equation derived from the enlarged data set, led to satisfactory results. However, it has to be pointed out that most sulfur-substituted paullones had been included in the enlarged data set that was employed for establishing the depicted regression equation. Two new derivatives were predicted (compounds 26 and 35, listed in table 7-1, chapter 7.4.2); one (compound 35) proved to be much more potent than expected, represented by the triangle furthest to the right in figure 4-2. This compound is the 2-methoxy-substituted sulfone **37b** which constitutes one of the most potent CDK1/cyclin B inhibitors discovered up to today (cf. chapter 3.1). A comparison of the observed and the calculated pIC_{50}-values of the 9-sulfur-substituted paullones is presented in table 4-7.

Table 4-7: Comparison of observed and calculated pIC_{50}-values of paullones with 9-sulfur-substituents

compound number	observed pIC_{50}-value	calculated pIC_{50}-value
12	6.40	6.47
13	6.40	6.36
14	6.55	6.70
24	6.75	6.47
25	6.45	6.36
26	7.10	6.70
35	8.05	6.88

The column “compound number” shows the numbers assigned to the substances in table 7-1, chapter 7.4.2.

The prediction of the inhibitory activity of the 9-carbonyl-substituted paullones resulted in much higher IC_{50}-values than observed in the biological testing (table 4-8).

Table 4-8: Comparison of observed and calculated pIC_{50}-values of paullones with 9-carbonyl-substituents

compound number	observed pIC_{50}-value	calculated pIC_{50}-value
30	4.60	7.29
31	5.16	6.69
33	4.89	7.32
36	4.60	6.99
38	5.38	7.11
39	4.33	6.80
41	4.40	5.61

The column “compound number” shows the numbers assigned to the substances in table 7-1, chapter 7.4.2.

The carbonyl derivatives are widely scattered within the graph depicted in figure 4-2, lacking a logical order. The seemingly random scattering is comprehensible when keeping in mind that the only structural difference between the paullone esters consists in the length of the ester chains. However, the chain length is mirrored by the steric descriptor, and that parameter plays a very insignificant role in the illustrated regression equation, exerting almost no influence on the result of the calculation of the pIC_{50}-value.

With respect to the overall poor inhibitory activity exhibited by the 9-carbonyl-substituted paullones, a self-evident explanation does not exist. Possibly, the carbonyl functionality provokes severe changes in the arrangement of these paullone derivatives at the active site. A putative reason might be the encumbrance of important interactions between the inhibitor molecule and the amino acids generating the ATP binding pocket. If the manner of binding of the paullones with 9-carbonyl-substituents differed from the one of the other paullone compounds, an essential requirement established for the performance of QSAR analyses would no longer be met: different mechanisms underlay the observed biological activity of the substances (cf. chapter 4.2). This reality would account for the fact that the paullones carrying carbonyl residues at the 9-position cannot be described by the established regression equation. The incompatibility of the 9-carbonyl-substituted derivatives with the primarily synthesized paullones would be explicable.

4.3.2 Cell Growth Inhibition

An additional multiple regression analysis was performed that focused on the inhibitory activity of paullone derivatives towards the whole cell, employing the observed cell growth inhibition of characteristic cancer cell lines as the dependent variable, respectively, within the regression equations.

Although the in vitro inhibition of cyclin-dependent kinases has been proven, the exact mechanism by which paullones unfold their antitumor effect has not been discovered up to now.[142] Therefore, it was investigated whether the inhibition of the enzymes CDK1/cyclin B, CDK5/p25, or GSK-3β played a role in the observed inhibition of the whole cell. Via multiple regression analysis, the degree of contribution made by each inhibited enzyme could also be determined if a correlation between enzyme inhibition and cell growth inhibition existed.

Besides the enzyme inhibition, the transport of the compounds across the cell membrane had to be taken into account. The ability to reach the interior of the cell, and thus the potential sites of action, was represented by the log P-values of the paullone derivatives which were calculated by means of the ACDLabs computer program (cf. chapter 7.4.4).

Regression analyses were performed separately with four different cancer cell lines: the colon cancer cell line HCT-116 (cf. chapter 7.4.5, regression equations 308-324), the leukemia cell line SR (cf. chapter 7.4.5, regression equations 325-341), the renal cancer cell line RXF 393 (cf. chapter 7.4.5, regression equations 342-355), and the melanoma cell line LOX IMVI (cf. chapter 7.4.5, regression equations 356-369). These cell lines were chosen because of their eminent sensibility to the anti-proliferative effects exerted by the paullones. In the correlation calculations, the determined pIC_{50}-values of the enzymes and/or the calculated log P-values of the paullone derivatives were employed as the explanatory variable(s). The number of compounds considered in the regression analyses ranged from 65 to 75, including the newly synthesized paullone derivatives. The enzyme inhibition data of the primarily produced paullones were taken from the article published by Leost[5].

All obtained regression equations had little or no predictive power. The obtained q^2-values all lay below 0.4, hinting the absence of a correlation between enzyme inhibition and cell growth inhibition. Thus, the antitumor effect exerted by the paullones can seemingly not be ascribed to their inhibitory activity towards CDK1/cyclin B, CDK5/p25, or GSK-3β. This assumption complies with the findings recently published by Lahusen[142] who reports on the investigation of the mechanism of the anti-proliferative effects of alsterpaullone (**2**), the most potent paullone derivative. Lahusen demonstrates that alsterpaullone induces apoptosis via caspase activation. The effects on the cell cycle machinery presumably occur irrespectively of the activation of caspases and are supposedly not sufficient for the induction of apoptosis. Concerning alsterpaullone, a correlation between CDK inhibition and the effects on tumor cells could not be discovered.

Finally, it was briefly analyzed whether the cell growth inhibition of the colon cancer cell line HCT-116 could be correlated with the physicochemical properties of the substituents located at the 9-position of the paullone molecules (cf. chapter 7.4.5, regression equations 301-307). The resulting regression equations had little or no predictive power – hence, the approach was not further pursued.

5 Summary

Paullones represent a class of cyclin-dependent kinase inhibitors, structurally defined as 7,12-dihydroindolo[3,2-*d*][1]benzazepin-6(5*H*)-ones. With a view to analyze structure-activity relationships, paullone derivatives with different substituents at the 9-position of the molecules were synthesized within the scope of this thesis. Focus was put on the introduction of electron-withdrawing sulfur and carbonyl residues.

The synthesized paullones underwent biological testing. None of the compounds unfolded an outstanding anti-proliferative activity like alsterpaullone (**2**), the most potent paullone derivative.

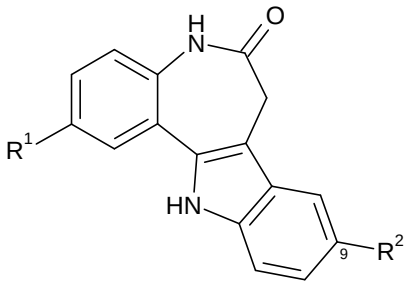

2 $R^1 = H, R^2 = NO_2$

37b $R^1 = OCH_3, R^2 = SO_2CH_3$

40a $R^1 = H, R^2 = COOC_2H_5$

With respect to the CDK1/cyclin B-inhibitory activity, the new compound **37b** was fourfold more active than alsterpaullone. The derivative **37b** thus embodies one of the strongest CDK1/cyclin B inhibitors existing so far.

The paullone **40a** proved to unfold inhibitory effects on the growth of *Trypanosoma cruzi*, the parasite causing the Chagas disease. As **40a** exhibits only moderate cytotoxic effects on host cells, it can be regarded as a new lead in the drug development for the treatment of trypanosomal infections.

In the course of the preparation of new compounds, the skeletal rearrangement of paullones to 11*H*-indolo[3,2-*c*]quinoline-6-carboxylic acids was discovered (scheme 5-1).

Scheme 5-1:

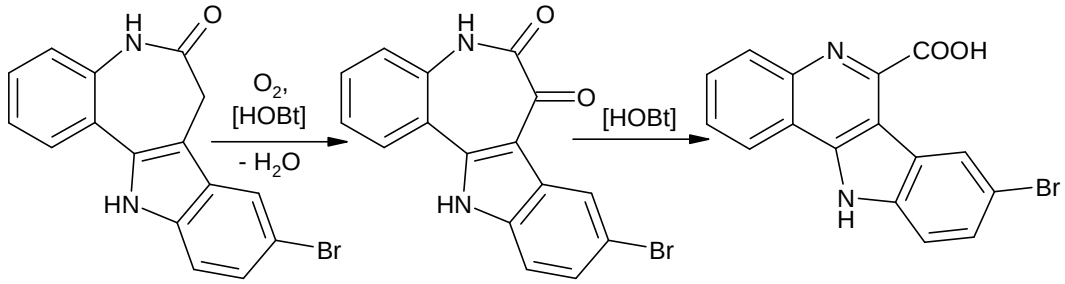

1 **90** **79c**

The mechanism presumably involves the aerobic oxidation of the paullone **1**, promoted by HOBt as a radical catalyst, followed by the conversion of the activated derivative **90** into the rearranged product **79c**, conceivably catalyzed by HOBt as well.

Using the obtained biological data, a paullone QSAR study was performed. It provided the insight that the quantitative relationship between the physicochemical properties of the substituents at the 9-position of the paullone molecules and the exhibited CDK1/cyclin B-inhibitory activity of the compounds can best be characterized by means of the regression equation

$$pIC_{50}(\text{CDK1/cyclin B}) = 4.92(\pm0.52) - 0.24(\pm0.16)\,\pi^2 + 2.55(\pm0.65)\,\sigma_m + 0.29(\pm0.20)\,\text{dist}$$

The electronic parameter σ_m constitutes the by far most significant descriptor. The established relationship becomes less significant if the variety within the applied data set is increased.

A correlation between enzyme inhibition (i.e., inhibition of CDK1/cyclin B, CDK5/p25, and/or GSK-3β) and cancer cell growth inhibition could not be derived. Therefore, the anti-proliferative effects exerted by the paullones cannot exclusively be ascribed to the observed CDK inhibition.

6 Zusammenfassung

Paullone stellen eine Klasse von Inhibitoren Cyclin-abhängiger Kinasen mit der Grundstruktur des 7,12-Dihydroindolo[3,2-*d*][1]benzazepin-6(5*H*)-ons dar. Um Untersuchungen zu Struktur-Aktivitäts-Beziehungen durchführen zu können, wurden im Rahmen dieser Arbeit Paullonderivate mit diversen Substituenten in 9-Position der Moleküle synthetisiert. Dabei stand die Einführung von elektronenziehenden Schwefel- und Carbonylresten im Mittelpunkt.

Die synthetisierten Paullone wurden biologischen Testungen unterzogen. Keine der Verbindungen zeigte eine so herausragende antiproliferative Aktivität wie Alsterpaullon (**2**), das potenteste Paullonderivat.

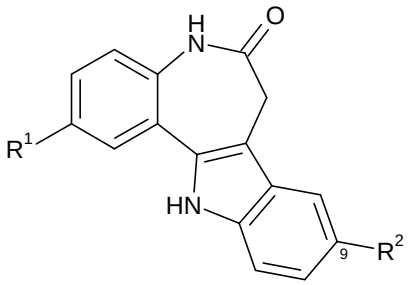

2 $R^1 = H$, $R^2 = NO_2$

37b $R^1 = OCH_3$, $R^2 = SO_2CH_3$

40a $R^1 = H$, $R^2 = COOC_2H_5$

Hinsichtlich der CDK1/Cyclin B-inhibitorischen Aktivität entfaltete die neue Verbindung **37b** eine vierfach stärkere Wirkung als Alsterpaullon. Das Derivat **37b** verkörpert so einen der potentesten CDK1/Cyclin B-Inhibitoren, die zur Zeit verfügbar sind.

Das Paullon **40a** erwies sich als Wachstumshemmstoff für *Trypanosoma cruzi*, den parasitären Erreger der Chagas-Krankheit. Da **40a** nur schwache Zytotoxizität gegenüber den Wirtszellen zeigt, kann es als eine neue Leitstruktur für die Entwicklung von Arzneistoffen gegen Trypanosomen-Infektionen angesehen werden.

Im Rahmen der Synthese neuer Paullone wurde deren Umlagerung zu 11*H*-Indolo[3,2-*c*]chinolin-6-carbonsäuren entdeckt (Schema 5-1).

Schema 5-1:

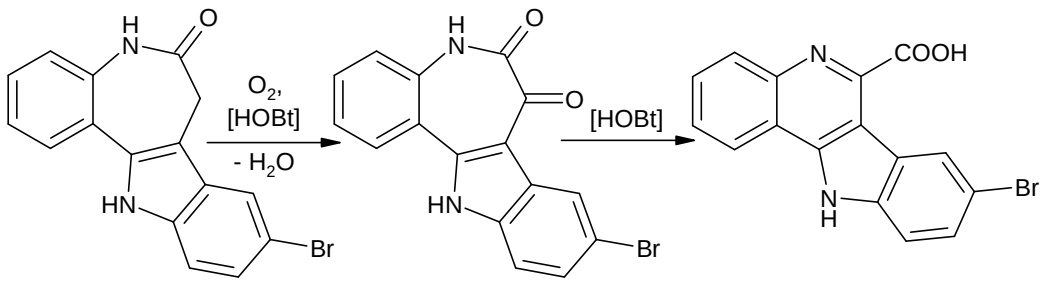

1 **90** **79c**

Der Mechanismus besteht vermutlich in der Oxidation des Paullons **1** durch Luftsauerstoff, bei der HOBt als Radikalstarter fungiert. Darauf folgt die Umwandlung des aktivierten Derivates **90** in das umgelagerte Produkt **79c**, bei der ebenfalls HOBt als Katalysator zu dienen scheint.

Unter Verwendung der erhaltenen biologischen Daten wurde eine QSAR-Studie mit Paullonen durchgeführt. Diese erbrachte die Erkenntnis, dass der quantitative Zusammenhang zwischen den physikochemischen Eigenschaften der Paullon-Substituenten in 9-Position und der CDK1/Cyclin B-inhibitorischen Aktivität der Verbindungen am besten durch die folgende Regressionsgleichung beschrieben wird:

$$pIC_{50}(\text{CDK1/cyclin B}) = 4.92(\pm0.52) - 0.24(\pm0.16)\,\pi^2 + 2.55(\pm0.65)\,\sigma_m + 0.29(\pm0.20)\,\text{dist}$$

Der elektronische Parameter σ_m stellt den bei weitem signifikantesten Deskriptor dar. Der ermittelte Zusammenhang verliert allerdings bei Erhöhung der Vielfalt innerhalb des verwendeten Datensatzes an Aussagekraft.

Eine Korrelation zwischen der Enzym-Inhibition (d. h. Inhibition von CDK1/Cyclin B, CDK5/p25 und/oder GSK-3β) und der Hemmung des Wachstums von Krebszellen konnte nicht abgeleitet werden. Die antiproliferativen Effekte der Paullone können demzufolge nicht ausschließlich auf die beobachtete CDK-Inhibition zurückgeführt werden.

7 Experimental Section

7.1 General Information

Melting Points:

IA 9100, Electrothermal, Southend-on-Sea, Essex, UK

IR Spectra:

PU 9712 Infrared Spectrophotometer, Philips, Cambridge, UK

FTIR-8300, Shimadzu, Kyoto, Japan

Recorded as KBr pellets

^{1}H-NMR Spectra and Two-Dimensional Spectra:

AMX 400 (400MHz), Bruker, Karlsruhe, Germany

DRX 500 (500 MHz), Bruker, Karlsruhe, Germany

Sample solvent: [D_6]-DMSO

Internal standard: tetramethylsilane

^{1}H chemical shifts quoted in delta (δ), values documented in ppm

Coupling constants (*J*): values documented in Hz

Determination of ratio of protons by integration

Abbreviations used for describing signal multiplicity: (s) = singlet, (d) = doublet, (t) = triplet, (q) = quartet, (quint) = quintet, (sext) = sextet, (sept) = septet, (m) = multiplet, (br) = broadened

^{13}C-NMR Spectra:

AMX 400 (100.6 MHz), Bruker, Karlsruhe, Germany

Sample solvent: [D_6]-DMSO

Internal standard: tetramethylsilane

^{13}C chemical shifts quoted in delta (δ), values documented in ppm

Spectra recorded spin-decoupled, additional PENDANT and DEPT experiments performed

Elemental Analyses:

C, H, N: CHN-O-Rapid, Heraeus, Hanau, Germany

EA 1108, Carlo Erba, Milan, Italy

Calculated (calcd.) and found (found) values documented in percent

Mass spectra:

VG 70-250S, VG Analytical, Manchester, U.K.

FAB xenon atom beam

Matrices: PEG 300, PEG 600

UV/VIS Spectra:

UV/VIS Recording Spectrophotometer UV-160A, Shimadzu, Kyoto, Japan

Thin Layer Chromatography:

Polygram Sil G/UV_{254} precoated microplates, Macherey-Nagel, Düren, Germany

Visualization accomplished by UV-illumination at 254 nm

Column Chromatography:

Adsorption of substances on silica gel 100-200 active, 60 Å, ICN, Eschwege, Germany

Column filling: silica gel 60 (< 0.063 mm), Merck, Darmstadt, Germany

Glass columns (∅ 3 cm)

Medium Pressure Liquid Chromatography:

Pump: Büchi 681, Büchi, Flawil, Switzerland

Column: Merck 310-25 Lobar-LiChroprep RP-18 (40-63 µm), Merck, Darmstadt, Germany

Detector: UV/VIS Filterphotometer (254 nm), Büchi, Flawil, Switzerland

Elution solvent: acetonitrile (ACN)/water (pH 1.5, adjusted with trifluoroacetic acid) gradients

Flow rate: 7 ml/min

High Performance Liquid Chromatography:

Merck Hitachi L-7000 series, connected to diode array detector L-7455, Merck Hitachi, Darmstadt, Germany

Column: LiChroCART 125-4, LiChrospher 100 RP-18 (5 µm), Merck, Darmstadt, Germany

Elution solvents: ACN/water and ACN/water (pH 1.5, adjusted with trifluoroacetic acid) gradients

Flow rate: 1 ml/min

Thermogravimety:

Thermobalance TG 760, Stanton Redcroft, London, U.K.

Aluminum Crucibles, Stanton Redcroft, London, U.K.

Data acquisition: LSB 36-III, Linseis, Selb, Germany

Water cooling flow rate: 100 ml/min

Nitrogen flow rate: 30 ml/min

Microwave-Assisted Synthesis:

Discover, CEM GmbH, Kamp-Lintfort, Germany

SmithCreator, Personal Chemistry GmbH, Konstanz, Germany

Purification of Chemicals:

The purification and drying of chemicals was performed according to methods stated in literature.[143]

7.2 Syntheses/Analytical Data

General Procedure A:
Synthesis of 7,12-Dihydroindolo[3,2-*d*][1]benzazepin-6(5*H*)-ones

An appropriate 3,4-dihydro-1*H*-1-benzazepine-2,5-dione (1 mmol) and an appropriate substituted phenylhydrazine (1.5 mmol) [or the appropriate substituted phenylhydrazine hydrochloride (1.5 mmol) and sodium acetate (123 mg, 1.5 mmol)] were suspended in glacial acetic acid (10 ml) and stirred for 1 h at 70-80 °C. Subsequently, concentrated sulfuric acid (0.1 ml) was added, and stirring was continued at 70-80 °C for 1 h. After cooling to room temperature, the reaction mixture was poured into a 5% aqueous sodium acetate solution (30 ml). The resulting precipitate was filtered off with suction, washed with water, and recrystallized from the given solvent.

General Procedure B:
Synthesis of 6-Oxo-5,6,7,12-tetrahydroindolo[3,2-*d*][1]benzazepine-9-carboxylic Acid Esters

To a suspension of 6-oxo-5,6,7,12-tetrahydroindolo[3,2-*d*][1]benzazepine-9-carboxylic acid (0.5 mmol) in freshly dried THF (3.5 ml), 2.5 equiv. of triphenylphosphine (1.25 mmol) and 2.5 equiv. of an appropriate anhydrous alcohol (1.25 mmol) were added. The reaction mixture was stirred in an ice bath for 30 min before adding 2.5 equiv. of di-*tert*-butyl azodicarboxylate (1.25 mmol), and stirring was continued for another 30 min. The ice bath was removed, and the mixture was allowed to warm up to room temperature. The reaction mixture was then stirred for a total of 24 h, adding 1 ml of the appropriate alcohol after 20 h. The solid was filtered off with suction and recrystallized from the given solvent.

General Procedure C:
Synthesis of 6-Oxo-5,6,7,12-tetrahydroindolo[3,2-*d*][1]benzazepine-9-carboxamides

A solution of 6-oxo-5,6,7,12-tetrahydroindolo[3,2-*d*][1]benzazepine-9-carboxylic acid (1 mmol), 1.3 equiv. of HOBt (1.3 mmol), and 1.3 equiv. of EDC (1.3 mmol) in DMF (10 ml) was stirred in an ice bath under nitrogen. After 20 min, 1 equiv. of an appropriate amine (1 mmol) was added to the reaction mixture, and the stirring under nitrogen was continued for 1 h in the ice bath, and subsequently for 24 h at room temperature. The solvent was evaporated in vacuo, and 0.1 M HCl (50 ml) was added to the oily residue. A precipitate was formed that was filtered off with suction and washed with water, saturated sodium hydrogen carbonate solution, and again water (50 ml each). The product was dried in vacuo and recrystallized from the given solvent.

General Procedure D:
Synthesis of 8-Aminocarbonyl-11*H*-indolo[3,2-*c*]quinoline-6-carboxylic Acids

A solution of 6-oxo-5,6,7,12-tetrahydroindolo[3,2-*d*][1]benzazepine-9-carboxylic acid (1 mmol), 1.3 equiv. of HOBt (1.3 mmol), and 1.3 equiv. of EDC (1.3 mmol) in DMF (10 ml) was stirred in an ice bath under nitrogen. After 20 min, 1 equiv. of an appropriate amine (1 mmol) was added to the reaction mixture, and the stirring was continued under nitrogen and in the ice bath for 1 h. Subsequently, the reaction mixture was stirred at room temperature and under air atmosphere for 3-14 d. The solvent was evaporated in vacuo, and 0.1 M HCl (50 ml) was added to the oily residue. A precipitate was formed that was filtered off with suction and washed with water, saturated sodium hydrogen carbonate solution, and again water (50 ml each). The product was dried in vacuo and recrystallized from the given solvent.

9-Bromo-7,12-dihydroindolo[3,2-*d*][1]benzazepin-6(5*H*)-one (**1**)

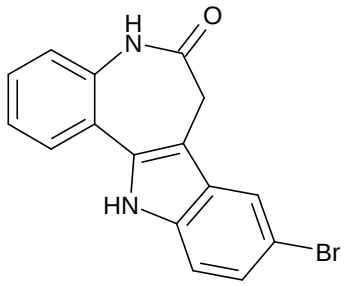

Prepared according to general procedure A with 175 mg (1 mmol) 3,4-dihydro-1*H*-1-benzazepine-2,5-dione, 335 mg (1.5 mmol) (4-bromophenyl)hydrazine hydrochloride, and 123 mg (1.5 mmol) sodium acetate. Recrystallization from ethanol afforded 228 mg (70%) of a yellow powder.

Mp: > 330 °C (Lit.[52]: > 330 °C)

Ethyl 2-amino-5-methoxybenzoate (**23b**)

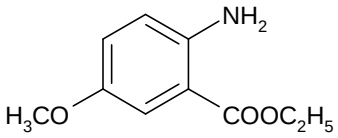

2-Amino-5-methoxybenzoic acid (**32**) (1.67 g, 10 mmol) was dissolved in dry ethanol (60 ml). Gaseous hydrogen chloride was bubbled through the reaction mixture until a clearly visible precipitate had formed (required approximately 20 min). The mixture was refluxed for 36 h, and subsequently evaporated to dryness. The residue was dissolved in water (50 ml), and the solution was neutralized by addition of 5% aqueous sodium carbonate solution. The neutral solution was extracted 5-10 times with dichloromethane (each portion 30 ml). The combined organic layers were washed with 5% aqueous sodium carbonate solution (30 ml) and dried by means of sodium sulfate. Evaporation to dryness afforded 1.54 g (79%) of a yellow oil which was used without further purification. (Lit: Wieking[115])

Ethyl 2-[(4-ethoxy-4-oxobutanoyl)amino]benzoate (**25a**)

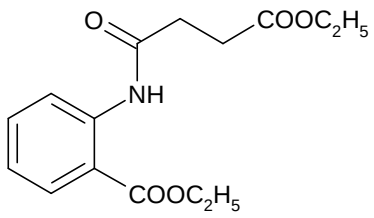

A solution of ethyl succinyl chloride (17.3 g, 105 mmol) in toluene (15 ml) was added drop by drop to a stirred solution of ethyl 2-aminobenzoate (14.5 g, 88 mmol) and pyridine (10 ml) in toluene (40 ml) at 0-10 °C. The resulting suspension was refluxed for 2 h. After cooling to room temperature, water (15 ml) was added to the reaction mixture. Using a separation funnel, the aqueous phase was discarded. The remaining organic phase was washed with 1 M HCl (15 ml) and 5% aqueous sodium carbonate solution (15 ml), dried by means of sodium sulfate, and evaporated in vacuo. After refluxing the resulting oil in ethanol (30 ml), the product crystallized. Recrystallization from ethanol afforded 22.21 g (86%) of colorless crystals.

Mp: 60 °C (Lit.[144]: 60 °C)

Ethyl 2-[(4-ethoxy-4-oxobutanoyl)amino]-5-methoxybenzoate (**25b**)

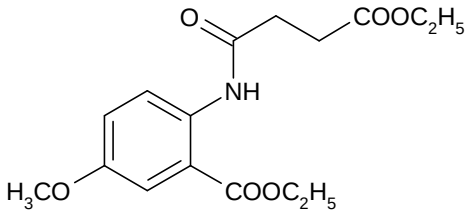

A solution of ethyl succinyl chloride (4.4 g, 27 mmol) in toluene (4 ml) was added drop by drop to a stirred solution of ethyl 2-amino-5-methoxybenzoate (**23b**) (3.9 g, 20 mmol) and pyridine (2.5 ml) in toluene (9 ml) at 0-10 °C. The resulting suspension was stirred at 80 °C for 2 h. After cooling to room temperature, water (6 ml) was added to the reaction mixture. Using a separation funnel, the aqueous phase was discarded. The remaining organic phase was washed with 1 M HCl (2.5 ml) and 5%

aqueous sodium carbonate solution (2.5 ml), dried by means of sodium sulfate, and evaporated to dryness. Recrystallization of the residue from ethanol afforded 5.09 g (79%) of colorless needles.

Mp: 67 °C (Lit.[115]: 68 °C)

Ethyl 5-hydroxy-2-oxo-2,3-dihydro-1*H*-1-benzazepine-4-carboxylate (**26a**)

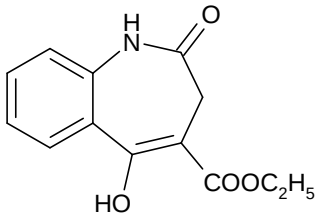

Under nitrogen atmosphere, 10 g of a 35% suspension of potassium hydride in mineral oil were washed three times with toluene (each portion 40 ml), and then suspended in toluene (75 ml). [**Be cautious when handling potassium hydride! Carefully keep away water or moisture!**] A solution of ethyl 2-[(4-ethoxy-4-oxobutanoyl)amino]benzoate (**25a**) (14.7 g, 50 mmol) in a mixture of DMF (22 ml) and toluene (150 ml) was added drop by drop to the stirred suspension under nitrogen with cooling. After the hydrogen evolution had ceased, the reaction mixture was stirred at 70 °C for 2-3 h. Neutralization of the mixture was performed by cautious addition of glacial acetic acid (8 ml). Subsequently, water (150 ml) was added drop by drop, and the slightly acidic suspension was stirred at 0-10 °C for 15 min. The precipitate was filtered off with suction and then washed with water and petrol ether. Recrystallization from ethanol afforded 10.6 g (86%) of colorless crystals.

Mp: 210 °C (Lit.[44]: 210-213 °C)

Ethyl 5-hydroxy-7-methoxy-2-oxo-2,3-dihydro-1*H*-1-benzazepine-4-carboxylate (**26b**)

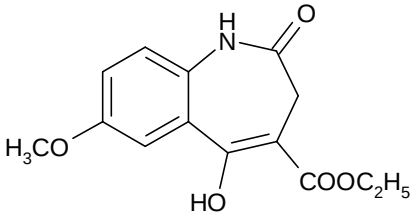

Under nitrogen atmosphere, 4.6 g of a 35% suspension of potassium hydride in mineral oil were washed three times with toluene (each portion 30 ml), and then suspended in toluene (30 ml). [**Be cautious when handling potassium hydride! Carefully keep away water or moisture!**] A solution of ethyl 2-[(4-ethoxy-4-oxobutanoyl)amino]-5-methoxybenzoate (**25b**) (6.5 g, 20 mmol) in a mixture of DMF (10 ml) and toluene (70 ml) was added drop by drop to the stirred suspension under nitrogen with cooling. After the hydrogen evolution had ceased, the reaction mixture was stirred at 70 °C for 3 h. Neutralization of the mixture was performed by cautious addition of glacial acetic acid (3 ml). Subsequently, water (70 ml) was added drop by drop, and the slightly acidic suspension was stirred at 0-10 °C for 15 min. The precipitate was filtered off with suction and then washed with water and petrol ether. Recrystallization from ethanol afforded 4.0 g (72%) of white needles.

Mp: 190-192 °C (degradation) (Lit.[115]: 191-193 °C (degradation))

3,4-Dihydro-1*H*-1-benzazepine-2,5-dione (**27a**)

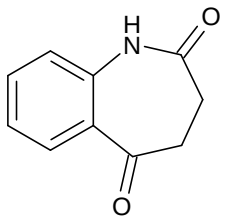

Water (0.5 ml) was added to a solution of ethyl 5-hydroxy-2-oxo-2,3-dihydro-1*H*-1-benzazepine-4-carboxylate (**26a**) (3.7 g, 15 mmol) in dimethyl sulfoxide (40 ml), and the mixture was stirred under nitrogen at

150 °C. After 1 and 3 h of stirring, further portions of water were added (0.5 ml, respectively). After stirring under nitrogen at 150 °C for a total of 4 h, the reaction mixture was allowed to cool to room temperature. Subsequently, the mixture was poured into water (300 ml) and stored in the refrigerator for 12 h. The resulting crystals were filtered off with suction, washed with petrol ether, and dried in vacuo. Recrystallization from ethanol afforded 2.18 g (83%) of colorless crystals.

Mp: 187 °C (Lit[145]: 187-188 °C)

7-Methoxy-3,4-dihydro-1*H*-1-benzazepine-2,5-dione (**27b**)

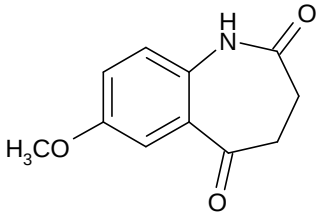

Water (0.5 ml) was added to a solution of ethyl 5-hydroxy-7-methoxy-2-oxo-2,3-dihydro-1*H*-1-benzazepine-4-carboxylate (**26b**) (4.2 g, 15 mmol) in dimethyl sulfoxide (40 ml), and the mixture was stirred under nitrogen at 150 °C. After 1 and 3 h of stirring, further portions of water were added (0.5 ml, respectively). After stirring under nitrogen at 150 °C for a total of 4 h, the reaction mixture was allowed to cool to room temperature. Subsequently, the mixture was poured into water (300 ml) and stored in the refrigerator for 12 h. The resulting crystals were filtered off with suction, washed with petrol ether, and dried in vacuo. Recrystallization from ethanol afforded 2.77 g (89%) of a yellow powder.

Mp: 180 °C (Lit[115]: 181 °C)

[4-(Methylthio)phenyl]hydrazine hydrochloride (**29a**)

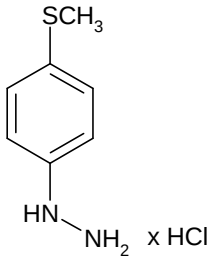

Under cooling, concentrated hydrochloric acid (30 ml) was rapidly added drop by drop to 4-(methylthio)aniline (4.2 g, 30 mmol), and the reaction mixture was stirred at 0 °C. To the resulting suspension, 20% aqueous sodium nitrite solution (12 ml) was slowly added drop by drop, and the stirring was continued at 0 °C for 0.5-1 h. The precipitate was filtered off with suction and discarded. Under continuous stirring at temperatures < 0 °C, the filtrate was cautiously added to a precooled 0.01% solution of tin(II) chloride in concentrated hydrochloric acid (21 ml). The reaction mixture was stored in the refrigerator for 12 h. The precipitate was filtered off with suction and washed with brine and petrol ether. Recrystallization from ethanol/water (2/1) at 70 °C afforded 2.91 g (50.6%) of white glistening crystals.

Mp: 196-197 °C (Lit[49]: 198-199 °C)

4-Hydrazinobenzenesulfonamide hydrochloride (**29b**)

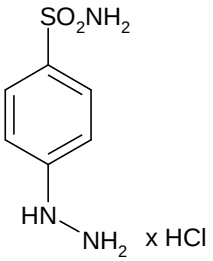

To a mixture of sulfanilamide (3.5 g, 20 mmol), concentrated hydrochloric acid (10 ml), and crushed ice (20 g) stirred at < 0 °C, a solution of sodium nitrite (1.4 g, 20 mmol) in water (5 ml) was slowly added drop by drop. Under vigorous stirring, the resulting diazonium salt solution was rapidly

added to a precooled solution of tin(II) chloride dihydrate (10 g, 44 mmol) in concentrated hydrochloric acid (15 ml). The reaction mixture was stored in the freezer compartment for 12 h. The precipitate was filtered off with suction and washed with brine and petrol ether. Drying in vacuo afforded 3.36 g (74%) of a white powder which was used without further purification. (Lit: Soliman[51])

4-[2-(2-Oxo-1,2,3,4-tetrahydro-5*H*-1-benzazepin-5-ylidene)hydrazino] benzenesulfonamide (**30c**)

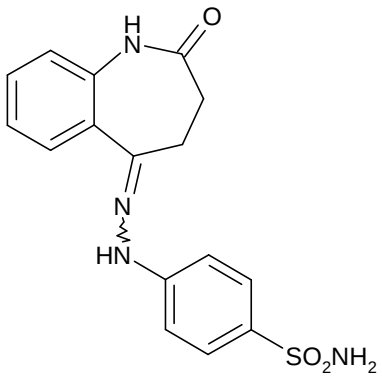

A suspension of 3,4-dihydro-1*H*-1-benzazepine-2,5-dione (**27a**) (260 mg, 1.5 mmol), 1.5 equiv. 4-hydrazinobenzenesulfonamide (500 mg, 2.25 mmol), and 1.5 equiv. sodium acetate (185 mg, 2.25 mmol) in glacial acetic acid (15 ml) was stirred for 1.5 h at 70 °C. After cooling to room temperature, the reaction mixture was poured into a 5% aqueous sodium acetate solution (50 ml). The resulting precipitate was filtered off with suction and washed with water. Recrystallization from ethanol afforded 425 mg (82%) of a yellow powder.

Mp: 303-305 °C (discoloration at 294 °C); IR (KBr): 3320 cm^{-1} (NH), 3200 cm^{-1} (NH), 3070 cm^{-1} (CH, aromatic), 1660 cm^{-1} (C=O), 1310 cm^{-1} and 1150 cm^{-1} (SO_2); ^{1}H-NMR ([D6]-DMSO, 400 MHz): δ (ppm) = 2.51-2.58 and 2.98-3.05 (m, AA'XX', 4H, CH_2-CH_2), 7.02 (d, *J* = 7.6 Hz, 1H, Ar H), 7.08 (s, 2H, SO_2NH_2), 7.17 ("dt", *J* = 7.6/7.6/1.0 Hz, 1H, Ar H), 7.28 (d, *J* = 8.6 Hz, 2H, Ar H), 7.35 ("dt", *J* = 7.6/7.6/1.5 Hz, 1H, Ar H), 7.63-7.69 (m, 3H, Ar H), 9.65 (s, 1H, NH), 9.76 (s, 1H, NH); ^{13}C-NMR ([D6]-DMSO, 100.6 MHz): δ (ppm) = 29.8, 30.7 (CH_2), 112.1, 121.8, 124.3, 127.1,

129.1, 129.6 (tert. C), 130.7, 134.0, 137.2, 145.8, 148.2, 172.9 (quat. C); $C_{16}H_{16}N_4O_3S$ (344.39); calcd. C 55.80, H 4.68, N 16.27; found C 55.39, H 4.65, N 15.88.

4-[2-(2-Oxo-1,2,3,4-tetrahydro-5*H*-1-benzazepin-5-ylidene)hydrazino] benzoic acid (**30d**)

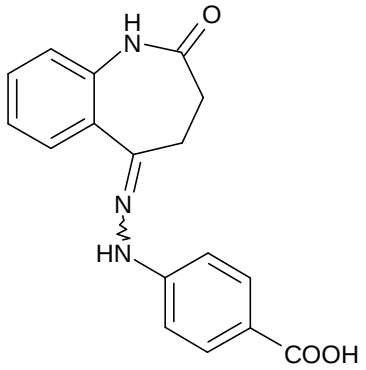

A suspension of 3,4-dihydro-1*H*-1-benzazepine-2,5-dione (**27a**) (175 mg, 1 mmol) and 1.5 equiv. 4-hydrazinobenzoic acid (230 mg, 1.5 mmol) in glacial acetic acid (10 ml) was stirred for 2 h at 80 °C. After cooling to room temperature, the reaction mixture was poured into a 5% aqueous sodium acetate solution (30 ml). The resulting precipitate was filtered off with suction and washed with water. Recrystallization from ethanol afforded 263 mg (85%) of a white powder.

^{1}H-NMR ([D6]-DMSO, 400 MHz): δ (ppm) = 2.51-2.58 and 2.98-3.05 (m, AA'XX', 4H, CH_2-CH_2), 7.02 (d, *J* = 8.2 Hz, 1H, Ar H), 7.17 ("t", *J* = ~7.1 Hz, 1H, Ar H), 7.23 (d, *J* = 8.6 Hz, 2H, Ar H), 7.34 ("dt", *J* = 7.6/7.6/1.4 Hz, 1H, Ar H), 7.65 (dd, *J* = 7.9/1.3 Hz, 1H, Ar H), 7.81 (d, *J* = 8.6, 2H, Ar H), 9.66 (s, 1H, NH), 9.76 (s, 1H, NH), 12.33 (br s, 1H, COOH); ^{13}C-NMR ([D6]-DMSO, 100.6 MHz): δ (ppm) = 29.8, 30.7 (CH_2), 112.1, 121.8, 124.3, 129.1, 129.6, 130.8 (tert. C), 120.9, 130.7, 137.2, 145.7, 149.2, 167.2, 172.9 (quat. C); $C_{17}H_{15}N_3O_3$ (309.32); calcd. C 66.01, H 4.89, N 13.58; found C 65.51, H 4.76, N 13.49.

The substance was not further characterized as it merely served as an intermediate within an alternative synthesis route leading to the fully characterized end product **39**.

2-Amino-5-methoxybenzoic acid (**32**)

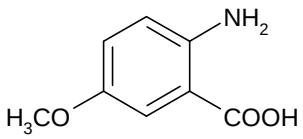

5-Methoxy-2-nitrobenzoic acid (2.96 g, 15 mmol) was added to a solution of tin(II) chloride dihydrate (14.6 g, 65 mmol) in concentrated hydrochloric acid (15 ml), and the reaction mixture was heated to 80 °C. After 15 min, concentrated hydrochloric acid (8 ml) was added, and the mixture was stirred at 0-10 °C for 20 min. The resulting precipitate was filtered off with suction, washed with concentrated hydrochloric acid, and again thoroughly filtered off with suction. Under stirring, the residue was dissolved by degrees in a 10% aqueous sodium carbonate solution (approximately 60 ml in total). The solution was alkalinized, and a grayish precipitate was formed which was filtered off and discarded. The yellow filtrate was cooled to 0-10 °C, pH-adjusted to pH 4 with 10% hydrochloric acid, and subsequently extracted with ethyl acetate until no product was left in the aqueous phase (i.e., 5-10 times, 30 ml each portion). The organic layers were combined and dried by means of sodium sulfate. Evaporation to dryness afforded 1.71 g (68%) of a yellow powder.

Mp: 147-148 °C (Lit[115]: 148 °C)

9-(Methylthio)-7,12-dihydroindolo[3,2-*d*][1]benzazepin-6(5*H*)-one (**35a**)

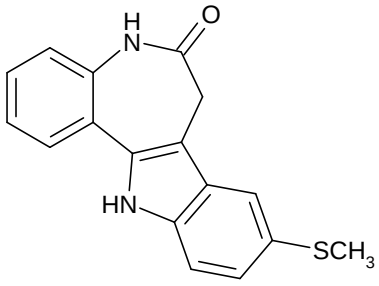

Prepared according to general procedure A with 265 mg (1.5 mmol) 3,4-dihydro-1*H*-1-benzazepine-2,5-dione (**27a**), 430 mg (2.25 mmol) [4-(methylthio)phenyl]hydrazine hydrochloride (**29a**), and 185

mg (2.25 mmol) sodium acetate in 15 ml glacial acetic acid. Recrystallization from ethanol afforded 265 mg (60%) of a beige powder.

Mp: > 330 °C; IR (KBr): 3210 cm^{-1} (NH), 1640 cm^{-1} (C=O); ^{1}H-NMR ([D6]-DMSO, 400 MHz): δ (ppm) = 2.51 (s, 3H, SCH_3), 3.51 (s, 2H, CH_2), 7.15 (dd, *J* = 8.4/1.5 Hz, 1H, Ar H), 7.23-7.30 (m, 2H, Ar H), 7.34-7.41 (m, 2H, Ar H), 7.64 (d, *J* = 1.5 Hz, 1H, Ar H), 7.73 (dd, *J* = 7.6/1.0 Hz, 1H, Ar H), 10.10 (s, 1H, lactam-NH), 11.63 (s, 1H, indole-NH); ^{13}C-NMR ([D6]-DMSO, 100.6 MHz): δ (ppm) = 17.2 (SCH_3), 31.4 (CH_2), 112.0, 117.3, 122.2, 123.1, 123.6, 126.8, 128.0 (tert. C), 107.0, 122.6, 127.0, 127.3, 133.2, 135.4, 135.9, 171.5 (quat. C); $C_{17}H_{14}N_2OS$ (294.38); calcd. C 69.36, H 4.79, N 9.52; found C 69.26, H 4.76, N 9.32.

2-Methoxy-9-(methylthio)-7,12-dihydroindolo[3,2-*d*][1]benzazepin-6(5*H*)-one (**35b**)

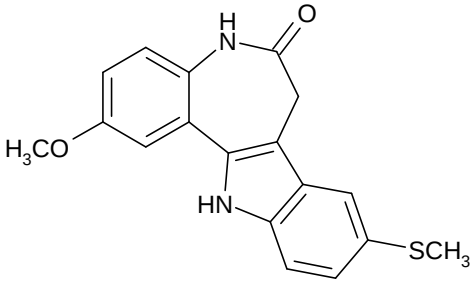

Prepared according to general procedure A with 205 mg (1 mmol) 7-methoxy-3,4-dihydro-1*H*-1-benzazepine-2,5-dione (**27b**), 286 mg (1.5 mmol) [4-(methylthio)phenyl]hydrazine hydrochloride (**29a**), and 123 mg (1.5 mmol) sodium acetate. Recrystallization from ethanol afforded 265 mg (82%) of a brownish powder.

Mp: > 330 °C; IR (KBr): 3200 cm^{-1} (NH), 3050 cm^{-1} (CH, aromatic), 2970 cm^{-1} (CH, aliphatic), 1640 cm^{-1} (C=O); ^{1}H-NMR ([D6]-DMSO, 400 MHz): δ (ppm) = 2.51 (s, 3H, SCH_3), 3.47 (s, 2H, CH_2), 3.84 (s, 3H, OCH_3), 6.98 (dd, *J* = 8.9/2.9 Hz, 1H, Ar H), 7.12-7.19 (m, 2H, Ar H), 7.26 (d, *J* = 3.0 Hz, 1H, Ar H), 7.40 (d, *J* = 8.7 Hz, 1H, Ar H), 7.63 (d, *J* = 1.0 Hz, 1H, Ar H), 9.89 (s, 1H, lactam-NH), 11.62 (s, 1H, indole-NH); ^{13}C-NMR ([D6]-DMSO, 100.6 MHz): δ (ppm) = 17.2 (SCH_3), 31.3 (CH_2), 55.4 (OCH_3),

110.4, 112.0, 114.9, 117.3, 123.2, 123.7 (tert. C), 107.3, 123.6, 127.0, 127.2, 129.0, 133.2, 135.7, 155.3, 171.2 (quat. C); $C_{18}H_{16}N_2O_2S$ (324.40); calcd. C 66.65, H 4.97, N 8.64; found C 66.51, H 5.00, N 8.75.

2-Methoxy-6-oxo-5,6,7,12-tetrahydroindolo[3,2-*d*][1]benzazepine-9-sulfonamide (**35c**)

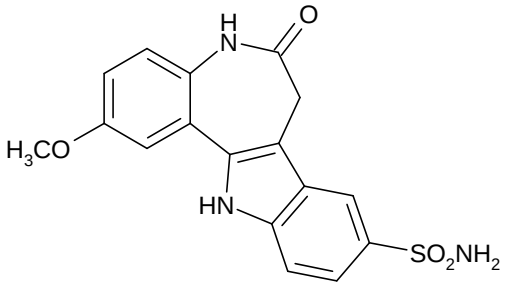

Prepared according to general procedure A with 205 mg (1 mmol) 7-methoxy-3,4-dihydro-1*H*-1-benzazepine-2,5-dione (**27b**), 336 mg (1.5 mmol) 4-hydrazinobenzenesulfonamide hydrochloride (**29b**) and 123 mg (1.5 mmol) sodium acetate. Recrystallization from ethanol afforded 207 mg (58%) of brownish crystals.

Mp: > 330 °C (discoloration at 303 °C); IR (KBr): 3380 cm^{-1} (NH), 3340 cm^{-1} (NH), 3290 cm^{-1} (NH), 3200 cm^{-1} (NH), 3080 cm^{-1} (CH, aromatic), 2970 cm^{-1} (CH, aliphatic), 1650 cm^{-1} (C=O), 1320 cm^{-1} and 1150 cm^{-1} (SO_2); ^{1}H-NMR ([D6]-DMSO, 400 MHz): δ (ppm) = 3.51 (s, 2H, CH_2), 3.86 (s, 3H, OCH_3), 7.03 (dd, *J* = 8.9/2.8 Hz, 1H, Ar H), 7.18 and 7.20 (s, 2H, SO_2NH_2 and d, *J* = 9.1 Hz, 1H, Ar H, overlapping), 7.31 (d, *J* = 2.6 Hz, 1H, Ar H), 7.58 (d, *J* = 8.6 Hz, 1H, Ar H), 7.65 (dd, *J* = 8.4/1.8 Hz, 1H, Ar H), 8.17 (d, *J* = 1.5 Hz, 1H, Ar H), 9.98 (s, 1H, lactam-NH), 12.05 (s, 1H, indole-NH); ^{13}C-NMR ([D6]-DMSO, 100.6 MHz): δ (ppm) = 31.4 (CH_2), 55.4 (OCH_3), 110.5, 111.5, 115.4, 116.4, 119.5, 123.8 (tert. C), 108.6, 123.1, 125.4, 129.2, 134.6, 135.3, 138.2, 155.4, 170.9 (quat. C); $C_{17}H_{15}N_3O_4S$ (357.39); calcd. C 57.13, H 4.23, N 11.76; found C 57.07, H 4.20, N 11.51.

9-(Methylsulfinyl)-7,12-dihydroindolo[3,2-*d*][1]benzazepin-6(5*H*)-one (**36a**)

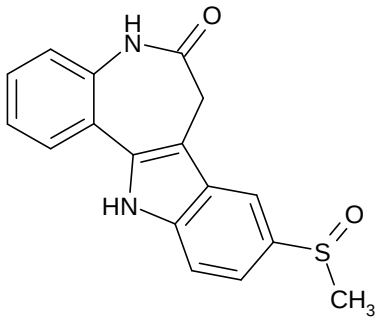

Under stirring, 9-(methylthio)-7,12-dihydroindolo[3,2-*d*][1]benzazepin-6(5*H*)-one (**35a**) (150 mg, 0.5 mmol) was dissolved in acetone (60 ml) and cooled down to temperatures < 0 °C. A solution of 141 mg *meta*-chloroperbenzoic acid (*m*-CPBA, 70%) in 14 ml acetone was slowly added drop by drop to the dissolved educt, maintaining temperatures < 0 °C and observing the progression of the reaction by TLC. After the completion of the reaction, the mixture was poured into 300 ml of water. The resulting precipitate was filtered off with suction and washed with 7% aqueous sodium hydrogen carbonate solution. Recrystallization from ethanol afforded 65 mg (42%) of a salmon colored powder.

Mp: > 330 °C; IR (KBr): 3200 cm^{-1} (NH), 3050 cm^{-1} (CH, aromatic), 2980 cm^{-1} (CH, aliphatic), 1650 cm^{-1} (C=O), 1040 cm^{-1} (S=O); ^{1}H-NMR ([D6]-DMSO, 400 MHz): δ (ppm) = 2.75 (s, 3H, $SOCH_3$), 3.57 (d, *J* = 2.6 Hz, 2H, CH_2), 7.25-7.33 (m, 2H, Ar H), 7.41 (“dt”, *J* = 7.7/7.5/1.5 Hz, 1H, Ar H), 7.48 (dd, *J* = 8.5/1.7 Hz, 1H, Ar H), 7.62 (d, *J* = 8.4 Hz, 1H, Ar H), 7.77 (dd, *J* = 7.9/1.3 Hz, 1H, Ar H), 8.04 (d, *J* = 1.2 Hz, 1H, Ar H), 10.14 (s, 1H, lactam-NH), 11.97 (s, 1H, indole-NH); ^{13}C-NMR ([D6]-DMSO, 100.6 MHz): δ (ppm) = 31.5 (CH_2), 43.6 ($SOCH_3$), 112.3, 114.3, 117.1, 122.2, 123.6, 126.9, 128.4 (tert. C), 108.0, 126.4, 134.3, 135.6, 136.3, 138.4, 171.4 (quat. C, lacking one: not detected under application of 3072 scans); $C_{17}H_{14}N_2O_2S$ (310.38); calcd. C 65.79, H 4.55, N 9.03; found C 65.78, H 4.58, N 8.82.

2-Methoxy-9-(methylsulfinyl)-7,12-dihydroindolo[3,2-*d*][1]benzazepin-6(5*H*)-one (**36b**)

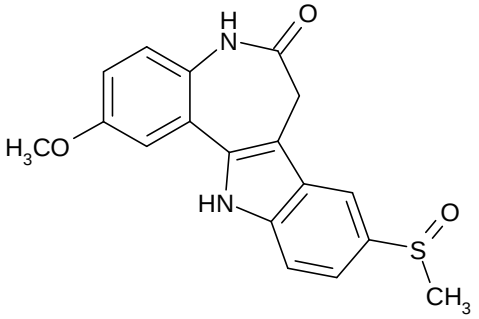

Under stirring, 2-methoxy-9-(methylthio)-7,12-dihydroindolo[3,2-*d*][1] benzazepin-6(5*H*)-one (**35b**) (162 mg, 0.5 mmol) was dissolved in acetone (60 ml) and cooled down to temperatures < 0 °C. A solution of 141 mg *meta*-chloroperbenzoic acid (*m*-CPBA, 70%) in 14 ml acetone was slowly added drop by drop to the dissolved educt, maintaining temperatures < 0 °C and observing the progression of the reaction by TLC. After the completion of the reaction, the mixture was poured into 300 ml of water. The resulting precipitate was filtered off with suction and washed with 7% aqueous sodium hydrogen carbonate solution. Recrystallization from ethanol afforded 73 mg (43%) of a greenish powder.

Mp: 308-310 °C (degradation); IR (KBr): 3180 cm^{-1} (NH), 3060 cm^{-1} (CH, aromatic), 2940 cm^{-1} (CH, aliphatic), 1650 cm^{-1} (C=O), 1040 cm^{-1} (S=O); ^{1}H-NMR ([D6]-DMSO, 400 MHz): δ (ppm) = 2.76 (s, 3H, $SOCH_3$), 3.53 (d, *J* = 2.8 Hz, 2H, CH_2), 3.85 (s, 3H, OCH_3), 7.02 (dd, *J* = 8.9/3.1 Hz, 1H, Ar H), 7.20 (d, *J* = 8.9 Hz, 1H, Ar H), 7.30 (d, *J* = 2.8 Hz, 1H, Ar H), 7.49 (dd, *J* = 8.5/1.7 Hz, 1H, Ar H), 7.63 (d, *J* = 8.4 Hz, 1H, Ar H), 8.04 (d, *J* = 1.0 Hz, 1H, Ar H), 9.94 (s, 1H, lactam-NH), 11.96 (s, 1H, indole-NH); ^{13}C-NMR ([D6]-DMSO, 100.6 MHz): δ (ppm) = 31.4 (CH_2), 43.6 ($SOCH_3$), 55.4 (OCH_3), 110.6, 112.3, 114.3, 115.2, 117.2, 123.8 (tert. C), 108.3, 123.2, 126.3, 129.2, 134.2, 136.4, 138.3, 155.4, 171.0 (quat. C); $C_{18}H_{16}N_2O_3S$ (340.40); calcd. C 63.51, H 4.74, N 8.23; found C 63.17, H 4.87, N 7.97.

9-(Methylsulfonyl)-7,12-dihydroindolo[3,2-*d*][1]benzazepin-6(5*H*)-one (**37a**)

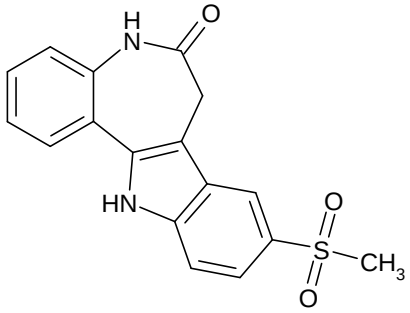

To a solution of 9-(methylthio)-7,12-dihydroindolo[3,2-*d*][1]benzazepin-6(5*H*)-one (**35a**) (150 mg, 0.5 mmol) in glacial acetic acid (28 ml), stirred at 70 °C, 35% aqueous hydrogen peroxide solution (0.25 ml, 2.5 mmol) was added. The reaction mixture was stirred at 60-80 °C for 3 h and subsequently poured into 15% aqueous sodium hydroxide solution (120 ml). The mixture was stored in the refrigerator for 12 h. The resulting precipitate was filtered off with suction and washed with water. Recrystallization from ethanol afforded 47 mg (29%) of a beige powder.

Mp: > 330 °C; IR (KBr): 3290 cm^{-1} (NH), 3200 cm^{-1} (NH), 3070 cm^{-1} (CH, aromatic), 2920 cm^{-1} (CH, aliphatic), 1650 cm^{-1} (C=O), 1280 cm^{-1} and 1150 cm^{-1} (SO_2); ^{1}H-NMR ([D6]-DMSO, 400 MHz): δ (ppm) = 3.21 (s, 3H, SO_2CH_3), 3.61 (s, 2H, CH_2), 7.26-7.34 (m, 2H, Ar H), 7.43 (“dt”, *J* = 7.6/7.6/1.5 Hz, 1H, Ar H), 7.64 (d, *J* = 8.6 Hz, 1H, Ar H), 7.69 (dd, *J* = 8.4/1.8 Hz, 1H, Ar H), 7.78 (dd, *J* = 7.8/1.1 Hz, 1H, Ar H), 8.31 (d, *J* = 1.5 Hz, 1H, Ar H), 10.18 (s, 1H, lactam-NH), 12.19 (s, 1H, indole-NH); ^{13}C-NMR ([D6]-DMSO, 100.6 MHz): δ (ppm) = 31.8 (CH_2), 44.8 (SO_2CH_3), 112.4, 118.8, 120.5, 122.8, 124.2, 127.4, 129.2 (tert. C), 109.1, 122.4, 126.3, 132.1, 135.6, 136.2, 139.8, 171.7 (quat. C); $C_{17}H_{14}N_2O_3S$ (326.38); calcd. C 62.56, H 4.32, N 8.58; found C 61.98, H 4.43, N 8.20; HRMS-FAB (m/z): $[M + H]^+$ calcd. 327.0804, $[M + H]^+$ found 327.0767.

2-Methoxy-9-(methylsulfonyl)-7,12-dihydroindolo[3,2-*d*][1]benzazepin-6(5*H*)-one (**37b**)

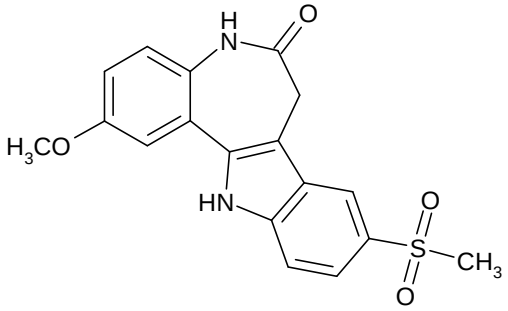

To a solution of 2-methoxy-9-(methylthio)-7,12-dihydroindolo[3,2-*d*][1] benzazepin-6(5*H*)-one (**35b**) (324 mg, 1 mmol) in glacial acetic acid (50 ml), stirred at 70 °C, 35% aqueous hydrogen peroxide solution (0.5 ml, 5 mmol) was added. The reaction mixture was stirred at 60-80 °C for 3 h and subsequently poured into 15% aqueous sodium hydroxide solution (200 ml). The mixture was stored in the refrigerator for 12 h. The resulting precipitate was filtered off with suction and washed with water. Recrystallization from ethanol afforded 164 mg (46%) of a beige powder.

Mp: > 330 °C (discoloration at 310 °C); IR (KBr): 3320 cm^{-1} (NH), 3190 cm^{-1} (NH), 3070 cm^{-1} (CH, aromatic), 2940 cm^{-1} (CH, aliphatic), 1650 cm^{-1} (C=O), 1280 cm^{-1} and 1150 cm^{-1} (SO_2); ^{1}H-NMR ([D6]-DMSO, 400 MHz): δ (ppm) = 3.21 (s, 3H, SO_2CH_3), 3.57 (s, 2H, CH_2), 3.86 (s, 3H, OCH_3), 7.04 (dd, *J* = 8.9/3.6 Hz, 1H, Ar H), 7.21 (d, *J* = 8.9 Hz, 1H, Ar H), 7.31 (d, *J* = 2.8 Hz, 1H, Ar H), 7.65 (d, *J* = 8.6 Hz, 1H, Ar H), 7.70 (dd, *J* = 8.5/1.7 Hz, 1H, Ar H), 8.31 (d, *J* = 1.2 Hz, 1H, Ar H), 10.00 (s, 1H, lactam-NH), 12.20 (s, 1H, indole-NH); ^{13}C-NMR ([D6]-DMSO, 100.6 MHz): δ (ppm) = 31.3 (CH_2), 44.3 (SO_2CH_3), 55.4 (OCH_3), 110.6, 111.9, 115.5, 118.3, 120.1, 123.8 (tert. C), 108.9, 122.9, 125.8, 129.3, 131.7, 135.1, 139.1, 155.4, 171.0 (quat. C); $C_{18}H_{16}N_2O_4S$ (356.40); calcd. C 60.66, H 4.52, N 7.86; found C 60.65, H 4.50, N 7.83.

6-Oxo-5,6,7,12-tetrahydroindolo[3,2-*d*][1]benzazepine-9-sulfonamide (**38**)

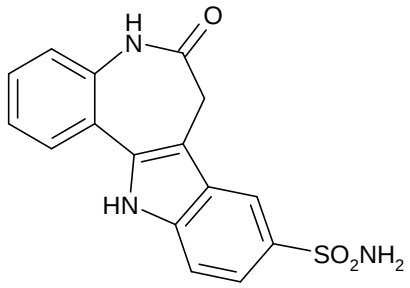

A solution of 4-[2-(2-oxo-1,2,3,4-tetrahydro-5*H*-1-benzazepin-5-ylidene) hydrazino]benzenesulfonamide (**30c**) (270 mg, 0.8 mmol) in diphenyl ether (150 ml) was refluxed for 4 h. After allowing the solution to cool to room temperature, petrol ether was added (350 ml). The resulting precipitate was filtered off with suction and washed with petrol ether. Recrystallization from ethanol afforded 91 mg (35%) of a beige powder.

Mp: > 330 °C; IR (KBr): 3370 cm^{-1} (NH), 3210 cm^{-1} (NH), 3060 cm^{-1} (CH, aromatic), 2920 cm^{-1} (CH, aliphatic), 1670 cm^{-1} (C=O); ^{1}H-NMR ([D6]-DMSO, 400 MHz): δ (ppm) = 3.54 (s, 2H, CH_2), 7.15 (s, 2H, SO_2NH_2), 7.26-7.34 (m, 2H, Ar H), 7.42 (“dt”, *J* = 7.6/7.6/1.5 Hz, 1H, Ar H), 7.57 (d, *J* = 8.6 Hz, 1H, Ar H), 7.64 (dd, *J* = 8.6/1.8 Hz, 1H, Ar H), 7.77 (dd, *J* = 7.9/1.3 Hz, 1H, Ar H), 8.17 (d, *J* = 1.6 Hz, 1H, Ar H), 10.15 (s, 1H, lactam-NH), 12.04 (s, 1H, indole-NH); ^{13}C-NMR ([D6]-DMSO, 100.6 MHz): δ (ppm) = 31.5 (CH_2), 111.5, 116.3, 119.4, 122.3, 123.7, 126.9, 128.5 (tert. C), 108.4, 122.1, 125.4, 134.6, 135.3, 135.7, 138.4, 171.2 (quat. C); $C_{16}H_{13}N_3O_3S$ (327.36); calcd. C 58.70, H 4.00, N 12.84; found C 58.87, H 3.95, N 12.60.

6-Oxo-5,6,7,12-tetrahydroindolo[3,2-*d*][1]benzazepine-9-carboxylic acid (**39**)

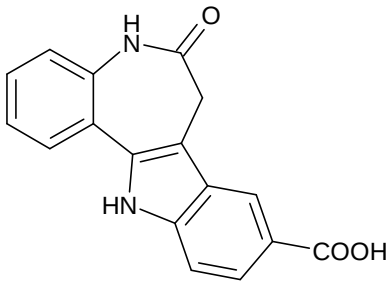

Method A:

Prepared according to general procedure A with 280 mg (1.6 mmol) 3,4-dihydro-1*H*-1-benzazepine-2,5-dione (**27a**), 365 mg (2.4 mmol) 4-hydrazinobenzoic acid in 15 ml glacial acetic acid at 90 °C. Recrystallization from ethanol afforded 364 mg (78%) of a grayish white powder.

Method B:

A solution of 4-[2-(2-oxo-1,2,3,4-tetrahydro-5*H*-1-benzazepin-5-ylidene) hydrazino]benzoic acid (**30d**) (185 mg, 0.6 mmol) in diphenyl ether (100 ml) was refluxed for 3 h. After allowing the solution to cool to room temperature, petrol ether was added (200 ml). The resulting precipitate was filtered off with suction and washed with petrol ether. Recrystallization from ethanol afforded 116 mg (66%) of a greenish powder.

Mp: > 330 °C; IR (KBr): 3200 cm^{-1} (NH), 3050 cm^{-1} (CH, aromatic), 2970 cm^{-1} (CH, aliphatic), 1670 cm^{-1} (C=O), 1650 cm^{-1} (C=O); ^{1}H-NMR ([D6]-DMSO, 400 MHz): δ (ppm) = 3.55 (s, 2H, CH_2), 7.25-7.33 (m, 2H, Ar H), 7.41 (“dt”, *J* = 7.8/7.6/1.2 Hz, 1H, Ar H), 7.50 (d, *J* = 8.6 Hz, 1H, Ar H), 7.76 (dd, *J* = 7.9/1.3 Hz, 1H, Ar H), 7.80 (dd, *J* = 8.7/1.5 Hz, 1H, Ar H), 8.32 (s, 1H, Ar H), 10.14 (s, 1H, lactam-NH), 11.96 (s, 1H, indole-NH), 12.50 (br s, 1H, COOH); ^{13}C-NMR ([D6]-DMSO, 100.6 MHz): δ (ppm) = 31.4 (CH_2), 111.2, 120.4, 122.3, 123.2, 123.6, 126.9, 128.4 (tert. C), 108.5, 121.7, 126.0, 134.0, 135.6, 139.7, 168.1, 171.3 (quat. C, lacking one: not detected under application of 2048 scans); $C_{17}H_{12}N_2O_3$ (292.29); calcd. C 69.86, H 4.14, N 9.58; found C 69.50, H 4.13, N 9.48.

Ethyl 6-oxo-5,6,7,12-tetrahydroindolo[3,2-*d*][1]benzazepine-9-carboxylate (**40a**)

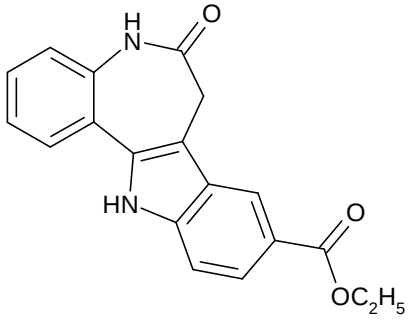

Method A:

To a suspension of 6-oxo-5,6,7,12-tetrahydroindolo[3,2-*d*][1]benzazepine-9-carboxylic acid (**39**) (292 mg, 1 mmol) in dry ethanol (50 ml), concentrated sulfuric acid (0.5 ml) was added. Adding another portion of concentrated sulfuric acid (0.5 ml) after 12 h, the reaction mixture was refluxed for a total of 24 h. Subsequently, the mixture was evaporated to dryness, and the residue was suspended in ice water and neutralized with a 10% aqueous sodium carbonate solution. The precipitate was filtered off with suction and washed with water. Recrystallization from ethanol afforded 119 mg (37%) of a brownish white powder.

Method B:

6-Oxo-5,6,7,12-tetrahydroindolo[3,2-*d*][1]benzazepine-9-carboxylic acid (**39**) (60 mg, 0.2 mmol) was dissolved in ethanolic hydrochloric acid (15 ml). The solution was refluxed for 36 h and then evaporated to dryness. The residue was suspended in water and alkalinized with 10% aqueous sodium carbonate solution (total volume of 200 ml). The precipitate was filtered off with suction. Recrystallization from ethanol afforded 31 g (47%) of a white powder.

Method C:

Prepared according to general procedure B with 88 mg (0.3 mmol) 6-oxo-5,6,7,12-tetrahydroindolo[3,2-*d*][1]benzazepine-9-carboxylic acid (**39**), 197 mg (0.75 mmol) triphenylphosphine, 35 mg (0.75 mmol) dry ethanol, and 180 mg (0.75 mmol) di-*tert*-butyl azodicarboxylate in 3 ml freshly

dried THF. Recrystallization from ethanol afforded 28 mg (29%) of a white powder.

Mp: > 330 °C; IR (KBr): 3380 cm^{-1} (NH), 3200 cm^{-1} (NH), 3070 cm^{-1} (CH, aromatic), 2980 cm^{-1} (CH, aliphatic), 1690 cm^{-1} (C=O), 1670 cm^{-1} (C=O); ^{1}H-NMR ([D6]-DMSO, 400 MHz): δ (ppm) = 1.37 (t, *J* = 7.1 Hz, 3H, CH_3), 3.56 (s, 2H, azepinone-CH_2), 4.34 (q, *J* = 7.1 Hz, 2H, ester-OCH_2), 7.25-7.33 (m, 2H, Ar H), 7.41 (“dt”, *J* = 7.8/7.6/1.4 Hz, 1H, Ar H), 7.52 (d, *J* = 8.6 Hz, 1H, Ar H), 7.77 (dd, *J* = 7.7/1.1 Hz, 1H, Ar H), 7.82 (dd, *J* = 8.6/1.5 Hz, 1H, Ar H), 8.34 (d, *J* = 1.3 Hz, 1H, Ar H), 10.15 (s, 1H, lactam-NH), 12.02 (s, 1H, indole-NH); ^{13}C-NMR ([D6]-DMSO, 100.6 MHz): δ (ppm) = 14.2 (CH_3), 31.4 (azepinone-CH_2), 60.1 (ester-OCH_2), 111.3, 120.3, 122.3, 122.9, 123.6, 126.9, 128.4 (tert. C), 108.6, 120.9, 122.2, 126.0, 134.2, 135.6, 139.8, 166.5, 171.2 (quat. C); $C_{19}H_{16}N_2O_3$ (320.35); calcd. C 71.24, H 5.03, N 8.74; found C 70.97, H 4.97, N 8.64.

Methyl 6-oxo-5,6,7,12-tetrahydroindolo[3,2-*d*][1]benzazepine-9-carboxylate (**40b**)

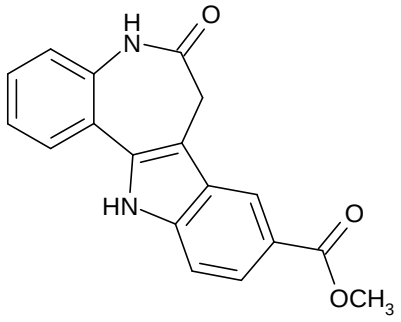

Prepared according to general procedure B with 155 mg (0.5 mmol) 6-oxo-5,6,7,12-tetrahydroindolo[3,2-*d*][1]benzazepine-9-carboxylic acid (**39**), 348 mg (1.25 mmol) triphenylphosphine, 40 mg (1.25 mmol) dry methanol, and 305 mg (1.25 mmol) di-*tert*-butyl azodicarboxylate in 3.5 ml freshly dried THF. Recrystallization from methanol afforded 38 mg (23%) of a white powder.

Mp: > 330 °C; IR (KBr): 3370 cm^{-1} (NH), 3200 cm^{-1} (NH), 3070 cm^{-1} (CH, aromatic), 2980 cm^{-1} (CH, aliphatic), 1690 cm^{-1} (C=O), 1670 cm^{-1} (C=O); ^{1}H-NMR ([D6]-DMSO, 400 MHz): δ (ppm) = 3.56 (s, 2H, CH_2), 3.87 (s,

3H, ester-OCH_3), 7.25-7.33 (m, 2H, Ar H), 7.41 (“dt”, *J* = 7.6/7.6/1.5 Hz, 1H, Ar H), 7.52 (d, *J* = 8.4 Hz, 1H, Ar H), 7.77 (dd, *J* = 7.8/1.4 Hz, 1H, Ar H), 7.81 (dd, *J* = 8.7/1.5 Hz, 1H, Ar H), 8.35 (d, *J* = 1.3 Hz, 1H, Ar H), 10.14 (s, 1H, lactam-NH), 12.03 (s, 1H, indole-NH); ^{13}C-NMR ([D6]-DMSO, 100.6 MHz): δ (ppm) = 31.4 (CH_2), 51.6 (ester-OCH_3), 111.4, 120.4, 122.3, 122.9, 123.6, 126.9, 128.4 (tert. C), 108.6, 120.6, 122.1, 126.0, 134.2, 135.6, 139.8, 167.0, 171.2 (quat. C); $C_{18}H_{14}N_2O_3$ (306.32); calcd. C 70.58, H 4.61, N 9.15; found C 70.06, H 4.56, N 9.07.

Propyl 6-oxo-5,6,7,12-tetrahydroindolo[3,2-*d*][1]benzazepine-9-carboxylate (**40c**)

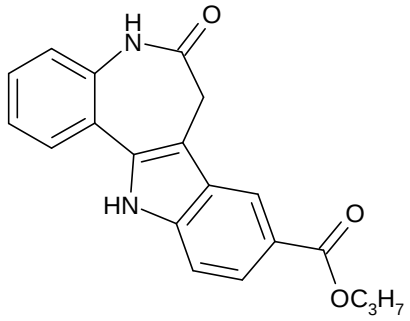

Prepared according to general procedure B with 89 mg (0.3 mmol) 6-oxo-5,6,7,12-tetrahydroindolo[3,2-*d*][1]benzazepine-9-carboxylic acid (**39**), 200 mg (0.75 mmol) triphenylphosphine, 45 mg (0.75 mmol) dry 1-propanol, and 183 mg (0.75 mmol) di-*tert*-butyl azodicarboxylate in 3 ml freshly dried THF. Lacking a reasonable amount of precipitate after the suction filtration, the filtrate was extracted with ethyl acetate, and the combined organic layers were evaporated to dryness. Recrystallization from methanol afforded 29 mg (28%) of a white powder.

Mp: 285 °C (degradation); IR (KBr): 3360 cm^{-1} (NH), 3200 cm^{-1} (NH), 3070 cm^{-1} (CH, aromatic), 2970 cm^{-1} (CH, aliphatic), 1690 cm^{-1} (C=O), 1670 cm^{-1} (C=O); ^{1}H-NMR ([D6]-DMSO, 400 MHz): δ (ppm) = 1.01 (t, *J* = 7.4 Hz, 3H, CH_3), 1.77 (“sext”, *J* = ~7.1 Hz, 2H, ester-CH_2), 3.56 (s, 2H, azepinone-CH_2), 4.25 (t, *J* = 6.7 Hz, 2H, ester-OCH_2), 7.25-7.33 (m, 2H, Ar H), 7.41 (“dt”, *J* = 7.8/7.6/1.4 Hz, 1H, Ar H), 7.52 (d, *J* = 8.4 Hz, 1H, Ar H), 7.77 (dd, *J* = 7.9/1.3 Hz, 1H, Ar H), 7.82 (dd, *J* = 8.5/1.7 Hz, 1H, Ar

H), 8.34 (d, *J* = 1.3 Hz, 1H, Ar H), 10.15 (s, 1H, lactam-NH), 12.01 (s, 1H, indole-NH); ^{13}C-NMR ([D6]-DMSO, 100.6 MHz): δ (ppm) = 10.4 (CH_3), 21.7 (ester-CH_2), 31.4 (azepinone-CH_2), 65.6 (ester-OCH_2), 111.4, 120.2, 122.3, 122.9, 123.7, 126.9, 128.4 (tert. C), 108.5, 120.9, 122.2, 126.0, 134.2, 135.6, 139.8, 166.6, 171.3 (quat. C); $C_{20}H_{18}N_2O_3$ (334.37); calcd. C 71.84, H 5.43, N 8.38; found C 71.56, H 5.51, N 8.16.

Butyl 6-oxo-5,6,7,12-tetrahydroindolo[3,2-*d*][1]benzazepine-9-carboxylate (**40d**)

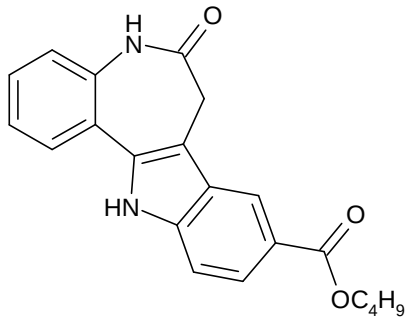

Prepared according to general procedure B with 88 mg (0.3 mmol) 6-oxo-5,6,7,12-tetrahydroindolo[3,2-*d*][1]benzazepine-9-carboxylic acid (**39**), 199 mg (0.75 mmol) triphenylphosphine, 56 mg (0.75 mmol) dry 1-butanol, and 183 mg (0.75 mmol) di-*tert*-butyl azodicarboxylate in 3 ml freshly dried THF. Recrystallization from methanol afforded 31 mg (30%) of a white powder.

Mp: > 330 °C (discoloration at 285 °C); IR (KBr): 3370 cm^{-1} (NH), 3200 cm^{-1} (NH), 3070 cm^{-1} (CH, aromatic), 2960 cm^{-1} (CH, aliphatic), 1690 cm^{-1} (C=O), 1670 cm^{-1} (C=O); ^{1}H-NMR ([D6]-DMSO, 400 MHz): δ (ppm) = 0.97 (t, *J* = 7.4 Hz, 3H, CH_3), 1.47 (“sext”, *J* = ~7.4 Hz, 2H, ester-CH_2), 1.74 (“quint”, *J* = ~7.1 Hz, 2H, ester-CH_2), 3.56 (s, 2H, azepinone-CH_2), 4.30 (t, *J* = 6.6 Hz, 2H, ester-OCH_2), 7.25-7.33 (m, 2H, Ar H), 7.41 (“dt”, *J* = 7.6/7.6/1.5 Hz, 1H, Ar H), 7.52 (d, *J* = 8.4 Hz, 1H, Ar H), 7.77 (dd, *J* = 7.9/1.3 Hz, 1H, Ar H), 7.81 (dd, *J* = 8.5/1.7 Hz, 1H, Ar H), 8.33 (d, *J* = 1.3 Hz, 1H, Ar H), 10.15 (s, 1H, lactam-NH), 12.01 (s, 1H, indole-NH); ^{13}C-NMR ([D6]-DMSO, 100.6 MHz): δ (ppm) = 14.0 (CH_3), 19.2, 30.8 (ester-CH_2), 31.9 (azepinone-CH_2), 64.3 (ester-OCH_2), 111.8, 120.7, 122.7,

123.4, 124.1, 127.3, 128.9 (tert. C), 109.0, 121.4, 122.6, 126.5, 134.7, 136.1, 140.3, 167.0, 171.7 (quat. C); $C_{21}H_{20}N_2O_3$ (348.40); calcd. C 72.40, H 5.79, N 8.04; found C 72.09, H 5.73, N 8.11.

Pentyl 6-oxo-5,6,7,12-tetrahydroindolo[3,2-*d*][1]benzazepine-9-carboxylate (**40e**)

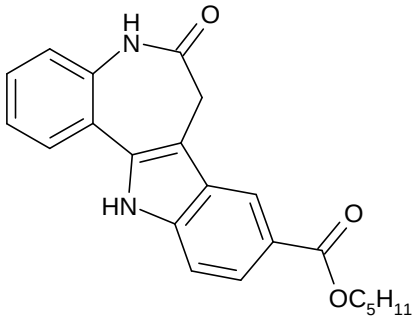

Prepared according to general procedure B with 120 mg (0.4 mmol) 6-oxo-5,6,7,12-tetrahydroindolo[3,2-*d*][1]benzazepine-9-carboxylic acid (**39**), 272 mg (1 mmol) triphenylphosphine, 88 mg (1 mmol) dry 1-pentanol, and 230 mg (1 mmol) di-*tert*-butyl azodicarboxylate in 3 ml freshly dried THF. Recrystallization from methanol afforded 22 mg (15%) of a white powder.

Mp: 293 °C (degradation); IR (KBr): 3370 cm^{-1} (NH), 3200 cm^{-1} (NH), 3070 cm^{-1} (CH, aromatic), 2960 cm^{-1} (CH, aliphatic), 1690 cm^{-1} (C=O), 1670 cm^{-1} (C=O); ^{1}H-NMR ([D6]-DMSO, 400 MHz): δ (ppm) = 0.92 (t, *J* = 7.1 Hz, 3H, CH_3), 1.33-1.47 (m, 4H, CH_2-CH_2), 1.76 (“quint”, *J* = ~7.0 Hz, 2H, ester-CH_2), 3.56 (s, 2H, azepinone-CH_2), 4.29 (t, *J* = 6.6 Hz, 2H, ester-OCH_2), 7.25-7.33 (m, 2H, Ar H), 7.41 (“dt”, *J* = 7.8/7.6/1.4 Hz, 1H, Ar H), 7.52 (d, *J* = 8.4 Hz, 1H, Ar H), 7.77 (dd, *J* = 7.6/1.3 Hz, 1H, Ar H), 7.81 (dd, *J* = 8.5/1.6 Hz, 1H, Ar H), 8.33 (d, *J* = 1.5 Hz, 1H, Ar H), 10.16 (s, 1H, lactam-NH), 12.03 (s, 1H, indole-NH); ^{13}C-NMR ([D6]-DMSO, 100.6 MHz): δ (ppm) = 13.8 (CH_3), 21.7, 27.7, 27.9 (ester-CH_2), 31.4 (azepinone-CH_2), 64.1 (ester-OCH_2), 111.4, 120.2, 122.3, 122.9, 123.7, 126.9, 128.4 (tert. C), 108.5, 120.9, 122.2, 126.0, 134.2, 135.6, 139.8, 166.6, 171.3 (quat. C); $C_{22}H_{22}N_2O_3$ (362.43); calcd. C 72.91, H 6.12, N

7.73; found C 72.04, H 6.09, N 7.62; HRMS-FAB (m/z): $[M + H]^+$ calcd. 363.1709, $[M + H]^+$ found 363.1702.

1-Methylbutyl 6-oxo-5,6,7,12-tetrahydroindolo[3,2-*d*][1]benzazepine-9-carboxylate (**40f**)

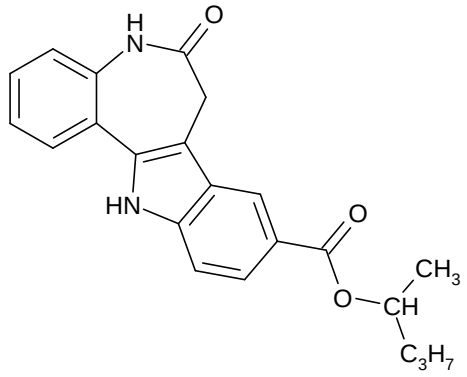

Prepared according to general procedure B with 125 mg (0.4 mmol) 6-oxo-5,6,7,12-tetrahydroindolo[3,2-*d*][1]benzazepine-9-carboxylic acid (**39**), 277 mg (1 mmol) triphenylphosphine, 88 mg (1 mmol) dry 2-pentanol, and 238 mg (1 mmol) di-*tert*-butyl azodicarboxylate in 3 ml freshly dried THF. Lacking a reasonable amount of precipitate after the suction filtration, the filtrate was extracted with ethyl acetate after having added water, and the combined organic layers were evaporated to dryness. Recrystallization from methanol afforded 30 mg (19%) of a white powder.

Mp: 265 °C (degradation); IR (KBr): 3330 cm^{-1} (NH), 3200 cm^{-1} (NH), 3070 cm^{-1} (CH, aromatic), 2960 cm^{-1} (CH, aliphatic), 1670 cm^{-1} (C=O); ^{1}H-NMR ([D6]-DMSO, 400 MHz): δ (ppm) = 0.93 (t, *J* = 7.4 Hz, 3H, CH_3), 1.33 (d, *J* = 6.1 Hz, 3H, CH_3), 1.34-1.48 (m, 2H, ester-CH_2), 1.55-1.79 (m, 2H, ester-CH_2), 3.56 (s, 2H, azepinone-CH_2), 5.11 (“sext”, *J* = ~6.2 Hz, 1H, ester-OCH), 7.25-7.33 (m, 2H, Ar H), 7.41 (“dt”, *J* = 7.8/7.6/1.4 Hz, 1H, Ar H), 7.52 (d, *J* = 8.6 Hz, 1H, Ar H), 7.77 (dd, *J* = 7.8/1.4 Hz, 1H, Ar H), 7.80 (dd, *J* = 8.5/1.6 Hz, 1H, Ar H), 8.31 (d, *J* = 1.3 Hz, 1H, Ar H), 10.17 (s, 1H, lactam-NH), 12.02 (s, 1H, indole-NH); ^{13}C-NMR ([D6]-DMSO, 100.6 MHz): δ (ppm) = 13.8, 19.9 (CH_3), 18.2 (ester-CH_2, lacking one: not detected under application of 4096 scans), 31.8 (azepinone-

CH_2), 70.2 (ester-OCH), 111.3, 120.1, 122.3, 122.9, 123.7, 126.9, 128.4 (tert. C), 109.3, 122.2, 134.1, 165.9, 171.3 (quat. C, lacking four: not detected under application of 4096 scans); $C_{22}H_{22}N_2O_3$ (362.43); calcd. C 72.91, H 6.12, N 7.73; found C 72.01, H 5.98, N 7.71; HRMS-FAB (m/z): $[M]^+$ calcd. 362.1630, $[M]^+$ found 362.1615.

Hexyl 6-oxo-5,6,7,12-tetrahydroindolo[3,2-*d*][1]benzazepine-9-carboxylate (**40g**)

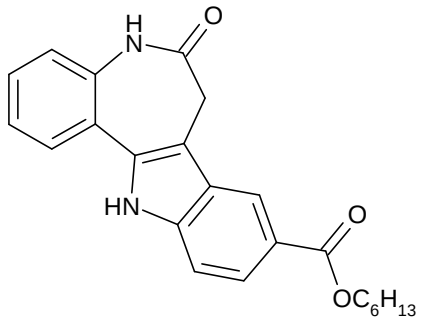

Prepared according to general procedure B with 154 mg (0.5 mmol) 6-oxo-5,6,7,12-tetrahydroindolo[3,2-*d*][1]benzazepine-9-carboxylic acid (**39**), 330 mg (1.25 mmol) triphenylphosphine, 128 mg (1.25 mmol) dry 1-hexanol, and 298 mg (1.25 mmol) di-*tert*-butyl azodicarboxylate in 3.5 ml freshly dried THF. Recrystallization from methanol afforded 55 mg (28%) of a white powder.

Mp: 280 °C (degradation); IR (KBr): 3370 cm^{-1} (NH), 3200 cm^{-1} (NH), 3070 cm^{-1} (CH, aromatic), 2930 cm^{-1} (CH, aliphatic), 1680 cm^{-1} (C=O), 1670 cm^{-1} (C=O); ^{1}H-NMR ([D6]-DMSO, 400 MHz): δ (ppm) = 0.89 (t, *J* = 7.0 Hz, 3H, CH_3), 1.28-1.49 (m, 6H, CH_2-CH_2-CH_2), 1.76 (“quint”, *J* = ~7.1 Hz, 2H, ester-CH_2), 3.56 (s, 2H, azepinone-CH_2), 4.29 (t, *J* = 6.6 Hz, 2H, ester-OCH_2), 7.25-7.33 (m, 2H, Ar H), 7.41 (“dt”, *J* = 7.6/7.6/1.5 Hz, 1H, Ar H), 7.52 (d, *J* = 8.7 Hz, 1H, Ar H), 7.77 (dd, *J* = 7.9/1.3 Hz, 1H, Ar H), 7.81 (dd, *J* = 8.6/1.5 Hz, 1H, Ar H), 8.33 (d, *J* = 1.5 Hz, 1H, Ar H), 10.16 (s, 1H, lactam-NH), 12.03 (s, 1H, indole-NH); ^{13}C-NMR ([D6]-DMSO, 100.6 MHz): δ (ppm) = 14.3 (CH_3), 22.4, 25.6, 28.6, 31.3 (ester-CH_2), 31.9 (azepinone-CH_2), 64.6 (ester-OCH_2), 111.8, 120.7, 122.7, 123.4, 124.1, 127.3, 128.9 (tert. C), 109.0, 121.4, 122.6, 126.5, 134.7, 136.1,

140.3, 167.0, 171.7 (quat. C); $C_{23}H_{24}N_2O_3$ (376.45); calcd. C 73.38, H 6.43, N 7.44; found C 73.21, H 6.38, N 7.50.

Octyl 6-oxo-5,6,7,12-tetrahydroindolo[3,2-*d*][1]benzazepine-9-carboxylate (**40h**)

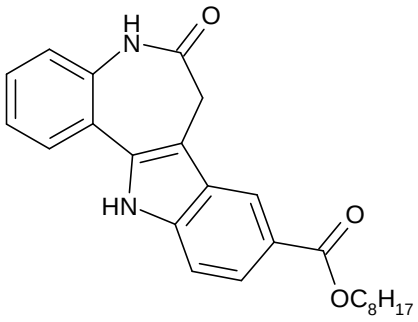

Prepared according to general procedure B with 152 mg (0.5 mmol) 6-oxo-5,6,7,12-tetrahydroindolo[3,2-*d*][1]benzazepine-9-carboxylic acid (**39**), 342 mg (1.25 mmol) triphenylphosphine, 163 mg (1.25 mmol) dry 1-octanol, and 305 mg (1.25 mmol) di-*tert*-butyl azodicarboxylate in 3.5 ml freshly dried THF. Recrystallization from methanol afforded 70 mg (33%) of a white powder.

Mp: 292 °C (degradation); IR (KBr): 3360 cm^{-1} (NH), 3200 cm^{-1} (NH), 3070 cm^{-1} (CH, aromatic), 2920 cm^{-1} (CH, aliphatic), 2850 cm^{-1} (CH, aliphatic), 1680 cm^{-1} (C=O), 1670 cm^{-1} (C=O); ^{1}H-NMR ([D6]-DMSO, 400 MHz): δ (ppm) = 0.86 (t, *J* = 6.7 Hz, 3H, CH_3), 1.21-1.48 (m, 10H, CH_2-CH_2-CH_2-CH_2-CH_2), 1.75 (“quint”, *J* = ~7.0 Hz, 2H, ester-CH_2), 3.55 (s, 2H, azepinone-CH_2), 4.28 (t, *J* = 6.6 Hz, 2H, ester-OCH_2), 7.25-7.33 (m, 2H, Ar H), 7.41 (“dt”, *J* = 7.8/7.6/1.5 Hz, 1H, Ar H), 7.52 (d, *J* = 8.6 Hz, 1H, Ar H), 7.77 (dd, *J* = 7.6/1.0 Hz, 1H, Ar H), 7.81 (dd, *J* = 8.6/1.5 Hz, 1H, Ar H), 8.32 (d, *J* = 1.3 Hz, 1H, Ar H), 10.15 (s, 1H, lactam-NH), 12.02 (s, 1H, indole-NH); ^{13}C-NMR ([D6]-DMSO, 100.6 MHz): δ (ppm) = 13.8 (CH_3), 22.0, 25.5, 28.2, 28.5, 28.6, 31.1 (ester-CH_2), 31.4 (azepinone-CH_2), 64.1 (ester-OCH_2), 111.4, 120.2, 122.3, 122.9, 123.6, 126.9, 128.4 (tert. C), 108.5, 120.9, 122.2, 126.0, 134.2, 135.6, 139.8, 166.5, 171.2 (quat. C); $C_{25}H_{28}N_2O_3$ (404.51); calcd. C 74.23, H 6.98, N 6.93; found C

73.65, H 7.02, N 6.92; HRMS-FAB (m/z): $[M + H]^+$ calcd. 405.2178, $[M + H]^+$ found 405.2175.

N-Isopropyl-*N*-[(isopropylamino)carbonyl]-6-oxo-5,6,7,12-tetrahydroindolo[3,2-*d*][1]benzazepine-9-carboxamide (**54**)

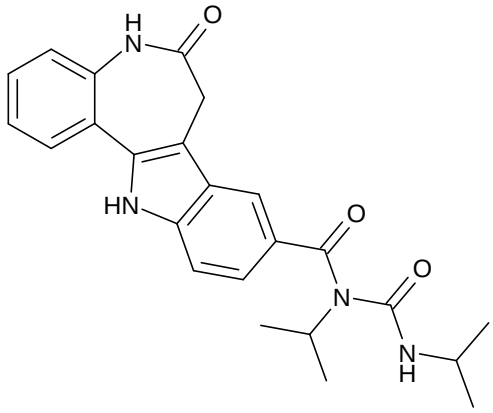

Diisopropylcarbodiimide (40 mg, 0.3 mmol) was added to a solution of 6-oxo-5,6,7,12-tetrahydroindolo[3,2-*d*][1]benzazepine-9-carboxylic acid (**39**) (100 mg, 0.3 mmol) in DMF (5 ml). After 2.5 h of stirring, *N*-ethyldiisopropylamine (388 mg, 3 mmol) and catalytic amounts of 4-dimethylaminopyridine (DMAP) were added to the reaction mixture which was then stirred for 24 h. The mixture was evaporated to dryness, the resulting residue suspended in water, and the precipitate filtered off with suction. Recrystallization from ethyl acetate afforded 68 mg (46%) of a yellow powder.

Mp: 180 °C (degradation); IR (KBr): 3470 cm^{-1} (NH), 3310 cm^{-1} (NH), 3200 cm^{-1} (NH), 3060 cm^{-1} (CH, aromatic), 2970 cm^{-1} (CH, aliphatic), 1670 cm^{-1} (C=O), 1650 cm^{-1} (C=O), 1630 cm^{-1} (C=O); ^{1}H-NMR ([D6]-DMSO, 400 MHz): δ (ppm) = 0.70 (d, *J* = 6.6 Hz, 6H, CH_3), 1.31 (d, *J* = 6.9 Hz, 6H, CH_3), 3.44-3.55 (m, 3H, azepinone-CH_2 [s, 2H] and isopropyl-CH [sept, 1H], overlapping), 4.60 (sept, *J* = 6.9 Hz, 1H, isopropyl-CH), 7.24-7.32 (m, 2H, Ar H), 7.35-7.43 (m, 3H, Ar H), 7.72-7.80 (m, 2H, Ar H [dd, 1H] and isopropylamino-NH [d, 1H], overlapping), 7.87 (s, 1H, Ar H), 10.12 (s, 1H, lactam-NH), 11.80 (s, 1H, indole-NH); ^{13}C-NMR ([D6]-DMSO, 100.6 MHz): δ (ppm) = 20.9, 21.8 (CH_3), 32.0 (azepinone-CH_2),

42.4, 46.5 (isopropyl-CH), 111.0, 118.1, 122.2, 122.7, 124.1, 127.3, 128.7 (tert. C), 108.5, 122.8, 125.9, 134.0, 135.9, 138.7, 155.0, 171.7 (quat. C); $C_{24}H_{26}N_4O_3$ (418.49); calcd. C 68.88, H 6.26, N 13.39; $C_{24}H_{26}N_4O_3 \times H_2O$ (436.50); calcd. C 66.04, H 6.47, N 12.84; found C 66.06, H 6.50, N 12.74.

N-Benzyl-6-oxo-5,6,7,12-tetrahydroindolo[3,2-*d*][1]benzazepine-9-carboxamide (**55a**)

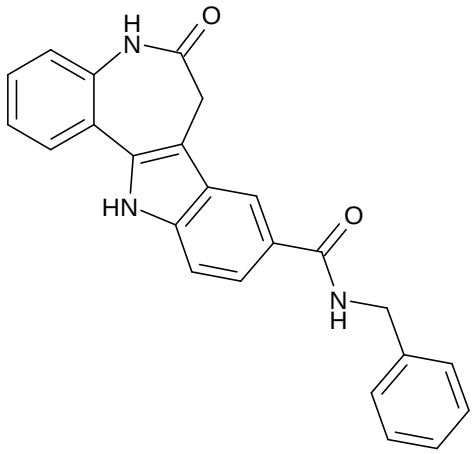

Prepared according to general procedure C with 440 mg (1.5 mmol) 6-oxo-5,6,7,12-tetrahydroindolo[3,2-*d*][1]benzazepine-9-carboxylic acid (**39**), 263 mg (1.95 mmol) HOBt, 374 mg (1.95 mmol) EDC, and 161 mg (1.5 mmol) benzylamine. Recrystallization from ethanol afforded 303 mg (53%) of a beige powder.

Mp: 286 °C; IR (KBr): 3230 cm^{-1} (NH), 3060 cm^{-1} (CH, aromatic), 2920 cm^{-1} (CH, aliphatic), 1660 cm^{-1} (C=O), 1650 cm^{-1} (C=O); ^{1}H-NMR ([D6]-DMSO, 400 MHz): δ (ppm) = 3.55 (s, 2H, azepinone-CH_2), 4.53 (d, *J* = 5.8 Hz, 2H, benzylamide-CH_2), 7.22-7.43 (m, 8H, Ar H), 7.47 (d, *J* = 8.4 Hz, 1H, Ar H), 7.77 (“dt”, *J* = 8.1/7.9/1.3 Hz, 2H, Ar H), 8.35 (s, 1H, Ar H), 8.96 (t, *J* = 5.9 Hz, 1H, benzylamide-NH), 10.12 (s, 1H, lactam-NH), 11.84 (s, 1H, indole-NH); ^{13}C-NMR ([D6]-DMSO, 100.6 MHz): δ (ppm) = 32.0 (azepinone-CH_2), 43.0 (benzylamide-CH_2), 111.4, 118.0, 122.3, 122.7, 124.1, 127.0, 127.3, 127.6, 128.6, 128.7 (tert. C), 108.8, 122.9, 125.8, 126.4, 134.1, 135.9, 139.3, 140.5, 167.3, 171.9 (quat. C); $C_{24}H_{19}N_3O_2$

(381.43); calcd. C 75.57, H 5.02, N 11.02; found C 74.13, H 4.94, N 11.03; HRMS-FAB (m/z): $[M + H]^+$ calcd. 382.1556, $[M + H]^+$ found 382.1557.

9-(Morpholin-4-ylcarbonyl)-7,12-dihydroindolo[3,2-*d*][1]benzazepin-6(5*H*)-one (**55b**)

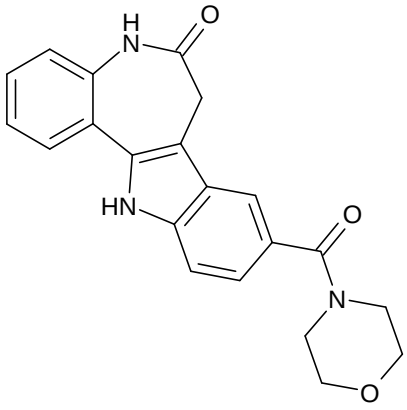

Prepared according to general procedure C with 186 mg (0.6 mmol) 6-oxo-5,6,7,12-tetrahydroindolo[3,2-*d*][1]benzazepine-9-carboxylic acid (**39**), 105 mg (0.8 mmol) HOBt, 150 mg (0.8 mmol) EDC, and 56 mg (1 mmol) morpholine. Recrystallization from ethanol afforded 70 mg (30%) of orange crystals.

Mp: 175 °C (degradation); IR (KBr): 3190 cm^{-1} (NH), 3050 cm^{-1} (CH, aromatic), 2920 cm^{-1} (CH, aliphatic), 1660 cm^{-1} (C=O), 1600 cm^{-1} (C=O); ^{1}H-NMR ([D6]-DMSO, 400 MHz): δ (ppm) = 3.50-3.67 (m, 10H, azepinone-CH_2 [s, 2H] and morpholine-CH_2 [m, 8H] overlapping), 7.23 and 7.24-7.32 (dd, *J* = 8.2/1.4 Hz, 1H, Ar H and m, 2H, Ar H, overlapping), 7.39 (“dt”, *J* = 7.8/7.6/1.3 Hz, 1H, Ar H), 7.47 (d, *J* = 8.5 Hz, 1H, Ar H), 7.75 and 7.77 (dd, *J* = 7.8/1.1 Hz, 1H, Ar H and s, 1H, Ar H, overlapping), 10.11 (s, 1H, lactam-NH), 11.81 (s, 1H, indole-NH); ^{13}C-NMR ([D6]-DMSO, 100.6 MHz): δ (ppm) = 31.4 (azepinone-CH_2), 66.1 (morpholine-CH_2, all overlapping), 111.1, 117.5, 121.4, 122.2, 123.6, 126.8, 128.2 (tert. C), 108.0, 122.4, 125.9, 126.4, 133.7, 135.5, 137.7, 170.3, 171.4 (quat. C); $C_{21}H_{19}N_3O_3$ (361.40); HRMS-FAB (m/z): $[M + H]^+$ calcd. 362.1505, $[M + H]^+$ found 362.1514.

N-Octadecyl-6-oxo-5,6,7,12-tetrahydroindolo[3,2-*d*][1]benzazepine-9-carboxamide (**55c**)

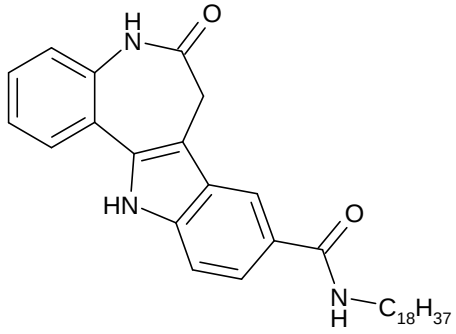

Prepared according to general procedure C with 197 mg (0.7 mmol) 6-oxo-5,6,7,12-tetrahydroindolo[3,2-*d*][1]benzazepine-9-carboxylic acid (**39**), 123 mg (0.9 mmol) HOBt, 174 mg (0.9 mmol) EDC, and 189 mg (1 mmol) octadecylamine. Recrystallization from ethanol afforded 125 mg (34%) of an ocher powder.

Mp: 270 °C (degradation); IR (KBr): 3310 cm^{-1} (NH), 3200 cm^{-1} (NH), 3070 cm^{-1} (CH, aromatic), 2920 cm^{-1} (CH, aliphatic), 2850 cm^{-1} (CH, aliphatic), 1670 cm^{-1} (C=O), 1640 cm^{-1} (C=O); ^{1}H-NMR ([D6]-DMSO, 400 MHz): δ (ppm) = 0.85 (t, *J* = 6.9 Hz, 3H, CH_3), 1.18-1.36 (m, 32H, octadecylamide-CH_2), 1.50-1.60 (m, 2H, octadecylamide-NCH_2), 3.55 (s, 2H, azepinone-CH_2), 7.24-7.32 (m, 2H, Ar H), 7.39 (“dt”, *J* = 7.6/7.2/1.3 Hz, 1H, Ar H), 7.44 (d, *J* = 8.6 Hz, 1H, Ar H), 7.72 and 7.75 (dd, *J* = 8.9/1.3 Hz, 1H, Ar H and d, *J* = 7.9 Hz, 1H, Ar H, overlapping), 8.26 (s, 1H, Ar H), 8.34 (t, *J* = 5.6 Hz, 1H, octadecylamide-NH), 10.12 (s, 1H, lactam-NH), 11.80 (s, 1H, indole-NH); ^{13}C-NMR ([D6]-DMSO, 100.6 MHz): δ (ppm) = 14.3 (CH_3), 22.4, 26.9, 29.0, 29.2, 29.4, 29.7 (octadecylamide-CH_2, partially overlapping), 31.6 (azepinone-CH_2), 111.3, 117.8, 122.2, 122.7, 124.1, 127.2, 128.6 (tert. C), 108.8, 122.9, 126.3, 126.3, 134.0, 135.9, 139.2, 167.1, 171.9 (quat. C); $C_{35}H_{49}N_3O_2$ (543.79); calcd. C 77.31, H 9.08, N 7.73; found C 76.95, H 9.01, N 7.76; HRMS-FAB (m/z): $[M + H]^+$ calcd. 544.3903, $[M + H]^+$ found 544.3887.

9-[(4-Benzylpiperazin-1-yl)carbonyl]-7,12-dihydroindolo[3,2-*d*][1] benzazepin-6(5*H*)-one (**55d**)

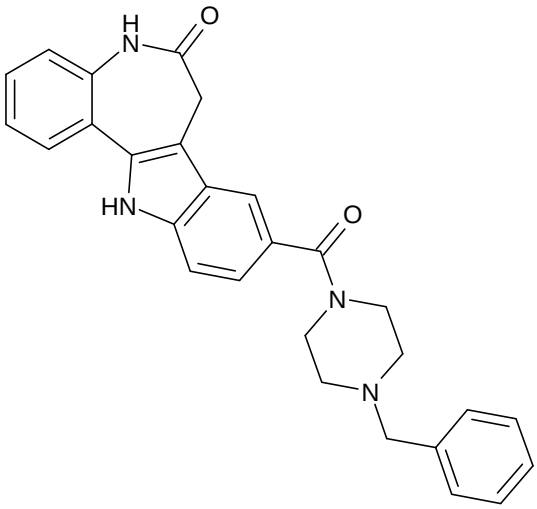

Prepared according to general procedure C with 201 mg (0.7 mmol) 6-oxo-5,6,7,12-tetrahydroindolo[3,2-*d*][1]benzazepine-9-carboxylic acid (**39**), 123 mg (0.9 mmol) HOBt, 174 mg (0.9 mmol) EDC, and 123 mg (0.7 mmol) 1-benzylpiperazine. The produced hydrochloride derivative was recrystallized from ethanol. The base was liberated by suspending the compound in 10% aqueous ammonia. The precipitate was filtered off with suction and washed with water. Drying in vacuo afforded 103 mg (33%) of an orange whitish powder.

Mp: 167 °C (degradation); IR (KBr): 3230 cm^{-1} (NH), 2910 cm^{-1} (CH, aliphatic), 2810 cm^{-1} (CH, aliphatic), 1660 cm^{-1} (C=O), 1600 cm^{-1} (C=O); ^{1}H-NMR ([D6]-DMSO, 400 MHz): δ (ppm) = 2.41 (“br s”, 4H, piperazine-CH_2), 3.52 and 3.53 and 3.49-3.62 (s, 2H, benzyl-CH_2 and s, 2H, azepinone-CH_2 and “br s”, 4H, piperazine-CH_2, overlapping), 7.20 (dd, *J* = 8.4/1.5 Hz, 1H, Ar H), 7.23-7.29 (m, 3H, Ar H), 7.30-7.35 (m, 4H, Ar H), 7.39 (“dt”, *J* = 7.6/7.6/1.3 Hz, 1H, Ar H), 7.46 (d, *J* = 8.1 Hz, 1H, Ar H), 7.72-7.77 (m, 2H, Ar H), 10.10 (s, 1H, lactam-NH), 11.80 (s, 1H, indole-NH); ^{13}C-NMR ([D6]-DMSO, 100.6 MHz): δ (ppm) = 31.4 (azepinone-CH_2), 52.5, 61.8 (benzylpiperazine-CH_2, only two detected under application of 1024 scans), 111.1, 117.4, 121.3, 122.2, 123.6, 126.8, 126.9, 128.1, 128.2, 128.8 (tert. C), 108.0, 122.4, 125.9, 126.8, 133.6, 135.5, 137.7, 170.2, 171.4 (quat. C, lacking one: not detected under

application of 1024 scans); $C_{28}H_{26}N_4O_2$ (450.55); HRMS-FAB (m/z): $[M + H]^+$ calcd. 451.2134, $[M + H]^+$ found 451.2143.

9-(Pyrrolidin-1-ylcarbonyl)-7,12-dihydroindolo[3,2-*d*][1]benzazepin-6(5*H*)-one (**55e**)

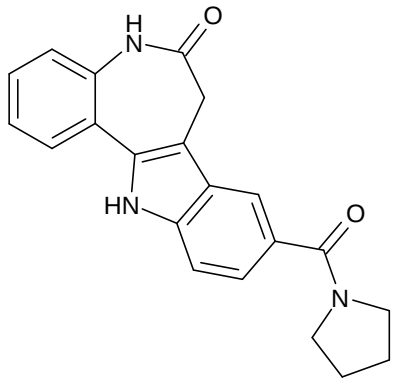

A solution of 6-oxo-5,6,7,12-tetrahydroindolo[3,2-*d*][1]benzazepine-9-carboxylic acid (**39**) (235 mg, 0.8 mmol), 1.3 equiv. of HOBt (135 mg, 1 mmol), and 1.3 equiv. of EDC (192 mg, 1 mmol) in DMF (10 ml) was stirred in an ice bath under nitrogen. After 20 min, 1 equiv. of pyrrolidine (57 mg, 0.8 mmol) was added to the reaction mixture, and the stirring under nitrogen was continued for 1 h in the ice bath, and subsequently, for 24 h at room temperature. A precipitate was formed that was filtered off with suction and washed with petrol ether. Recrystallization from ethanol afforded 105 mg (38%) of a yellowish powder.

Mp: 242 °C (degradation); IR (KBr): 3200 cm^{-1} (NH), 3060 cm^{-1} (CH, aromatic), 2970 cm^{-1} (CH, aliphatic), 2870 cm^{-1} (CH, aliphatic), 1660 cm^{-1} (C=O), 1590 cm^{-1} (C=O); ^{1}H-NMR ([D6]-DMSO, 400 MHz): δ (ppm) = 1.77-1.94 (m, 4H, pyrrolidine-CH_2), 3.50 (t, *J* = 6.6 Hz, 4H, pyrrolidine-CH_2), 3.54 (s, 2H, azepinone-CH_2), 7.24-7.32 (m, 2H, Ar H), 7.35 and 7.39 (dd, *J* = 8.5/1.4 Hz, 1H, Ar H and "dt", *J* = 7.7/7.6/1.4 Hz, 1H, Ar H, overlapping), 7.45 (d, *J* = 8.4 Hz, 1H, Ar H), 7.75 (dd, *J* = 7.6/1.3 Hz, 1H, Ar H), 7.88 (s, 1H, Ar H), 10.10 (s, 1H, lactam-NH), 11.78 (s, 1H, indole-NH); ^{13}C-NMR ([D6]-DMSO, 100.6 MHz): δ (ppm) = 31.4 (azepinone-CH_2), 46.0, 49.2 (pyrrolidine-CH_2), 110.8, 117.4, 121.6, 122.2, 123.6, 126.8, 128.1 (tert. C), 108.1, 122.5, 125.7, 128.2, 133.5, 135.5, 137.8,

169.3, 171.4 (quat. C); $C_{21}H_{19}N_3O_2$ (345.40); HRMS-FAB (m/z): $[M + H]^+$ calcd. 346.1556, $[M + H]^+$ found 346.1586.

N-Butyl-6-oxo-5,6,7,12-tetrahydroindolo[3,2-*d*][1]benzazepine-9-carboxamide (**55f**)

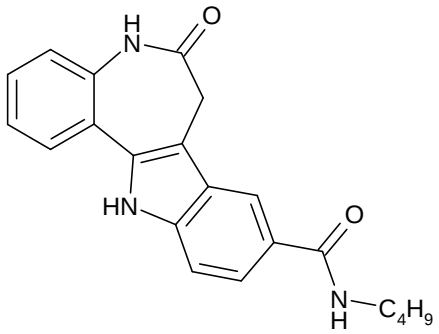

Prepared according to general procedure C with 230 mg (0.8 mmol) 6-oxo-5,6,7,12-tetrahydroindolo[3,2-*d*][1]benzazepine-9-carboxylic acid (**39**), 135 mg (1 mmol) HOBt, 191 mg (1 mmol) EDC, and 59 mg (0.8 mmol) butylamine. The substance was recrystallized from ethanol, and further purified by column chromatography, eluting with ethyl acetate. Evaporation to dryness of the pure fraction afforded 11 mg (4%) of a yellow powder.

Mp: 291 °C (degradation); IR (KBr): 3320 cm^{-1} (NH), 3200 cm^{-1} (NH), 3070 cm^{-1} (CH, aromatic), 2960 cm^{-1} (CH, aliphatic), 2930 cm^{-1} (CH, aliphatic), 2870 cm^{-1} (CH, aliphatic), 1670 cm^{-1} (C=O), 1640 cm^{-1} (C=O); ^{1}H-NMR ([D6]-DMSO, 400 MHz): δ (ppm) = 0.93 (t, *J* = 7.4 Hz, 3H, CH_3), 1.37 (“sext”, *J* = ~7.4 Hz, 2H, butylamide-CH_2), 1.55 (“quint”, *J* = ~7.3 Hz, 2H, butylamide-CH_2), 3.31 (“q”, *J* = ~6.4 Hz, 2H, butylamide-NCH_2, partially hidden under water signal), 3.56 (s, 2H, azepinone-CH_2), 7.25-7.33 (m, 2H, Ar H), 7.39 (“dt”, *J* = 7.6/7.6/1.3 Hz, 1H, Ar H), 7.46 (d, *J* = 8.6 Hz, 1H, Ar H), 7.71-7.79 (m, 2H, Ar H), 8.27 (s, 1H, Ar H), 8.35 (t, *J* = 5.6 Hz, 1H, butylamide-NH), 10.13 (s, 1H, lactam-NH), 11.81 (s, 1H, indole-NH); ^{13}C-NMR ([D6]-DMSO, 100.6 MHz): δ (ppm) = 13.7 (CH_3), 19.6, 31.4, 31.6 (azepinone-CH_2 and butylamide-CH_2, lacking one: not detected under application of 3072 scans), 110.8, 117.3, 121.8, 122.2, 123.6, 126.8, 128.2 (tert. C), 108.3, 122.4, 125.8, 125.9, 133.6, 135.5,

138.7, 166.7, 171.4 (quat. C); $C_{21}H_{21}N_3O_2$ (347.42); calcd. C 72.60, H 6.09, N 12.09; found C 72.10, H 6.33, N 11.44; HRMS-FAB (m/z): $[M + H]^+$ calcd. 348.1712, $[M + H]^+$ found 348.1721.

N-(4-Methoxybenzyl)-6-oxo-5,6,7,12-tetrahydroindolo[3,2-*d*][1] benzazepine-9-carboxamide (**55g**)

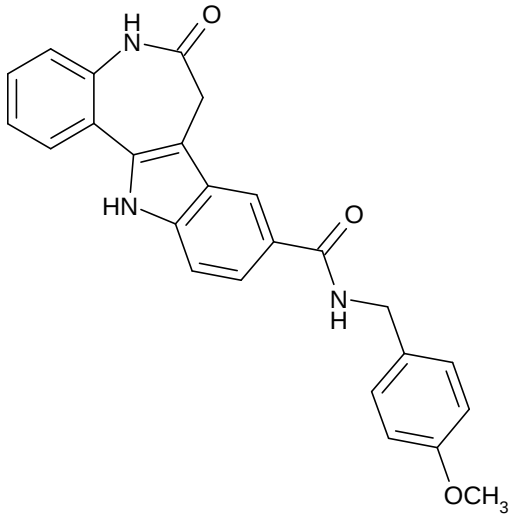

Prepared according to general procedure C with 242 mg (0.8 mmol) 6-oxo-5,6,7,12-tetrahydroindolo[3,2-*d*][1]benzazepine-9-carboxylic acid (**39**), 142 mg (1 mmol) HOBt, 199 mg (1 mmol) EDC, and 110 mg (0.8 mmol) 4-methoxybenzylamine. Recrystallization from ethanol afforded 162 mg (48%) of a beige powder.

Mp: 290 °C (degradation); IR (KBr): 3420 cm^{-1} (NH), 3270 cm^{-1} (NH), 3060 cm^{-1} (CH, aromatic), 2920 cm^{-1} (CH, aliphatic), 1660 cm^{-1} (C=O), 1640 cm^{-1} (C=O); ^{1}H-NMR ([D6]-DMSO, 400 MHz): δ (ppm) = 3.55 (s, 2H, azepinone-CH_2), 3.73 (s, 3H, OCH_3), 4.45 (d, *J* = 5.9 Hz, 2H, methoxybenzylamide-CH_2), 6.90 (d, *J* = 8.6 Hz, 2H, Ar H), 7.24-7.32 (m, 4H, Ar H), 7.39 (“dt”, *J* = 7.6/7.6/1.3 Hz, 1H, Ar H), 7.47 (d, *J* = 8.4 Hz, 1H, Ar H), 7.74-7.79 (m, 2H, Ar H), 8.33 (s, 1H, Ar H), 8.89 (t, *J* = 6.0 Hz, 1H, methoxybenzylamide-NH), 10.12 (s, 1H, lactam-NH), 11.83 (s, 1H, indole-NH); ^{13}C-NMR ([D6]-DMSO, 100.6 MHz): δ (ppm) = 31.5 (azepinone-CH_2), 42.0 (methoxybenzylamide-CH_2), 55.0 (OCH_3), 110.9, 113.6, 117.4, 121.8, 122.2, 123.6, 126.8, 128.2, 128.5 (tert. C), 108.3,

122.4, 125.5, 125.9, 132.0, 133.6, 135.5, 138.8, 158.1, 166.7, 171.4 (quat. C); $C_{25}H_{21}N_3O_3$ (411.46); calcd. C 72.98, H 5.14, N 10.21; found C 72.62, H 5.14, N 10.28; HRMS-FAB (m/z): $[M + H]^+$ calcd. 412.1661, $[M + H]^+$ found 412.1673.

N-(2,4-Dichlorobenzyl)-6-oxo-5,6,7,12-tetrahydroindolo[3,2-*d*][1]benzazepine-9-carboxamide (**55h**)

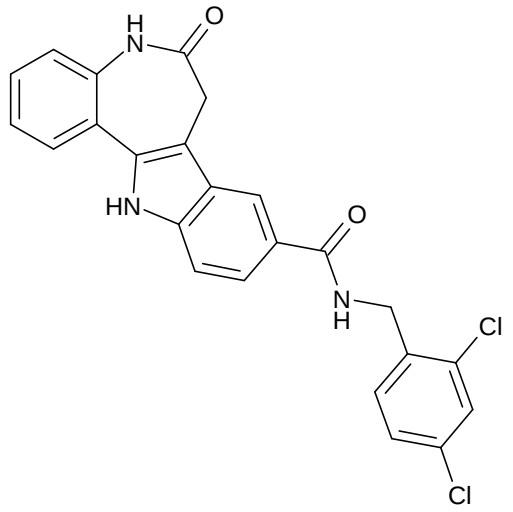

Prepared according to general procedure C with 234 mg (0.8 mmol) 6-oxo-5,6,7,12-tetrahydroindolo[3,2-*d*][1]benzazepine-9-carboxylic acid (**39**), 144 mg (1 mmol) HOBt, 201 mg (1 mmol) EDC, and 141 mg (0.8 mmol) 2,4-dichlorobenzylamine. Recrystallization from ethanol afforded 162 mg (48%) of a salmon colored powder.

Mp: 302 °C (degradation); IR (KBr): 3350 cm^{-1} (NH), 3200 cm^{-1} (NH), 3060 cm^{-1} (CH, aromatic), 2970 cm^{-1} (CH, aliphatic), 1670 cm^{-1} (C=O), 1650 cm^{-1} (C=O); ^{1}H-NMR ([D6]-DMSO, 400 MHz): δ (ppm) = 3.57 (s, 2H, azepinone-CH_2), 4.56 (d, *J* = 5.8 Hz, 2H, dichlorobenzylamide-CH_2), 7.25-7.33 (m, 2H, Ar H), 7.37-7.44 (m, 3H, Ar H), 7.49 (d, *J* = 8.6 Hz, 1H, Ar H), 7.63 (d, *J* = 1.5 Hz, 1H, Ar H), 7.78 (“dt”, *J* = 7.4/7.1/1.5 Hz, 2H, Ar H), 8.37 (d, *J* = 1.0 Hz, 1H, Ar H), 9.00 (t, *J* = 5.7 Hz, 1H, dichlorobenzylamide-NH), 10.14 (s, 1H, lactam-NH), 11.87 (s, 1H, indole-NH); ^{13}C-NMR ([D6]-DMSO, 100.6 MHz): δ (ppm) = 32.0 (azepinone-CH_2), 40.6 (dichlorobenzylamide-CH_2), 111.5, 118.1, 122.3, 122.7, 124.1,

127.3, 127.7, 128.7, 128.9, 130.4 (tert. C), 108.8, 122.8, 125.4, 126.4, 132.4, 133.2, 134.2, 136.0, 136.4, 139.4, 167.6, 171.9 (quat. C); $C_{24}H_{17}Cl_2N_3O_2$ (450.32); calcd. C 64.01, H 3.81, N 9.33; found C 64.06, H 3.84, N 9.78; HRMS-FAB (m/z): $[M + H]^+$ calcd. 450.0776, $[M + H]^+$ found 450.0819.

6-Oxo-5,6,7,12-tetrahydroindolo[3,2-*d*][1]benzazepine-9-carbonitrile (**74**)

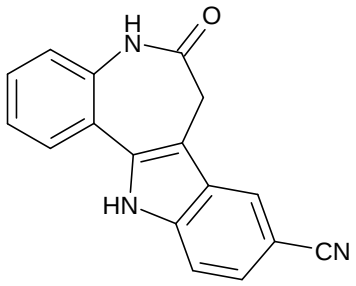

A mixture of 9-bromo-7,12-dihydroindolo[3,2-*d*][1]benzazepin-6(5*H*)-one (**1**) (502 mg, 1.5 mmol) and copper(I) cyanide (358 mg, 4 mmol) in *N*-methyl-2-pyrrolidone (15 ml) was refluxed for 8 h. After allowing the reaction mixture to cool to room temperature, water was added (15 ml) and the mixture was stirred for 20 min at room temperature. The resulting precipitate was filtered off with suction and subsequently suspended in 1,2-diaminoethane (4 ml) and water (15 ml). After 30 min of stirring, the precipitate was filtered off with suction and washed with 10% aqueous sodium cyanide solution (20 ml) and water. Drying in vacuo afforded 403 mg (98%) of a brown powder which was used without further purification. (Lit: Schultz[6])

9-(1*H*-Tetrazol-5-yl)-7,12-dihydroindolo[3,2-*d*][1]benzazepin-6(5*H*)-one (**75**)

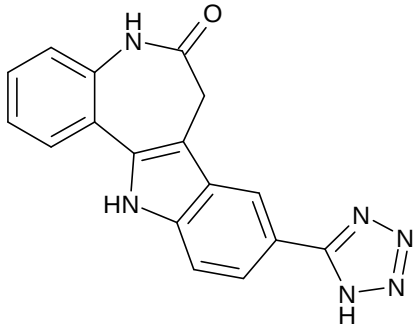

6-Oxo-5,6,7,12-tetrahydroindolo[3,2-*d*][1]benzazepine-9-carbonitrile (**74**) (75 mg, 0.3 mmol) and trimethyltin azide (**76**) (520 mg, 2.5 mmol) were suspended in toluene (30 ml) and refluxed for 66 h. After adding another portion of the reagent **76** (205 mg, 1 mmol), the reaction mixture was refluxed for another 123 h. The mixture was allowed to cool to room temperature, and the precipitate was filtered off with suction and subsequently suspended in THF (2 ml) and toluene (15 ml). Under cooling, gaseous hydrogen chloride was bubbled through the reaction mixture for 20 min, continuously stirring. The precipitate was filtered off with suction and washed with toluene. Further purification was performed by MPLC, eluting with acetonitrile/water pH 1.5 (pH-adjusted with trifluoroacetic acid) gradients. Previously, the substance had been dissolved in a mixture of DMSO and elution solvent in order to prevent the precipitation of the product on the column. Evaporation to dryness of the pure fraction afforded 7 mg (9%) of a brown powder.

Mp: 184 °C (degradation); IR (KBr): 3230 cm^{-1} (NH), 3050 cm^{-1} (CH, aromatic), 2910 cm^{-1} (CH, aliphatic), 1650 cm^{-1} (C=O); ^{1}H-NMR ([D6]-DMSO, 400 MHz): δ (ppm) = 3.58 (s, 2H, CH_2), 7.26-7.34 (m, 2H, Ar H), 7.42 (“dt”, *J* = 7.6/7.6/1.5 Hz, 1H, Ar H), 7.64 (d, *J* = 8.4 Hz, 1H, Ar H), 7.79 (dd, *J* = 7.9/1.3 Hz, 1H, Ar H), 7.89 (dd, *J* = 8.5/1.6 Hz, 1H, Ar H), 8.40 (d, *J* = 1.2 Hz, 1H, Ar H), 10.18 (s, 1H, lactam-NH), 12.04 (s, 1H, indole-NH), 16.57 (br s, 1H, tetrazole-NH); ^{13}C-NMR ([D6]-DMSO, 100.6 MHz): δ (ppm) = 31.6 (CH_2), 112.4, 117.2, 120.9, 122.3, 123.7, 126.9, 128.5 (tert. C), 108.1, 122.2, 134.2, 135.6, 138.6, 171.3 (quat. C, lacking

three: not detected under application of 3072 scans); $C_{17}H_{12}N_6O$ (316.32); HRMS-FAB (m/z): $[M + H]^+$ calcd. 317.1151, $[M + H]^+$ found 317.1180.

Trimethyltin azide (**76**)

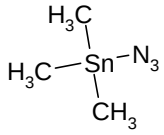

Sodium azide (39 mg, 6 mmol) was dissolved in water (2 ml) and stirred at 0 °C. Trimethyltin chloride (863 mg, 4.3 mmol) was added to the solution, and the stirring was continued for a total of 6 h, adding another portion of water (2 ml) after 2 h and maintaining the temperature at 0-10 °C. Filtering off the precipitate with suction afforded 616 mg (69%) of a white powder which was used without further purification. (Lit: Kricheldorf[89], Luijten[90])

IR (KBr): 2980 cm^{-1} (CH, aliphatic), 2900 cm^{-1} (CH, aliphatic), 2050 cm^{-1} (N_3); ^{1}H-NMR ([D6]-DMSO, 400 MHz): δ (ppm) = 0.35 (s, 9H, CH_3); ^{13}C-NMR ([D6]-DMSO, 100.6 MHz): δ (ppm) = 0.8 (CH_3).

8-[(Benzylamino)carbonyl]-11*H*-indolo[3,2-*c*]quinoline-6-carboxylic acid (**79a**)

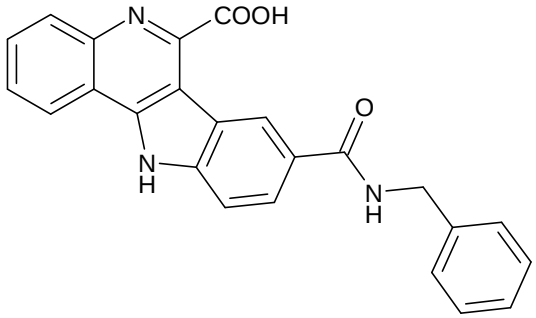

Prepared according to general procedure D with 190 mg (0.7 mmol) 6-oxo-5,6,7,12-tetrahydroindolo[3,2-*d*][1]benzazepine-9-carboxylic acid (**39**), 123 mg (0.9 mmol) HOBt, 174 mg (0.9 mmol) EDC, and 75 mg

(0.7 mmol) benzylamine. Stirred for 3 d under air atmosphere. Recrystallization from hexanol/ethyl acetate (1/1) and subsequently from ethanol afforded 56 mg (22%) of a yellow powder.

Mp: > 330 °C; IR (KBr): 3200 cm^{-1} (NH), 1660 cm^{-1} (C=O), 1640 cm^{-1} (C=O); ^{1}H-NMR ([D6]-DMSO, 400 MHz): δ (ppm) = 4.52 (d, *J* = 6.1 Hz, 2H, benzylamide-CH_2), 7.22-7.27 (m, 1H, Ar H), 7.32-7.43 (m, 5H, Ar H), 7.56-7.66 (m, 3H, Ar H), 7.93 (dd, *J* = 8.6/1.5 Hz, 1H, Ar H), 8.25 (d, *J* = 7.6 Hz, 1H, Ar H), 8.91 (d, *J* = 1.5 Hz, 1H, Ar H), 9.12 (t, *J* = 6.0 Hz, 1H, benzylamide-NH), 11.53 (s, 1H, indole-NH), 12.85 (“br s”, 1H, COOH); ^{13}C-NMR ([D6]-DMSO, 100.6 MHz): δ (ppm) = 43.1 (benzylamide-CH_2), 112.0, 121.8, 122.0, 124.1, 125.0, 127.0, 127.6, 127.7, 128.6, 131.5 (tert. C), 129.4, 135.9, 140.4, 161.8, 167.2 (quat. C, lacking six: not detected under application of 5120 scans); $C_{24}H_{17}N_3O_3$ (395.41); HRMS-FAB (m/z): $[M + H]^+$ calcd. 396.1348, $[M + H]^+$ found 396.1357.

8-{[(4-Methoxybenzyl)amino]carbonyl}-11*H*-indolo[3,2-*c*]quinoline-6-carboxylic acid (**79b**)

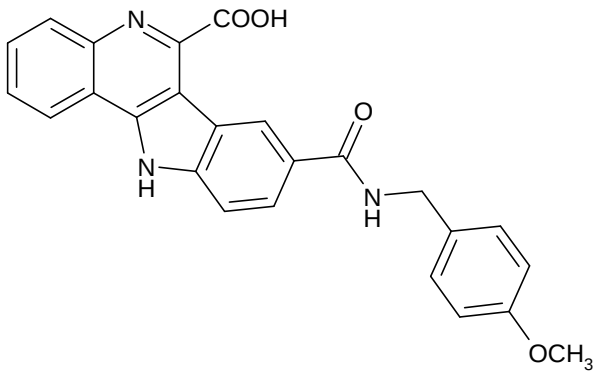

Prepared according to general procedure D with 190 mg (0.7 mmol) 6-oxo-5,6,7,12-tetrahydroindolo[3,2-*d*][1]benzazepine-9-carboxylic acid (**39**), 123 mg (0.9 mmol) HOBt, 174 mg (0.9 mmol) EDC, and 96 mg (0.7 mmol) (4-methoxybenzyl)amine. Stirred for 3 d under air atmosphere. Recrystallization from ethanol/toluene (2/1) and subsequently from ethanol afforded 34 mg (12%) of a yellow fluffy powder.

Mp: > 330 °C; IR (KBr): 3210 cm^{-1} (NH), 1650 cm^{-1} (C=O), 1640 cm^{-1} (C=O); ^{1}H-NMR ([D6]-DMSO, 400 MHz): δ (ppm) = 3.73 (s, 3H, OCH_3),

4.45 (d, *J* = 6.1 Hz, 2H, methoxybenzylamide-CH_2), 6.90 (d, *J* = 8.9 Hz, 2H, Ar H), 7.29 (d, *J* = 8.6 Hz, 2H, Ar H), 7.41 ("dt", *J* = 7.4/7.4/1.3 Hz, 1H, Ar H), 7.57-7.67 (m, 3H, Ar H), 7.92 (dd, *J* = 8.5/1.6 Hz, 1H, Ar H), 8.23 (d, *J* = 8.1 Hz, 1H, Ar H), 8.89 (d, *J* = 1.3 Hz, 1H, Ar H), 9.06 (t, *J* = 5.8 Hz, 1H, methoxybenzylamide-NH), 11.55 (s, 1H, indole-NH), 12.85 ("br s", 1H, COOH); ^{13}C-NMR ([D6]-DMSO, 100.6 MHz): δ (ppm) = 42.6 (methoxybenzylamide-CH_2), 55.4 (OCH_3), 111.8, 114.0, 121.9, 121.9, 124.2, 125.1, 127.5, 129.0, 131.5 (tert. C), 117.4, 126.8, 129.6, 132.4, 135.9, 139.1, 143.0, 158.5, 161.8, 167.1 (quat. C, lacking two: not detected under application of 1600 scans); $C_{25}H_{19}N_3O_4$ (425.45); calcd. C 70.58, H 4.50, N 9.88; found C 70.41, H 4.61, N 9.70; HRMS-FAB (m/z): $[M + H]^+$ calcd. 426.1454, $[M + H]^+$ found 426.1440.

8-Bromo-11*H*-indolo[3,2-*c*]quinoline-6-carboxylic acid (**79c**)

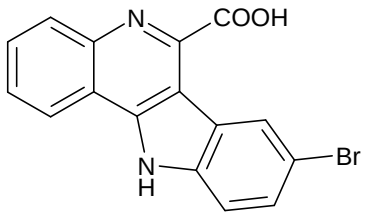

A solution of 230 mg (0.7 mmol) 9-bromo-7,12-dihydroindolo[3,2-*d*][1] benzazepin-6(5*H*)-one (**1**), 123 mg (0.9 mmol) HOBt, and 174 mg (0.9 mmol) EDC in DMF (10 ml) was stirred in an ice bath under nitrogen for 1 h. Subsequently, the reaction mixture was stirred at room temperature and under air atmosphere for 14 d. A precipitate was formed that was filtered off with suction and washed with water (50 ml). Drying in vacuo afforded 121 mg (50%) of a yellow powder.

Mp: > 330 °C; IR (KBr): 3210 cm^{-1} (NH), 1620 cm^{-1} (C=O); ^{1}H-NMR ([D6]-DMSO, 400 MHz): δ (ppm) = 7.40 ("dt", *J* = 7.5/7.4/1.4 Hz, 1H, Ar H), 7.53 and 7.54 and 7.59 and 7.63 (dd, *J* = 8.5/1.9 Hz, 1H, Ar H and d, *J* = 8.4 Hz, 1H, Ar H and "dt", *J* = 7.5/7.5/1.3 Hz, 1H, Ar H and dd, *J* = 8.3/1.4 Hz, 1H, Ar H, overlapping), 8.21 (dd, *J* = 8.0/0.9 Hz, 1H, Ar H), 8.48 (d, *J* = 1.3 Hz, 1H, Ar H), 11.55 (s, 1H, indole-NH), 12.85 ("br s", 1H, COOH); ^{13}C-NMR ([D6]-DMSO, 100.6 MHz): δ (ppm) = 113.8, 121.4, 123.7, 123.9,

127.0, 127.7, 131.2 (tert. C), 113.3, 115.0, 116.5, 128.6, 135.6, 135.8, 142.4, 160.9, 175.0 (quat. C); $C_{16}H_9BrN_2O_2$ (341.16); calcd. C 56.33, H 2.66, N 8.21; found C 56.29, H 2.73, N 8.36.

8-[(4-Methylpiperidin-1-yl)carbonyl]-11*H*-indolo[3,2-*c*]quinoline-6-carboxylic acid (**79d**)

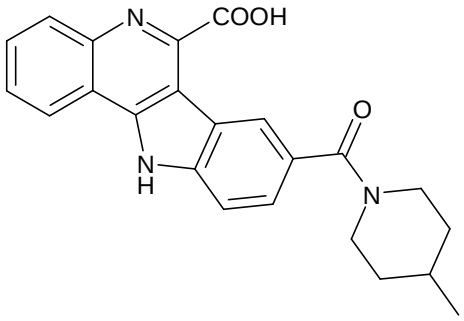

Prepared according to general procedure D with 200 mg (0.7 mmol) 6-oxo-5,6,7,12-tetrahydroindolo[3,2-*d*][1]benzazepine-9-carboxylic acid (**39**), 123 mg (0.9 mmol) HOBt, 174 mg (0.9 mmol) EDC, and 69 mg (0.7 mmol) 4-methylpiperidine. Stirred for 3 d under air atmosphere. Recrystallization from ethanol/toluene (2/1) and subsequently from ethanol afforded 96 mg (37%) of a yellow powder.

Mp: > 330 °C; IR (KBr): 3190 cm^{-1} (NH), 3070 cm^{-1} (CH, aromatic), 2920 cm^{-1} (CH, aliphatic), 1630 cm^{-1} (C=O); ^{1}H-NMR ([D6]-DMSO, 400 MHz): δ (ppm) = 0.95 (d, *J* = 6.1 Hz, 3H, CH_3), 1.04-1.20 (m, 2H, methylpiperidine-CH_2), 1.65 (“br s”, 3H, methylpiperidine-CH_2 and methylpiperidine-CH, overlapping), 2.93 (“br s”, 2H, methylpiperidine-CH_2), 3.58-4.64 (m, 2H, methylpiperidine-CH_2; very broad signal due to coalescence phenomenon), 7.37-7.45 (m, 2H, Ar H), 7.55-7.67 (m, 3H, Ar H), 8.24 (d, *J* = 8.1 Hz, 1H, Ar H), 8.36 (s, 1H, Ar H), 11.56 (s, 1H, indole-NH), 12.84 (“br s”, 1H, COOH); ^{13}C-NMR ([D6]-DMSO, 100.6 MHz): δ (ppm) = 21.5 (CH_3), ~35, ~35 (methylpiperidine-CH_2, only two detected and only by means of HMQC), 30.4 (methylpiperidine-CH), 111.7, 120.6, 121.4, 123.7, 124.3, 127.0, 131.1 (tert. C), 116.8, 126.3, 130.6, 135.6, 137.4, 142.4, 161.1, 175.1 (quat. C, lacking two: not detected under

application of 3072 scans); $C_{23}H_{21}N_3O_3$ (387.44); HRMS-FAB (m/z): $[M + H]^+$ calcd. 388.1661, $[M + H]^+$ found 388.1704.

7.3 Biological Data

7.3.1 CDK-Assays

The CDK-inhibitory activity exerted by the synthesized compounds was assayed by the group of Laurent Meijer (CNRS, Station Biologique, Roscoff, France). The activity of the kinases CDK1/cyclin B and CDK5/p25 was determined by measuring the CDK-catalyzed phosphorylation of histone H1, that is, the incorporation of radioactive labeled phosphate into the histone.

CDK1/cyclin B[6,146,147]

CDK1/cyclin B was purified from M phase oocytes of the starfish *Marthasterias glacialis* by affinity chromatography on $p9^{CKShs1}$-sepharose beads and subsequent elution with free $p9^{CKShs1}$. The CDK1 assay solution, holding a final volume of 30 µl, contained 0.5-1 µl purified enzyme, 5 µl histone H1 (5 mg/ml), 5 µl [γ-^{32}P]ATP (15 µM, 3000 Ci/mmol, 1 mCi/ml) and 3 µl of the inhibitor (0.1-1000 µM), all in reaction buffer C (60 mM β-glycerolphosphate, 15 mM *p*-nitrophenyl phosphate, 25 mM MOPS (pH 7.2), 5 mM EGTA, 15 mM magnesium chloride, 1 mM dithiothreitol, 1 mM sodium vanadate, 1 mM phenyl phosphate, 10 µg/ml leupeptin, 10 µg/ml aprotinin, 10 µg/ml soybean trypsin inhibitor, 100 µM benzamidine). For the determination of the maximum phosphate incorporation, buffer C was used instead of the inhibitor. Nonspecific binding was determined in the absence of histone H1 in the reaction mixture and subtracted from the values obtained with the assay solutions. The assays were started by the addition of radioactive ATP, and after a 10-min incubation at 30 °C, 25 µl aliquots of the supernatant were spotted onto pieces (2.5 x 3 cm) of Whatman P81 phosphocellulose paper. After 20 s, the filters were washed five times (for at least 5 min each time) in 0.1% phosphoric acid. The wet filters were transferred into 1 ml ACS scintillation cocktail (Amersham), and after mixing, ^{32}P radioactivity was measured by means of a Packard Tri-Carb counter. Controls were performed with appropriate dilutions of DMSO as the inhibitors had been dissolved in DMSO as 100 mM stock solutions. However, the final DMSO concentration never exceeded 1% in the

reaction mixture. The kinase activity is expressed as pmol of phosphate groups incorporated into histone H1 during a 10-min incubation or in percent of the maximum kinase activity. Dose-response curves were constructed for every compound tested and used for the calculation of the corresponding IC_{50}-values. All assays were carried out in triplicate.

CDK5/p25[5,147,148]

CDK5/p25 was reconstituted by mixing equal amounts of recombinant mammalian CDK5 and p25 expressed in *E. coli* as GST (glutathione-S-transferase) fusion proteins. Purification was performed by affinity chromatography on glutathione agarose. The kinase activity was assayed in buffer C as described for CDK1/cyclin B.

7.3.2 GSK-3b-Assay[5,147,148]

The GSK-inhibitory activity exerted by the synthesized compounds was assayed by the group of Laurent Meijer (CNRS, Station Biologique, Roscoff, France). The activity of the kinase GSK-3β was determined by measuring the GSK-catalyzed phosphorylation of glutathione synthase-1 (GS-1) peptide, that is, the incorporation of radioactive labeled phosphate into the peptide.

GSK-3β was expressed in and purified from insect Sf9 cells. Subsequent to a 1/100 dilution in 1 mg bovine serum albumin (BSA)/ml 10 mM dithiotreitol, the kinase activity was assayed in buffer A (10 mM $MgCl_2$, 1 mM EGTA, 1 mM dithiotreitol, 25 mM Tris-HCl (pH 7.5), 50 µg/ml heparin) with 5 µl of 40 µM GS-1 peptide as a substrate in the presence of 15 µM [γ-^{32}P]ATP (3000 Ci/mmol, 1 mCi/ml), constituting a final volume of 30 µl. After a 30-min incubation at 30 °C, 25 µl aliquots of the supernatant were spotted onto pieces (2.5 x 3 cm) of Whatman P81 phosphocellulose paper and further analyzed as described for CDK1/cyclin B.

7.3.3 NCI Human Tumor Cell Line Anti-Cancer Drug Screen

The in vitro antitumor activity exhibited by the compounds synthesized within the scope of this thesis was investigated by the National Cancer Institute, Bethesda, Maryland, USA by means of the NCI anti-cancer drug screen.[6,120]

In this procedure, the anti-proliferative activity is determined by testing the compounds against 60 different human tumor cell lines. The cancer cell lines comprise 9 tumor types, grouped as subpanels: leukemia, non-small cell lung cancer, colon cancer, CNS cancer, melanoma, ovarian cancer, renal cancer, prostate cancer, and breast cancer.

The tumor cell lines are inoculated into microtiter plates and incubated with five different inhibitor concentrations (10^{-4} to 10^{-8} M). After 48 hours of exposure, the medium is removed, and the cells are fixated and washed. Treatment with sulforhodamine B, a dye binding to basic amino residues in proteins, allows a photometric determination of the cell mass. By measuring the solubilized, dyed residue present in the cavities of the microtiter plates, the percentage of cell growth inhibition can be determined.

For each cell line, concentration-effect curves are constructed. The molar concentrations of the tested inhibitor causing 50% cell growth inhibition (GI_{50}), total cell growth inhibition (TGI), and 50% cell death (LC_{50}) are stated as the corresponding $\log_{10}$-values, respectively. For each of these parameters, a “meangraph midpoint” ($\log_{10}$ MG_MID) is calculated by averaging the log parameters of all 60 cell lines. Insensitive cell lines are included with the highest test concentration, therefore the MG_MID-value does not necessarily represent the actual mean value.

Furthermore, a bar graph is established for each tested compound, depicting the mean graphs of each response parameter (i.e., GI_{50}, TGI, and LC_{50}). The mean graphs facilitate the visual scanning of data for patterns of selectivity for particular cell lines or subpanels with respect to a selected response parameter. The three $\log_{10}$ MG_MID-values constitute the central axis of the mean graphs. Bars extending to the right represent sensitivity of the cell line to the tested inhibitor compound in excess of the average sensitivity of all tested cell lines, and bars extending to the left correspondingly imply sensitivity less than the mean.

The length of the bars corresponds to the relative sensitivity of the cell line compared to the $\log_{10}$ MG_MID-value. The bar scale is logarithmic, thus, if a compound achieved the response parameter for a cell line at a concentration one-tenth the mean concentration required over all cell lines, the bar would extend one unit to the right.

7.3.4 Trypanosoma-Assays

In vitro assays investigating the antiprotozoic activity of the synthesized paullone derivatives were performed by the Swiss Tropical Institute, Basel, Switzerland.[149,150]

Trypanosoma brucei rhodesiense

Minimum Essential Medium (50 µl) supplemented according to Baltz[149] with 2-mercaptoethanol and 15% heat-inactivated horse serum was added to each well of a 96-well microtiter plate. Serial drug dilutions were added to the wells. Then, 50 µl of trypanosome suspension (*T. b. rhodesiense* STIB 900) were added to each well, and the plate was incubated at 37 °C under a 5% CO_2 atmosphere for 72 hours. Alamar Blue (10 µl) was then added to each well, and incubation was continued for further 2-4 hours. The plate was then read with a Millipore Cytofluor 2300 using an excitation wavelength of 530 nm and emission wavelength of 590 nm, as stated by Räz[150]. Fluorescence development was expressed as percentage of the control, and IC_{50}-values were determined. Cytotoxicity was assessed using the same assay and rat skeletal myoblasts (L-6 cells).

Trypanosoma cruzi

Rat skeletal myoblasts (L-6 cells) were seeded in 96-well microtiter plates at 2000 cells/well/100µl in RPMI 1640 medium with 10% FBS and 2 mM L-glutamine. After 24 hours, 5000 trypomastigotes of *T. cruzi* (Tulahuen strain C2C4 containing the β-galactosidase (Lac Z) gene) were added in 100 µl per well with 2x of a serial drug dilution. The plates were incubated

at 37°C in 5% CO_2 for 4 days. After 96 hours, the minimum inhibitory concentration (MIC) was determined microscopically. For measurement of the IC_{50}, the substrate CPRG/Nonidet was added to the wells. The color reaction which developed during the following 2-4 hours was read photometrically at 540 nm. From the sigmoidal inhibition curve, IC_{50}-values were calculated.

7.4 QSAR

7.4.1 Computer Program

For the performance of the multiple linear regression analyses, the computer program MULREG was employed, kindly provided by Dr. K.-J. Schaper, Forschungszentrum Borstel, 23845 Borstel, Germany.

7.4.2 Selection of Compounds

The following table (table 7-1) gives an overview of the paullone derivatives that were incorporated into the calculations dealing with the correlation of substituent properties and enzyme inhibition.

Table 7-1: Compounds employed in the QSAR analyses dealing with substituent properties and enzyme inhibition

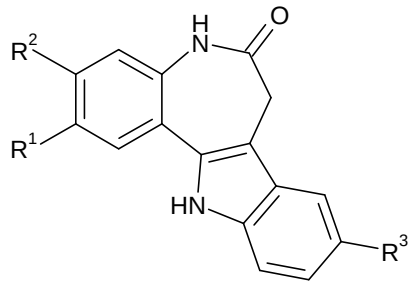

#	R^1	R^2	R^3	thesis ID
1	H	H	H	
2	H	H	Br	**1**
3	H	H	Cl	
4	H	H	OCH_3	
5	H	H	CH_3	
6	H	H	F	

Table 7-1: Compounds employed in the QSAR analyses dealing with substituent properties and enzyme inhibition (continuation)

#	R^1	R^2	R^3	thesis ID
7	H	H	CF_3	
8	H	H	CN	**74**
9	H	H	NO_2	**2**
10	H	H	NH_2	
11	H	H	$NHCOCH_3$	
12	H	H	SO_2NH_2	**38**
13	H	H	SCH_3	**35a**
14	H	H	$SOCH_3$	**36a**
15	OCH_3	OCH_3	Br	
16	OCH_3	OCH_3	H	
17	OCH_3	OCH_3	CF_3	
18	OCH_3	OCH_3	CN	
19	OCH_3	OCH_3	NO_2	
20	OCH_3	H	Br	
21	H	OCH_3	Br	
22	OCH_3	H	CF_3	
23	H	OCH_3	CF_3	
24	OCH_3	H	SO_2NH_2	**35c**
25	OCH_3	H	SCH_3	**35b**
26	OCH_3	H	$SOCH_3$	**36b**
27	H	OCH_3	CN	
28	H	OCH_3	NO_2	
29	OCH_3	H	NO_2	
30	H	H	$COOC_2H_5$	**40a**

Table 7-1: Compounds employed in the QSAR analyses dealing with substituent properties and enzyme inhibition (continuation)

#	R^1	R^2	R^3	thesis ID
31	H	H	$COOC_6H_{13}$	**40g**
32	H	H	$COOC_4H_9$	**40d**
33	H	H	$COOC_3H_7$	**40c**
34	H	H	$CON(C_3H_7)CONH(C_3H_7)$	**54**
35	OCH_3	H	SO_2CH_3	**37b**
36	H	H	$COOC_5H_{11}$	**40e**
37	H	H	$CH(CH_3)(C_3H_7)$	**40f**
38	H	H	$COOCH_3$	**40b**
39	H	H	COOH	**39**
40	H	H	$CONHC_{18}H_{37}$	**55c**
41	H	H	$COOC_8H_{17}$	**40h**

The column “thesis ID” lists the numbers that were assigned to the particular compounds within the scope of this thesis.

The order of appearance of the compounds within this table corresponds to the chronology of the obtainment of the biological test results.

7.4.3 Literature Parameters

Numerous regression equations were established under employment of the substituent parameters stated in literature (cf. chapter 7.4.5, regression equations 1-79, 137-147, 164-261, and 301-307). The values for the utilized substituent constants are listed in table 7-2, originating from publications by Hansch[140,151] and Seydel[152].

Table 7-2: Literature parameters employed in the paullone QSAR study

substituents	π	σ_m	σ_p	F	R	MR	E_s[a]	L	B_1	B_4	dist
H	0.00	0.00	0.00	0.00	0.00	1.03	0.00	2.06	1.00	1.00	0.00
Br	0.86	0.39	0.23	0.44	-0.17	8.88	-1.16	3.83	1.95	1.95	2.70
Cl	0.71	0.37	0.23	0.41	-0.15	6.03	-0.97	3.52	1.80	1.80	2.43
OCH_3	-0.02	0.12	-0.27	0.26	-0.51	7.87	-0.55	3.98	1.35	2.87	3.64
CH_3	0.56	-0.07	-0.17	-0.04	-0.13	5.65	-1.24	3.00	1.52	2.04	0.99
F	0.14	0.34	0.06	0.43	-0.34	0.92	-0.46	2.65	1.35	1.35	2.88
CF_3	0.88	0.43	0.54	0.38	0.19	5.02	-2.40	3.30	1.98	2.61	2.21
CN	-0.57	0.56	0.66	0.51	0.19	6.33	-0.51	4.23	1.60	1.60	3.53
NO_2	-0.28	0.71	0.78	0.67	0.16	7.36	-1.01	3.44	1.70	2.44	3.47
NH_2	1.23	-0.16	-0.66	0.02	-0.68	5.42	-0.61	2.93	1.50	1.84	4.60
$NHCOCH_3$	-0.97	0.21	0.00	0.28	-0.26	14.93	-1.82	5.15	1.50	3.61	4.06
SO_2NH_2	-1.82	0.46	0.57	0.41	0.19	12.28	-2.62	3.82	2.11	3.07	4.40
SCH_3	0.61	0.15	0.00	0.20	-0.18	13.82	-1.07	4.30	1.70	3.26	2.00

Table 7-2: Literature parameters employed in the paullone QSAR study (continuation)

substituents	π	σ_m	σ_p	F	R	MR	E_s [a]	L	B_1	B_4	dist
$SOCH_3$	-1.58	0.52	0.49	0.52	0.01	13.70	n/a	4.03	1.60	3.36	2.04
$COOC_2H_5$	0.51	0.37	0.45	0.33	0.15	17.47	n/a	5.96	1.52	4.28	3.27
$COOC_6H_{13}$	n/a	n/a	n/a	n/a	n/a	n/a	n/a	n/a	n/a	n/a	n/a
$COOC_4H_9$	n/a	n/a	n/a	n/a	n/a	n/a	n/a	n/a	n/a	n/a	n/a
$COOC_3H_7$	1.07	n/a	n/a	0.34	0.11	22.20	n/a	6.90	1.90	4.83	3.58
$CON(C_3H_7)CONH(C_3H_7)$	n/a	n/a	n/a	n/a	n/a	n/a	n/a	n/a	n/a	n/a	n/a
SO_2CH_3	-1.63	0.60	0.72	0.54	0.22	13.49	n/a	4.37	2.11	3.15	3.96
$COOC_5H_{11}$	n/a	n/a	n/a	n/a	n/a	n/a	n/a	n/a	n/a	n/a	n/a
$CH(CH_3)(C_3H_7)$	n/a	n/a	n/a	n/a	n/a	n/a	n/a	n/a	n/a	n/a	n/a
$COOCH_3$	-0.01	0.37	0.45	0.33	0.15	12.87	n/a	4.85	1.90	3.36	3.05
COOH	-0.32	0.37	0.45	0.33	0.15	6.93	n/a	3.91	1.60	2.66	3.67
$CONHC_{18}H_{37}$	n/a	n/a	n/a	n/a	n/a	n/a	n/a	n/a	n/a	n/a	n/a
$COOC_8H_{17}$	n/a	n/a	n/a	n/a	n/a	n/a	n/a	n/a	n/a	n/a	n/a

[a] All values refer to E_S (H) = 0.00, that is, E_S (CH_3) = -1.24.

"N/a" stands for "not applicable": The parameter values corresponding to the particular substituents were not available in literature.

7.4.4 Calculated Parameters

The ACDLabs computer program “ChemSketch” provided the values for the parameters MR, MV, σ_p, and σ_m.

The values for the substituent constant “dist” [Å] were obtained through individual 3D-optimization of the particular derivative structures and subsequent determination of the distance between the C9-carbon of the paullone basic ring structure and the most remote atom of the substituent. The ACDLabs computer program “3D Viewer” was utilized.

The π-value of a substituent was acquired manually by subtracting the log P-value of the unsubstituted paullone from the log P-value of the paullone derivative equipped with the particular substituent. Prior to that, the log P-values had been determined by means of the ACDLabs computer program "log P dB".

The calculated parameters were compared to the literature parameters by evaluating the intercorrelation matrices resulting from the correlation calculations performed for this purpose. The results, depicted in table 7-3, were satisfactory, thus “validating” the calculated parameters which are listed in table 7-4. The calculated parameters were used in regression equations 80-136, 148-163, and 262-300 (cf. chapter 7.4.5).

Table 7-3: Intercorrelation between literature and calculated parameters

literature parameter	calculated parameter	intercorrelation (r-value)
π	π	0.844
σ_m	σ_m	1.000
σ_p	σ_p	0.999
MR	MR	0.972
L	dist	0.789
dist	dist	0.648

It is worth pointing out that the definition for the literature parameter “dist” is not similar to the one of the calculated parameter - the low intercorrelation is thus explicable.

Table 7-4: Calculated parameters employed in the paullone QSAR study

substituents	dist	MR	MV	σ_p	σ_m	π	log P
H	1.10	n/a	n/a	0.00	0.00	0.00	3.16
Br	1.88	8.76	27.46	0.23	0.39	0.86	4.02
Cl	1.72	5.87	25.67	0.23	0.37	0.78	3.94
OCH_3	3.35	7.40	37.15	-0.27	0.12	-0.09	3.07
CH_3	2.16	5.66	30.79	-0.17	-0.07	0.46	3.62
F	1.33	1.19	19.73	0.06	0.34	0.14	3.30
CF_3	2.35	6.11	47.18	0.51	0.43	0.57	3.73
CN	2.58	5.57	24.17	0.66	0.56	0.21	3.37
NO_2	2.42	7.05	27.06	0.78	0.71	0.39	3.55
NH_2	2.23	4.56	17.96	-0.66	-0.16	-1.44	1.72
$NHCOCH_3$	4.23	13.91	53.23	-0.07	0.21	-1.40	1.76
SO_2NH_2	3.64	13.46	38.99	0.60	0.53	-1.89	1.27
SCH_3	3.83	13.65	44.76	-0.08	0.15	0.48	3.64

Table 7-4: Calculated parameters employed in the paullone QSAR study (continuation)

substituents	dist	MR	MV	σ_p	σ_m	π	log P
$SOCH_3$	3.86	14.52	40.29	0.49	0.52	-1.67	1.49
$COOC_2H_5$	5.71	16.70	67.28	0.41	0.37	0.97	4.13
$COOC_6H_{13}$	10.93	35.23	133.31	0.44	0.35	3.09	6.25
$COOC_4H_9$	8.32	25.96	100.30	0.44	0.36	2.03	5.19
$COOC_3H_7$	6.97	21.33	83.79	0.44	0.36	1.50	4.66
$CON(C_3H_7)CONH(C_3H_7)$	8.24	45.38	157.40	n/a	n/a	-0.04	3.12
SO_2CH_3	3.89	14.46	51.82	0.70	0.60	-1.71	1.45
$COOC_5H_{11}$	9.50	30.60	116.80	0.44	0.35	2.56	5.72
$CH(CH_3)(C_3H_7)$	8.22	30.56	117.18	0.46	0.37	2.38	5.54
$COOCH_3$	4.45	12.07	50.78	0.43	0.37	0.44	3.60
COOH	3.32	7.22	25.41	0.41	0.37	-0.33	2.83
$CONHC_{18}H_{37}$	26.32	92.67	333.84	0.34	0.26	7.67	10.83
$COOC_8H_{17}$	13.55	44.50	166.32	0.44	0.36	4.16	7.32

7.4.5 Regression Equations and Statistical Data

The correlation calculations led to regression equations of the following type:

$$Y = I(\pm ci_I) + sl_1(\pm ci_1)\, X_1 + sl_2(\pm ci_2)\, X_2 + sl_3(\pm ci_3)\, X_3 + sl_4(\pm ci_4)\, X_4$$

where Y is the dependent variable,

$X_{1\text{-}4}$ are the explanatory variables,

I is the ordinate intercept,

$sl_{1\text{-}4}$ are the slopes corresponding to the explanatory variables,

ci_I is the confidence interval corresponding to the intercept,

$ci_{1\text{-}4}$ are the confidence intervals corresponding to the explanatory variables $X_{1\text{-}4}$.

The employed variables and the values corresponding to the particular intercept, slopes, and confidence intervals are presented in table 7-5a.

The statistical quantities corresponding to the regression equations in table 7-5a are shown in table 7-5b. The definitions for n, r, s, t, F, and q^2 have been discussed in chapter 4.2.2. The values for $t_{1\text{-}4}$ correspond to the explanatory variables $X_{1\text{-}4}$, the value for t_I corresponds to the ordinate intercept.

Identification codes have been used in table 7-5a for enzymes and cancer cell lines:

CDK1 ≡ CDK1/cyclin B
CDK5 ≡ CDK5/p25
GSK3 ≡ GSK-3β
HCT ≡ HCT-116 (colon cancer cell line)
SR ≡ SR (leukemia cell line)
RXF ≡ RXF 393 (renal cancer cell line)
LOX ≡ LOX IMVI (melanoma cell line)

Table 7-5a: Regression equations, parameters with corresponding slopes and confidence intervals

#	Y [pIC_{50}]	X_1	sl_1	ci_1 [95%]	X_2	sl_2	ci_2 [95%]	X_3	sl_3	ci_3 [95%]	X_4	sl_4	ci_4 [95%]	I	ci_I [95%]
1	CDK1	π	0.15	±0.30	σ_p	1.59	±0.64	MR	0.04	±0.06				5.63	±0.53
2	CDK1	σ_p	1.59	±0.64	MR	0.03	±0.06							5.70	±0.51
3	CDK1	σ_p	1.62	±0.66	MR^2	0.00	±0.00							5.84	±0.38
4	CDK1	MR	0.25	±0.43	MR^2	-0.01	±0.03							5.09	±1.57
5	CDK1	σ_p	1.51	±0.59	MR	0.19	±0.20	MR^2	-0.01	±0.01				5.22	±0.73
6	CDK1	π	-0.10	±0.42	π^2	-0.22	±0.39	σ_p	1.73	±0.66				6.05	±0.36
7	CDK1	π^2	-0.30	±0.24	σ_p	1.67	±0.52	MR	0.06	±0.05				5.66	±0.41
8	CDK1	π^2	-0.15	±0.49	σ_p	1.65	±0.98	E_s	-0.00	±0.63				6.01	±0.58
9	CDK1	π	0.17	±0.28	σ_m	2.60	±0.95	MR	0.03	±0.06				5.21	±0.52
10	CDK1	π^2	-0.26	±0.25	σ_m	2.65	±0.83	MR	0.05	±0.06				5.25	±0.44
11	CDK1	π^2	-0.22	±0.33	F	2.93	±1.33	MR	0.05	±0.07				5.08	±0.63
12	CDK1	π^2	-0.31	±0.40	R	2.07	±1.25	MR	0.08	±0.09				6.09	±0.69

Table 7-5b: Statistical quantities corresponding to the regression equations in table 7-5a

#	n	r	s	t_1	t_2	t_3	t_4	t_l	F	q^2
1	14	0.885	0.411	1.12	5.55	1.42		23.84	12.02	0.607
2	14	0.869	0.415	5.48	1.05			24.77	17.02	0.602
3	14	0.859	0.430	5.43	0.55			33.60	15.53	0.587
4	14	0.360	0.819	1.28	1.23			7.12	0.82	-0.304
5	14	0.906	0.373	5.75	2.14	1.90		15.99	15.26	0.638
6	14	0.880	0.418	0.54	1.27	5.87		37.20	11.50	0.639
7	14	0.928	0.329	2.75	7.22	2.58		30.95	20.64	0.716
8	12	0.835	0.470	0.72	3.86	0.001		23.93	6.12	0.231
9	14	0.901	0.382	1.31	6.10	1.29		22.24	14.45	0.670
10	14	0.927	0.331	2.35	7.15	2.05		26.55	20.24	0.731
11	14	0.864	0.443	1.51	4.92	1.40		17.92	9.85	0.491
12	14	0.797	0.532	1.73	3.70	1.99		19.79	5.81	0.332

Table 7-5a: Regression equations, parameters with corresponding slopes and confidence intervals (continuation)

#	Y [pIC_{50}]	X_1	sl_1	ci_1 [95%]	X_2	sl_2	ci_2 [95%]	X_3	sl_3	ci_3 [95%]	X_4	sl_4	ci_4 [95%]	I	ci_I [95%]
13	CDK1	F	2.33	±1.30	R	1.06	±1.03							5.57	±0.54
14	CDK1	π^2	-0.15	±0.24	F	2.39	±1.27	R	1.14	±1.01				5.69	±0.56
15	CDK1	F	2.22	±1.37	R	1.07	±1.06	MR	0.02	±0.06				5.44	±0.65
16	CDK1	π^2	-0.28	±0.24	F	2.14	±1.10	R	1.25	±0.86	MR	0.06	±0.05	5.45	±0.52
17	CDK1	σ_m	1.84	±2.65	σ_p	0.56	±1.67							5.57	±0.55
18	CDK1	π^2	-0.28	±0.24	σ_p	1.25	±0.86	F	0.99	±1.65	MR	0.06	±0.05	5.45	±0.53
19	CDK1	π	-0.09	±0.34	π^2	-0.36	±0.35	σ_p	1.68	±0.54	MR	0.06	±0.06	5.69	±0.45
20	CDK1	π^2	-0.26	±0.28	σ_p	1.70	±0.59	MR^2	0.00	±0.00				5.90	±0.35
21	CDK1	π^2	-0.39	±0.51	σ_p^2	2.24	±2.09	MR	0.10	±0.11				5.33	±0.90
22	CDK1	π^2	-0.20	±0.57	MR	0.08	±0.13							5.77	±0.95
23	CDK1	π^2	-0.30	±0.19	σ_p	1.60	±0.42	MR	0.22	±0.14	MR^2	-0.01	±0.01	5.19	±0.51
24	CDK1	π^2	-0.22	±0.33	F	2.93	±1.33	MR	0.05	±0.07				5.08	±0.63

Table 7-5b: Statistical quantities corresponding to the regression equations in table 7-5a (continuation)

#	n	r	s	t_1	t_2	t_3	t_4	t_l	F	q^2
13	14	0.883	0.394	3.94	2.27			22.60	19.46	0.622
14	14	0.903	0.379	1.39	4.19			22.68	14.71	0.635
15	14	0.891	0.399	3.62	2.26	0.85		18.52	12.90	0.589
16	14	0.941	0.315	2.67	4.43	3.29	2.34	23.55	17.36	0.711
17	14	0.882	0.396	1.53	0.73			22.23	19.30	0.620
18	14	0.941	0.316	2.67	3.27	1.36	2.35	23.47	17.24	0.710
19	14	0.931	0.340	0.59	2.37	7.00	2.47	28.87	14.55	0.666
20	14	0.903	0.379	2.03	6.40	1.58		37.81	14.67	0.651
21	14	0.670	0.654	1.67	2.39	2.00		13.16	2.72	-0.095
22	14	0.369	0.781	0.77	1.31			13.31	0.87	-0.345
23	14	0.960	0.259	3.42	8.66	3.52	2.66	22.88	26.64	0.811
24	14	0.864	0.443	1.51	4.92	1.40		17.92	9.85	0.491

Table 7-5a: Regression equations, parameters with corresponding slopes and confidence intervals (continuation)

#	Y [pIC_{50}]	X_1	sl_1	ci_1 [95%]	X_2	sl_2	ci_2 [95%]	X_3	sl_3	ci_3 [95%]	X_4	sl_4	ci_4 [95%]	I	ci_I [95%]
25	CDK1	π	0.13	±0.44	R	1.90	±1.37	MR	0.05	±0.09				6.04	±0.79
26	CDK1	π	0.16	±0.29	F	2.26	±1.36	R	1.05	±1.05	MR	0.03	±0.06	5.36	±0.67
27	CDK1	F	2.29	±1.39	R	1.06	±1.08	MR^2	0.00	±0.00				5.54	±0.61
28	CDK1	F	2.45	±1.46	R	1.19	±1.20	E_s	0.12	±0.39				5.71	±0.75
29	CDK1	π^2	-0.21	±0.54	F	2.99	±1.58	E_s^2	0.06	±0.22				5.29	±0.61
30	CDK1	π^2	-0.19	±0.35	σ_p	1.82	±0.63	MR	0.08	±0.06	E_s	0.25	±0.49	5.73	±0.47
31	CDK1	π^2	-0.10	±0.65	σ_p	1.89	±0.60	MR	0.07	±0.06	E_s^2	-0.12	±0.17	5.65	±0.41
32	CDK1	π^2	-0.19	±0.42	σ_m	2.74	±1.02	MR	0.05	±0.06	E_s^2	-0.03	±0.18	5.22	±0.52
33	CDK1	π^2	-0.26	±0.22	σ_m	2.52	±0.75	MR	0.19	±0.16	MR^2	-0.01	±0.01	4.87	±0.58
34	CDK1	π	0.46	±0.54	σ_p^2	2.62	±2.18	MR	0.09	±0.10				5.10	±0.96
35	CDK1	F	2.38	±1.38	R	1.36	±1.19	E_s^2	-0.07	±0.13				5.75	±0.65
36	CDK1	π^2	-0.37	±0.23	σ_p	1.47	±0.52	σ_p^2	0.90	±1.06	MR	0.07	±0.05	5.50	±0.41

Table 7-5b: Statistical quantities corresponding to the regression equations in table 7-5a (continuation)

#	n	r	s	t_1	t_2	t_3	t_4	t_I	F	q^2
25	14	0.740	0.593	0.68	3.09	1.31		17.01	4.03	0.181
26	14	0.908	0.390	1.23	3.77	2.26		18.16	10.55	0.631
27	14	0.885	0.410	3.68	2.18	0.41		20.39	12.05	0.563
28	13	0.892	0.416	3.80	2.25	0.68		17.10	11.68	0.362
29	13	0.840	0.499	0.89	4.28	0.63		19.60	7.21	0.360
30	13	0.938	0.340	1.23	6.69	2.74		27.89	14.52	0.693
31	13	0.946	0.315	0.65	7.32	2.92	1.68	31.51	17.17	0.729
32	13	0.928	0.363	1.06	6.19	1.95	0.37	23.18	12.45	0.666
33	14	0.950	0.291	2.64	7.59	2.60	1.99	19.07	20.68	0.788
34	14	0.695	0.633	1.91	2.67	2.04		11.83	3.12	0.009
35	13	0.904	0.395	3.91	2.58	1.24		19.98	13.33	0.535
36	14	0.949	0.292	3.55	6.42	1.93	3.29	30.12	20.59	0.703

Table 7-5a: Regression equations, parameters with corresponding slopes and confidence intervals (continuation)

#	Y [pIC_{50}]	X_1	sl_1	ci_1 [95%]	X_2	sl_2	ci_2 [95%]	X_3	sl_3	ci_3 [95%]	X_4	sl_4	ci_4 [95%]	I	ci_I [95%]
37	CDK1	π^2	-0.28	±0.24	σ_m	1.34	±2.21	σ_p	0.88	±1.39	MR	0.06	±0.05	5.45	±0.53
38	CDK1	π^2	-0.24	±0.52	σ_p	1.53	±0.97	σ_p^2	0.61	±1.74	E_s	-0.06	±0.64	5.92	±0.63
39	CDK1	π^2	-0.21	±0.19	σ_p	1.59	±0.47	L	0.36	±0.24				4.79	±0.86
40	CDK1	π	0.14	±0.24	σ_p	1.52	±0.54	L	0.34	±0.29				4.73	±1.03
41	CDK1	π^2	-0.20	±0.21	σ_p	1.63	±0.51	L^2	0.04	±0.04				5.48	±0.52
42	CDK1	π^2	-0.24	±0.22	σ_p	1.52	±0.55	L	0.34	±0.27	B_1	0.23	±0.91	4.52	±1.41
43	CDK1	π^2	-0.20	±0.28	σ_p	1.58	±0.51	MR	-0.01	±0.12	L	0.40	±0.58	4.72	±1.43
44	CDK1	σ_p	1.49	±0.52	MR	-0.06	±0.09	L	0.62	±0.52				4.20	±1.33
45	CDK1	π^2	-0.10	±0.31	σ_p	1.70	±0.54	E_s	0.23	±0.42	L	0.41	±0.27	4.77	±0.91
46	CDK1	σ_p	1.80	±0.46	E_s^2	-0.12	±0.09	L	0.38	±0.22				4.76	±0.78
47	CDK1	π^2	-0.03	±0.32	σ_p	1.78	±0.52	E_s^2	-0.11	±0.14	L	0.38	±0.24	4.76	±0.84
48	CDK1	π^2	-0.25	±0.13	σ_p	1.45	±0.33	L	2.24	±1.20	L^2	-0.26	±0.16	1.60	±2.11

Table 7-5b: Statistical quantities corresponding to the regression equations in table 7-5a (continuation)

#	n	r	s	t_1	t_2	t_3	t_4	t_l	F	q^2
37	14	0.941	0.315	2.68	1.37	1.44		23.29	17.32	0.710
38	13	0.885	0.455	1.05	3.63	0.81	0.23	21.76	7.23	0.175
39	14	0.943	0.293	2.51	7.60	3.31		12.45	26.90	0.712
40	14	0.920	0.345	1.31	6.22	2.65		10.23	18.38	0.668
41	14	0.930	0.325	2.13	7.07	2.65		21.21	21.21	0.605
42	14	0.945	0.303	2.43	6.23	2.94	0.57	7.23	18.90	0.637
43	14	0.943	0.308	1.65	7.05	0.15	1.54	7.45	18.21	0.652
44	14	0.926	0.334	6.33	1.60	2.66		7.05	19.93	0.666
45	13	0.952	0.298	0.77	7.23	1.23	3.49	12.13	19.53	0.707
46	13	0.960	0.260	8.89	3.26	3.92		13.88	34.69	0.801
47	13	0.960	0.275	0.25	7.88	1.82	3.72	13.14	23.32	0.753
48	14	0.977	0.199	4.28	9.82	4.21	3.57	1.72	47.01	0.851

Table 7-5a: Regression equations, parameters with corresponding slopes and confidence intervals (continuation)

#	Y [pIC_{50}]	X_1	sl_1	ci_1 [95%]	X_2	sl_2	ci_2 [95%]	X_3	sl_3	ci_3 [95%]	X_4	sl_4	ci_4 [95%]	I	ci_I [95%]
49	CDK1	π^2	-0.19	±0.23	σ_p	1.57	±0.50	L	0.42	±0.40	B_4	-0.08	±0.42	4.75	±0.93
50	CDK1	π^2	-0.29	±0.29	σ_p	1.57	±0.69	B_1	0.39	±1.11	B_4	0.23	±0.34	4.98	±1.66
51	CDK1	σ_p	1.51	±0.55	L	0.30	±0.29							4.84	±1.03
52	CDK1	F	1.90	±1.30	R	1.18	±0.95	L	0.26	±0.31				4.81	±1.05
53	CDK5	π^2	-0.28	±0.28	σ_p	1.82	±0.59	MR	0.02	±0.06				5.63	±0.47
54	CDK5	π^2	-0.28	±0.26	σ_p	1.76	±0.54	MR	0.17	±0.19	MR^2	-0.01	±0.01	5.21	±0.67
55	CDK5	π^2	-0.26	±0.23	σ_p	1.78	±0.57	L	0.18	±0.30				5.15	±1.05
56	CDK5	π	0.11	±0.33	σ_p	1.74	±0.70	MR	0.00	±0.07				5.62	±0.58
57	CDK5	π^2	-0.25	±0.22	F	2.80	±1.02	R	1.04	±0.80	MR	0.01	±0.05	5.25	±0.49
58	CDK5	π^2	-0.22	±0.18	F	2.85	±0.95	R	1.01	±0.75				5.30	±0.42
59	CDK5	π^2	-0.18	±0.31	F	2.82	±1.06	R	1.14	±0.88	E_s	0.14	±0.40	5.43	±0.55
60	CDK5	π^2	-0.23	±0.19	F	2.73	±1.08	R	1.06	±0.80	L	0.08	±0.26	5.07	±0.87

Table 7-5b: Statistical quantities corresponding to the regression equations in table 7-5a (continuation)

#	n	r	s	t_1	t_2	t_3	t_4	t_l	F	q^2
49	14	0.944	0.305	1.90	7.17	2.37	0.45	11.57	18.62	0.655
50	14	0.914	0.376	2.23	5.17	0.79	1.56	6.79	11.47	0.573
51	14	0.906	0.356	6.00	2.33			10.35	25.08	0.653
52	14	0.914	0.357	3.26	2.76	1.86		10.21	17.02	0.649
53	14	0.912	0.377	2.25	6.87	0.87		26.86	16.56	0.605
54	14	0.938	0.337	2.47	7.31	2.07	1.86	17.62	16.36	0.640
55	14	0.921	0.359	2.46	6.93	1.36		10.92	18.59	0.570
56	14	0.872	0.450	0.75	5.56	0.02		21.71	10.61	0.533
57	14	0.953	0.294	2.51	6.20	2.92	0.52	24.28	22.31	0.759
58	14	0.952	0.283	2.75	6.71	3.00		28.27	31.98	0.812
59	13	0.956	0.297	1.32	6.12	2.98	0.80	22.60	21.30	0.647
60	14	0.954	0.291	2.75	5.73	2.98	0.67	13.20	22.78	0.727

Table 7-5a: Regression equations, parameters with corresponding slopes and confidence intervals (continuation)

#	Y [pIC_{50}]	X_1	sl_1	ci_1 [95%]	X_2	sl_2	ci_2 [95%]	X_3	sl_3	ci_3 [95%]	X_4	sl_4	ci_4 [95%]	I	ci_I [95%]
61	CDK5	π^2	-0.23	±0.22	F	2.84	±1.03	R	1.02	±0.81	B_4	0.02	±0.27	5.26	±0.65
62	CDK5	σ_p	1.66	±0.64	L	0.39	±0.51	B_4	-0.34	±0.49				5.03	±1.22
63	CDK5	π^2	-0.23	±0.23	σ_p	1.84	±0.58							5.77	±0.29
64	CDK5	π^2	-0.19	±0.23	F	3.46	±1.08							4.95	±0.43
65	CDK5	π^2	-0.25	±0.22	F	2.80	±1.02	R	1.04	±0.80	MR	0.01	±0.05	5.25	±0.49
66	GSK3	π^2	-0.47	±0.40	σ_p	2.01	±0.84	MR	0.27	±0.29	MR^2	-0.02	±0.02	6.32	±1.04
67	GSK3	π^2	-0.42	±0.45	σ_p	2.14	±0.94	MR^2	0.01	±0.01				7.16	±0.55
68	GSK3	π^2	-0.41	±0.47	F	2.30	±2.15	R	1.91	±1.71	MR^2	-0.01	±0.01	7.03	±0.96
69	GSK3	σ_p	2.00	±1.06	MR^2	-0.01	±0.01							7.06	±0.62
70	CDK1	π^2	-0.30	±0.19	σ_p	1.67	±0.43	MR	0.08	±0.04				5.48	±0.34
71	CDK1	π^2	-0.23	±0.19	σ_m	2.63	±0.67	MR	0.06	±0.04				5.17	±0.37
72	CDK1	π^2	-0.24	±0.25	σ_p	1.75	±0.56	dist	0.16	±0.18				5.62	±0.53

Table 7-5b: Statistical quantities corresponding to the regression equations in table 7-5a (continuation)

#	n	r	s	t_1	t_2	t_3	t_4	t_l	F	q^2
61	14	0.952	0.298	2.38	6.21	2.85	0.18	18.42	21.67	0.752
62	14	0.896	0.408	5.76	1.67	1.56		9.18	13.65	0.570
63	14	0.905	0.373	2.14	7.04			43.16	25.04	0.678
64	14	0.906	0.371	1.80	7.06			25.46	25.23	0.734
65	14	0.953	0.294	2.51	6.20	2.92	0.53	24.28	22.31	0.759
66	14	0.940	0.523	2.71	5.41	2.08	3.13	13.80	17.10	0.718
67	14	0.910	0.603	2.12	5.05	3.31		28.85	16.05	0.694
68	14	0.913	0.627	1.99	2.42	2.53	3.22	16.65	11.20	0.589
69	14	0.866	0.692	4.16	4.47			25.22	16.57	0.596
70	25	0.889	0.355	3.22	8.15	3.84		33.63	26.29	0.700
71	25	0.890	0.353	2.51	8.22	2.72		29.37	26.73	0.718
72	14	0.913	0.359	2.13	6.92	1.98		23.63	16.70	0.648

Table 7-5a: Regression equations, parameters with corresponding slopes and confidence intervals (continuation)

#	Y [pIC_{50}]	X_1	sl_1	ci_1 [95%]	X_2	sl_2	ci_2 [95%]	X_3	sl_3	ci_3 [95%]	X_4	sl_4	ci_4 [95%]	I	ci_I [95%]
73	CDK1	π^2	-0.24	±0.20	σ_p	1.59	±0.47	dist	0.22	±0.16				5.49	±0.41
74	CDK1	π^2	-0.15	±0.27	σ_m	2.74	±0.99	dist	0.02	±0.21				5.47	±0.59
75	CDK1	π^2	-0.14	±0.21	σ_m	2.60	±0.81	dist	0.07	±0.17				5.36	±0.43
76	CDK1	π	0.07	±0.29	σ_p	1.65	±0.65							5.92	±0.28
77	CDK1	π	-0.03	±0.22	σ_p	1.58	±0.55							5.88	±0.24
78	CDK1	π	0.10	±0.26	σ_m	2.70	±0.95							5.44	±0.36
79	CDK1	π	-0.03	±0.19	σ_m	2.64	±0.76							5.42	±0.31
80	CDK1	σ_p	1.20	±0.88										5.64	±0.42
81	CDK1	σ_m	2.55	±1.24										5.10	±0.54
82	CDK1	MR	-0.03	±0.02										6.46	±0.42
83	CDK1	MV	-0.01	±0.01										6.52	±0.44
84	CDK1	dist	-0.10	±0.07										6.39	±0.44

Table 7-5b: Statistical quantities corresponding to the regression equations in table 7-5a (continuation)

#	n	r	s	t_1	t_2	t_3	t_4	t_l	F	q^2
73	25	0.863	0.392	2.44	6.98	2.90		27.63	20.38	0.639
74	14	0.894	0.394	1.26	6.18	0.24		20.49	13.34	0.644
75	25	0.854	0.403	1.43	6.70	0.90		25.69	18.90	0.628
76	14	0.860	0.429	0.57	5.58			46.34	15.56	0.612
77	25	0.789	0.465	0.30	5.98			50.00	18.13	0.527
78	14	0.884	0.393	0.84	6.27			33.50	19.66	0.679
79	25	0.838	0.413	0.28	7.17			36.52	26.04	0.625
80	38	0.419	0.878	2.77				27.14	7.68	0.101
81	38	0.569	0.795	4.15				19.17	17.24	0.260
82	38	0.474	0.950	3.23				30.87	10.44	-0.106
83	38	0.493	0.939	3.40				30.34	11.53	-0.180
84	40	0.413	0.969	2.79				29.69	7.80	-0.152

Table 7-5a: Regression equations, parameters with corresponding slopes and confidence intervals (continuation)

#	Y [pIC_{50}]	X_1	sl_1	ci_1 [95%]	X_2	sl_2	ci_2 [95%]	X_3	sl_3	ci_3 [95%]	X_4	sl_4	ci_4 [95%]	I	ci_I [95%]
85	CDK1	π	-0.21	±0.19										6.09	±0.34
86	CDK1	MR	-0.00	±0.03	σ_m	2.40	±1.33	π	-0.18	±0.24				5.28	±0.68
87	CDK1	MR	-0.01	±0.03	σ_p	1.18	±0.84	π	-0.20	±0.26				5.85	±0.51
88	CDK1	MR	-0.08	±0.06	σ_p	1.24	±0.82	π^2	0.09	±0.09				6.42	±0.62
89	CDK1	MR	-0.07	±0.05	σ_m	2.45	±1.30	π^2	0.08	±0.08				5.78	±0.76
90	CDK1	MR	-0.07	±0.05	MR^2	-0.00	±0.00	σ_m	2.45	±1.33	π^2	0.09	±0.27	5.78	±0.78
91	CDK1	MR	-0.05	±0.05	σ_m	2.41	±1.27	π	-0.18	±0.23	π^2	0.08	±0.08	5.68	±0.76
92	CDK1	MV	-0.02	±0.01	σ_m	2.31	±1.25	π^2	0.09	±0.08				5.99	±0.77
93	CDK1	dist	-0.27	±0.15	σ_m	2.42	±1.12	π^2	0.10	±0.07				5.98	±0.66
94	CDK1	dist	-0.31	±0.16	σ_p	1.33	±0.74	π^2	0.11	±0.07				6.57	±0.56
95	CDK1	dist	-0.25	±0.16	$dist^2$	-0.01	±0.02	σ_m	2.39	±1.14	π^2	0.15	±0.22	5.94	±0.68
96	CDK1	dist	-0.02	±0.02	σ_m	2.34	±1.28	π^2	0.19	±0.24				5.25	±0.58

Table 7-5b: Statistical quantities corresponding to the regression equations in table 7-5a (continuation)

#	n	r	s	t_1	t_2	t_3	t_4	t_l	F	q^2
85	39	0.349	1.002	2.26				36.46	5.12	0.016
86	36	0.654	0.760	0.21	3.68	1.49		15.90	7.98	0.055
87	36	0.593	0.809	0.40	2.85	1.58		23.44	5.78	-0.089
88	36	0.619	0.789	2.80	3.05	2.06		21.03	6.61	0.046
89	36	0.674	0.742	2.56	3.83	1.96		15.42	8.86	0.123
90	36	0.674	0.754	2.52	0.06	3.76	0.66	15.18	6.44	-4.386
91	36	0.705	0.724	1.93	3.87	1.63	2.07	15.31	7.66	0.065
92	36	0.707	0.711	3.18	3.76	2.46		15.82	10.65	0.270
93	36	0.736	0.676	3.70	4.41	2.86		18.40	8.86	0.123
94	37	0.695	0.718	3.94	3.68	2.96		24.01	10.25	0.382
95	37	0.738	0.683	3.13	0.54	4.28	1.41	17.74	9.59	-1.026
96	37	0.637	0.769	1.74	3.73	1.56		18.57	7.51	-1.450

Table 7-5a: Regression equations, parameters with corresponding slopes and confidence intervals (continuation)

#	Y [pIC_{50}]	X_1	sl_1	ci_1 [95%]	X_2	sl_2	ci_2 [95%]	X_3	sl_3	ci_3 [95%]	X_4	sl_4	ci_4 [95%]	I	ci_I [95%]
97	CDK1	σ_m	2.38	±1.22	π	-0.20	±0.14							5.26	±0.55
98	CDK1	MV	-0.00	±0.01	σ_m	2.39	±1.33	π	-0.15	±0.27				5.31	±0.71
99	CDK1	MV	-0.00	±0.01	σ_p	1.18	±0.84	π	-0.16	±0.28				5.91	±0.54
100	CDK1	dist	-0.03	±0.09	σ_m	2.36	±1.23	π	-0.12	±0.24				5.38	±0.63
101	CDK1	σ_p	1.22	±0.81	π	-0.24	±0.15							5.77	±0.40
102	CDK1	σ_m	2.46	±1.31	π^2	-0.02	±0.03							5.20	±0.59
103	CDK1	σ_m^2	3.59	±1.73	π	-0.16	±0.14							5.48	±0.43
104	CDK1	σ_p^2	1.80	±1.47	π	-0.18	±0.16							5.76	±0.46
105	CDK1	σ_m^2	3.84	±1.80	π^2	-0.02	±0.03							5.40	±0.45
106	CDK1	MR	-0.00	±0.03	σ_m	3.55	±1.85	π	-0.15	±0.24				5.51	±0.55
107	CDK1	MV	-0.00	±0.01	σ_m^2	3.53	±1.86	π	-0.13	±0.26				5.53	±0.60
108	CDK1	dist	-0.03	±0.09	σ_m^2	3.56	±1.75	π	-0.10	±0.24				5.58	±0.54

Table 7-5b: Statistical quantities corresponding to the regression equations in table 7-5a (continuation)

#	n	r	s	t_1	t_2	t_3	t_4	t_l	F	q^2
97	37	0.660	0.738	3.97	2.80			19.58	13.15	0.299
98	36	0.656	0.759	0.37	3.65	1.17		15.16	8.04	0.034
99	36	0.598	0.805	0.68	2.87	1.14		22.11	5.94	-0.136
100	37	0.667	0.743	0.75	3.92	1.04		17.24	8.84	0.051
101	37	0.595	0.790	3.07	3.17			29.60	9.30	0.203
102	37	0.593	0.791	3.82	1.54			17.96	9.21	-0.596
103	37	0.676	0.724	4.21	2.27			25.78	14.32	0.328
104	37	0.549	0.821	2.48	2.31			25.31	7.33	0.158
105	37	0.635	0.759	4.33	1.26			24.39	11.47	-0.353
106	36	0.670	0.746	0.13	3.91	1.28		20.32	8.69	0.149
107	36	0.671	0.745	0.26	3.87	1.03		18.89	8.72	0.129
108	37	0.682	0.730	0.68	4.13	0.81		21.15	9.56	0.133

Table 7-5a: Regression equations, parameters with corresponding slopes and confidence intervals (continuation)

#	Y [pIC_{50}]	X_1	sl_1	ci_1 [95%]	X_2	sl_2	ci_2 [95%]	X_3	sl_3	ci_3 [95%]	X_4	sl_4	ci_4 [95%]	I	ci_I [95%]
109	CDK1	dist	-0.06	±0.05	σ_m^2	3.74	±1.66							5.60	±0.48
110	CDK1	dist	-0.06	±0.06	σ_m	0.73	±2.90	σ_m^2	2.76	±4.28				5.53	±0.57
111	CDK1	dist	-0.06	±0.06	σ_p	-1.50	±2.10	σ_m	4.64	±3.28				5.07	±0.76
112	CDK1	MR	-0.01	±0.02	σ_m^2	3.66	±1.86							5.59	±0.54
113	CDK1	MV	-0.00	±0.01	σ_m^2	3.57	±1.85							5.64	±0.56
114	CDK1	σ_m^2	4.07	±1.72										5.30	±0.41
115	CDK1	σ_m^2	3.59	±1.75	π	-0.21	±0.22	π^2	0.01	±0.04				5.46	±0.44
116	CDK1	MR	-0.05	±0.05	MR^2	0.00	±0.00	σ_m^2	3.56	±1.84				5.89	±0.69
117	CDK1	dist	-0.31	±0.39	MV	0.02	±0.03	σ_m^2	3.75	±1.83				5.63	±0.54
118	CDK1	MR	0.04	±0.10	MV	-0.01	±0.03	σ_m^2	3.45	±1.89				5.70	±0.58
119	CDK1	σ_p	1.54	±0.53										5.91	±0.24
120	CDK1	σ_m	2.59	±0.74										5.43	±0.30

Table 7-5b: Statistical quantities corresponding to the regression equations in table 7-5a (continuation)

#	n	r	s	t_1	t_2	t_3	t_4	t_l	F	q^2
109	38	0.681	0.719	2.18	4.56			23.72	15.09	0.199
110	38	0.683	0.727	2.22	0.51	1.31		19.65	9.94	0.124
111	38	0.688	0.723	2.02	1.45	2.88		13.58	10.17	0.152
112	36	0.649	0.753	1.79	4.01			20.99	12.00	0.161
113	36	0.657	0.746	1.97	3.91			20.64	12.53	0.129
114	38	0.625	0.755	4.80				26.39	23.03	0.319
115	37	0.680	0.731	4.17	1.92	0.60		25.35	9.49	-0.161
116	36	0.675	0.741	1.95	1.43	3.95		17.45	8.939	-2.607
117	36	0.689	0.728	1.63	1.32	4.18		21.10	9.66	0.163
118	36	0.665	0.750	0.78	1.10	3.72		19.93	8.46	0.138
119	25	0.779	0.464	5.96				51.57	35.48	0.537
120	25	0.833	0.410	7.21				51.99	51.99	0.639

Table 7-5a: Regression equations, parameters with corresponding slopes and confidence intervals (continuation)

#	Y [pIC_{50}]	X_1	sl_1	ci_1 [95%]	X_2	sl_2	ci_2 [95%]	X_3	sl_3	ci_3 [95%]	X_4	sl_4	ci_4 [95%]	I	ci_I [95%]
121	CDK1	MR	0.02	±0.08										6.23	±0.76
122	CDK1	MV	-0.01	±0.03										6.57	±1.06
123	CDK1	dist	0.24	±0.33										5.72	±0.89
124	CDK1	π	0.13	±0.33										6.35	±0.30
125	CDK1	MR	0.03	±0.06	σ_m	2.41	±0.86	π	0.15	±0.22				5.21	±0.59
126	CDK1	MR	0.04	±0.06	σ_p	1.39	±0.52	π	0.15	±0.23				5.69	±0.55
127	CDK1	MR	0.07	±0.06	σ_p	1.44	±0.45	π^2	-0.26	±0.19				5.66	±0.45
128	CDK1	MR	0.06	±0.06	σ_m	2.49	±0.75	π^2	-0.26	±0.18				5.18	±0.50
129	CDK1	MR	0.08	±0.23	MR^2	-0.00	±0.01	σ_m	2.48	±0.78	π^2	-0.25	±0.20	5.11	±0.96
130	CDK1	MR	0.07	±0.05	σ_m	2.61	±0.73	π	-0.28	±0.35	π^2	-0.48	±0.33	5.29	±0.50
131	CDK1	MV	-0.00	±0.02	σ_m	2.50	±0.85	π^2	-0.13	±0.17				5.62	±0.72
132	CDK1	dist	0.29	±0.20	σ_m	2.55	±0.65	π^2	-0.24	±0.16				4.92	±0.52

Table 7-5b: Statistical quantities corresponding to the regression equations in table 7-5a (continuation)

#	n	r	s	t_1	t_2	t_3	t_4	t_l	F	q^2
121	23	0.108	0.693	0.50				17.06	0.25	-0.158
122	23	0.074	0.695	0.34				12.85	0.12	-0.250
123	25	0.293	0.708	1.47				13.36	2.16	-0.048
124	24	0.169	0.704	0.81				44.19	0.65	-0.160
125	23	0.820	0.419	1.25	5.88	1.44		18.39	13.04	0.562
126	23	0.809	0.431	1.32	5.63	1.38		21.69	12.01	0.550
127	23	0.857	0.378	2.41	6.67	2.86		26.11	17.51	0.645
128	23	0.867	0.365	2.37	6.99	2.96		21.70	19.17	0.665
129	23	0.867	0.375	0.74	0.18	6.66	2.70	11.18	13.66	0.487
130	23	0.886	0.349	2.69	7.51	1.67	3.07	22.27	16.45	0.672
131	23	0.824	0.415	0.11	6.15	1.64		16.31	13.36	0.544
132	24	0.893	0.338	3.03	8.18	3.28		19.63	26.15	0.738

Table 7-5a: Regression equations, parameters with corresponding slopes and confidence intervals (continuation)

#	Y [pIC_{50}]	X_1	sl_1	ci_1 [95%]	X_2	sl_2	ci_2 [95%]	X_3	sl_3	ci_3 [95%]	X_4	sl_4	ci_4 [95%]	I	ci_I [95%]
133	CDK1	dist	0.31	±0.22	σ_p	1.50	±0.44	π^2	-0.23	±0.17				5.34	±0.54
134	CDK1	dist	0.62	±1.26	$dist^2$	-0.06	±0.23	σ_m	2.47	±0.72	π^2	-0.23	±0.16	4.53	±1.54
135	CDK1	$dist^2$	0.05	±0.04	σ_m	2.61	±0.66	π^2	-0.25	±0.16				5.27	±0.36
136	CDK1	σ_m	2.48	±0.80	π	0.09	±0.19							5.47	±0.33
137	CDK1	σ_p	1.59	±0.53										5.88	±0.24
138	CDK1	σ_m	2.65	±0.74										5.42	±0.30
139	CDK1	MR	0.06	±0.07										5.89	±0.64
140	CDK1	dist	0.21	±0.24										5.74	±0.71
141	CDK1	π	-0.08	±0.34										6.31	±0.31
142	CDK1	π	0.02	±0.20	σ_m	2.56	±0.76	MR	0.03	±0.05				5.20	±0.43
143	CDK1	π	0.04	±0.21	σ_p	1.56	±0.51	MR	0.05	±0.05				5.51	±0.43
144	CDK1	π^2	-0.22	±0.19	σ_m	2.51	±0.74	MR	0.12	±0.16	MR^2	-0.00	±0.01	5.02	±0.52

Table 7-5b: Statistical quantities corresponding to the regression equations in table 7-5a (continuation)

#	n	r	s	t_1	t_2	t_3	t_4	t_l	F	q^2
133	24	0.866	0.375	2.96	7.11	2.81		20.53	19.98	0.686
134	24	0.895	0.343	1.04	0.57	7.18	3.00	6.15	19.03	0.715
135	24	0.888	0.344	2.84	8.21	3.18		30.65	24.92	0.723
136	24	0.823	0.415	6.49	0.96			34.27	22.02	0.605
137	25	0.788	0.456	6.14				51.10	37.66	0.555
138	25	0.838	0.404	7.36				37.36	54.17	0.650
139	25	0.307	0.705	1.55				19.13	2.40	-0.039
140	25	0.351	0.693	1.80				16.61	3.23	-0.095
141	25	0.096	0.737	0.46				42.80	0.22	-0.144
142	25	0.855	0.402	0.21	7.04	1.47		24.99	19.00	0.626
143	25	0.830	0.433	0.40	6.32	2.11		26.57	15.45	0.577
144	25	0.894	0.355	2.45	7.06	1.58	0.85	20.11	19.97	0.708

Table 7-5a: Regression equations, parameters with corresponding slopes and confidence intervals (continuation)

#	Y [pIC_{50}]	X_1	sl_1	ci_1 [95%]	X_2	sl_2	ci_2 [95%]	X_3	sl_3	ci_3 [95%]	X_4	sl_4	ci_4 [95%]	I	ci_I [95%]
145	CDK1	π	-0.16	±0.21	π^2	-0.33	±0.23	σ_m	2.65	±0.64	MR	0.06	±0.04	5.25	±0.37
146	CDK1	π^2	-0.15	±0.22	σ_m	2.64	±0.99	dist	0.03	±0.58	$dist^2$	0.01	±0.11	5.39	±0.59
147	CDK1	π^2	-0.15	±0.21	σ_m	2.67	±0.76	$dist^2$	0.01	±0.03				5.41	±0.36
148	CDK1	MR	0.06	±0.05	σ_p	1.47	±0.41	π^2	-0.30	±0.18				5.84	±0.38
149	CDK1	MR	0.06	±0.06	σ_m	2.39	±0.77	π^2	-0.31	±0.20				5.33	±0.46
150	CDK1	dist	0.26	±0.19	σ_p	1.55	±0.37	π^2	-0.28	±0.15				5.56	±0.50
151	CDK1	dist	0.26	±0.23	σ_m	2.53	±0.73	π^2	-0.29	±0.18				5.04	±0.63
152	CDK1	σ_p	1.49	±0.55	π	0.15	±0.23							6.04	±0.25
153	CDK1	σ_m	2.42	±0.96	π	0.18	±0.24							5.55	±0.39
154	CDK1	σ_p	1.46	±0.53	π	0.08	±0.21							5.96	±0.24
155	CDK1	MR	-0.09	±0.07	σ_p	1.22	±1.13	π^2	0.11	±0.10				6.39	±0.73
156	CDK1	MR	-0.08	±0.06	σ_m	2.41	±1.78	π^2	0.10	±0.09				5.80	±0.84

Table 7-5b: Statistical quantities corresponding to the regression equations in table 7-5a (continuation)

#	n	r	s	t_1	t_2	t_3	t_4	t_l	F	q^2
145	25	0.903	0.340	1.61	3.05	8.58	2.81	29.68	22.21	0.707
146	25	0.854	0.413	1.38	5.59	0.11	0.17	19.15	13.52	0.598
147	25	0.854	0.403	1.46	7.27	0.91		31.20	18.92	0.625
148	13	0.952	0.261	2.48	8.13	3.75		34.89	29.26	0.801
149	13	0.938	0.297	2.31	7.00	3.42		25.95	21.92	0.769
150	13	0.961	0.237	3.05	9.59	4.22		25.30	35.96	0.857
151	13	0.943	0.284	2.58	7.85	3.60		18.03	24.24	0.798
152	13	0.897	0.359	6.03	1.48			54.11	20.55	0.693
153	13	0.884	0.379	5.61	1.65			31.77	17.91	0.681
154	24	0.790	0.448	5.77	0.81			52.23	17.43	0.539
155	21	0.648	0.787	2.90	2.27	2.34		18.60	4.11	-0.038
156	21	0.699	0.739	2.86	2.85	2.35		14.58	5.43	0.044

Table 7-5a: Regression equations, parameters with corresponding slopes and confidence intervals (continuation)

#	Y [pIC_{50}]	X_1	sl_1	ci_1 [95%]	X_2	sl_2	ci_2 [95%]	X_3	sl_3	ci_3 [95%]	X_4	sl_4	ci_4 [95%]	I	ci_I [95%]
157	CDK1	dist	-0.34	±0.19	σ_p	1.21	±1.00	π^2	0.12	±0.08				6.65	±0.71
158	CDK1	dist	-0.30	±0.17	σ_m	2.27	±1.61	π^2	0.11	±0.08				6.06	±0.82
159	CDK1	σ_p	0.89	±1.22	π	-0.19	±0.20							5.64	±0.52
160	CDK1	σ_m	2.09	±1.96	π	-0.16	±0.18							5.17	±0.76
161	CDK1	Y/N	-0.13	±0.73	MR	-0.08	±0.06	σ_p	1.29	±0.89	π^2	0.10	±0.09	6.46	±0.67
162	CDK1	Y/N	-0.26	±0.57	dist	-0.29	±0.16	σ_m	2.52	±1.14	π^2	0.10	±0.07	6.07	±0.69
163	CDK1	Y/N	0.14	±0.59	σ_m	2.32	±1.26	π	-0.20	±0.14				5.25	±0.55
164	CDK1	π	-0.25	±0.37	σ_p	1.39	±0.93	MR	-0.05	±0.10				6.08	±0.87
165	CDK1	π	-0.13	±0.33	σ_p	1.28	±0.81	MR	0.01	±0.07				5.71	±0.68
166	CDK1	σ_p	1.45	±0.94	MR	-0.02	±0.09							5.87	±0.82
167	CDK1	σ_p	1.47	±0.93	MR^2	-0.00	±0.01							5.85	±0.57
168	CDK1	σ_p	1.36	±0.92	MR	0.25	±0.36	MR^2	-0.01	±0.02				4.82	±1.58

Table 7-5b: Statistical quantities corresponding to the regression equations in table 7-5a (continuation)

#	n	r	s	t_1	t_2	t_3	t_4	t_l	F	q^2
157	21	0.729	0.709	3.79	2.55	3.05		19.89	6.41	0.332
158	21	0.757	0.676	3.63	2.98	2.95		15.54	7.61	0.375
159	21	0.479	0.883	1.54	2.03			22.65	2.67	-0.105
160	21	0.564	0.830	2.24	1.86			14.27	4.19	0.027
161	36	0.621	0.800	0.37	2.74	2.96	2.06	19.61	4.86	0.005
162	37	0.743	0.677	0.91	3.79	4.49	2.99	17.85	9.88	0.428
163	37	0.663	0.746	0.49	3.73	2.77		19.27	8.65	0.270
164	28	0.585	0.783	1.41	3.09	0.97		14.50	4.17	0.040
165	33	0.560	0.765	0.78	3.25	0.27		17.26	4.41	0.093
166	28	0.537	0.798	3.17	0.41			14.74	5.06	0.071
167	28	0.548	0.792	3.27	0.77			21.06	5.35	0.019
168	28	0.596	0.776	3.05	1.44	1.58		6.31	4.41	-0.096

Table 7-5a: Regression equations, parameters with corresponding slopes and confidence intervals (continuation)

#	Y [pIC_{50}]	X_1	sl_1	ci_1 [95%]	X_2	sl_2	ci_2 [95%]	X_3	sl_3	ci_3 [95%]	X_4	sl_4	ci_4 [95%]	I	ci_I [95%]
169	CDK1	π	-0.07	±0.46	π^2	0.14	±0.42	σ_p	1.35	±0.93				5.63	±0.60
170	CDK1	π^2	0.30	±0.35	σ_p	1.50	±0.91	MR	-0.06	±0.10				5.96	±0.79
171	CDK1	π^2	0.19	±0.32	σ_p	1.29	±0.79	MR	-0.00	±0.07				5.66	±0.64
172	CDK1	π^2	0.06	±0.35	σ_p	1.50	±0.66	E_s	0.28	±0.43				6.14	±0.48
173	CDK1	π	-0.12	±0.33	σ_m	2.29	±1.35	MR	-0.00	±0.08				5.37	±0.94
174	CDK1	π	-0.11	±0.31	σ_m	2.34	±1.17	MR	0.00	±0.07				5.32	±0.70
175	CDK1	π^2	0.20	±0.31	σ_m	2.35	±1.29	MR	-0.01	±0.08				5.29	±0.86
176	CDK1	π^2	0.20	±0.29	σ_m	2.35	±1.13	MR	-0.01	±0.07				5.29	±0.66
177	CDK1	π^2	0.25	±0.35	R	1.15	±1.35	MR	-0.05	±0.08				6.53	±0.72
178	CDK1	F	3.26	±1.98	R	-0.12	±1.41							4.95	±0.85
179	CDK1	π^2	0.19	±0.28	F	3.34	±1.96	R	-0.25	±1.41				4.75	±0.88
180	CDK1	F	3.18	±2.04	R	-0.06	±1.46	MR	-0.01	±0.06				5.12	±1.13

Table 7-5b: Statistical quantities corresponding to the regression equations in table 7-5a (continuation)

#	n	r	s	t_1	t_2	t_3	t_4	t_l	F	q^2
169	28	0.575	0.790	0.33	0.71	3.00		19.35	3.96	0.134
170	28	0.609	0.766	1.78	3.41	1.29		15.47	4.72	0.084
171	33	0.578	0.753	1.24	3.34	0.06		18.08	4.85	0.096
172	22	0.754	0.508	0.39	4.77	1.36		26.96	7.91	0.366
173	31	0.593	0.737	0.75	3.48	0.02		11.69	4.88	0.103
174	33	0.637	0.712	0.76	4.09	0.07		15.54	6.59	0.216
175	31	0.617	0.720	1.35	3.73	0.31		12.57	5.52	0.139
176	33	0.657	0.696	1.40	4.25	0.33		16.43	7.35	0.234
177	32	0.427	0.847	1.46	1.75	1.41		18.65	2.09	-0.135
178	32	0.591	0.742	3.36	0.17			11.95	7.78	0.204
179	32	0.625	0.731	1.38	3.50	0.36		11.01	5.99	0.191
180	32	0.595	0.753	3.19	0.08	0.48		9.31	5.13	0.120

Table 7-5a: Regression equations, parameters with corresponding slopes and confidence intervals (continuation)

#	Y [pIC_{50}]	X_1	sl_1	ci_1 [95%]	X_2	sl_2	ci_2 [95%]	X_3	sl_3	ci_3 [95%]	X_4	sl_4	ci_4 [95%]	I	ci_I [95%]
181	CDK1	π^2	0.25	±0.30	F	3.18	±1.98	R	-0.14	±1.42	MR	-0.03	±0.07	5.09	±1.09
182	CDK1	σ_m	4.57	±4.03	σ_p	-1.14	±2.40							4.82	±0.92
183	CDK1	π^2	0.34	±0.32	σ_p	0.08	±1.38	F	3.62	±2.84	MR	-0.06	±0.09	4.94	±1.07
184	CDK1	π	-0.10	±0.46	π^2	0.24	±0.44	σ_p	1.46	±0.93	MR	-0.06	±0.10	6.03	±0.87
185	CDK1	π^2	0.32	±0.34	σ_p	1.50	±0.88	MR^2	-0.00	±0.01				5.74	±0.55
186	CDK1	π^2	0.25	±0.38	σ_p^2	1.98	±1.69	MR	-0.03	±0.11				5.75	±0.96
187	CDK1	π^2	0.28	±0.36	MR	-0.05	±0.08							6.48	±0.74
188	CDK1	π^2	0.28	±0.34	σ_p	1.41	±0.89	MR	0.19	±0.36	MR^2	-0.01	±0.02	5.00	±1.54
189	CDK1	π^2	0.25	±0.30	F	3.06	±1.59	MR	-0.04	±0.06				5.15	±0.92
190	CDK1	F	3.05	±2.03	R	0.02	±1.44	MR^2	-0.00	±0.00				5.17	±0.96
191	CDK1	F	1.10	±1.71	R	1.45	±1.36	E_s	0.24	±0.37				6.30	±1.07
192	CDK1	π^2	-0.07	±0.34	F	3.21	±1.17	E_s^2	-0.00	±0.12				4.90	±0.58

Table 7-5b: Statistical quantities corresponding to the regression equations in table 7-5a (continuation)

#	n	r	s	t_1	t_2	t_3	t_4	t_l	F	q^2
181	32	0.645	0.729	1.69	3.29	0.21	1.09	9.57	4.82	0.131
182	28	0.642	0.726	2.34	0.98			10.76	8.76	0.239
183	28	0.719	0.686	2.22	0.11	2.64	1.37	9.57	6.16	0.199
184	28	0.614	0.779	0.47	1.13	3.24	1.31	14.36	3.48	0.015
185	28	0.631	0.749	1.98	3.51	1.67		21.43	5.29	0.087
186	28	0.500	0.836	1.33	2.42	0.50		12.36	2.67	-0.100
187	32	0.305	0.877	1.57	1.27			17.94	1.49	-0.118
188	28	0.653	0.747	1.70	3.28	1.08	1.50	6.72	4.28	0.030
189	32	0.645	0.716	1.71	3.93	1.15		11.46	6.64	0.197
190	32	0.610	0.742	3.08	0.02	1.01		10.99	5.53	0.142
191	25	0.729	0.496	1.35	2.22	1.34		12.19	7.95	0.313
192	25	0.793	0.491	0.42	5.69	0.04		17.67	11.84	0.458

Table 7-5a: Regression equations, parameters with corresponding slopes and confidence intervals (continuation)

#	Y [pIC_{50}]	X_1	sl_1	ci_1 [95%]	X_2	sl_2	ci_2 [95%]	X_3	sl_3	ci_3 [95%]	X_4	sl_4	ci_4 [95%]	I	ci_I [95%]
193	CDK1	π^2	-0.13	±0.46	σ_p	1.34	±0.70	MR	0.08	±0.13	E_s	0.18	±0.45	5.65	±0.92
194	CDK1	π^2	-0.12	±0.53	σ_p	1.34	±0.35	MR	0.08	±0.14	E_s^2	-0.05	±0.16	5.56	±0.84
195	CDK1	π^2	-0.11	±0.38	σ_m	2.14	±0.96	MR	0.06	±0.07	E_s^2	-0.01	±0.13	5.21	±0.71
196	CDK1	π^2	0.18	±0.30	σ_m	2.18	±1.30	MR	0.20	±0.34	MR^2	-0.01	±0.02	4.52	±1.47
197	CDK1	π^2	0.19	±0.29	σ_m	2.08	±1.23	MR	0.13	±0.26	MR^2	-0.01	±0.01	4.90	±0.95
198	CDK1	π	-0.08	±0.47	σ_p^2	1.85	±2.03	MR	0.00	±0.11				5.77	±1.19
199	CDK1	F	1.04	±1.71	R	1.53	±1.38	E_s^2	-0.08	±0.12				6.20	±0.91
200	CDK1	π^2	0.29	±0.36	σ_p	1.26	±1.17	σ_p^2	0.65	±1.99	MR	-0.06	±0.10	5.83	±0.89
201	CDK1	π^2	0.34	±0.32	σ_m	4.92	±3.85	σ_p	-1.27	±2.31	MR	-0.06	±0.09	4.92	±1.08
202	CDK1	π^2	0.08	±0.36	σ_p	1.65	±0.90	σ_p^2	-0.36	±1.47	E_s	0.31	±0.46	6.22	±0.59
203	CDK1	π^2	0.20	±0.30	σ_p	1.55	0.91±	L	-0.35	±0.49				6.84	±1.81
204	CDK1	π	-0.21	±0.33	σ_p	1.50	±0.92	L	-0.37	±0.49				7.08	±1.82

Table 7-5b: Statistical quantities corresponding to the regression equations in table 7-5a (continuation)

#	n	r	s	t_1	t_2	t_3	t_4	t_l	F	q^2
193	22	0.780	0.498	0.60	4.03	1.32	0.85	12.99	6.62	0.413
194	22	0.777	0.501	0.48	3.85	1.16	0.73	14.02	6.49	0.413
195	25	0.743	0.498	0.59	4.66	1.67	0.21	15.28	6.15	0.346
196	31	0.648	0.710	1.23	3.45	1.23	1.33	6.30	4.70	0.064
197	33	0.676	0.692	1.32	3.47	1.02	1.15	10.60	5.91	0.167
198	28	0.446	0.864	0.35	1.88	0.02		10.03	1.99	-0.237
199	25	0.734	0.493	1.26	2.31	1.47		14.15	8.18	0.338
200	28	0.619	0.775	1.68	2.23	0.68	1.13	13.47	3.58	-0.620
201	28	0.720	0.685	2.23	2.64	1.14	1.37	9.41	6.17	0.201
202	22	0.759	0.519	0.48	3.87	0.52	1.43	22.10	5.76	0.185
203	28	0.620	0.758	1.38	3.52	1.49		7.80	5.00	0.097
204	28	0.617	0.760	1.31	3.36	1.57		8.03	4.91	0.097

Table 7-5a: Regression equations, parameters with corresponding slopes and confidence intervals (continuation)

#	Y [pIC_{50}]	X_1	sl_1	ci_1 [95%]	X_2	sl_2	ci_2 [95%]	X_3	sl_3	ci_3 [95%]	X_4	sl_4	ci_4 [95%]	I	ci_I [95%]
205	CDK1	π^2	0.19	±0.29	σ_p	1.54	±0.89	L^2	-0.05	±0.06			±	6.21	±0.90
206	CDK1	π^2	0.22	±0.34	σ_p	1.61	±1.02	L	-0.36	±0.50	B_1	-0.25	±1.66	7.27	±3.42
207	CDK1	π^2	0.20	±0.47	σ_p	1.55	±0.93	MR	0.00	±0.21	L	-0.35	±1.03	6.84	±2.69
208	CDK1	σ_p	1.57	±0.92	MR	0.07	±0.13	L	-0.64	±0.77			±	7.51	±2.15
209	CDK1	π^2	-0.02	±0.39	σ_p	1.31	±0.78	E_s	0.16	±0.50	L	0.32	±0.68	4.97	±2.51
210	CDK1	σ_p	1.33	±0.66	E_s^2	-0.06	±0.10	L	0.32	±0.58			±	4.89	±2.06
211	CDK1	π^2	0.01	±0.41	σ_p	1.33	±0.78	E_s^2	-0.06	±0.16	L	0.31	±0.67	4.91	±2.32
212	CDK1	π^2	0.13	±0.29	σ_p	1.29	±0.92	L	2.80	±3.58	L^2	-0.37	±0.42	0.54	±7.29
213	CDK1	π^2	0.32	±0.32	σ_p	1.64	±0.87	L	-0.07	±0.56	B_4	-0.50	±0.57	6.87	±1.73
214	CDK1	π^2	0.36	±0.35	σ_p	1.69	±0.94	B_1	-0.30	±1.54	B_4	-0.56	±0.47	7.20	±2.78
215	CDK1	σ_p	1.58	±0.92	L	-0.34	±0.49			±			±	6.95	±1.83
216	CDK1	F	2.98	±1.98	R	0.15	±1.43	L	-0.24	±0.33			±	6.00	±1.67

Table 7-5b: Statistical quantities corresponding to the regression equations in table 7-5a (continuation)

#	n	r	s	t_1	t_2	t_3	t_4	t_l	F	q^2
205	28	0.634	0.747	1.34	3.59	1.73		14.18	5.39	0.114
206	28	0.622	0.772	1.33	3.28	1.49	0.31	4.40	3.64	0.049
207	28	0.620	0.774	0.87	3.44	0.01	0.71	5.26	3.60	0.010
208	28	0.604	0.770	3.52	1.04	1.70		7.21	4.59	0.049
209	22	0.770	0.508	0.10	3.56	0.67	1.00	4.17	6.19	0.360
210	22	0.772	0.492	4.19	1.22	1.15		4.50	8.84	0.403
211	22	0.772	0.506	0.03	3.61	0.77	0.98	4.46	6.26	0.362
212	28	0.681	0.722	0.89	2.92	1.62	1.84	0.15	4.97	0.268
213	28	2.10	3.87	0.26	1.84			8.22	4.97	0.140
214	28	0.682	0.721	2.14	3.72	0.40	2.43	5.36	5.01	0.172
215	28	0.580	0.771	3.53	1.41			7.82	6.33	0.090
216	32	0.630	0.727	3.08	0.21	1.49		7.37	6.15	0.205

Table 7-5a: Regression equations, parameters with corresponding slopes and confidence intervals (continuation)

#	Y [pIC_{50}]	X_1	sl_1	ci_1 [95%]	X_2	sl_2	ci_2 [95%]	X_3	sl_3	ci_3 [95%]	X_4	sl_4	ci_4 [95%]	I	ci_I [95%]
217	CDK5	π^2	0.29	±0.40	σ_p	1.74	±0.97	MR	-0.10	±0.17			±	5.95	±0.87
218	CDK5	π^2	0.25	±0.39	σ_p	1.64	±0.95	MR	0.20	±0.38	MR^2	-0.02	±0.02	4.80	±1.64
219	CDK5	π^2	0.12	±0.32	σ_p	1.83	±0.96	L	-0.57	±0.55				7.39	±1.99
220	CDK5	π	-0.33	±0.39	σ_p	1.61	±0.96	MR	-0.09	±0.10				6.13	±0.91
221	CDK5	π^2	0.28	±0.32	F	4.09	±2.04	R	-0.35	±1.47	MR	-0.08	±0.07	4.84	±1.12
222	CDK5	π^2	0.12	±0.32	F	4.40	±2.22	R	-0.51	±1.60				4.08	±1.02
223	CDK5	π^2	0.01	±0.29	F	1.81	±1.47	R	1.58	±1.19	E_s	0.35	±0.40	5.91	±0.94
224	CDK5	π^2	0.14	±0.28	F	3.91	±1.95	R	-0.05	±1.42	L	-0.49	±0.32	6.19	±1.63
225	CDK5	π^2	0.25	±0.30	F	3.59	±2.06	R	0.09	±1.49	B_4	-0.52	±0.38	5.65	±1.46
226	CDK5	σ_p	1.92	±0.94	L	-0.36	±0.61	B_4	-0.36	±0.55				7.53	±1.94
227	CDK5	π^2	0.08	±0.34	σ_p	1.55	±0.99							5.39	±0.60
228	CDK5	π^2	0.10	±0.31	F	3.98	±1.78							4.27	±0.83

Table 7-5b: Statistical quantities corresponding to the regression equations in table 7-5a (continuation)

#	n	r	s	t_1	t_2	t_3	t_4	t_l	F	q^2
217	27	0.631	0.819	1.47	3.69	1.78		14.18	5.06	-0.127
218	27	0.683	0.788	1.35	3.58	1.07	1.69	6.05	4.81	-0.805
219	27	0.657	0.796	0.76	3.94	2.17		7.69	5.81	-0.028
220	27	0.647	0.804	1.75	3.49	1.81		13.98	5.53	0.064
221	31	0.743	0.739	1.77	4.12	0.49	2.54	8.90	8.03	0.305
222	31	0.665	0.810	0.74	4.07	0.66		8.20	7.12	0.264
223	25	0.855	0.428	0.08	2.57	2.75	1.81	13.14	13.59	0.561
224	31	0.773	0.701	1.04	4.13	0.07	3.17	7.80	9.64	0.408
225	31	0.757	0.722	1.69	3.58	0.12	2.84	7.97	8.75	0.356
226	27	0.679	0.775	4.22	1.22	1.36		8.02	6.55	0.054
227	27	0.561	0.855	0.50	3.24			18.57	5.50	0.186
228	31	0.658	0.802	0.64	4.58			10.52	10.68	0.318

Table 7-5a: Regression equations, parameters with corresponding slopes and confidence intervals (continuation)

#	Y [pIC_{50}]	X_1	sl_1	ci_1 [95%]	X_2	sl_2	ci_2 [95%]	X_3	sl_3	ci_3 [95%]	X_4	sl_4	ci_4 [95%]	I	ci_I [95%]
229	CDK5	π^2	0.28	±0.32	F	4.09	±2.04	R	-0.35	±1.47	MR	-0.08	±0.07	4.84	±1.12
230	GSK3	π^2	0.02	±0.49	σ_p	1.40	±1.00	MR	0.22	±0.49	MR^2	-0.02	±0.03	6.15	±1.96
231	GSK3	π^2	-0.03	±0.48	σ_p	1.44	±0.99	MR^2	-0.01	±0.01				6.99	±0.63
232	GSK3	π^2	0.26	±0.29	F	3.88	±1.95	R	-0.25	±1.40	MR^2	-0.00	±0.00	4.60	±0.95
233	GSK3	σ_p	1.45	±0.96	MR^2	-0.01	±0.01							6.99	±0.62
234	CDK1	π^2	0.03	±0.34	F	1.10	±1.75	R	1.47	±1.42	E_s	0.26	±0.48	6.31	±1.11
235	CDK1	σ_m	1.10	±1.73	R	1.16	±1.74	E_s	0.24	±0.37				6.30	±1.08
236	CDK1	σ_m	3.11	±2.02	R	-0.83	±1.80	MR	0.01	±0.07				4.93	±1.13
237	CDK1	σ_m	2.40	±1.31	MR^2	-0.00	±0.00							5.34	±0.70
238	CDK1	π^2	0.06	±0.35	σ_p	1.50	±0.66	E_s	0.28	±0.63				6.14	±0.48
239	CDK1	π^2	0.25	±0.35	R	1.15	±1.35	MR	-0.05	±0.08				6.53	±0.72
240	CDK1	π^2	0.25	±0.30	F	3.18	±1.98	R	-0.14	±1.42	MR	-0.03	±0.07	5.09	±1.09

Table 7-5b: Statistical quantities corresponding to the regression equations in table 7-5a (continuation)

#	n	r	s	t_1	t_2	t_3	t_4	t_l	F	q^2
229	31	0.743	0.739	1.77	4.12	0.49	2.54	8.90	8.03	0.305
230	27	0.712	0.835	0.07	2.89	0.94	1.72	6.50	5.67	-0.056
231	27	0.698	0.833	0.13	3.00	2.74		22.87	7.30	0.330
232	31	0.773	0.702	1.84	4.09	0.36	3.16	9.97	9.62	0.397
233	27	0.698	0.816	3.11	4.19			23.36	11.40	0.384
234	25	0.730	0.508	0.17	1.32	2.17	1.15	11.82	5.70	0.253
235	25	0.729	0.497	1.33	1.39	1.34		12.10	7.92	0.310
236	31	0.599	0.732	3.17	0.94	0.40		8.97	5.05	0.114
237	31	0.580	0.732	3.76	0.02			15.60	7.09	0.117
238	22	0.754	0.508	0.39	4.77	1.36		26.96	7.908	0.366
239	32	0.427	0.847	1.46	1.75	1.41		18.65	2.09	-0.135
240	32	0.645	0.729	1.69	3.29	0.21	1.09		4.82	0.131

Table 7-5a: Regression equations, parameters with corresponding slopes and confidence intervals (continuation)

#	Y [pIC_{50}]	X_1	sl_1	ci_1 [95%]	X_2	sl_2	ci_2 [95%]	X_3	sl_3	ci_3 [95%]	X_4	sl_4	ci_4 [95%]	I	ci_I [95%]
241	CDK1	σ_p	1.36	±0.77										5.77	±0.38
242	CDK1	σ_m	2.44	±1.11										5.32	±0.49
243	CDK1	MR	-0.00	±0.07										6.21	±0.67
244	CDK1	dist	0.17	±0.29										5.72	±0.89
245	CDK1	π	-0.28	±0.34										6.19	±0.31
246	CDK1	π	0.02	±0.39	π^2	0.21	±0.38	σ_m	2.36	±1.17	MR	-0.01	±0.07	5.27	±0.70
247	CDK1	π^2	0.23	±0.28	σ_m	2.56	±1.23	dist	-0.12	±0.27				5.43	±0.71
248	CDK1	π^2	0.18	±0.31	σ_p	1.27	±0.81	dist	0.02	±0.28				5.60	±0.76
249	CDK1	π^2	0.23	±0.30	σ_m	2.51	±1.43	dist	-0.05	±0.92	$dist^2$	-0.01	±0.18	5.39	±0.97
250	CDK1	π^2	0.24	±0.29	σ_m	2.47	±1.15	$dist^2$	-0.02	±0.05				5.34	±0.58
251	CDK1	π	-0.12	±0.29	σ_m	2.34	±1.14							5.34	±0.50
252	CDK1	π^2	0.17	±0.54	σ_p	1.16	±1.29	MR	-0.04	±0.11				5.88	±0.98

Table 7-5b: Statistical quantities corresponding to the regression equations in table 7-5a (continuation)

#	n	r	s	t_1	t_2	t_3	t_4	t_l	F	q^2
241	33	0.540	0.751	3.57				30.96	12.76	0.216
242	33	0.626	0.696	4.47				22.11	19.94	0.324
243	34	0.001	0.910	0.003				18.75	0.00	-0.176
244	34	0.206	0.891	1.19				13.08	1.42	-0.072
245	34	0.282	0.873	1.66				41.16	2.76	-0.028
246	33	0.657	0.708	0.10	1.15	4.15	0.33	15.36	5.33	0.198
247	33	0.667	0.688	1.64	4.25	0.89		15.68	7.74	0.312
248	33	0.578	0.753	1.21	3.21	0.15		15.01	4.86	0.163
249	33	0.667	0.700	1.58	3.61	0.12	0.15	11.34	5.62	0.286
250	33	0.667	0.688	1.66	4.37	0.89		18.83	7.75	0.309
251	33	0.637	0.700	0.83	4.19			21.96	10.22	0.311
252	17	0.496	0.881	0.68	1.93	0.72		13.00	1.41	-0.265

Table 7-5a: Regression equations, parameters with corresponding slopes and confidence intervals (continuation)

#	Y [pIC_{50}]	X_1	sl_1	ci_1 [95%]	X_2	sl_2	ci_2 [95%]	X_3	sl_3	ci_3 [95%]	X_4	sl_4	ci_4 [95%]	I	ci_I [95%]
253	CDK1	π^2	0.14	±0.49	σ_m	2.38	±1.93	MR	-0.04	±0.10				5.46	±0.97
254	CDK1	π^2	0.13	±0.54	σ_p	1.06	±1.28	dist	-0.05	±0.42				5.76	±1.28
255	CDK1	π^2	0.13	±0.49	σ_m	2.39	±1.94	dist	-0.15	±0.39				5.55	±1.17
256	CDK1	π	-0.04	±0.56	σ_p	1.08	±1.23							5.70	±0.54
257	CDK1	π	-0.00	±0.51	σ_m	2.27	±1.86							5.26	±0.70
258	CDK1	π^2	0.20	±0.33	σ_p	1.27	±0.85	MR	-0.00	±0.08	Y/N	0.03	±0.69	5.65	±0.72
259	CDK1	π^2	0.22	±0.29	σ_m	2.59	±1.33	Y/N	-0.04	±0.61	dist	-0.12	±0.28	5.44	±0.75
260	CDK1	π	-0.14	±0.31	σ_p	1.29	±0.79							5.78	±0.38
261	CDK1	π	-0.11	±0.30	σ_m	2.37	±1.21	Y/N	-0.04	±0.61				5.34	±0.51
262	CDK1	dist	0.14	±0.35	σ_m	2.27	±1.09	π^2	0.01	±0.26				5.08	±0.95
263	CDK1	dist	0.09	±0.38	σ_m	2.00	±1.29	π^2	-0.14	±0.58				5.35	±1.14
264	CDK1	dist	0.30	±0.28	σ_m	2.21	±0.84	π^2	-0.10	±0.21				4.85	±0.74

Table 7-5b: Statistical quantities corresponding to the regression equations in table 7-5a (continuation)

#	n	r	s	t_1	t_2	t_3	t_4	t_l	F	q^2
253	17	0.611	0.804	0.63	2.67	0.85		12.13	2.58	-0.008
254	17	0.469	0.897	0.52	1.79	0.26		9.75	1.22	-0.215
255	17	0.608	0.806	0.59	2.66	0.80		10.20	2.54	0.086
256	17	0.452	0.873	0.15	1.88			22.78	1.79	-0.056
257	17	0.575	0.800	0.002	2.62			16.14	3.46	0.141
258	33	0.578	0.766	1.22	3.07	0.03	0.10	16.02	3.52	0.048
259	33	0.667	0.700	1.56	4.00	0.14	0.88	14.89	5.62	0.275
260	33	0.558	0.753	0.93	3.33			30.90	6.79	0.203
261	33	0.637	0.712	0.75	3.99	0.13		21.53	6.59	0.275
262	30	0.663	0.650	0.80	4.26	0.11		11.01	6.81	0.266
263	25	0.636	0.667	0.48	3.23	0.52		9.74	4.76	0.225
264	29	0.770	0.499	2.17	5.40	0.98		13.57	12.16	0.471

Table 7-5a: Regression equations, parameters with corresponding slopes and confidence intervals (continuation)

#	Y [pIC_{50}]	X_1	sl_1	ci_1 [95%]	X_2	sl_2	ci_2 [95%]	X_3	sl_3	ci_3 [95%]	X_4	sl_4	ci_4 [95%]	I	ci_I [95%]
265	CDK1	dist	0.26	±0.19	σ_m	2.35	±0.64	π^2	-0.20	±0.15				4.98	±0.50
266	CDK1	dist	0.30	±0.20	σ_m	2.58	±0.65	π^2	-0.23	±0.15				4.87	±0.52
267	CDK1	dist	0.27	±0.23	σ_m	2.39	±0.76	π^2	-0.18	±0.18				4.92	±0.62
268	CDK1	dist	0.29	±0.25	σ_m	2.22	±0.78	π^2	-0.19	±0.19				4.94	±0.65
269	CDK1	dist	0.30	±0.19	σ_m	2.50	±0.61	π^2	-0.22	±0.15				4.88	±0.51
270	CDK1	dist	0.32	±0.23	σ_m	2.64	±0.70	π^2	-0.17	±0.17				4.76	±0.59
271	CDK1	dist	-0.06	±0.24	σ_m	2.56	±0.97	π^2	-0.06	±0.22				5.62	±0.71
272	CDK1	dist	0.17	±0.17	σ_m	2.57	±0.66	π^2	-0.26	±0.16				5.21	±0.46
273	CDK1	dist	-0.03	±0.20	σ_m	2.58	±0.87	π^2	-0.12	±0.21				5.60	±0.59
274	CDK1	dist	0.05	±0.19	σ_m	2.60	±0.78	π^2	-0.24	±0.19				5.48	±0.52
275	CDK1	dist	0.10	±0.22	σ_m	2.52	±0.81	π^2	-0.10	±0.18				5.26	±0.63
276	CDK1	dist	0.13	±0.32	σ_m	2.51	±1.05	π^2	-0.09	±0.25				5.14	±0.87

Table 7-5b: Statistical quantities corresponding to the regression equations in table 7-5a (continuation)

#	n	r	s	t_1	t_2	t_3	t_4	t_l	F	q^2
265	22	0.886	0.316	2.91	7.66	2.74		21.07	21.98	0.708
266	25	0.891	0.340	3.18	8.29	3.09		19.61	26.91	0.735
267	26	0.834	0.407	2.44	6.53	2.11		16.60	16.74	0.612
268	26	0.810	0.431	2.45	5.90	2.01		15.72	14.00	0.546
269	26	0.892	0.337	3.19	8.52	3.02		19.88	28.53	0.740
270	27	0.871	0.394	2.98	7.76	2.09		16.81	24.11	0.680
271	27	0.753	0.538	0.56	5.45	0.59		16.49	10.02	0.153
272	27	0.878	0.370	2.04	8.01	3.41		23.44	25.90	0.501
273	27	0.794	0.482	0.33	6.15	1.25		19.52	13.11	0.211
274	27	0.847	0.435	0.57	6.89	2.58		21.68	19.42	0.257
275	27	0.808	0.448	0.91	6.46	1.17		17.21	14.37	0.472
276	27	0.726	0.581	0.82	4.95	0.77		12.26	8.53	0.379

Table 7-5a: Regression equations, parameters with corresponding slopes and confidence intervals (continuation)

#	Y [pIC_{50}]	X_1	sl_1	ci_1 [95%]	X_2	sl_2	ci_2 [95%]	X_3	sl_3	ci_3 [95%]	X_4	sl_4	ci_4 [95%]	I	ci_I [95%]
277	CDK1	dist	0.29	±0.20	σ_m	2.47	±0.62	π^2	-0.14	±0.08				4.84	±0.51
278	CDK1	dist	0.25	±0.19	σ_m	2.55	±0.62	π^2	-0.28	±0.13				5.04	±0.48
279	CDK1	dist	-0.19	±0.17	σ_m	2.52	±1.05	π^2	0.01	±0.18				5.87	±0.59
280	CDK1	dist	0.29	±0.21	σ_m	2.49	±0.67	π^2	-0.13	±0.09				4.85	±0.54
281	CDK1	dist	0.10	±0.24	σ_m	2.34	±0.91	π^2	-0.18	±0.18				5.37	±0.66
282	CDK1	dist	-0.26	±0.14	σ_m	2.54	±1.06	π^2	0.09	±0.07				5.89	±0.61
283	CDK1	dist	0.02	±0.30	σ_m	2.34	±1.06	π^2	0.08	±0.25				5.27	±0.82
284	CDK1	dist	0.17	±0.36	σ_m	2.23	±1.08	π^2	0.01	±0.26				5.02	±0.87
285	CDK1	dist	0.28	±0.70	σ_m	2.01	±1.39	π^2	-0.21	±0.61				4.99	±1.18
286	CDK1	dist	0.27	±0.61	σ_m	2.32	±1.25	π^2	-0.20	±0.54				4.94	±1.04
287	CDK1	dist	0.30	±0.27	σ_m	2.21	±0.79	π^2	-0.10	±0.20				4.85	±0.66
288	CDK1	dist	0.30	±0.24	σ_m	2.48	±0.74	π^2	-0.13	±0.18				4.81	±0.59

Table 7-5b: Statistical quantities corresponding to the regression equations in table 7-5a (continuation)

#	n	r	s	t_1	t_2	t_3	t_4	t_l	F	q^2
277	27	0.895	0.343	3.09	8.29	3.47		19.55	31.00	-0.820
278	27	0.910	0.346	2.78	8.47	4.52		21.85	37.16	0.628
279	29	0.788	0.554	2.30	4.96	0.05		20.43	13.61	0.453
280	25	0.889	0.353	2.90	7.68	3.27		18.74	26.32	-2.625
281	31	0.785	0.543	0.88	5.28	2.04		16.65	14.43	0.515
282	38	0.739	0.671	3.65	4.89	2.81		19.68	13.61	0.446
283	32	0.672	0.655	0.16	4.53	0.66		13.19	7.70	0.280
284	30	0.691	0.647	0.98	4.25	0.09		11.83	7.92	0.310
285	21	0.804	0.519	0.85	3.05	0.71		8.89	10.34	0.479
286	20	0.863	0.452	0.94	3.95	0.78		10.10	15.60	0.623
287	30	0.795	0.489	2.31	5.73	1.00		15.19	14.89	0.526
288	29	0.845	0.437	2.58	6.91	1.45		16.86	20.86	0.633

Table 7-5a: Regression equations, parameters with corresponding slopes and confidence intervals (continuation)

#	Y [pIC_{50}]	X_1	sl_1	ci_1 [95%]	X_2	sl_2	ci_2 [95%]	X_3	sl_3	ci_3 [95%]	X_4	sl_4	ci_4 [95%]	I	ci_I [95%]
289	CDK1	dist	0.32	±0.21	σ_m	2.63	±0.66	π^2	-0.17	±0.17				4.77	±0.52
290	CDK1	dist	0.02	±0.29	σ_m	2.69	±1.07	π^2	0.03	±0.24				5.24	±0.78
291	CDK1	σ_m	5.55	±57.5										2.84	±20.7
292	CDK1	dist	-0.06	±0.13										5.31	±1.18
293	CDK1	π	-0.14	±0.32										5.13	±0.78

Table 7-5b: Statistical quantities corresponding to the regression equations in table 7-5a (continuation)

#	n	r	s	t_1	t_2	t_3	t_4	t_l	F	q^2
289	28	0.885	0.386	3.14	8.19	2.13		18.92	28.94	0.717
290	30	0.729	0.625	0.15	5.18	0.29		13.74	9.81	0.372
291	6	0.133	0.414	0.27				0.38	0.07	-1.469
292	6	0.512	0.359	1.19				12.52	1.42	-0.745
293	6	0.518	0.357	1.21				18.17	1.47	-0.727

Table 7-5a: Regression equations, parameters with corresponding slopes and confidence intervals (continuation)

#	Y [pGI_{50}]	X_1	sl_1	ci_1 [95%]	X_2	sl_2	ci_2 [95%]	X_3	sl_3	ci_3 [95%]	X_4	sl_4	ci_4 [95%]	I	ci_I [95%]
294	HCT	σ_p	1.12	±0.80										4.84	±0.42
295	HCT	σ_m	2.07	±1.15										4.41	±0.54
296	HCT	MR	-0.03	±0.05										5.55	±0.58
297	HCT	dist	-0.09	±0.17										5.52	±0.59
298	HCT	π	0.14	±0.34										5.23	±0.37
299	HCT	MR	0.05	±0.12	σ_m	1.79	±1.67	π^2	-0.30	±0.51				4.42	±0.80
300	HCT	dist	-0.05	±0.35	σ_m	2.13	±1.36	π^2	-0.07	±0.38				4.58	±0.78
301	HCT	σ_p	1.15	±0.80										4.88	±0.43
302	HCT	σ_m	2.09	±1.17										4.45	±0.56
303	HCT	MR	0.04	±0.12										5.07	±0.85
304	HCT	dist	0.05	±0.32										5.18	±1.00
305	HCT	π	0.26	±0.44										5.33	±0.36

Table 7-5b: Statistical quantities corresponding to the regression equations in table 7-5a (continuation)

#	n	r	s	t_1	t_2	t_3	t_4	t_l	F	q^2
294	23	0.534	0.667	2.90				24.02	8.39	0.173
295	23	0.632	0.612	3.74				16.91	13.96	0.304
296	21	0.246	0.781	1.10				20.12	1.22	-0.069
297	23	0.237	0.767	1.12				19.52	1.25	-0.047
298	22	0.190	0.787	0.86				29.68	0.75	-0.182
299	21	0.691	0.616	0.82	2.26	1.26		11.59	5.19	0.279
300	22	0.693	0.609	0.27	3.30	0.39		12.31	5.54	0.296
301	21	0.567	0.664	3.00				23.95	9.01	0.205
302	21	0.651	0.613	3.73				16.73	13.94	0.327
303	21	0.153	0.797	0.67				12.50	0.45	-0.157
304	21	0.070	0.805	0.30				10.84	0.09	-0.223
305	21	0.269	0.777	1.22				31.34	1.48	-0.070

Table 7-5a: Regression equations, parameters with corresponding slopes and confidence intervals (continuation)

#	Y [pGI_{50}]	X_1	sl_1	ci_1 [95%]	X_2	sl_2	ci_2 [95%]	X_3	sl_3	ci_3 [95%]	X_4	sl_4	ci_4 [95%]	I	ci_I [95%]
306	HCT	π^2	-0.37	±0.50	σ_m	1.79	±1.47	MR	0.04	±0.15				4.55	±0.69
307	HCT	π^2	-0.22	±0.37	σ_m	2.19	±1.30	dist	-0.07	±0.30				4.76	±0.78
308	HCT	CDK1	0.32	±0.11										3.35	±0.69
309	HCT	CDK5	0.27	±0.10										3.79	±0.57
310	HCT	GSK3	0.28	±0.10										3.37	±0.71
311	HCT	log P	-0.07	±0.17										5.50	±0.64
312	HCT	log P	0.19	±0.16	CDK1	0.39	±0.13							2.19	±1.17
313	HCT	log P	0.24	±0.18	CDK5	0.34	±0.11							2.46	±1.12
314	HCT	log P	0.11	±0.15	GSK3	0.32	±0.11							2.72	±1.12
315	HCT	log P	0.23	±0.18	CDK1	0.15	±0.28	CDK5	0.15	±0.23	GSK3	0.10	±0.18	2.00	±1.19
316	HCT	CDK1	0.22	±0.27	CDK5	0.10	±0.23							3.40	±0.74
317	HCT	CDK1	0.20	±0.19	GSK3	0.14	±0.18							3.17	±0.72

Table 7-5b: Statistical quantities corresponding to the regression equations in table 7-5a (continuation)

#	n	r	s	t_1	t_2	t_3	t_4	t_l	F	q^2
306	21	0.717	0.595	1.54	2.56	0.58		13.88	5.98	0.371
307	21	0.715	0.596	1.23	3.55	0.52		12.95	5.93	0.332
308	67	0.572	0.527	5.62				9.72	31.62	0.275
309	66	0.550	0.538	5.26				13.19	27.72	0.250
310	67	0.557	0.533	5.41				9.52	29.25	0.262
311	68	0.101	0.636	0.82				17.16	0.67	-0.052
312	67	0.619	0.508	2.40	6.24			3.72	19.83	0.320
313	66	0.613	0.513	2.73	6.14			4.41	18.96	0.312
314	67	0.577	0.528	1.48	5.59			4.84	15.99	0.273
315	66	0.645	0.504	2.51	1.06	1.31	1.14	3.34	10.87	0.286
316	66	0.575	0.531	1.62	0.85			9.13	15.54	0.232
317	67	0.593	0.521	2.01	1.53			8.82	17.32	0.279

Table 7-5a: Regression equations, parameters with corresponding slopes and confidence intervals (continuation)

#	Y [pGI_{50}]	X_1	sl_1	ci_1 [95%]	X_2	sl_2	ci_2 [95%]	X_3	sl_3	ci_3 [95%]	X_4	sl_4	ci_4 [95%]	I	ci_I [95%]
318	HCT	CDK5	0.14	±0.15	GSK3	0.18	±0.17							3.27	±0.74
319	HCT	log P^2	-0.01	±0.02										5.43	±0.33
320	HCT	log P^2	0.02	±0.02	CDK1	0.39	±0.13							2.65	±0.97
321	HCT	log P^2	0.03	±0.02	CDK5	0.34	±0.12							2.97	±0.89
322	HCT	log P^2	0.01	±0.02	GSK3	0.33	±0.12							2.86	±0.97
323	HCT	log P^2	0.03	±0.02	CDK1	0.14	±0.29	CDK5	0.14	±0.23	GSK3	0.13	±0.18	2.38	±1.02
324	HCT	log P	0.52	±0.59	log P^2	-0.04	±0.07	CDK1	0.38	±0.13				1.66	±1.48
325	SR	CDK1	0.31	±0.13										3.53	±0.81
326	SR	CDK5	0.21	±0.13										4.21	±0.72
327	SR	GSK3	0.26	±0.12										3.68	±0.77
328	SR	log P	-0.02	±0.17										5.39	±0.68
329	SR	log P	0.20	±0.18	CDK1	0.37	±0.15							2.40	±1.30

Table 7-5b: Statistical quantities corresponding to the regression equations in table 7-5a (continuation)

#	n	r	s	t_1	t_2	t_3	t_4	t_l	F	q^2
318	66	0.590	0.524	1.85	2.11			8.83	16.83	0.280
319	68	0.151	0.632	1.24				32.49	1.54	-0.028
320	67	0.605	0.515	1.97	5.92			5.45	18.46	0.298
321	66	0.598	0.520	2.34	5.84			6.69	17.57	0.287
322	67	0.578	0.528	1.51	5.51			5.90	16.05	0.276
323	66	0.638	0.508	2.31	0.97	1.22	1.44	4.66	10.49	0.273
324	67	0.629	0.507	1.76	1.17	5.90		2.25	13.75	0.332
325	75	0.467	0.689	4.51				8.67	20.34	0.167
326	72	0.365	0.715	3.28				11.63	10.79	0.076
327	73	0.467	0.673	4.45				9.51	19.83	0.171
328	78	0.023	0.771	0.20				15.84	0.04	-0.054
329	75	0.517	0.672	2.19	5.12			3.69	13.11	0.197

Table 7-5a: Regression equations, parameters with corresponding slopes and confidence intervals (continuation)

#	Y [pGI_{50}]	X_1	sl_1	ci_1 [95%]	X_2	sl_2	ci_2 [95%]	X_3	sl_3	ci_3 [95%]	X_4	sl_4	ci_4 [95%]	I	ci_I [95%]
330	SR	log P	0.27	±0.21	CDK5	0.30	±0.14							2.77	±1.32
331	SR	log P	0.10	±0.17	GSK3	0.29	±0.13							3.15	±1.21
332	SR	log P	0.20	±0.22	CDK1	0.21	±0.18	CDK5	-0.01	±0.31	GSK3	0.16	±0.21	2.39	±1.52
333	SR	CDK1	0.32	±0.35	CDK5	-0.03	±0.30							3.67	±0.93
334	SR	CDK1	0.09	±0.22	GSK3	0.21	±0.19							3.47	±0.90
335	SR	CDK5	0.02	±0.19	GSK3	0.25	±0.19							3.67	±0.89
336	SR	log P^2	-0.01	±0.02										5.43	±0.37
337	SR	log P^2	0.02	±0.02	CDK1	0.37	±0.15							2.87	±1.09
338	SR	log P^2	0.04	±0.03	CDK5	0.30	±0.14							3.22	±1.08
339	SR	log P^2	0.01	±0.02	GSK3	0.30	±0.13							3.28	±1.06
340	SR	log P^2	0.03	±0.03	CDK1	0.20	±0.36	CDK5	-0.01	±0.31	GSK3	0.18	±0.20	2.63	±1.31
341	SR	log P	0.62	±0.68	log P^2	-0.06	±0.09	CDK1	0.35	±0.15				1.78	±1.61

Table 7-5b: Statistical quantities corresponding to the regression equations in table 7-5a (continuation)

#	n	r	s	t_1	t_2	t_3	t_4	t_l	F	q^2
330	72	0.458	0.688	2.57	4.22			4.19	9.14	0.142
331	73	0.482	0.672	1.13	4.57			5.22	10.59	0.168
332	70	0.490	0.678	1.82	1.18	0.07	1.52	3.13	5.12	0.093
333	72	0.416	0.703	1.82	0.23			7.90	7.23	0.081
334	72	0.473	0.679	0.80	2.20			7.72	9.93	0.144
335	70	0.435	0.690	0.21	2.57			8.25	7.83	0.109
336	78	0.078	0.769	0.68				29.33	0.46	-0.049
337	75	0.500	0.680	1.77	4.88			5.24	12.02	0.163
338	72	0.448	0.692	2.41	4.15			5.95	8.66	0.129
339	73	0.481	0.673	1.09	4.46			6.18	10.54	0.165
340	70	0.492	0.677	1.89	1.14	0.07	1.79	4.00	5.20	0.097
341	75	0.532	0.669	1.80	1.27	4.73		2.20	9.35	0.195

Table 7-5a: Regression equations, parameters with corresponding slopes and confidence intervals (continuation)

#	Y [pGI_{50}]	X_1	sl_1	ci_1 [95%]	X_2	sl_2	ci_2 [95%]	X_3	sl_3	ci_3 [95%]	X_4	sl_4	ci_4 [95%]	I	ci_I [95%]
342	RXF	CDK1	0.18	±0.15										4.09	±0.90
343	RXF	CDK5	0.21	±0.11										3.99	±0.64
344	RXF	GSK3	0.29	±0.11										3.22	±0.73
345	RXF	log P	0.01	±0.16										5.10	±0.62
346	RXF	log P	0.25	±0.19	CDK1	0.31	±0.17							2.34	±1.55
347	RXF	log P	0.27	±0.18	CDK5	0.32	±0.13							2.37	±1.24
348	RXF	log P	0.12	±0.14	GSK3	0.34	±0.12							2.47	±1.15
349	RXF	log P	0.22	±0.18	CDK1	-0.17	±0.27	CDK5	0.29	±0.24	GSK3	0.23	±0.18	2.22	±1.34
350	RXF	$\log P^2$	0.00	±0.02										5.18	±0.35
351	RXF	$\log P^2$	0.03	±0.02	CDK1	0.29	±0.17							3.02	±1.30
352	RXF	$\log P^2$	0.03	±0.03	CDK5	0.30	±0.14							3.05	±1.03
353	RXF	$\log P^2$	0.01	±0.02	GSK3	0.35	±0.13							2.63	±1.05

Table 7-5b: Statistical quantities corresponding to the regression equations in table 7-5a (continuation)

#	n	r	s	t_1	t_2	t_3	t_4	t_l	F	q^2
342	67	0.290	0.687	2.44				9.09	5.96	0.030
343	65	0.423	0.593	3.71				12.56	13.73	0.126
344	67	0.548	0.555	5.28				8.79	27.89	0.259
345	70	0.016	0.717	0.13				16.35	0.02	-0.084
346	67	0.422	0.655	2.71	3.65			3.01	6.94	0.075
347	65	0.531	0.559	2.99	4.94			3.81	12.19	0.214
348	67	0.574	0.548	1.66	5.53			4.28	15.71	0.277
349	65	0.596	0.539	2.45	1.21	2.36	2.54	3.32	8.26	0.247
350	70	0.030	0.717	0.25				29.84	0.06	-0.095
351	67	0.386	0.667	2.22	3.33			4.66	5.62	0.018
352	65	0.493	0.574	2.30	4.44			5.93	9.97	0.170
353	67	0.570	0.550	1.52	5.28			5.01	15.38	0.273

Table 7-5a: Regression equations, parameters with corresponding slopes and confidence intervals (continuation)

#	Y [pGI_{50}]	X_1	sl_1	ci_1 [95%]	X_2	sl_2	ci_2 [95%]	X_3	sl_3	ci_3 [95%]	X_4	sl_4	ci_4 [95%]	I	ci_I [95%]
354	RXF	log P^2	0.03	±0.02	CDK1	-0.19	±0.27	CDK5	0.28	±0.25	GSK3	0.27	±0.18	2.59	±1.18
355	RXF	log P	0.64	±0.65	log P^2	-0.05	±0.08	CDK1	0.30	±0.17				1.70	±1.86
356	LOX	CDK1	0.24	±0.12										3.69	±0.76
357	LOX	CDK5	0.20	±0.11										4.04	±0.62
358	LOX	GSK3	0.28	±0.12										3.29	±0.80
359	LOX	log P	-0.09	±0.15										5.46	±0.60
360	LOX	log P	0.09	±0.17	CDK1	0.28	±0.15							3.11	±1.35
361	LOX	log P	0.12	±0.20	CDK5	0.25	±0.13							3.34	±1.30
362	LOX	log P	0.04	±0.15	GSK3	0.29	±0.13							3.06	±1.19
363	LOX	log P	0.05	±0.20	CDK1	0.05	±0.28	CDK5	0.04	±0.24	GSK3	0.25	±0.21	2.80	±1.36
364	LOX	log P^2	-0.01	±0.02										5.32	±0.32
365	LOX	log P^2	0.01	±0.02	CDK1	0.28	±0.15							3.34	±1.10

Table 7-5b: Statistical quantities corresponding to the regression equations in table 7-5a (continuation)

#	n	r	s	t_1	t_2	t_3	t_4	t_l	F	q^2
354	65	0.587	0.543	2.23	1.36	2.27	2.98	4.39	7.90	0.234
355	67	0.444	0.653	1.94	1.22	3.54		1.82	5.16	0.043
356	65	0.441	0.552	3.90				9.73	15.22	0.141
357	64	0.420	0.562	3.64				12.99	13.27	0.117
358	65	0.510	0.529	4.70				8.23	22.14	0.207
359	66	0.136	0.605	1.10				18.21	1.21	-0.038
360	65	0.457	0.552	1.05	3.86			4.61	8.17	0.122
361	64	0.443	0.559	1.23	3.71			5.14	7.44	0.109
362	65	0.513	0.532	0.52	4.54			5.13	11.08	0.190
363	64	0.533	0.537	0.51	0.35	0.31	2.34	4.13	5.85	0.129
364	66	0.157	0.603	1.27				33.34	1.62	-0.029
365	65	0.452	0.553	0.87	3.73			6.05	7.96	0.117

Table 7-5a: Regression equations, parameters with corresponding slopes and confidence intervals (continuation)

#	Y [pGI_{50}]	X_1	sl_1	ci_1 [95%]	X_2	sl_2	ci_2 [95%]	X_3	sl_3	ci_3 [95%]	X_4	sl_4	ci_4 [95%]	I	ci_I [95%]
366	LOX	log P^2	0.01	±0.03	CDK5	0.24	±0.14							3.62	±1.03
367	LOX	log P^2	0.01	±0.02	GSK3	0.31	±0.14							2.99	±1.07
368	LOX	log P^2	0.01	±0.03	CDK1	0.05	±0.28	CDK5	0.04	±0.24	GSK3	0.25	±0.21	2.82	±1.17
369	LOX	log P	0.24	±0.63	log P^2	-0.02	±0.08	CDK1	0.28	±0.15				2.86	±1.69

Table 7-5b: Statistical quantities corresponding to the regression equations in table 7-5a (continuation)

#	n	r	s	t_1	t_2	t_3	t_4	t_l	F	q^2
366	64	0.437	0.561	1.04	3.56			7.02	7.19	0.097
367	65	0.518	0.530	0.84	4.54			5.61	11.37	0.195
368	64	0.535	0.536	0.66	0.33	0.36	2.47	4.83	5.91	0.126
369	65	0.460	0.555	0.76	0.49	3.74		3.39	5.46	0.095

8 References

1. Kunick, C.: Fused azepinones with antitumor activity. *Curr. Pharm. Des.* **1999**, 5, 181-194.

2. Zaharevitz, D. W.; Gussio, R.; Leost, M.; Senderowicz, A.; Lahusen, T.; Kunick, C.; Meijer, L. and Sausville, E. A.: Discovery and initial characterization of the paullones, a novel class of small-molecule inhibitors of cyclin-dependent kinases. *Cancer Res.* **1999**, 59, 2566-2569.

3. Kelland, L. R.: Flavopiridol, the first cyclin-dependent kinase inhibitor to enter the clinic: current status. *Expt. Opin. Invest. Drugs* **2000**, 9, 2903-2911.

4. Zhai, S.; Senderowicz, A.; Sausville, E. and Figg, W. D.: Flavopiridol, a novel cyclin-dependent kinase inhibitor, in clinical development. *Ann. Pharmacother.* **2002**, 36, 905-911.

5. Leost, M.; Schultz, C.; Link, A.; Wu, Y.-Z.; Biernat, J.; Mandelkow, E.-M.; Bibb, J. A.; Snyder, G. L.; Greengard, P.; Zaharevitz, D. W.; Gussio, R.; Senderowicz, A.; Sausville, E.; Kunick, C. and Meijer, L.: Paullones are potent inhibitors of glycogen synthase kinase-3β and cyclin dependent kinase 5/p25. *Eur. J. Biochem.* **2000**, 267, 1-13.

6. Schultz, C.; Link, A.; Leost, M.; Zaharevitz, D. W.; Gussio, R.; Sausville, E. A.; Meijer, L. and Kunick, C.: Paullones, a series of cyclin-dependent kinase inhibitors: synthesis, evaluation of CDK1/ cyclin B inhibition, and in vitro antitumor activity. *J. Med. Chem.* **1999**, 42, 2909-2919.

7. Morgan, D. O.: Cyclin-dependent kinases: engines, clocks, and microprocessors. *Annu. Rev. Cell Dev. Biol.* **1997**, 13, 261-291.

8. Sielecki, T. M.; Boylan, J. F.; Benfield, P. A. and Trainor, G. L.: Cyclin-dependent kinase inhibitors: useful targets in cell cycle regulation. *J. Med. Chem.* **2000**, 43, 1-18.

9. Berman, H. M.; Westbrook, J.; Feng, Z.; Gilliland, G.; Bhat, T. N.; Weissig, H.; Shindyalov, I. N. and Bourne, P. E.: The Protein Data Bank. *Nucleic Acids Res.* **2000**, 28, 235-242.

10. Russo, A. A.; Jeffrey, P. D. and Pavletich, N. P.: Structural basis of cyclin-dependent kinase activation by phosphorylation. *Nat. Struct. Biol.* **1996**, 3, 696-700.

11. SYBYL 6.7, Tripos Inc., 1699 South Hanley Rd., St. Louis, Missouri, 63144, USA.

12. Lauenroth, K.: Paullonderivate mit veränderter heterozyklischer Grundstruktur als Inhibitoren Cyclin-abhängiger Kinasen. *Dissertation Universität Hamburg* **2001**.

13. Webster, K. R.: The therapeutic potential of targeting the cell cycle. *Exp. Opin. Invest. Drugs* **1998**, 7, 865-887.

14. Draetta, G. and Pagano, M.: Cell cycle control and cancer. *Annu. Rep. Med. Chem.* **1996**, 31, 241-248.

15. Pavletich, N. P.: Mechanisms of cyclin-dependent kinase regulation: structures of CDKs, their cyclin activators, and CIP and INK4 inhibitors. *J. Mol. Biol.* **1999**, 287, 821-828.

16. Coleman, K. G.; Lyssikatos, J. P. and Ynag, B. V.: Chemical inhibitors of cyclin-dependent kinases. *Annu. Rep. Med. Chem.* **1997**, 32, 171-179.

17. Kimball, S. D. and Webster, K. R.: Cell cycle kinases and checkpoint regulation in cancer. *Annu. Rep. Med. Chem.* **2001**, 36, 139-148.

18. Kim, S.-H.: Structure-based inhibitor design for CDK2, a cell cycle controlling protein kinase. *Pure Appl. Chem.* **1998**, 70, 555-565.

19. Davis, S. T.; Benson, B. G.; Bramson, H. N.; Chapman, D. E.; Dickerson, S. H.; Dold, K. M.; Eberwein, D. J.; Edelstein, M.; Frye, S. V.; Gampe, R. T., Jr.; Griffin, R. J.; Harris, P. A.; Hassell, A. M.; Holmes, W. D.; Hunter, R. N.; Knick, V. B.; Lackey, K.; Lovejoy, B.; Luzzio, M. J.; Murray, D.; Parker, P.; Rocque, W. J.; Shewchuk, L.; Veal, J. M.; Walker, D. H. and Kuyper, L. F.: Prevention of

chemotherapy-induced alopecia in rats by CDK inhibitors. *Science* **2001**, 291, 134-137.

20. Bramson, H. N.; Corona, J.; Davis, S. T.; Dickerson, S. H.; Edelstein, M.; Frye, S. V.; Gampe, R. T., Jr.; Harris, P. A.; Hassall, C. H.; Holmes, W. D.; Hunter, R. N.; Lackey, K.; Lovejoy, B.; Luzzio, M. J.; Montana, V.; Rocque, W. J.; Rusnak, D.; Shewchuk, L.; Veal, J. M.; Walker, D. H. and Kuyper, L. F.: Oxindole-based inhibitors of cyclin-dependent kinase 2 (CDK2): design, synthesis, enzymatic activities, and X-ray crystallographic analysis. *J. Med. Chem.* **2001**, 44, 4339-4358.

21. Schoepfer, J.; Fretz, H.; Chaudhuri, B.; Muller, L.; Seeber, E.; Meijer, L.; Lozach, O.; Vangrevelinghe, E. and Furet, P.: Structure-based design and synthesis of 2-benzylidene-benzofuran-3-ones as flavopiridol mimics. *J. Med. Chem.* **2002**, 45, 1741-1747.

22. Barvian, M.; Boschelli, D. H.; Cossrow, J.; Dobrusin, E.; Fattaey, A.; Fritsch, A.; Fry, D.; Harvey, P.; Keller, P.; Garrett, M.; La, F.; Leopold, W.; McNamara, D.; Quin, M.; Trumpp-Kallmeyer, S.; Toogood, P.; Wu, Z. and Zhang, E.: Pyrido[2,3-*d*]pyrimidin-7-one inhibitors of cyclin-dependent kinases. *J. Med. Chem.* **2000**, 43, 4606-4616.

23. Nugiel, D. A.; Vidwans, A.; Etzkorn, A.-M.; Rossi, K. A.; Benfield, P. A.; Burton, C. R.; Cox, S.; Doleniak, D. and Seitz, S. P.: Synthesis and evaluation of indenopyrazoles as cyclin-dependent kinase inhibitors. 2. Probing the indeno ring substituent pattern. *J. Med. Chem.* **2002**, 45, 5224-5232.

24. Yue, E. W.; Higley, C. A.; DiMeo, S. V.; Carini, D. J.; Nugiel, D. A.; Benware, C.; Benfield, P. A.; Burton, C. R.; Cox, S.; Grafstrom, R. H.; Sharp, D. M.; Sisk, L. M.; Boylan, J. F.; Muckelbauer, J. K.; Smallwood, A. M.; Chen, H.; Chang, C.-H.; Seitz, S. P. and Trainor, G. L.: Synthesis and evaluation of indenopyrazoles as cyclin-dependent kinase inhibitors. 3. Structure activity relationships at C3. *J. Med. Chem.* **2002**, 45, 5233-5248.

25. Kim, K. S.; Kimball, S. D.; Misra, R. N.; Rawlins, D. B.; Hunt, J. T.; Xiao, H.-Y.; Lu, S.; Qian, L.; Han, W.-C.; Shan, W.; Mitt, T.; Cai, Z.-W.; Poss, M. A.; Zhu, H.; Sack, J. S.; Tokarski, J. S.; Chang, C. Y.;

Pavletich, N. P.; Kamath, A.; Humphreys, W. G.; Marathe, P.; Bursuker, I.; Kellar, K. A.; Roongta, U.; Batorsky, R.; Mulheron, J. G.; Bol, D.; Fairchild, C. R.; Lee, F. Y. and Webster, K. R.: Discovery of aminothiazole inhibitors of cyclin-dependent kinase 2: synthesis, X-ray crystallographic analysis, and biological activities. *J. Med. Chem.* **2002**, 45, 3905-3927.

26. Krystof, V.; Lenobel, R.; Havlicek, L.; Kuzma, M. and Strnad, M.: Synthesis and biological activity of olomoucine II. *Bioorg. Med. Chem. Lett.* **2002**, 12, 3283-3286.

27. Meijer, L.; Leclerc, S. and Leost, M.: Properties and potential applications of chemical inhibitors of cyclin-dependent kinases. *Pharmacol. Ther.* **1999**, 82, 279-284.

28. Gray, N.; Detivaud, L.; Doerig, C. and Meijer, L.: ATP-site directed inhibitors of cyclin-dependent kinases. *Curr. Med. Chem.* **1999**, 6, 859-875.

29. Meijer, L.: Cyclin-dependent kinases inhibitors as potential anticancer, antineurogenerative, antiviral and antiparasitic agents. *Drug Resist. Updates* **2000**, 3, 83-88.

30. Ruetz, S.; Woods-Cook, K.; Solf, R.; Meyer, T.; Zimmermann, J. and Fabbro, D.: Effect of CGP 60474 on cyclin-dependent kinases (CDKs), cell cycle proliferation and onset of apoptosis in normal and transformed cells. *Proc. Am. Assoc. Cancer Res.* **1998**, 39, 558.

31. Bresnahan, W. A.; Boldogh, I.; Chi, P.; Thompson, E. A. and Albrecht, T.: Inhibition of cellular Cdk2 activity blocks human cytomegalovirus replication. *Virology* **1997**, 231, 239-247.

32. Schang, L. M.; Phillips, J. and Schaffer, P. A.: Requirement for cellular cyclin-dependent kinases in herpes simplex virus replication and transcription. *J. Virol.* **1998**, 72, 5626-5637.

33. Ye, M.; Duus, K. M.; Peng, J.; Price, D. H. and Grose, C.: Varicella-zoster virus Fc receptor component gI is phosphorylated on its endodomain by a cyclin-dependent kinase. *J. Virol.* **1999**, 73, 1320-1330.

34. Markus, M. A.; Kahle, P. J.; Winkler, A.; Horstmann, S.; Anneser, J. M. H. and Borasio, G. D.: Survival-promoting activity of inhibitors of cyclin-dependent kinases on primary neurons correlates with inhibition of c-jun kinase-1. *Neurobiol. Dis.* **1997**, 4, 122-133.

35. Imahori, K. and Uchida, T.: Physiology and pathology of tau protein kinases in relation to Alzheimer's disease. *J. Biochem. (Tokyo)* **1997**, 121, 179-188.

36. Mandelkow, E.: The tangled tale of tau. *Nature* **1999**, 402, 588-589.

37. Garcia-Perez, J.; Avila, J. and Diaz-Nido, J.: Implication of cyclin-dependent kinases and glykogen synthase kinase 3 in the phosphorylation of microtubule-associated protein 1B in developing neuronal cells. *J. Neurosci. Res.* **1998**, 52, 445-452.

38. Vincent, I.; Jicha, G.; Rosado, M. and Dickson, D. W.: Aberrant expression of mitotic cdc2/cyclin B1 kinase in degenerating neurons of Alzheimer's disease brain. *J.Neurosci.* **1997**, 17, 3588-3598.

39. Kappes, B.; Doerig, C. D. and Graeser, R.: An overview of *Plasmodium* protein kinases. *Parasitol. Today* **1999**, 15, 449-454.

40. Doerig, C.: Signal transduction in malaria parasites. *Parasitol. Today* **1997**, 13, 307-313.

41. Gomez, E. B.; Kornblihtt, A. R. and Tellez-Inon, M. T.: Cloning of cdc2-related protein kinase from *Trypanosoma cruzi* that interacts with mammalian cyclins. *Mol. Biochem. Parasitol.* **1998**, 91, 337-351.

42. Mottram, J. C.; Kinnaird, J.; Shiels, B.; Tait, A. and Barry, J. D.: A novel CDC2-related protein kinase from *Leishmania mexicana*, lmmCRK1, is post-translationally regulated during the life cycle. *J. Biol. Chem.* **1993**, 268, 21044-21051.

43. Wastling, J. M. and Kinnaird, J. H.: Isolation and characterisation of a genomic clone encoding a cdc2-related kinase of Toxoplasma gondii. *Mol. Biochem. Parasitol.* **1998**, 94, 143-148.

44. Kunick, C.: Synthese [*b*]-kondensierter Azepindione durch Dealkoxycarbonylierung. *Arch. Pharm. (Weinheim)* **1991**, 324, 579-581.

45. Link, A.: Antitumoraktive Pyrido[3,2-*d*]-1-benzazepine. *Dissertation Universität Hamburg* **1996**.

46. Schultz, C.: Antitumoraktive [*d*]-anellierte [1]Benzazepin-2-one. *Dissertation Universität Hamburg* **1999**.

47. Robinson, B.: The Fischer indole synthesis. *Chem. Rev.* **1963**, 63, 373-401.

48. Smith, M. E.; Elisberg, E. and Sherrill, M. L.: Quinazoline Derivatives. II. Synthesis of 4-(4´-Diethylamino-1´-methylbutylamino)-6-methoxyquinazoline (SN 12,253). *J. Am. Chem. Soc.* **1946**, 68, 1301-1303.

49. Hodgson, H. and Handley, F.: Studies in colour and constitution. Part III. The influence of methylthiol, methoxy-, and chlorine groups on the colours of the nitrobenzaldehydephenylhydrazones. *J. Chem. Soc.* **1928**, 130, 1882-1886.

50. Enders: Arylhydrazine und Arylhydrazone. Herstellung von Arylhydrazinen. Arylhydrazine durch Reduktion von Diazoverbindungen. In: Müller, E.: *Methoden der Organischen Chemie (Houben-Weyl)*. **1967**, Georg Thieme Verlag, Stuttgart, 180-223.

51. Soliman, R.: Preparation and antidiabetic activity of some sulfonylurea derivatives of 3,5-disubstituted pyrazoles. *J. Med. Chem.* **1979**, 22, 321-325.

52. Kunick, C.: Synthese von 7,12-Dihydro-indolo[3,2-*d*][1]benzazepin-6-(5*H*)-onen und 6,11-Dihydro-thieno-[3',2':2,3]azepino[4,5-*b*]indol-5(4*H*)-on. *Arch. Pharm. (Weinheim)* **1992**, 325, 297-299.

53. Potts, K. T.; Cipullo, M. J.; Ralli, P. and Theodoridis, G.: Synthesis of 2,6-disubstituted pyridines, polypyridinyls, and annulated pyridines. *J. Org. Chem.* **1982**, 47, 3027-3038.

54. Page, P. C. B.; Graham, A. E.; Bethell, D. and Park, B. K.: A simple and convenient method for the oxidation of sulphides. *Synth. Commun.* **1993**, 23, 1507-1514.

55. Bordwell, F. G. and Boutan, P. J.: Synthesis of aryl methyl sulfoxides and determination of the conjugative effect of the methylsulfinyl group. *J. Am. Chem. Soc.* **1957**, 79, 717-722.

56. Ternay, J., A.L.; Ens, L.; Herrmann, J. and Evans, S.: The stereochemistry of thioxanthene sulfoxide and its C-9 methylated analogs. The control of conformational distribution in folded molecules by *peri* substitution. *J. Org. Chem.* **1969**, 34, 940-945.

57. Roth, H. J.; Müller, C. E. and Folkers, G.: Stereochemie der Arzneistoffe I: Chirale Verbindungen. In: *Stereochemie & Arzneistoffe*. **1998**, Wissenschaftliche Verlagsgesellschaft, Stuttgart, 33-104.

58. Hesse, M.; Meier, H. and Zeeh, B.: Kernresonanz-Spektren. NMR-Spektren und Molekülstruktur. In: *Spektroskopische Methoden in der organischen Chemie*. **1995**, Georg Thieme Verlag, Stuttgart, 86-100.

59. Lidström, P.; Tierney, J.; Wathey, B. and Westman, J.: Microwave assisted organic synthesis. *Tetrahedron* **2001**, 57, 9225-9283.

60. Dzierba, C. D. and Combs, A. P.: Microwave-assisted chemistry as a tool for drug discovery. *Annu. Rep. Med. Chem.* **2002**, 37, 247-256.

61. Fischer, E. and Speier, A.: Darstellung der Ester. *Chem. Ber.* **1895**, 28, 3252-3258.

62. Mitsunobu, O. and Yamada, M.: Preparation of esters of carboxylic and phosphoric acid via quaternary phosphonium salts. *Chem. Soc. Jpn.* **1967**, 40, 2380-2382.

63. Mitsunobu, O.: The use of diethyl azodicarboxylate and triphenylphosphine in synthesis and transformation of natural products. *Synthesis* **1981**, 1-28.

64. Walter, W. and Francke, W.: Derivate aliphatischer Monocarbonsäuren. In: Beyer, H. and Walter, W.: *Lehrbuch der Organischen Chemie*. **1998**, S. Hirzel Verlag, Stuttgart, 266-286.

65. Benz, G.: Synthesis of amides and related compounds. In: Trost, B.M.: *Comprehensive Organic Synthesis*. **1991**, Pergamon Press, Oxford, 381-417.

66. Kurzer, F. and Douraghi-Zadeh, K.: Advances in the chemistry of carbodiimides. *Chem. Rev.* **1967**, 67, 107-152.

67. Hudson, D.: Methodological implications of simultaneous solid-phase peptide synthesis. 1. Comparison of different coupling procedures. *J. Org. Chem.* **1988**, 53, 617-624.

68. Ito, H.; Takamatsu, N. and Ichikizaki, I.: The peptide synthesis using unsymmetrical carbodiimides. *Chem. Lett.* **1977**, 539-542.

69. Tartar, A. and Gesquiere, J.-C.: Formation of CH_2Cl_2-soluble urea derivatives during solid phase peptide synthesis with unsymmetrical carbodiimides. *J. Org. Chem.* **1979**, 44, 5000-5002.

70. March, J.: Aliphatic nucleophilic substitution. In: *Advanced Organic Chemistry: Reactions, Mechanisms and Structure*. **1985**, John Wiley & Sons, New York, 255-446.

71. Wackerle, L.: Racemisierungsfreie Aktivierung von α-Aminosäuren mittels Isocyaniden. *Synthesis* **1979**, 197-198.

72. Aigner, H. and Marquarding, D.: Synthese von Amiden aus Carbonsäuren und Amiden in Gegenwart von Isocyaniden. *Tetrahedron Lett.* **1978**, 3325-3326.

73. Prabhakaran, P. V.; Jayadev, S.; Nema, S. K. and Rao, K. V. C.: Nucleophilic substitution of urea on aromatic carboxylic acids via phosphorylation. *Indian J. Chem. Sect. B* **1991**, 30, 1072-1073.

74. Harada, H.; Morie, T.; Hirokawa, Y.; Terauchi, H.; Fujiwara, I.; Yoshida, N. and Kato, S.: Development of potent serotonin -3 (5-HT_3) receptor antagonists. II. Structure-activity relationships of N-(1-benzyl-4-methylhexahydro-1*H*-1,4-diazepin-6-yl)carboxamides. *Chem. Pharm. Bull.* **1995**, 43, 1912-1930.

75. Walter, W. and Francke, W.: Aminosaeuren, Peptide und Proteine. In: Beyer, H. and Walter, W.: *Lehrbuch der Organischen Chemie*. **1998**, S. Hirzel Verlag, Stuttgart, 881-917.

76. Bailey, P. D.; Collier, I. D. and Morgan, K. M.: Amides. In: Katritzky, A.; Meth-Cohn, A. and Rees, C.W.: *Comprehensive Organic Functional Group Transformations*. **1995**, Pergamon Press, Cambridge, 257-307.

77. Madson, P.; Lundbeck, J. M.; Jakobsen, P.; Varming, A. R. and Westergaard, N.: Glucose-6-phosphatase catalytic enzyme inhibitors: synthesis and in vitro evaluation of novel 4,5,6,7-tetrahydrothieno[3,2-c]- and [2,3-c] pyridines. *Bioorg. Med. Chem.* **2000**, 8, 2277-2289.

78. Albrecht, M.; Napp, M. and Schneider, M.: The synthesis of amino acid bridged dicatechol derivatives. *Synthesis* **2001**, 468-472.

79. Herr, R. J.: 5-Substituted-1*H*-tetrazoles as carboxylic acid isosteres: medicinal chemistry and synthetic methods. *Bioorg. Med. Chem.* **2002**, 10, 3379-3393.

80. Alterman, M. and Hallberg, A.: Fast microwave-assisted preparation of aryl and vinyl nitriles and the corresponding tetrazoles from organo-halides. *J. Org. Chem.* **2000**, 65, 7984-7989.

81. Agarwal, A.; Jalluri, R. K.; DeWitt Blanton, J., C. and Taylor, E. W.: A new synthesis of the potent 5-HT_1 receptor ligand, 5-carboxyamidotryptamine (5-CT). *Synth. Commun.* **1993**, 23, 1101-1110.

82. Finnegan, W. G.; Henry, R. A. and Lofquist, R.: An improved synthesis of 5-substituted tetrazoles. *J. Am. Chem. Soc.* **1958**, 80, 3908-3911.

83. Peet, N. P.: An unexpected aminolysis in the synthesis of 5-substituted 3-(1*H*-tetrazol-5-yl)pyrazolo[1,5-α]quinazolines. *J. Heterocycl. Chem.* **1989**, 26, 713-716.

84. Ried, W. and Aboul-Fetouh, S.: Synthese neuer substituierter 5,6-Dihydro-tetrazolo-[1,5-c]chinazoline, Tetrazolo[1,5-c]chinazoline,

5,6-Dihydro-pyrimido[5,4-e]tetrazolo[1,5-c]pyrimidine und 5,6-Dihydro-tetrazolo[1,5-c]pyrimidine. *Chem.-Ztg.* **1988**, 112, 135-140.

85. Ried, W. and Laoutidis, J.: Synthese neuer heterocyclischer Phane aus 1,2,3-Triazolo-4,5-dicarbonitril. *Chem.-Ztg.* **1989**, 113, 384-385.

86. Herbst, R. M. and Wilson, K. R.: Apparent acidic dissociation of some 5-aryltetrazoles. *J. Org. Chem.* **1957**, 22, 1142-1145.

87. Arnold, J., C. and Thatcher, D. N.: Preparation and reactions of 5-vinyltetrazole. *J. Org. Chem.* **1969**, 34, 1141-1142.

88. Duncia, J. V.; Pierce, M. E. and Santella, J. B. I.: Three synthetic routes to a sterically hindered tetrazole. A new one-step mild conversion of an amide into a tetrazole. *J. Org. Chem.* **1991**, 56, 2395-2400.

89. Kricheldorf, H. R. and Leppert, E.: Synthese von Isocyanaten, Alkyl-carbamaten und Harnstoffen aus Carbonsäure-Derivaten und Tributylstannyl-azid. *Synthesis* **1976**, 329-330.

90. Luijten, J. G. A.; Janssen, M. J. and Van der Kerk, G. J. M.: New organotin compounds containing a tin-nitrogen linkage. *Recl. Trav. Chim. Pays Bas* **1962**, 81, 202-205.

91. Riesen, R. and Widmann, G.: Thermogravimetrie. In: Oehme, F.: *Thermoanalyse - Anwendungen, Begriffe, Methoden*. **1984**, Hüthig Verlag, Heidelberg, 108-109.

92. MacPhillamy, H. B.; Dziemian, R. L.; Lucas, R. A. and Kuehne, M. E.: The alkaloids of *Tabernanthe iboga*. Part VI. The synthesis of the selenium dehydrogenation products from ibogamine. *J. Am. Chem. Soc.* **1958**, 80, 2172-2178.

93. Hörlein, U. and Geiger, W.: Hydroxycarbostyril-alkancarbonsäuren und Dihydro-benzazepinolon-carbonsäureester. IV. Mitt. *Arch. Pharm. (Weinheim)* **1971**, 304, 167-175.

94. Moore, H. W.; Shelden, H. R. and Weyler, J., W.: Rearrangement of azidoquinones IV. Ring expansion of 4-azido-1,2-naphtoquinone. *Tetrahedron Lett.* **1969**, 1243-1246.

95. Rees, A. H. and Simon, K.: Some derivatives of 1-benzazepine. *Can. J. Chem.* **1969**, 47, 1227-1230.

96. Hughes, C. G. and Rees, A. H.: 2,3-Dihydro-2,3-dioxo-1-benzazepine. *Chem. Ind. (London)* **1971**, 50, 1439.

97. Jones, G.: Synthesis of the quinoline ring system. In: Weissberger, A. and Taylor, E.C.: *The Chemistry of Heterocyclic Compounds. Quinolines, Part I.* **1977**, John Wiley & Sons, London, 93-318.

98. Thomas, G.: Structure de l'acide quinaldique deduite de l'examen de ses spectres infrarouges. *Bull. Soc. Chim. Fr.* **1962**, 796-799.

99. Goher, M. A. S. and Hafez, A. K.: Studies on some quinoline derivatives. I. Copper(I) complexes of quinaldic acid and methyl and ethyl quinaldates. *Bull. Soc. Chim. Fr.* **1980**, 287-293.

100. Hesse, M.; Meier, H. and Zeeh, B.: Kernresonanz-Spektren. ^{1}H-Kernresonanz-Spektroskopie. In: *Spektroskopische Methoden in der organischen Chemie*. **1995**, Georg Thieme Verlag, Stuttgart, 100-142.

101. Skoog, D. A. and Leary, J. J.: Application of molecular ultraviolet/visible absorption spectroscopy. In: *Principles of Instrumental Analysis*. **1992**, Saunders College Publishing, Fort Worth, 150-173.

102. Li, K.; Helm, R. F. and Eriksson, K.-E. L.: Mechanistic studies of the oxidation of a non-phenolic lignin model compound by the laccase/1-hydroxybenzotriazole redox system. *Biotechnol. Appl. Biochem.* **1998**, 27, 239-243.

103. Xu, F.; Kulys, J. J.; Duke, K.; Li, K.; Krikstopaitis, K.; Deussen, H.-J. W.; Abbate, E.; Galinyte, V. and Schneider, P.: Redox chemistry in laccase-catalyzed oxidation of N-hydroxy compounds. *Appl. Environ. Microbiol.* **2000**, 66, 2052-2056.

104. Niku-Paavola, M.-L. and Viikari, L.: Enzymatic oxidation of alkenes. *J. Molec. Catal. B: Enzym.* **2000**, 10, 435-444.

105. Xu, F.; Deussen, H.-J. W.; Lopez, B. and Li, K.: Enzymatic and electrochemical oxidation of N-hydroxy compounds. Redox potential, electron-transfer kinetics, and radical stability. *Eur. J. Biochem.* **2001**, 268, 4169-4176.

106. Ishii, Y.; Nakayama, K.; Takeno, M.; Sakaguchi, S.; Iwahama, T. and Nishiyama, Y.: A novel catalysis of N-hydroxyphthalimide in the oxidation of organic substrates by molecular oxygen. *J. Org. Chem.* **1995**, 60, 3934-3935.

107. Matsunaka, K.; Iwahama, T.; Sakaguchi, S. and Ishii, Y.: A remarkable effect of quaternary ammonium bromide for the N-hydroxyphthalimide-catalyzed aerobic oxidation of hydrocarbons. *Tetrahedron Lett.* **1999**, 40, 2165-2168.

108. Miniski, F.; Punta, C.; Recupero, F.; Fontana, F. and Pedulli, G. F.: A new, highly selective synthesis of aromatic aldehydes by aerobic free-radical oxidation of benzylic alcohols, catalysed by *n*-hydroxyphthalimide under mild conditions. Polar and enthalpic effects. *Chem. Commun.* **2002**, 688-689.

109. Howard, J. A.: Free radical reaction mechanisms involving peroxides in solution. In: Patai, S.: *The Chemistry of Functional Groups. The chemistry of peroxides*. **1983**, John Wiley & Sons, Chichester, 235-258.

110. Criegee, R.: Herstellung und Umwandlung von Peroxyden. In: Müller, E.: *Methoden der Organischen Chemie (Houben-Weyl). Sauerstoffverbindungen III*. **1952**, Georg Thieme Verlag, Stuttgart, 5-74.

111. Cullis, C. F. and Fish, A.: Carbonyl-forming oxidations. In: Patai, S.: *The Chemistry of Functional Groups. The chemistry of the carbonyl group*. **1966**, John Wiley & Sons, London, 79-176.

112. Robertson, A. and Waters, W. A.: Studies on the autoxidation of tetralin. Part II. The decomposition of tetralin hydroperoxide. *J. Chem. Soc.* **1948**, 150, 1578-1585.

113. Frame, S. and Cohen, P.: GSK3 takes centre stage more than 20 years after its discovery. *Biochem. J.* **2001**, 359, 1-16.

114. Martinez, A.; Castro, A.; Dorronsoro, I. and Alonso, M.: Glygogen synthase kinase 3 (GSK-3) inhibitors as new promising drugs for diabetes, neurodegeneration, cancer and inflammation. *Med. Res. Rev.* **2002**, 22, 373-384.

115. Wieking, K.: Strukturmodifikationen und Affinitätsuntersuchungen zur Aufklärung des Wirkmechanismus von Paullonen. *Dissertation Universität Hamburg* **2001**.

116. Weinstein, J. N.; Myers, T. G.; O'Connor, P. M.; Friend, S. H.; Fornace, A. J., Jr.; Kohn, K. W.; Fojo, T.; Bates, S. E.; Rubinstein, L. V.; Anderson, N. L.; Buolamwini, J. K.; van Osdol, W. W.; Monks, A. P.; Scudiero, D. A.; Sausville, E. A.; Zaharevitz, D. W.; Bunow, B.; Viswanadhan, V. N.; Johnson, G. S.; Wittes, R. E. and Paull, K. D.: An information-intensive approach to the molecular pharmacology of cancer. *Science* **1997**, 275, 343-349.

117. Boyd, M. R.: Status of the NCI preclinical antitumor drug discovery screen. *Principles Practice Oncol.* **1989**, 3, 1-12.

118. Grever, M. R.; Schepartz, S. A. and Chabner, B. A.: The National Cancer Institute: cancer drug discovery and development program. *Semin. Oncol.* **1992**, 19, 622-638.

119. Monks, A.; Scudiero, D.; Skehan, P.; Shoemaker, R.; Paull, K.; Vistica, D.; Hose, C.; Langley, J.; Cronise, P.; Vaigro-Wolff, A.; Gray-Goodrich, M.; Campbell, H.; Mayo, J. and Boyd, M.: Feasibility of a high-flux anticancer drug screen using a diverse panel of cultured human tumor cell lines. *J. Natl. Cancer Inst.* **1991**, 83, 757-766.

120. Monks, A.; Scudiero, D. A.; Johnson, G. S.; Paull, K. D. and Sausville, E. A.: The NCI anti-cancer drug screen: a smart screen to identify effectors of novel targets. *Anti-Cancer Drug Des.* **1997**, 12, 533-541.

121. Robert, J.: Anticancer screening with in vitro models. *Drugs Fut.* **1997**, 22, 739-746.

122. Salvati, L.; Bolognesi, M. and Ascenzi, P.: Does inhibition of *Trypanosoma cruzi* key enzymes affect parasite life cycle and geographic distribution? *IUBMB Life* **2002**, 53, 45-47.

123. Urbina, J. A.: Specific treatment of Chagas disease: current status and new developments. *Curr. Opin. Infect. Dis.* **2001**, 14, 733-741.

124. Kunick, C. and Lemcke, T.: Paullone als selektive Kinase-Inhibitoren. *Pharm. Ztg.* **2002**, 147, 2428-2435.

125. Gussio, R.; Zaharevitz, D. W.; McGrath, C. F.; Pattabiraman, N.; Kellogg, G. E.; Schultz, C.; Link, A.; Kunick, C.; Leost, M.; Meijer, L. and Sausville, E.: Structure-based design modifications of the paullone molecular scaffold for cyclin-dependent kinase inhibition. *Anti-Cancer Drug Des.* **2000**, 15, 53-66.

126. Gerber, P. R. and Müller, K.: MAB, a generally applicable molecular force field for structure modelling in medicinal chemistry. *J. Comput.-Aided Mol. Design* **1995**, 9, 251-268.

127. Gerber, P. R.: Charge distribution from a simple molecular orbital type calculation and non-bonding interaction terms in the force field MAB. *J. Comput.-Aided Mol. Design* **1998**, 12, 37-51.

128. Böhm, H.-J.; Klebe, G. and Kubinyi, H.: Quantitative Struktur-Wirkungsbeziehungen. In: *Wirkstoffdesign*. **1996**, Spektrum Akademischer Verlag, Heidelberg, 363-380.

129. Kubinyi, H.: Der Schlüssel zum Schloß. II. Hansch-Analyse, 3D-QSAR und *De novo*-Design. *Pharm. Unserer Zeit* **1994**, 23, 281-290.

130. Lee, A. D.; Ren, S. and Lien, E. J.: Purine analogs as CDK enzyme inhibitory agents: A survey and QSAR analysis. *Prog. Drug Res.* **2001**, 56, 155-193.

131. Hansch, C.; Rockwell, S. D.; Jow, P. Y. C.; Leo, A. and Steller, E. E.: Substituent constants for correlation analysis. *J. Med. Chem.* **1977**, 20, 304-306.

132. Seydel, J. K. and Schaper, K.-J.: Statistische Auswertung durch Regressionsanalysen. In: *Chemische Struktur und biologische Aktivität von Wirkstoffen*. **1979**, Verlag Chemie, Weinheim, 242-255.

133. Seydel, J. K. and Schaper, K.-J.: Darstellung der für Struktur-Wirkung-Beziehungen wichtigen physiko-chemischen Struktur-Parameter. In: *Chemische Struktur und biologische Aktivität von Wirkstoffen*. **1979**, Verlag Chemie, Weinheim, 57-91.

134. Wilkowska, E. and Golebiewski, W. M.: Review of methods applied to search structure-activity relationship. *Pestycydy (Warsaw)* **2001**, 53-64.

135. Hansch, C.; Leo, A.; Unger, S. H.; Kim, K. H.; Nikaitani, D. and Lien, E. J.: "Aromatic" substituent constants for structure-activity correlations. *J. Med. Chem.* **1973**, 16, 1207-1216.

136. Swain, C. G. and Lupton, E. C., Jr.: Field and resonance components of substituent effects. *J. Amer. Chem. Soc.* **1968**, 90, 4328-4337.

137. Silipo, C. and Vittoria, A.: Three-dimensional structure of drugs. In: Ramsden, C.A.: *Comprehensive Medicinal Chemistry. Quantitative Drug Design*. **1990**, Pergamon Press, Oxford, 153-204.

138. Coburn, R. A. and Solo, A. J.: Quantitative structure-activity relationships among steroids. Investigations of the use of steric parameters. *J. Med. Chem.* **1976**, 19, 748-754.

139. Tute, M. S.: History and objectives of quantitative drug design. In: Hansch, C.; Sammes, P.G. and Taylor, J.B.: *Comprehensive Medicinal Chemistry. Quantitative Drug Design*. **1990**, Pergamon Press, Oxford, 1-31.

140. Hansch, C. and Leo, A.: Table 13-10: Substituents arranged according to their distance from hydrogen. In: *Exploring QSAR. Fundamentals and Applications in Chemistry and Biology*. **1995**, American Chemical Society, Washington, DC, 522-528.

141. Shorter, J.: Introduction to statistical methods necessary for correlation analysis. In: Atkins, P.W.; Holker, J.S.E. and Holliday, A.K.: *Correlation analysis in organic chemistry: an introduction to linear free-energy relationships*. **1973**, Oxford University Press, Oxford, 103-109.

142. Lahusen, T.; De Siervi, A.; Kunick, C. and Senderowicz, A. M.: Alsterpaullone, a novel cyclin-dependent kinase inhibitor, induces apoptosis by activation of caspase-9 due to perturbation in mitochondrial membrane potential. *Mol. Carcinog.* **2003**, 36, 183-194.

143. Perrin, D. D. and Armarego, W. L. F.: In: *Purification of Laboratory Chemicals*. **1988**, Pergamon Press, Oxford, 57-371.

144. Balasubramaniyan, V. and Argade, N.: Reactions of cyclic anhydrides: Part XIII - Facile synthesis of 1,2,3,4-tetrahydro-10*H*-

pyridazino[6,1-*b*]quinazoline-2,10-diones. *Indian J. Chem.* **1988**, 27B, 906-908.

145. Moriconi, E. J. and Maniscalco, I. A.: π-Equivalent heterocyclic congeners of tropone. Azatropones. *J. Org. Chem.* **1972**, 37, 208-215.

146. Meijer, L.; Borgne, A.; Mulner, O.; Chong, J. P. J.; Blow, J. J.; Inagaki, N.; Inagaki, M.; Delcros, J.-G. and Moulinoux, J.-P.: Biochemical and cellular effects of roscovitine, a potent and selective inhibitor of the cyclin-dependent kinases cdc2, cdk2 and cdk5. *Eur. J. Biochem.* **1997**, 243, 527-536.

147. Mettey, Y.; Gompel, M.; Thomas, V.; Garnier, M.; Leost, M.; Ceballos-Picot, I.; Noble, M.; Endicott, J.; Vierfond, J.-M. and Meijer, L.: Aloisines, a new family of CDK/GSK-3 inhibitors. SAR study, crystal structure in complex with CDK2, enzyme selectivity, and cellular effects. *J. Med. Chem.* **2003**, 46, 222-236.

148. Leclerc, S.; Garnier, M.; Hoessel, R.; Marko, D.; Bibb, J. A.; Snyder, G. L.; Greengard, P.; Biernat, J.; Wu, Y.-Z.; Mandelkow, E.-M.; Eisenbrand, G. and Meijer, L.: Indirubins inhibit glycogen synthase kinase-3β and CDK5/p25, two protein kinases involved in abnormal tau phosphorylation in Alzheimer's disease. *J. Biol. Chem.* **2001**, 276, 251-260.

149. Baltz, T.; Baltz, D.; Giroud, C. and Crockett, J.: Cultivation in a semi-defined medium of animal infective forms of *Trypanosoma brucei*, *T. equiperdum*, *T. evansi*, *T. rhodesiense* and *T. gambiense*. *EMBO J.* **1985**, 4, 1273-1277.

150. Räz, B.; Iten, M.; Grether-Bühler, R.; Kaminsky, R. and Brun, R.: The Alamar Blue assay to describe drug sensitivity of African trypanosomes (*T. b. rhodesiense* and *T. b. gambiense*) in vitro. *Acta trop.* **1997**, 68, 139-147.

151. Hansch, C.: *Rélations structure-activité. Séminaire*. **1974**, Société de Chimie Thérapeutique, Paris.

152. Seydel, J. K. and Schaper, K.-J.: Tab. 12.6: Substituenten-Konstanten. In: *Chemische Struktur und biologische Aktivität von Wirkstoffen*. **1979**, Verlag Chemie, Weinheim, 266-288.

9 Hazardous Substances

Concerning the toxicological properties of the compounds synthesized within the scope of this thesis and those of certain chemicals employed in the performed syntheses, the data called for by the Chemicals Act is not available. Hazardous properties cannot be excluded. Therefore, the chemicals should be regarded as hazardous substances and be treated with the appropriate caution.

The chemicals employed within the scope of this thesis that are listed below are classified in the appendix of the Ordinance on Hazardous Substances:

Acetic acid (100%):	C Corrosive
	R 10-35 Flammable - Causes severe burns
	S 23.2-26-45 Do not breathe vapor - In case of contact with eyes, rinse immediately with plenty of water and seek medical advice - In case of accident or if you feel unwell, seek medical advice immediately (show the label where possible)
Acetone:	F Highly flammable
	Xi Irritant
	R 11-36-66-67 Highly flammable - Irritating to eyes - Repeated exposure may cause skin dryness or cracking - Vapors may cause drowsiness and dizziness
	S 9-16-26 Keep container in a well ventilated place - Keep away from sources of ignition - No Smoking! - In case of contact with eyes, rinse immediately with plenty of water and seek medical advice

Acetonitrile:	F Highly flammable Xn Harmful R 11-20/21/22-36 Highly flammable - Harmful by inhalation, in contact with the skin and if swallowed - Irritating to eyes S 16-36/37 Keep away from sources of ignition - No Smoking! - Wear suitable protective clothing and gloves
Benzylamine:	C Corrosive R 21/22-34 Harmful in contact with the skin and if swallowed - Causes burns S 26-36/37/39-45 In case of contact with eyes, rinse immediately with plenty of water and seek medical advice - Wear suitable protective clothing, gloves and eye/face protection - In case of accident or if you feel unwell, seek medical advice immediately (show the label where possible)
1-Benzylpiperazine:	C Corrosive R 34 Causes burns S 26-36/37/39-45 In case of contact with eyes, rinse immediately with plenty of water and seek medical advice - Wear suitable protective clothing, gloves and eye/face protection - In case of accident or if you feel unwell, seek medical advice immediately (show the label where possible)
1-Butanol:	Xn Harmful R 10-22-37/38-41-67 Flammable - Harmful if swallowed - Irritating to respiratory system and skin - Risk of serious damage to eyes - Vapors may cause drowsiness and dizziness

S 7/9-13-26-37/39-46 Keep container tightly closed and in a well ventilated place - Keep away from food, drink and animal feedstuffs - In case of contact with eyes, rinse immediately with plenty of water and seek medical advice - Wear suitable gloves and eye/face protection - If swallowed, seek medical advice immediately and show the container or label

Butylamine:

F Highly flammable

C Corrosive

R 11-20/21/22-35 Highly flammable - Harmful by inhalation, in contact with the skin and if swallowed - Causes severe burns

S 3-16-26-29-36/37/39-45 Keep in a cool place - Keep away from sources of ignition - No Smoking! - In case of contact with eyes, rinse immediately with plenty of water and seek medical advice - Do not empty into drains - Wear suitable protective clothing, gloves and eye/face protection - In case of accident or if you feel unwell, seek medical advice immediately (show the label where possible)

tert-Butyl isocyanide:

F Highly flammable

T Toxic

R 11-23 Highly flammable - Toxic by inhalation

S 16-45 Keep away from sources of ignition - No Smoking! - In case of accident or if you feel unwell, seek medical advice immediately (show the label where possible)

N,*N'*-Carbonyldiimidazole:	Xi Irritant
	C Corrosive
	R 22-34-36/37/38 Harmful if swallowed - Causes burns - Irritating to eyes, respiratory system and skin
	S 26-36/37/39-45 In case of contact with eyes, rinse immediately with plenty of water and seek medical advice - Wear suitable protective clothing, gloves and eye/face protection - In case of accident or if you feel unwell, seek medical advice immediately (show the label where possible)
m-Chloroperbenzoic acid:	O Oxidative
	Xi Irritant
	R 5-8-36/37/38 Heating may cause an explosion - Contact with combustible material may cause fire - Irritating to eyes, respiratory system and skin
	S 17-26-36 Keep away from combustible material - In case of contact with eyes, rinse immediately with plenty of water and seek medical advice - Wear suitable protective clothing
Copper(I) cyanide:	T+ Very toxic
	N Environmentally dangerous compounds
	R 26/27/28-32-50/53 Very toxic by inhalation, in contact with the skin and if swallowed - Contact with acids liberates very toxic gas - Very toxic to aquatic organisms, may cause long term adverse effects in the aquatic environment
	S 7-28.1-29-45-60-61 Keep container tightly closed - After contact with skin, wash

	immediately with plenty of water - Do not empty into drains - In case of accident or if you feel unwell, seek medical advice immediately (show the label where possible) - This material and/or its container must be disposed of as hazardous waste - Avoid release to the environment. Refer to special instructions/ material safety data sheet
1,2-Diaminoethane:	C Corrosive
	R 10-21/22-34-42/43 Flammable - Harmful in contact with the skin and if swallowed - Causes burns - May cause sensitization by inhalation and skin contact
	S 23.2-26-36/37/39-45 Do not breathe vapor - In case of contact with eyes, rinse immediately with plenty of water and seek medical advice - Wear suitable protective clothing, gloves and eye/face protection - In case of accident or if you feel unwell, seek medical advice immediately (show the label where possible)
Di-*tert*-butyl	Xi Irritant
azodicarboxylate:	R 36/37/38 Irritating to eyes, respiratory system and skin
	S 26-36 In case of contact with eyes, rinse immediately with plenty of water and seek medical advice - Wear suitable protective clothing
2,4-Dichlorobenzylamine:	C Corrosive
	R 34 Causes burns
	S 26-36/37/39-45 In case of contact with eyes, rinse immediately with plenty of water and seek medical advice - Wear suitable protective clothing, gloves and eye/face protection - In case of accident or if you feel unwell, seek

	medical advice immediately (show the label where possible)
Dichloromethane:	Xn Harmful
	R 40 Possible risk of irreversible effects
	S 23.2-24/25-36/37 Do not breathe vapor - Avoid contact with skin and eyes - Wear suitable protective clothing and gloves
N,*N'*-Diisopropyl-	T+ Very toxic
carbodiimide:	R 10-26-41 Flammable - Very toxic by inhalation - Risk of serious damage to eyes
	S 24-26-28.1-39-45 Avoid contact with the skin - In case of contact with eyes, rinse immediately with plenty of water and seek medical advice - After contact with skin, wash immediately with plenty of water - Wear eye/face protection - In case of accident or if you feel unwell, seek medical advice immediately (show the label where possible)
4-Dimethylaminopyridine:	T Toxic
	R 24/25-36/38 Toxic in contact with the skin and if swallowed - Irritating to eyes and skin
	S 22-36/37 Do not breathe dust - Wear suitable protective clothing and gloves
N,*N*-Dimethylformamide:	T Toxic
	R 61-20/21-36 May cause harm to the unborn child - Harmful by inhalation and in contact with the skin - Irritating to eyes
	S 53-45 Avoid exposure - obtain special instructions before use - In case of accident or if you feel unwell, seek medical advice immediately (show the label where possible)

Dimethyl sulfoxide:	Xi Irritant
	R 36/38 Irritating to eyes and skin
	S 26 In case of contact with eyes, rinse immediately with plenty of water and seek medical advice
EDC:	Xi Irritant
	R 36/37/38 Irritating to eyes, respiratory system and skin
	S 26-36 In case of contact with eyes, rinse immediately with plenty of water and seek medical advice - Wear suitable protective clothing
Ethanol:	F Highly flammable
	R 11 Highly flammable
	S 7-16 Keep container tightly closed - Keep away from sources of ignition - No Smoking!
Ethyl acetate:	F Highly flammable
	Xi Irritant
	R 11-36-66-67 Highly flammable - Irritating to eyes - Repeated exposure may cause skin dryness or cracking - Vapors may cause drowsiness and dizziness
	S 16-26-33 Keep away from sources of ignition - No Smoking! - In case of contact with eyes, rinse immediately with plenty of water and seek medical advice - Take precautionary measures against static discharges
N-Ethyldiisopropylamine:	F Highly flammable
	C Corrosive
	R 11-22-34-52/53 Highly flammable - Harmful if swallowed - Causes burns - Harmful to

	aquatic organisms, may cause long term adverse effects in the aquatic environment
	S 16-26-36/37/39-45-61 Keep away from sources of ignition - No Smoking! - In case of contact with eyes, rinse immediately with plenty of water and seek medical advice - Wear suitable protective clothing, gloves and eye/face protection - In case of accident or if you feel unwell, seek medical advice immediately (show the label where possible) - Avoid release to the environment. Refer to special instructions/ material safety data sheet
Ethyl succinyl chloride:	C Corrosive
	R 34 Causes burns
	S 24/25 Avoid contact with skin and eyes
1-Hexanol:	X_n Harmful
	R 22 Harmful if swallowed
	S24/25 Avoid contact with skin and eyes
4-Hydrazinobenzoic acid:	Xi Irritant
	R 36/37/38 Irritating to eyes, respiratory system and skin
	S 26-36 In case of contact with eyes, rinse immediately with plenty of water and seek medical advice - Wear suitable protective clothing
Hydrochloric acid (37%):	C Corrosive
	R 34-37 Causes burns - Irritating to respiratory system
	S 26-36/37/39-45 In case of contact with eyes, rinse immediately with plenty of water and seek medical advice - Wear suitable protective clothing, gloves and eye/face protection - In

	case of accident or if you feel unwell, seek medical advice immediately (show the label where possible)
Hydrogen chloride	T Toxic
(gaseous):	C Corrosive
	R 23-35 Toxic by inhalation - Causes severe burns
	S 9-26-36/37/39-45 Keep container in a well ventilated place - In case of contact with eyes, rinse immediately with plenty of water and seek medical advice - Wear suitable protective clothing, gloves and eye/face protection - In case of accident or if you feel unwell, seek medical advice immediately (show the label where possible)
Hydrogen peroxide	C Corrosive
solution (35%):	R 34 Causes burns
	S28.1-36/39-45 After contact with skin, wash immediately with plenty of water - Wear suitable protective clothing and eye/face protection - In case of accident or if you feel unwell, seek medical advice immediately (show the label where possible)
1-Hydroxy-1*H*-benzotriazole (anhydrous):	R 44 Risk of explosion if heated under confinement S 15-36 Keep away from heat - Wear suitable protective clothing
Methanol:	F Highly flammable
	T Toxic
	R 11-23/24/25-39/23/24/25 Highly flammable - Toxic by inhalation, in contact with the skin and if swallowed - Toxic: danger of very

	serious irreversible effects through inhalation, in contact with skin and if swallowed
	S 7-16-36/37-45 Keep container tightly closed - Keep away from sources of ignition - No Smoking! - Wear suitable protective clothing and gloves - In case of accident or if you feel unwell, seek medical advice immediately (show the label where possible)
(4-Methoxybenzyl)amine:	C Corrosive
	R 34-37 Causes burns - Irritating to respiratory system
	S 26-36/37/39-45 In case of contact with eyes, rinse immediately with plenty of water and seek medical advice - Wear suitable protective clothing, gloves and eye/face protection - In case of accident or if you feel unwell, seek medical advice immediately (show the label where possible)
4-Methylpiperidine:	F Highly flammable
	C Corrosive
	R 11-34 Highly flammable - Causes burns
	S 16-26-36/37/39-45 Keep away from sources of ignition - No Smoking! - In case of contact with eyes, rinse immediately with plenty of water and seek medical advice - Wear suitable protective clothing, gloves and eye/face protection - In case of accident or if you feel unwell, seek medical advice immediately (show the label where possible)
1-Methyl-2-pyrrolidone:	Xi Irritant
	R 36/38 Irritating to eyes and skin
	S 41 In case of fire and/or explosion do not breath fumes

Morpholine:	C Corrosive
	R 10-20/21/22-34 Flammable - Harmful by inhalation, in contact with the skin and if swallowed - Causes burns
	S 23.2-36-45 Do not breathe vapor - Wear suitable protective clothing - In case of accident or if you feel unwell, seek medical advice immediately (show the label where possible)
Octadecylamine:	Xi Irritant
	R 36/37/38 Irritating to eyes, respiratory system and skin
	S 26-36 In case of contact with eyes, rinse immediately with plenty of water and seek medical advice - Wear suitable protective clothing
1-Octanol:	Xi Irritant
	R 36/38 Irritating to eyes and skin
	S26 In case of contact with eyes, rinse immediately with plenty of water and seek medical advice
1-Pentanol/2-Pentanol:	Xn Harmful
	R 10-20 Flammable - Harmful by inhalation
	S 24/25 Avoid contact with skin and eyes
Petrol ether:	F Highly flammable
	Xn Harmful
	N Environmentally dangerous compounds
	R 11-38-48/20-51/53-62-65-67 Highly flammable - Irritating to skin - Harmful: danger of serious damage to health by prolonged exposure through inhalation - Toxic to aquatic organisms, may cause long term adverse

effects in the aquatic environment - Possible risk of impaired fertility - Harmful: may cause lung damage if swallowed - Vapors may cause drowsiness and dizziness

S 16-23.2-24-33-36/37-61-62 Keep away from sources of ignition - No Smoking! - Do not breathe vapor - Avoid contact with the skin - Take precautionary measures against static discharges - Wear suitable protective clothing and gloves - Avoid release to the environment. Refer to special instructions/material safety data sheet - If swallowed, do not induce vomiting: seek medical advice immediately and show the container or label

Phenylhydrazine: T Toxic

N Environmentally dangerous compounds

R 45-23/24/25-36/38-43-48/23/24/25-50-68 May cause cancer - Toxic by inhalation, in contact with the skin and if swallowed - Irritating to eyes and skin - May cause sensitization by skin contact - Toxic: danger of serious damage to health by prolonged exposure through inhalation, in contact with the skin and if swallowed - Very toxic to aquatic organisms - Harmful: possible risk of irreversible effects

S 53-45-61 Avoid exposure - obtain special instructions before use - In case of accident or if you feel unwell, seek medical advice immediately (show the label where possible) - Avoid release to the environment. Refer to special instructions/ material safety data sheet

Piperidine:	F Highly flammable T Toxic R 11-23/24-34 Highly flammable - Toxic by inhalation and in contact with the skin - Causes burns S 16-26-27-45 Keep away from sources of ignition - No Smoking! - In case of contact with eyes, rinse immediately with plenty of water and seek medical advice - Take off immediately all contaminated clothing - In case of accident or if you feel unwell, seek medical advice immediately (show the label where possible)
Potassium hydride:	F Highly flammable C Corrosive R 15-34 Contact with water liberates highly flammable gases - Causes burns S 7/8-26-36/37/39-43.6-45 Keep container tightly closed and dry - In case of contact with eyes, rinse immediately with plenty of water and seek medical advice - Wear suitable protective clothing, gloves and eye/face protection - In case of fire, use sand, not water - In case of accident or if you feel unwell, seek medical advice immediately (show the label where possible)
1-Propanol:	F Highly flammable Xi Irritant R 11-41-67 Highly flammable - Risk of serious damage to eyes - Vapors may cause drowsiness and dizziness S 7-16-24-26-39 Keep container tightly closed - Keep away from sources of ignition - No

	Smoking! - Avoid contact with the skin - In case of contact with eyes, rinse immediately with plenty of water and seek medical advice - Wear eye/face protection
Pyrrolidine:	F Highly flammable
	C Corrosive
	R 11-20/22-34 Highly flammable - Harmful by inhalation and if swallowed - Causes burns
	S 16-26-36/37/39-45 Keep away from sources of ignition - No Smoking! - In case of contact with eyes, rinse immediately with plenty of water and seek medical advice - Wear suitable protective clothing, gloves and eye/face protection - In case of accident or if you feel unwell, seek medical advice immediately (show the label where possible)
Sodium azide:	T+ Very toxic
	N Environmentally dangerous compounds
	R 28-32-50/53 Very toxic if swallowed - Contact with acids liberates very toxic gas - Very toxic to aquatic organisms, may cause long term adverse effects in the aquatic environment
	S 28.1-45-60-61 After contact with skin, wash immediately with plenty of water - In case of accident or if you feel unwell, seek medical advice immediately (show the label where possible) - This material and/or its container must be disposed of as hazardous waste - Avoid release to the environment. Refer to special instructions/ material safety data sheet

Sodium hydroxide:	C Corrosive
	R 35 Causes severe burns
	S 26-37/39-45 In case of contact with eyes, rinse immediately with plenty of water and seek medical advice - Wear suitable gloves and eye/face protection - In case of accident or if you feel unwell, seek medical advice immediately (show the label where possible)
Sodium nitrite:	O Oxidative
	T Toxic
	N Environmentally dangerous compounds
	R 8-25-50 Contact with combustible material may cause fire - Toxic if swallowed - Very toxic to aquatic organisms
	S 45-61 In case of accident or if you feel unwell, seek medical advice immediately (show the label where possible) - Avoid release to the environment. Refer to special instructions/ material safety data sheet
Sulfuric acid (95-98%):	C Corrosive
	R 35 Causes severe burns
	S 26-30-45 In case of contact with eyes, rinse immediately with plenty of water and seek medical advice - Never add water to this product - In case of accident or if you feel unwell, seek medical advice immediately (show the label where possible)
Tetrahydrofuran:	F Highly flammable
	Xi Irritant
	R 11-19-36/37 Highly flammable - May form explosive peroxides - Irritating to eyes and respiratory system

S 16-29-33 Keep away from sources of ignition - No Smoking! - Do not empty into drains - Take precautionary measures against static discharges

Tin(II) chloride: Xn Harmful

R 22-36/37/38-43 Harmful if swallowed - Irritating to eyes, respiratory system and skin - May cause sensitization by skin contact

S 24-26-37 Avoid contact with the skin - In case of contact with eyes, rinse immediately with plenty of water and seek medical advice - Wear suitable gloves

Toluene: F Highly flammable

Xn Harmful

R 11-20 Highly flammable - Harmful by inhalation

S 16-25-29-33 Keep away from sources of ignition - No Smoking! - Avoid contact with eyes - Do not empty into drains - Take precautionary measures against static discharges

Trimethyltin chloride: T+ Very toxic

N Environmentally dangerous compounds

R 26/27/28-50/53 Very toxic by inhalation, in contact with the skin and if swallowed - Very toxic to aquatic organisms, may cause long term adverse effects in the aquatic environment

S 26-27-28.1-45-60-61 In case of contact with eyes, rinse immediately with plenty of water and seek medical advice - Take off immediately all contaminated clothing - After contact with skin, wash immediately with

plenty of water - In case of accident or if you feel unwell, seek medical advice immediately (show the label where possible) - This material and/or its container must be disposed of as hazardous waste - Avoid release to the environment. Refer to special instructions/ material safety data sheet

Triphenylphosphine: Xn Harmful

R 22-43-53 Harmful if swallowed - May cause sensitization by skin contact - May cause long-term adverse effects in the aquatic environment

S 24-37-61 Avoid contact with the skin - Wear suitable gloves - Avoid release to the environment. Refer to special instructions/ material safety data sheet

Triphenyl phosphite: Xi Irritant

N Environmentally dangerous compounds

R 36/38-50/53 Irritating to eyes and skin - Very toxic to aquatic organisms, may cause long term adverse effects in the aquatic environment

S 28.1-60-61 After contact with skin, wash immediately with plenty of water - This material and/or its container must be disposed of as hazardous waste - Avoid release to the environment. Refer to special instructions/ material safety data sheet

Curriculum Vitae

Name	Tanja Stephanie Pies
Date of Birth	23 April 1974
Place of Birth	Darmstadt, Germany
1980 – 1984	Elementary school, Frankenthal/Pfalz, Germany
1984 – 1987	High school “Karolinen-Gymnasium”, Frankenthal/Pfalz, Germany
1987 – 1989	Brazoswood High School, Clute, Texas, USA
1989 – 1993	High school “Karolinen-Gymnasium", Frankenthal/Pfalz, Germany
04/94 – 04/98	Studies of pharmacy, University of Hamburg, Germany
05/98 – 11/98	Internship at Knoll Pharmaceutical Company, Pharmaceutical Development Department, Whippany, New Jersey, USA
12/98 – 06/99	Internship at the pharmacy “City Apotheke”, Hamburg-Harburg, Germany
08/99	Degree in pharmacy (Approbation)
10/99 – 03/03	Scientific assistant and Ph.D. student at the Department of Pharmaceutical Chemistry, Institute of Pharmacy, University of Hamburg, Germany